ISSN 2634-1379

The Herpetological Journal

Volume 32, Number 3
July 2022

Published by the British Herpetological Society

British Herpetological Society

The Herpetological Journal is published quarterly by the British Herpetological Society and is issued free to members. Articles are listed in Current Awareness in Biological Sciences, Current Contents, Science Citation Index and Zoological Record. Applications to purchase copies and/or for details of membership should be made to the Hon. Secretary, British Herpetological Society, The Zoological Society of London, Regent's Park, London, NW1 4RY, UK. Instructions to authors are printed inside the back cover. All contributions should be addressed to the Scientific Editor.

Front cover: A metamorphosing Wangyal's torrent frog from eastern Bhutan, see article on page 142.

Herpetological Journal

Volume 32, Number 3, 2022

Contents

Full papers

Short notes

Volume 32, Number 2 was published on 1 April 2022

Volume 32 (July 2022), 93–101

Herpetological Journal

FULL PAPER

https://doi.org/10.33256/32.3.93101

Published by the British Herpetological Society

Potential distribution of hybrids between *Crocodylus acutus* and *Crocodylus moreletii* on the Mexican Pacific coast outside the natural hybridisation zone

Gerardo J. Soria-Ortiz[1*], Patricia G. García-Navarrete[2], Leticia M. Ochoa-Ochoa[2] & Armando Rincón-Gutiérrez[3]

[1]Instituto de Ecología, Universidad Nacional Autónoma de México, Circuito exterior s/n anexo al Jardín Botánico, C.P. 04500, Ciudad de México, México

[2]Museo de Zoología, Departamento de Biología Evolutiva Facultad de Ciencias, Universidad Nacional Autónoma de México, Circuito exterior s/n, C.P. 04510, Ciudad de México, México

[3]Instituto de Biología, Universidad Nacional Autónoma de México, Tercer circuito s/n, Ciudad Universitaria, Alcaldía Coyoacán, 04510 México City, México

In Mexico, *Crocodylus acutus* is widely distributed along the Pacific coast, while *C. moreletii* occurs on the Gulf of Mexico. Both species converge in the Yucatán peninsula where natural hybridisation is reported, and later it was also reported in the Gulf of Mexico. Unfortunately, due to translocations and stochastic events, currently there are hybrids of both species on the coast of Oaxaca and Guerrero. In this study, we evaluated the potential colonisation areas of the hybrids on the Pacific coast through ecological niche analyses. The results indicate that the hybrid crocodiles and the parent species share preferences in at least three climatic variables: average temperature range, isothermality, and minimum temperature of the coldest month. Furthermore, it was found that the climatic niche of the hybrids is more similar to that of the *C. moreletii* leaving reminiscent areas for *C. moreletii* in Nuevo León, San Luis Potosí and small areas far from the coast in Veracruz, coinciding with what was previously reported by molecular analysis. On the other hand, the climatic niche of the hybrid crocodiles is also sufficiently similar to that of *C. acutus*, having the possibility to colonise the Pacific coast extensively, leaving reminiscent small areas for *C. acutus* on the northern coast of Sinaloa, southern of Sonora, central coast of Oaxaca and small inland areas of the Pacific coast.

Keywords: Crocodilians, ecological niche, hybrids, species model distributions, conservation, Mexico

INTRODUCTION

American crocodile *Crocodylus acutus* and Morelet's crocodile *C. moreletii* belong to the Crocodylidae family, both are included in the Official Mexican Standard (SEMARNAT, 2010) which aims to identify the species or populations of wild flora and fauna at risk in the Mexican Republic; under the category of Special Protection (Pr) and have a wide distribution in Mexico. In Mexico, the first one is distributed along the Pacific coast, from Sinaloa to Chiapas, reaching the coast of Quintana Roo and Yucatán (Thorbjarnarson, 2010), while *C. moreletii* occurs throughout the entire Gulf of Mexico coast, from Tamaulipas to Quintana Roo (Platt et al., 2010). Both species are highly dependent on water bodies; *C. acutus* prefers brackish water and *C. moreletii* prefers fresh water (Álvarez del Toro, 1974; Hekkala et al., 2015).

The natural zone of contact and hybridisation between *C. acutus* and *C. moreletii* in Mexico is found along the coast of Yucatán, Quintana Roo and Campeche (Cedeño-Vázquez et al., 2008; Escobedo-Galván & González-Salazar, 2011; Pacheco-Sierra et al., 2016; Pacheco-Sierra et al., 2018). It is suggested that this hybridisation zone began 2 to 3 million years ago (Pacheco-Sierra et al., 2018) and currently hybrids have been able to colonise other areas beyond the natural contact zone, throughout the Gulf of Mexico, up to Tamaulipas (Pacheco-Sierra et al., 2016).

Regarding the presence of hybrid crocodiles on the Pacific coast, in the 1970s an unknown number of individuals with hybrid descent were translocated from the Yucatán area to the Chacahua crocodile farm within the Lagunas de Chacahua National Park (Parque Nacional Lagunas de Chacahua; PNLCH) (Soria-Ortiz, 2019). Several crocodiles from the farm escaped to the adjacent lagoons of the PNLCH and interbred with the native *C. acutus*, which has resulted in a set of hybrids in the PNLCH. Currently, the PNLCH is a focal point of hybridisation on the Pacific coast, with hybrids having even been reported outside the PNLCH in relatively near lagoons (~ 10 km away, Soria-Ortiz, 2019). It was reported that at least two hybrids are housed in Playa Linda at Ixtapa Zihuatanejo, Guerrero (Pacheco-Sierra et al., 2018). That hybrids exist in the PNLCH and wider Pacific coast poses a threat that the native species, *C. acutus*, will be displaced by hybrids, similar to what happened in the Gulf of Mexico with *C. moreletii* (Pacheco-Sierra et al., 2016).

Ecological niche studies used to determine the limiting environmental variables of a species are essential to

Correspondence: Gerardo J. Soria Ortiz (gsoria@ecologia.unam.mx)

know the geographic space that species may occupy. Also, they allow us to estimate areas with high environmental suitability outside the natural range of the species and to project them geographically in areas where it is not distributed, to explore the potential invasion that a species might have (Peterson & Vieglais, 2001). Predicting and understanding the potential invasion processes of a species, combined with ecological niche models of native species, is fundamental for management and making effective conservation plans (Gallien et al., 2010).

In this article we aim to evaluate the risk of displacement that the species *C. acutus* may suffer due to the presence of hybrid crocodiles on the Pacific coast of Mexico, for which we intended to: i) estimate the ecological niche (only the climatic part) of *C. acutus*, *C. moreletii* and the hybrids between both species in Mexico, ii) to compare the climatic space of *C. acutus*, *C. moreletii* and hybrids, and finally, iii) identify the remaining distribution areas of *C. acutus* by evaluating the colonisation potential of hybrid crocodiles on the coast of the Pacific Ocean.

MATERIALS & METHODS

Obtaining and cleaning the primary data

Presence records of *C. acutus* and *C. moreletii* were obtained from SNIB (Sistema Nacional de Información sobre Biodiversidad), CONABIO (http://www.snib.mx/), GBIF (Global Biodiversity Information Facility, http://www.gbif.org) databases, and the iNaturalista platform (http://www.naturalista.mx). Presence records were restricted to Mexico, with dates from the decade 1970 to 2019, because in previous years the identification of these particular species was not adequate, and the records do not agree with their known distribution; fossil records and records outside the known range of these species were discarded. Finally, records of captures of both species were obtained from Pacheco-Sierra et al. (2016; 2018) and records of hybrid crocodiles from collection points reported by Pacheco-Sierra et al. (2016; 2018) and Soria-Ortiz (2019) where used. Records were cleaned by eliminating duplicates, and only one point per pixel (~1 km^2) was kept. The records of hybrids were compared with those of the parental species and, in the event of a duplicate record between the two, we kept only the hybrid record. Finally, in the case of records located outside the environmental layers (e.g. the sea), they were moved to the closest environmental pixel to avoid information loss.

Study area and climatic variables

We used 19 climatic variables in ASCII format at a resolution of 1 km^2 developed by Cuervo-Robayo et al. (2014), which include information from the entire 20th century and the first decade of the 21st century, and the layers are also restricted to Mexico and southern United States of America. The climatic layers were trimmed based on the selection of the accessible area "M" (Peterson et al., 2011); that is, those areas where each species is or could be given the biological knowledge, its dispersal capacities, large barriers or environmental discontinuities that limit their establishment (Martínez-Méndez et al., 2016). The area "M" was determined independently for *C. acutus*, *C. moreletii* and hybrids. The herpetofaunal provinces of Mexico was taken as a basis (Casas-Andreu & Reyna-Trujillo, 1990), these coincide with the main mountain ranges in which it is known that there will hardly be any crocodile species. For *C. moreletii*, the provinces of Petén, Tamaulipeca, Yucateca, and Veracruzana were used; for the area "M" of *C. acutus* the provinces used were Petén, Yucateca, Veracruzana, Mexicana del Oeste and Desierto de Colorado-Sonora; and for the hybrids the provinces of Petén, Tamaulipeca, Yucateca, Veracruzana and Mexicana del Oeste (see Fig. S1 and Table S1 in Appendix I).

To avoid overfitting in the niche models, the number of environmental variables used for each parental species and hybrids was reduced. Test runs were carried out with the MaxEntsoftware version 3.4.1 (Phillips et al., 2006) using the 19 climatic variables within the "M" used for each species. From the table of values of contribution to the model and individual importance of each climatic variable, those variables that in sum contributed at least 80 % of the variance of the model and the variables that alone contributed 10 % of permutation were selected. Additionally, a correlation analysis was carried out with the values from the 19 environmental variables that the locality records have. We eliminated one of the variables that presented collinearity, giving preference to the variable that could be more biologically relevant ($r > 0.8$). With the final selected variables, a final model was performed for each parental species and hybrid crocodiles.

Determination of the niche volume

From the selection of variables for each species, three environmental variables that coincided between *C. acutus*, *C. moreletii* and hybrids were chosen, in addition to analysing the 19 variables together. A principal component analysis (PCA) was performed for both sets of variables to identify the volume of the niche occupied by each of the parental species and the hybrids. Subsequently, a multivariate non-parametric analysis of variance (MANOVA) was performed to identify if there was a significant difference between the climatic niche for each species. Paired t tests were performed for each environmental variable to identify the variables that differ between *C. acutus*, *C. moreletii* and the hybrids. To compare the climatic niche of each species, box and whisker plots were made, and the distribution was observed as the relationships between the set of variables shared by the two crocodile parental species and the hybrids. The results were presented in a table containing minimum and maximum values, averages and standard deviation.

To quantify niche overlap of *C. acutus*, *C. moreletii* and hybrids, we calculated the average pairwise Czekanowski niche overlap. This metric is bounded between zero and one, with zero indicating no overlap, and one indicating complete overlap between all species pairs; to test the significance we compared the observed overlap vs the mean of simulate index. If the simulated index is higher than observed there is niche difference. Results were considered significant if they were < 0.05. All analyses were performed in R 3.6.2 using ade4, vegan, stats, MNOVA.RM, and EcoSimR packages (Stéphane et al., 2020; Oksanen et al., 2017; R Core Team, 2013; Friedrich et al., 2019; Gotelli et al., 2015).

Distribution ranges overlap

From the suitability models resulting from *C. moreletii*, *C. acutus* and hybrids, binary presence-absence maps were generated using two threshold values, one was 0 % omission (strict scenario) of the test records (minimum training presence), and the second in which 10 % of omission (relaxed scenario) of the test records was allowed (10th percentile). To estimate the remaining geographic areas that *C. acutus* could occupy on the Pacific coast, the distribution model of *C. acutus* was compared, projecting the potential distribution of hybrids in the geographic space of the province Mexicana del Oeste and Desiertode Colorado-Sonora along the Pacific coast. To compare this result, the same procedure was performed with *C. moreletii* and the hybrids in the Gulf of Mexico, hoping that the reminiscent areas of *C. moreletii* distribution would coincide with the non-hybrid and isolated populations determined by Pacheco-Sierra et al. (2016; 2018).

RESULTS

The species more represented was *C. moreletii* (2,362 records) while *C. acutus* and the hybrids presented a similar number of records (285 and 277, respectively). In the case of hybrids, information was only taken from literature since these were records genetically validated (Table S2 in Appendix I). For each species and hybrids, eight important climatic variables were identified, of which three coincide: average temperature interval (Bio2), isothermality (Bio3) and minimum temperature of the coldest month (Bio6) (Table 1). For the niche volume analyses, 231 environmental values were used for *C. acutus*, 584 for *C. moreletii*, and 219 for hybrid crocodiles.

Niche volume

We found that the climatic niche volumes, determined as the climatic environmental spaces for hybrids and *C. moreletii* are very similar, unlike the climatic niche volume occupied by *C. acutus*. PCA with 19 climatic variables and three shared variables, respectively, show that the polygons that include 95 % of the climatic data between hybrids and *C. moreletii* widely overlap, while the ellipse for *C. acutus* shifts from the trainers (Figs. 1 & 2). The relationships between the shared climatic variables show the same observed pattern as in the PCAs, in which *C. acutus* differs from both hybrids and *C. moreletii* (Fig. 3). It can also be observed that the distribution of the mean diurnal range (Bio2) is extremely similar between *C. moreletii* and hybrids, while the distribution of the values for *C. acutus* is different (Table S3 in Appendix I). Likewise, the variation of the minimum temperature of the coldest month (Bio6) in *C. acutus* is greater compared to the restricted variation presented by *C. moreletii* and

Table 1. Climate variables selected for each species of crocodile and hybrids. Shared variables (among the three groups) are shown in bold.

C. acutus	*C. moreletii*	Hybrids
Bio2	**Bio2**	**Bio2**
Bio3	**Bio3**	**Bio3**
Bio5	Bio5	Bio4
Bio6	**Bio6**	**Bio6**
Bio10	Bio7	Bio7
Bio13	Bio9	Bio13
Bio14	Bio18	Bio14
Bio15	Bio19	Bio18

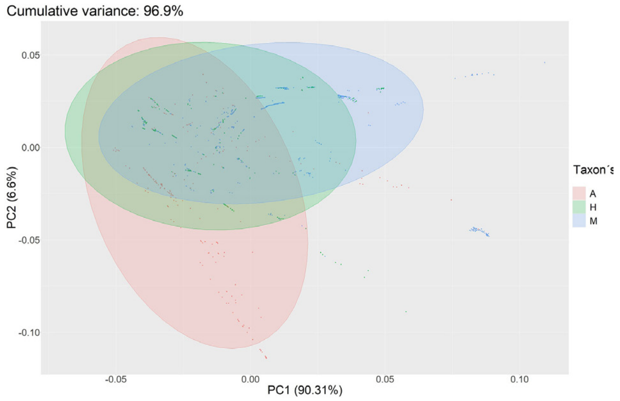

Figure 1. Principal Component Analysis (PCA) using all 19 climatic variables. In blue the variables for *C. moreletii* **(M)** are shown, in red the variables for *C. acutus* **(A)**, and in green the variables for the hybrid crocodiles **(H)**.

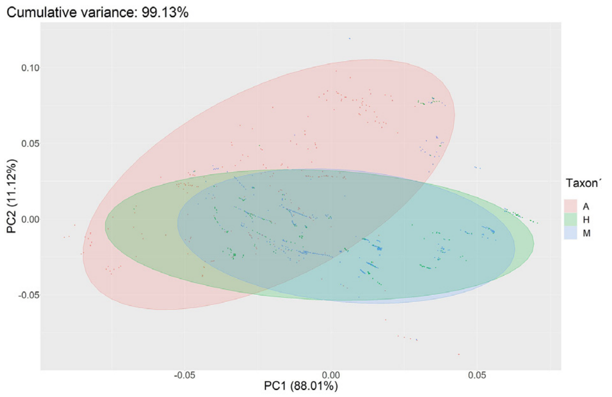

Figure 2. Principal Component Analysis (PCA) using shared climatic variables. Annual Mean Diurnal Range (Bio2), Isothermality (Bio3) and Min Temperature of Coldest Month (Bio6). In blue the variables for *C. moreletii* **(M)** are shown, in red the variables for *C. acutus* **(A)** and in green the variables for hybrid crocodiles **(H)**.

hybrids (Fig. 3).

One of the crocodilian groups analysed was found to be different statistically (MANOVA, F = 60.411, gl = 2, p = 0.0001) and the paired comparisons between the shared environmental variables (Bio2, Bio3, Bio6) shows that *C. acutus* is the one which differs from both *C. moreletii* and hybrids (Table 2). In all niche overlap comparisons between *C. acutus* x hybrids, *C. acutus* x *C. moreletii* and *C. moreletii* x hybrids, the observed index (Oi) was always higher than expected under the random model (simulated index, Si) (Oi = 0.8512 vs Si = 0.2979; Oi = 0.8684 vs Si = 0.2979; Oi = 0.8957 vs Si = 0.2977, respectively, p < 0.05), which means that their environmental niche overlap in all cases is larger than expected under a null hypothesis scenario (p < 0.05, Fig. S2 in Appendix I). We can also observe that there is more niche overlap between *C. moreletii* and hybrids than between *C. acutus* and hybrids.

In the box-and-whisker plot (Fig. 4) the differences between the values of the shared climatic variables are represented; in which it can be observed that *C. acutus* differs considerably from *C. moreletii* in Bio2 and Bio6, while in Bio3 it can be observed that the hybrids present intermediate values between the parental species. In general, *C. acutus* differs from *C. moreletii* and hybrids mainly in the precipitation variables, particularly at the lowest values (Bio12–Bio14, Bio16–Bio19), except for Bio15 (seasonality of precipitation) which presents the highest value (Table S3 & Fig. S3 in Appendix I). In summary, regarding the climatic variables of temperature, the hybrids have a similar pattern to that of *C. moreletii*, while, in the precipitation variables, the hybrids show an intermediate pattern between the two parental species (Fig. 4, Table S3 & Fig. S3 in Appendix I).

Geographical space

The modelled distribution of *C. acutus* is mostly restricted to the Pacific coast, from southern Sonora to Chiapas (Fig. 5, in red). In the Yucatán peninsula the modelled distribution is greater inland than the known distribution, however, on the coast the suitability values are higher (Fig. S4 in Appendix I); also in Tabasco and Veracruz there are suitable climatic values for its presence. The modelled distribution of *C. moreletii* coincides with the known distribution, which goes from Tamaulipas to Quintana Roo on the Atlantic coast of Mexico (Fig. 5, in blue). Likewise, it can also be observed that there are suitable climatic conditions in the coastal plains of the Gulf of Mexico, without being so restricted to the coastal zone (Fig. S5 in Appendix I). The hybrid crocodiles have a modelled distribution in the Gulf of Mexico and Mexican Caribbean that is somewhat more restricted to the coast (Fig. 5, in green), but with greater climatic suitability. Moreover, it can be observed that the modelled distribution of hybrids on the Pacific coast is limited to the coast, ranging from Sinaloa to Chiapas (Fig. S6 in Appendix I).

The suitable zones for *C. acutus*, due to the possible potential distribution of the hybrid crocodiles on the Pacific and Atlantic coasts of Mexico, in the strict scenario (0 % omission) are the southern area of the Sonora and the northern of Sinaloa, central Oaxaca and inland areas far from the Pacific coast (Fig. 6A). While in the case of *C. moreletii* it is evident that the only suitable areas would be found between Nuevo León, San Luis Potosí, and small inland areas far from the coast in Veracruz, Chiapas, and Quintana Roo (Fig. 6B).

Table 2. Result of multivariate variance analysis (MANOVA) and t-paired tests between climatic variables: Annual Mean Diurnal Range (Bio2), Isothermality (Bio3) and Min Temperature of Coldest Month (Bio6). At *** significant p-values between comparisons.

MANOVA (19 Bios)	F = 60.411	P < 0.0001***
	C. moreletii	*C. acutus*
C. acutus	Bio2 - 0.0001*** Bio3 - 0.0001*** Bio6 - 0.0001***	
Hybrids	Bio2 - 1 Bio3 - 0.66 Bio6 - 1	Bio2 - 0.0001*** Bio3 - 0.0001*** Bio6 - 0.0001***

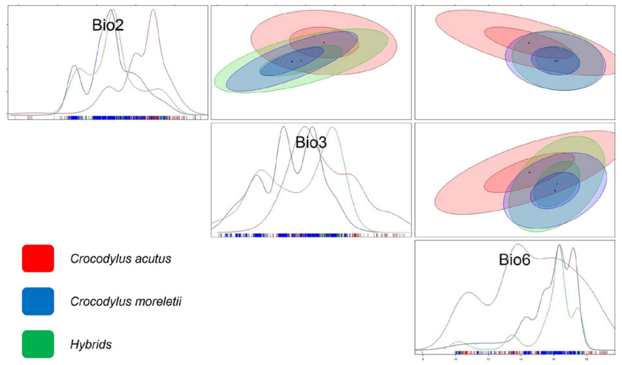

Figure 3. Matrix of relationship between shared climatic variables: Annual Mean Diurnal Range (Bio2), Isothermality (Bio3), and Min Temperature of Coldest Month (Bio6). The diagonal shows the distribution of each climatic variable, while above the diagonal the relationship between them is shown.

DISCUSSION

Niche volume

At first glance it can be observed that the climatic niche or climatic space occupied by *C. acutus* is different from that occupied by *C. moreletii* and hybrid crocodiles (Figs. 1 & 2). This may point to two possibilities: 1) that the climatic conditions on the Pacific coast, and the Gulf of Mexico and Mexican Caribbean may be different or 2) that in geographic spaces occupied by *C. acutus* on the Pacific coast, where *C. moreletii* is absent, and vice versa on the coast of the Gulf of Mexico where *C. moreletii* occurs but *C. acutus* is absent (Thorbjarnarson, 2010; Platt et al., 2010). In this sense, *C. acutus* occupies an important extension of the environmental-geographical space throughout the Pacific coast that it does not share with hybrids or with *C. moreletii*, which suggests that *C. acutus* could have a distinctive evolutionary and ecological imprint, such as it has been seen with other species (Martínez-Méndez et al., 2016). However, it is necessary to carry out analysis from a perspective of conservatism or divergence of climatic niche and combine them with phylogeographic analyses. Luna-Aranguré et al. (2020) analysed the *Ursus* genus and found that the most derived branches of each species coincided with the extreme environmental values, and that although there were species with great environmental space overlap, they occupy different geographical spaces.

According to what we obtained, the shared geographic space is mainly concentrated in the Yucatán Peninsula (Escobedo-Galván & Gonzales-Salazar, 2011; Sánchez-Méndez, 2016), where there is a presence of the three studied groups (Pacheco-Sierra et al., 2016). According to Pacheco-Sierra et al. (2018), the first contact between *C. acutus* and *C. moreletii* was in the Yucatán Peninsula, and later hybridisation between these species occurred, hence, the climatic niche similarity between the three taxa studied is because they occupy the same geographical space in south-eastern Mexico (Figs. 1 & 2 and Figs. S4, S5 & S6 in Appendix I). Furthermore, it was found that the climatic niche between *C. moreletii* and hybrids is very similar as they shared similar geographic space, corroborated by the modelled distribution overlap (Fig.6). This is mainly due to the fact that the hybrids managed to move from the Yucatán Peninsula to the Gulf of Mexico (Pacheco-Sierra et al., 2018). In the PCA (Figs. 2 & 3) the environmental ellipse of the hybrids completely encompasses the environmental space used by *C. moreletii*, even the observed index overlap was the largest (Oi = 0.8957). Due to the similarity of the environmental niche, the hybrid taxon would have the possibility of occupying the entire geographic space of *C. moreletii*, leaving few geographic areas for the unique presence of *C. moreletii*, which coincides with the existing

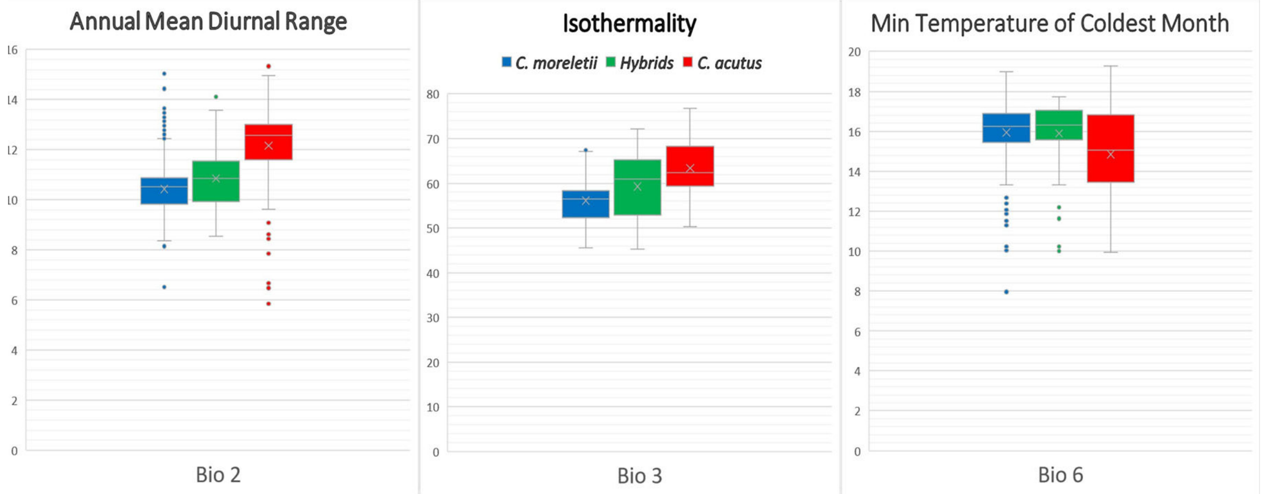

Figure 4. Box-and-whisker graphs between shared climatic variables: Annual Mean Diurnal Range (Bio2), Isothermality (Bio3), and Min Temperature of Coldest Month (Bio6).

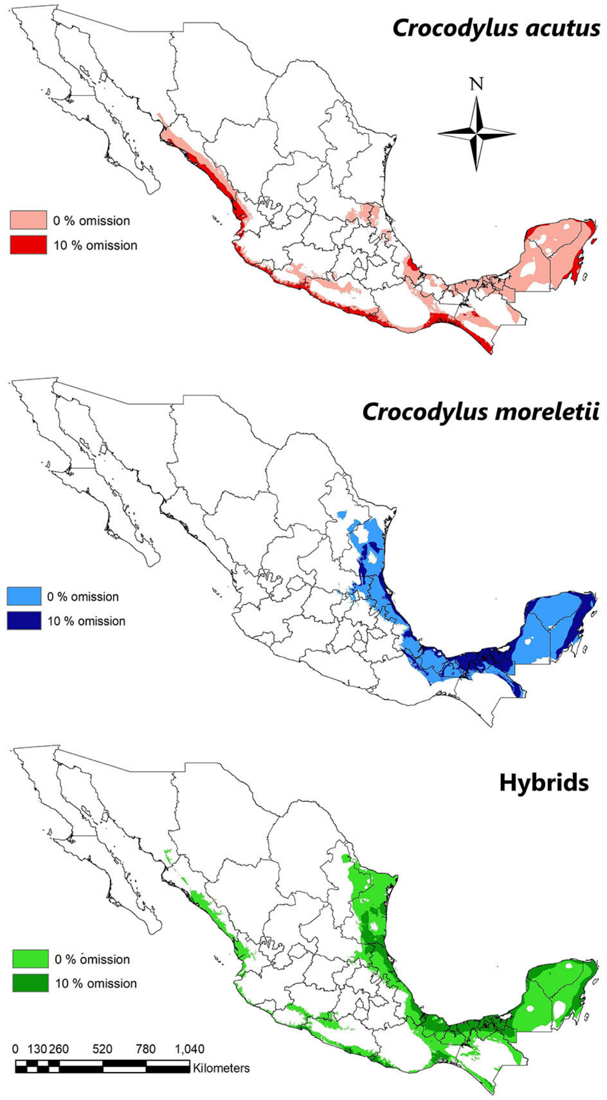

Figure 5. Modelled distribution areas of *C. acutus* (red), *C. moreletii* (blue), and hybrid crocodiles (green), with two threshold values, 0 % omission (clear tonality) and 10 % record omission (darker tonality).

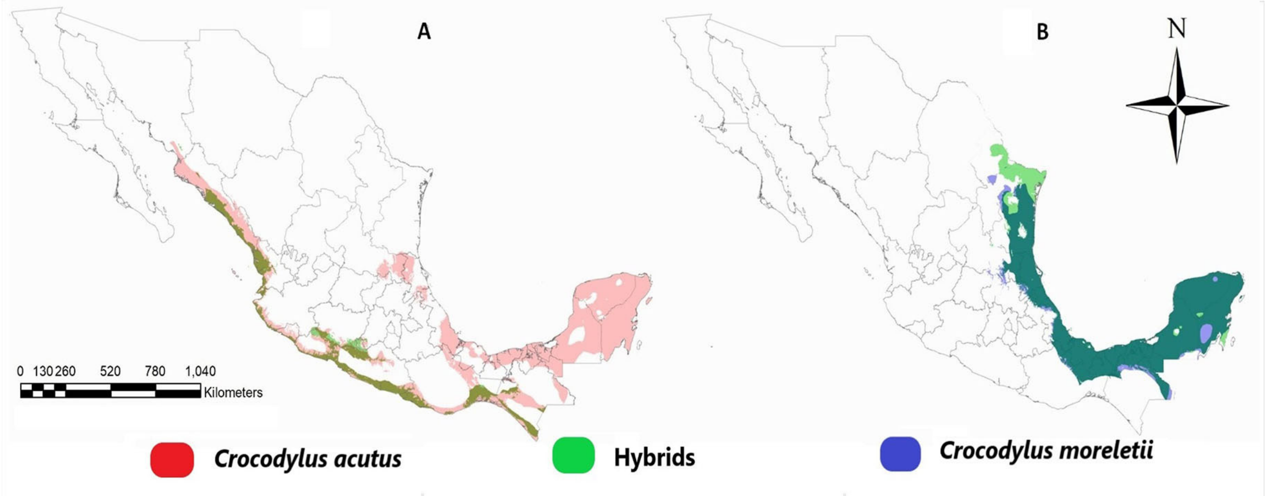

Figure 6. Reminiscent areas for *C. acutus* in the Pacific versant **(A)**, and for *C. moreletii* in the Gulf of Mexico and Mexican Caribbean **(B)**. Binary maps with 0 % omission.

pure populations of *C. moreletii* reported for the Gulf of Mexico (Pacheco-Sierra et al., 2016; 2018).

The similarity of the environmental niche used in the Yucatán Peninsula by the three crocodiles taxons may cause a competition for geographic space (see Figs. S4, S5 & S6 in Appendix I), which, in theory, is a problem ecologically, since species with similar niches cannot occupy the same geographic space due to competition (Hardin, 1960). Therefore, the consequence would be that one of the species will be displaced. In this case, due to our findings and those from previous works, it seems that hybrids are the taxon that has managed to displace the parental species. The evidence points out that although there could be competitive coexistence, hybrids have achieved a large presence in the Yucatán Peninsula, Mexico (Cedeño-Vázquez et al., 2008; Rodriguez et al., 2008; Pacheco-Sierra et al., 2016), displacing non-admixed *C. acutus* to the islands of Banco Chinchorro and Cozumel (MacHkour-M'Rabet et al., 2009; Pacheco-Sierra et al., 2016), and non-admixed *C. moreletii* to remote areas of the Gulf of Mexico (Pacheco-Sierra et al., 2016).

Species distribution models

The geographically projected models agree with the potential distribution of *C. acutus* and *C. moreletii*, which are widely known (Platt et al., 2010; Thorbjarnarson, 2010). Regarding the geographic projection of *C. acutus*, it can be observed that, in the northern zone of Veracruz in the Gulf of Mexico, there are suitable conditions for the presence of this species, as suggested by Escobedo-Galván & Gonzales-Salazar (2011). However, these areas are not continuous, so it can be assumed that the state of Veracruz has not the most adequate environmental suitability for *C. acutus*. It can also be observed that in the state of Tabasco and the Yucatán Peninsula there are areas with suitable conditions for the presence of this species; however, between Veracruz, Tabasco, and Campeche there are less than 10 records, which means that there are probably no established populations of *C. acutus* in that area. Without the presence of geographic barriers between Tabasco and Veracruz, probably the main cause of the absence of *C. acutus* is due to competition of *C. moreletii* and the hybrids that exist in these areas (Escobedo-Galván & González-Salazar, 2011; Pacheco-Sierra et al., 2016). Hypothetically *C. acutus* would have the ability to move to these areas and gradually colonise them; however, there must first be some type of interaction with *C. moreletii* or a hybrid crocodile with great possibilities of hybridisation, causing the displacement of *C. acutus* to be ineffective. Thus, for *C. acutus* what may exist is a biological barrier to its movement through the Gulf of Mexico coast. Regarding the Pacific coast, the distribution of *C. acutus* is restricted to the coast, but it is wide and continuous from Chiapas to southern Sonora, with the northern coast of Sinaloa and southern Sonora being possible areas of invasion, since according to the locality records, there are only presence records of *C. acutus* up to the central coast of Sinaloa.

The modelled distribution of *C. moreletii* coincides with the known distribution for this species (Platt et al., 2010). The areas with high suitable conditions for the presence of *C. moreletii* are found from Tamaulipas to Quintana Roo, and these are not restricted to the coast, unlike what was found for *C. acutus* in the Pacific coast. This remoteness from the coastal zones may be due to the preferences of *C. moreletii* for "fresh" water bodies (Álvarez del Toro, 1974; Hekkala et al., 2015), allowing this species to invade inland areas (Fig. 5). Also, the topography in the Gulf of Mexico is very different from that of the Pacific coast. In the Gulf of Mexico, the slope is much lower and there is a huge plain between the coast and the Sierra Madre Oriental (27 km in the central zone of Veracruz to 200 km in Tamaulipas), whereas in the Sierra Madre del Sur there are certain accessible zones (126 km in Oaxaca), the Chiapas highlands and the entire Yucatán Peninsula, as accessible areas for *C. moreletii*.

The potential hybridisation zone had previously been reported using the ecological niche approach; however, this was restricted to the Yucatán Peninsula due to the hybrid records at that time (Escobedo-Galván & González-Salazar, 2011). In this work, the records of hybrids (genetically identified) from all of Mexico were collected (Pacheco-Sierra et al., 2016; Soria-Ortiz, 2019) and a projection of the potential distribution of hybrids to all of Mexico was performed. According to our models, suitable environmental conditions were found for the hybrids to invade the coast of the Pacific Ocean, the Gulf of Mexico and the Yucatán Peninsula, even with the ability to cross the Isthmus of Tehuantepec unlike what is known found for *C. acutus* (Fig. 5). Based on the potential distribution of the hybrids, it is estimated that they could colonise sites from Sinaloa to Chiapas along the Pacific Ocean coast, with a discontinuity in central Oaxaca. In the Gulf of Mexico and the Yucatán Peninsula, it is observed that the hybrids present a distribution that practically reaching the border with the United States; therefore, like *C. moreletii*, they have capacity to invade the plain of the Gulf and the Yucatán Peninsula.

Considerations in conservation

There are only two antecedents focused on modelling the ecological niche of crocodiles in Mexico (Escobedo-Galván & Gonzales-Salazar, 2011; Sánchez-Méndez, 2016). Studies trying to identify the potential invasion that a species could have when it is mobilised to a new area using ecological niche modelling have been useful and effective in the implementation of conservation measures (Zambrano et al., 2006; Ramírez-Albores et al., 2016; Suárez-Mota et al., 2016). In Mexico, the situation is the following: hybrids from the Yucatán Peninsula and the Gulf of Mexico appeared due to natural contact between *C. acutus* and *C. moreletii* (Pacheco-Sierra et al., 2018). Nevertheless, hybridisation in the Pacific is a different story, if hybridisation had occurred naturally, it would be expected that the geographic hybridisation pattern would be clinal, from the Yucatán Peninsula to the Pacific coast, expecting to find a lower degree of hybridisation in areas further away from the Yucatán Peninsula, such as what happened in the Gulf of Mexico with *C. moreletii* (Pacheco-Sierra et al., 2016). However, it is known that hybridisation in the Pacific was caused by human-mediated movement of individuals from Yucatán to Oaxaca(Soria-Ortiz, 2019), and evidence of hybrid individuals in Guerrero of unknown origin, with two independent points of hybridisation in Guerrero and Oaxaca that are not continuous.

Thanks to the species distribution model for hybrids in the Pacific versant, it can be observed that there are suitable environmental conditions for hybrids to invade and colonise practically the entire Pacific coast, except for the northern Sinaloa and part of central Oaxaca, these being the only reminiscent areas for *C. acutus* (Fig. 6). In the case of *C. acutus* it is related to marine or estuarine areas (Taplin et al., 1982; Thorbjarnarson, 2010) and when competing or being displaced by hybrids it could have ecological consequences due to the need to adapt to new environments, and that might not necessarily happen. It has been reported that hybrids have managed to have an important presence in the PNLCH in the wild in a short time (Serrano-Gómez et al., 2016; Soria-Ortiz, 2019), that hybrids may have a greater suitable space (climatic niche volume) than parental species (Hekkala et al., 2015), and that hybridisation in the Yucatán Peninsula resulted in the only populations of pure *C. acutus* being isolated on the islands of Banco Chinchorro and Cozumel (MacHkour-M'Rabet et al., 2009). Furthermore, in the Gulf of Mexico, hybrids displaced *C. moreletii* to small isolated populations of pure lineages in Tabasco and San Luis Potosí (Pacheco-Sierra et al., 2016).

The aforementioned (in the absence of more ecological studies, reproduction, mobility, connectivity, among others), points to that *C. acutus* may be displaced by hybrids soon, promoting that isolated *C. acutus* populations may remain. Thus, it is essential that the potential invasion of hybrids on the Pacific coast - where *C. acutus* would be affected - is not taken lightly and preventive actions should be implemented.One option could be the containment and extraction of hybrid crocodiles in Oaxaca (PNLCH) and Guerrero (Ixtapa Zihuatanejo, in the absence of extensive local analysis) where hybrids are already known to be found in the wild. Design policies to reduce anthropogenic hybridisation (Allendorf et al., 2001), to avoid making movements of crocodiles to areas where they are not naturally distributed (e.g. *C. acutus* to the Gulf of Mexico or *C. moreletii* to the Pacific). Even make a proper genetic identification of crocodiles, because they could be handling hybrids without knowing it. In the absence of the option to do molecular analysis, morphological identification has proven to be effective (Pacheco et al., 2016; Soria-Ortiz, 2019). Therefore, implementing conservation actions at an early stage of hybridisation is advisable before it becomes an even more difficult problem.

ACKNOWLEDGEMENTS

To Angela Cuervo-Robayo and Enrique Martínez Meyer, professors of the subject "Tools for Spatial Analysis of Biodiversity", taught at the Institute of Biology of UNAM, from which this project was derived. The first two authors thank to the Posgradoen Ciencias Biológicas from UNAM and to CONACyT. Also, we thank two anonymous reviewers for their comments. This research did not receive any specific grant from funding agencies in the public, commercial, or not-for-profit sectors

Authors' Contribution

G.J.S-O, P.N.G-N and A.R-G designed the research; G.J.S-O, P.N.G-N, A.R-G, and L.M.O-O performed the statistical analyses; G.J.S-O analysed the results and drafted the manuscript with the help of P.N.G-N, A.R-G, and L.M.O-O. All the authors corrected and approved the final version of the manuscript. The authors declare that they have no conflicts of interest.

REFERENCES

Allendorf, F.W., Leary, R.F., Spruell, P. & J.K. Wenburg. (2001). The problems with hybrids: setting conservation guidelines. *Trends in Ecology and Evolution*, 16, 613–622.

Álvarez del Toro, M. (1974). *Los Crocodylia de México*. (1st ed.)

Mexico city: Instituto Mexicano de Recursos naturales A.C., México D.F., 70 pp.

Casas-Andreu, G. & Reyna-Trujillo, T. (1990). Herpetofauna (anfibios y reptiles). Mapa IV.8.6. In Atlas nacional de México, vol. III. Instituto de Geografía, UNAM, México, D.F.

Cedeño-Vázquez, J.R., Rodriguez, D., Calmé, S., Ross, J.P., Densmore III, L.D. & Thorbjarnarson, J.B. (2008). Hybridization betwen *Crocodylus acutus* and *Crocodylus moreletii* in the Yucatan Peninsula: I: Evidence from mitochondrial DNA and morphology. *Journal of Experimental Zoology Part A: Ecological Genetics and Physiology,* 309, 661–673.

Cuervo-Robayo, A.P., Téllez-Valdés, O., Gómez-Albores, M.A., Venegas-Barrera, C.S., Manjarrez, J. & Martínez-Meyer, E. (2014). An update of high-resolution monthly climate surfaces for Mexico. *International Journal of Climatology,* 34, 2427–2437.

Escobedo-Galván, A.H. & González-Salazar, C. (2011). Aplicando modelos de nicho ecológico para predecir áreas potenciales de hibridación entre *Crocodylus acutus* y *C. moreletii*. *Quehacer Científico En Chiapas,* 1, 27–35.

Friedrich, S., Konietschke, F. & Pauly, M. (2019). MANOVA. RM: Resampling-Based Analysis of Multivariate Data and Repeated Measures Designs. R package version: 0.3.4.

Gallien, L., Münkemüller, T., Albert, C.H., Boulangeat, I. & Thuiller, W. (2010). Predicting potential distributions of invasive species: Where to go from here? *Diversity and Distributions,* 16, 331–342.

Gotelli, N., Hart, E. & Ellison, A. (2015). EcoSimR: Null Model Analysis for Ecological Data. R package version: 0.1.0.

Hardin, G. (1960). The competitive exclusion principle. *Science,* 131, 1292-1297.

Hekkala, E.R., Platt, S.G., Thorbjarnarson, J.B., Rainwater, T.R., Tessler, M., Cunningham, S.W., ... Amato, G. (2015). Integrating molecular, phenotypic and environmental data to elucidate patterns of crocodile hybridization in Belize. *Royal Society Open Science,* 2, 150409.

Luna-Aranguré, C., Soberón, J. & Vázquez-Domínguez, E. (2020). A tale of four bears: Environmental signal on the phylogeographical patterns within the extant *Ursus* species. *Journal of Biogeography,* 47, 472–486.

MacHkour-M'Rabet, S., Hénaut, Y., Charruau, P., Gevrey, M., Winterton, P. & Legal, L. (2009). Between introgression events and fragmentation, islands are the last refuge for the American crocodile in Caribbean Mexico. *Marine Biology,* 156, 1321–1333.

Martínez-Méndez, N., Aguirre-Planter, E., Eguiarte, L.E. & Jaramillo-Correa, J.P. (2016). Modelado de nicho ecológico de las especies del género *Abies* (pinaceae) en México: Algunas implicaciones taxonómicas y para la conservación. *Botanical Sciences,* 94, 362–371.

Oksanen, J., Guillaume Blanchet, F., Friendly, M., Kindt, R., Legendre, P., McGlinn, D., Minchin, P.R., O'Hara, R.B., Simpson, G.L., Solymos, P., Stevens, M.H.H., Szoecs, E. & Wagner, H. (2017). vegan: Community Ecology Package. R package version 2.4-4.

Pacheco-Sierra, G., Gompert, Z., Domínguez-Laso, J. & Vázquez-Domínguez, E. (2016). Genetic and morphological evidence of a geographically widespread hybrid zone between two crocodile species, *Crocodylus acutus* and *Crocodylus moreletii*. *Molecular Ecology,* 25, 3484–3498.

Pacheco-Sierra, G., Vázquez-Domínguez, E., Pérez-Alquicira, J., Suárez-Atilano, M. & Domínguez-Laso, J. (2018). Ancestral hybridization yields evolutionary distinct hybrids lineages and species boundaries in crocodiles, posing unique conservation conundrums. *Frontiers in Ecology and Evolution,* 6, 138.

Peterson, A.T. & Vieglais, D.A. (2001). Predicting species invasions using ecological niche modeling: New approaches from bioinformatics attack a pressing problem. *BioScience,* 51, 363–371.

Peterson A.T., Soberón J., Pearson R.G., Anderson R.P., MartínezMeyer E., Nakamura M. & Araújo M.B. (2011). Ecological Niches and Geographic Distributions. *Princeton University Press*, New Jersey, USA. 314 pp.

Phillips, S.J., Dudík, M. & Schapire, R.E. (2006). Maximum entropy modeling of species geographic distributions. *Ecological Modelling,* 190, 231–259.

Platt, S.G., Sigler, L. & Rainwater, T.R. (2010). Morelet´s Crocodile *Crocodylus moreletii*. In Manolis, S.C. & Stevenson, C. (eds.) Crocodiles. *Status Survey and Conservation Action Plan* (pp. 79–83). Crocodile Specialist Group.

R Core Team (2013). R: A language and environment for statistical computing. R Foundation for Statistical Computing, Vienna, Austria. ISBN 3-900051-07-0, URL http://www.R-project.org/.

Ramírez-Albores, J.E., Bustamante, R.O. & Badano, E.I. (2016). Improved predictions of the geographic distribution of invasive plants using climatic niche models. *PLoS ONE,* 11, 1–14.

Rodriguez, D., Cedeño-Vázquez, J.R., Forstner, M.R. & Demnsmore III, L.D. (2008). Hybridization between *Crocodylus acutus* and *Crocodylus moreletii* in the Yucatan Peninsula: II. Evidence from microsatellites. *Journal of Experimental Zoology Part A: Ecological Genetics and Physiology,* 309, 674–686.

Sánchez-Méndez, W.D. (2016). Distribución e idoneidad del hábitat de *Crocodylus acutus*, *Crocodylus moreletii* y cocodrilos híbridos en Quintana Roo, México. MSc Thesis. El Colegio de la Frontera Sur, ECOSUR, México. 37 pp.

SEMARNAT, S. de M.A. y R.N. (2010). Norma Oficial Mexicana NOM-059-ECOL-2010. Mexico city.

Serrano-Gómez, S.S., Guevara-Chumacero, L.M., Barriga-Sosa, I.D.L.A., Ullóa-Arvízu, R., González-Guzmán, S. & Vázquez-Peláez, C.G. (2016). Low levels of genetic diversity in *Crocodylus acutus* in Oaxaca and Guerrero, Mexico, and molecular-morphological evidence of the presence of *C. moreletii*. *Biochemical Systematics and Ecology,* 69, 51–59.

Soria-Ortiz, G.J. (2019). Introgresión genética en la especie nativa *Crocodylus acutus* en los sistemas acuáticos del Parque Nacional Lagunas de Chacahua, Oaxaca México. MSc Thersis. Universidad Nacional Autónoma de México, UNAM, México. 54 pp.

Suárez-Mota, M.E., Ortiz, E., Villaseñor, J.L. & Espinosa-García, F.J. (2016). Ecological niche modeling of invasive plant species according to invasion status and management needs: The case of Chromolaena odorata (asteraceae) in South Africa. Polish Journal of Ecology 64, 369–383.

Stéphane, D., Anne-Béatrice, D. & Thioulouse, J. (2020). Ade4: Analysis of Ecological Data: Exploratory and Euclidean Methods in Environmental Sciences. R package version 1.7-15.

Taplin, L.E., Grigg, G.C., Harlow, P., Ellis, T.M. & Dunson, W.A. (1982). Lingual salt glands in *Crocodylus acutus* and *C. johnstoni* and their absence from Alligator mississipiensis and Caiman crocodilus. *Journal of Comparative Physiology,* 149, 43–47.

Thorbjarnarson, J.B. (2010). American Crocodile *Crocodylus acutus*. In Manolis, S.C. & Stevenson, C. (eds.), *Crocodiles status survey and conservation action plan* (pp. 46–53). Crocodile Specialist Group.

Zambrano, L., Martínez-Meyer, E., Menezes, N. & Peterson, A.T. (2006). Invasive potential of common carp (Cyprinus carpio) and Nile tilapia (Oreochromis niloticus) in American freshwater systems. Canadian Journal of Fisheries and Aquatic Sciences 63, 1903–1910.

Accepted: 10 April 2022

Please note that the Supplementary Material for this article is available online via the Herpetological Journal website: https://thebhs.org/publications/the-herpetological-journal/volume-32-number-3-july-2022

Herpetological Journal

FULL PAPER

https://doi.org/10.33256/32.3.102108

Published by the British Herpetological Society

Factors contributing to the biodiversity value of an archaeological landscape in Jordan

Omar Attum[1], Sufian Malkawi[2], Nashat Hamidan[2]

[1]Department of Biology, Indiana University Southeast, New Albany, IN, USA

[2]The Royal Society for the Conservation of Nature, P.O. Box 1215, Jubeiha 11941, Jordan

Archeological landscapes are important places because they protect areas of historical importance, shape cultural and national identity, are recreational spaces, and vital sources of tourism revenue. Archaeological landscapes have the potential to assist in reptile conservation. The objective of this study was to compare the diurnal reptile richness of an archaeological site to the reptile richness of a nature reserve (treatment control for biodiversity value) and a modern olive grove (treatment control for poor biodiversity value). Our results suggest that archaeological landscapes provide valuable reptile habitat, as our archaeological site supported similar reptile richness as the natural site, with both sites having higher species richness than the modern olive tree farm. The high reptile richness and densities were the result of high potential food availability and habitat mosaic of relatively low tree density and open areas with exposed, tall, rocky ruins. Reptile richness had a negative relationship with tree density. The ruins and high food availability of the archaeological site supported higher densities of saxaphilic lizard species as the density of these species increased as mean maximum rock height and percentage of green ground vegetation cover increased. Promoting the reptile richness of archaeological sites provides another justification for the protection and visitor appreciation for archaeological sites as places of historical, cultural and biodiversity importance.

Keywords: *Stellagama stellio*, *Ptyodactylus puiseuxi*, reptile richness, rock outcroppings, vegetation greenness indices

INTRODUCTION

Archaeological landscapes have the potential to be valuable spaces of wildlife conservation. Historical human activity sometimes increases environmental or habitat heterogeneity that increases flora and wildlife biodiversity (Celesti-Grapow et al., 2006; Dambrine et al., 2007; Vanderplank et al., 2014). For example, remains of historic human disturbance, such as shell middens from hunters, was found to change soil composition and increase microsite habitat structural heterogeneity, which in turn resulted in increased plant diversity (Vanderplank et al., 2014). Species richness and coexistence is often related to the availability and diversity of habitat and food (Schoener, 1974). Heterogeneous and structurally diverse habitats often favour a greater number of species as a result of the greater availability of refuge, nesting, and foraging niches (Pianka, 1966).

Archaeological sites can be viewed as a landscape of rock outcrops, a habitat recognised as having high biodiversity value because of their habitat heterogeneity. Archaeological ruins often consist of structures with different states of preservation creating a mosaic of irregular remains of walls, buildings, and rock piles that can be used for basking, perching and refuge by different wildlife (Celesti-Grapow et al., 2006; Dambrine et al., 2007; Fitzsimons & Micheal, 2017). These anthropogenic rock piles have a long history of abandonment, which would allow species from neighbouring natural habitats to colonise and utilise the semi-modified landscape (Celesti-Grapow et al., 2006; Dambrine et al., 2007).

Biologists often quantify food availability to examine the relationship between food availability and biodiversity. However, trapping and quantifying insects as a measure of food availability for reptiles can be time consuming and may require some entomological taxonomic specialisation (Newbold & Macmahon, 2014). In arid environments, vegetation availability is sometimes used as a proxy to quantify food availability for higher trophic levels (Hunter & Price, 1992). Vegetation greenness indices are often used to assess precipitation quantity and resultant vegetation quality at a large scale, which is used to correlate greener and presumably higher nutritional vegetation with wildlife populations (Creech et al., 2016). Therefore, an indirect measurement of percent green vegetation cover measured on the microhabitat scale would be useful to represent the availability of potential food for reptiles at the immediate site (Patrignani & Ochsner, 2015).

Despite the potential for archaeological landscapes to contain high biodiversity or rare species, this aspect is often not studied or appreciated (Ruben & Disi, 2006; Celesti-Grapow et al., 2006; Damhoureyeh et al., 2011). The objective of this study was to compare the diurnal reptile richness between an archaeological site, a nature reserve (treatment control for biodiversity value) and a modern olive grove (treatment control for poorer biodiversity value) in northern Jordan. Jordan is an ideal field site because of its high reptile diversity and numerous large archaeological sites, which are habitat to a variety of reptile species (Disi et al., 2001). We then examined which habitat factors had a significant relationship with reptile richness and the abundance of the two most common rock dwelling lizards in order to understand why some species may have high densities at archaeological sites.

Correspondence: Omar Attum (oattum@ius.edu)

METHODS

Study site

We surveyed three sites between 22 May 2018 and 8 June 2018 in northern Jordan. The three sites were Umm Qais Archaeological Park, Yarmouk Protected Area, and a modern olive tree farm (Fig. 1). The three sites are part of the Mediterranean biogeographic zone characterised by warm summers and relatively cold winters, with mean precipitation of 400 mm / year. The area consists of plateaus, hills, and mountains with deeply dissected valleys that feed into the Yarmouk river. The Umm Qais town is the closest urban center to all three study habitats. The Umm Qais archaeological park (45 ha) consists of a partially excavated Greco-Roman site on a plateau covered by newer Byzantine and Ottoman village and cemetery. The archeological structures consist of columns, buildings, walls, and rubble outcroppings in different states of preservation. The site also contains a historic olive grove, which contains olive trees as old as several hundred years, with old growth olive trees being the most abundant and widespread tree in the archaeological park. The olives are harvested using traditional farming by hand and are not sprayed with pesticides. Native trees such as deciduous oak *Quercus aegilops* and Atlantic pistachio *Pistacia atlantica* are also found in the archeological site, while native shrubs, grasses, and other flowering plants occur. Grazing mostly occurs in the periphery of the park by a small herd of cows and sheep throughout the spring and early summer. The entire park is enclosed by a wired fence.

Yarmouk Nature Preserve (2000 ha^2), borders the Umm Qais archaeological site, overlooks Yarmouk river, and consists of deciduous oak forest (roughly 85 percent of Jordan's surviving oak cover) on mountains (500 m), deep valleys (seasonally flowing riverbeds), limestone rocky outcroppings, and open grassland habitats. The tree community is dominated by deciduous oak with other prominent species including carob *Ceratonia siliqua*, Atlantic pistachio, white willow *Salix alba*, and Aleppo pine *Pinus halepensis*. The Yarmouk Nature Preserve served as our control treatment for high species richness.

The modern olive tree farm (roughly 100 ha) consisted of an olive tree farm on a plateau that is less than twenty years old and was considered the treatment control for poor species richness. In order to accommodate vehicles such as tractors, most of the large rocks have been removed, while some native trees and vegetation remain. Herbicides and pesticides are also applied to remove herbaceous ground cover and reduce insect populations. The modern olive tree farm is adjacent to Yarmouk protected area and the archaeological site.

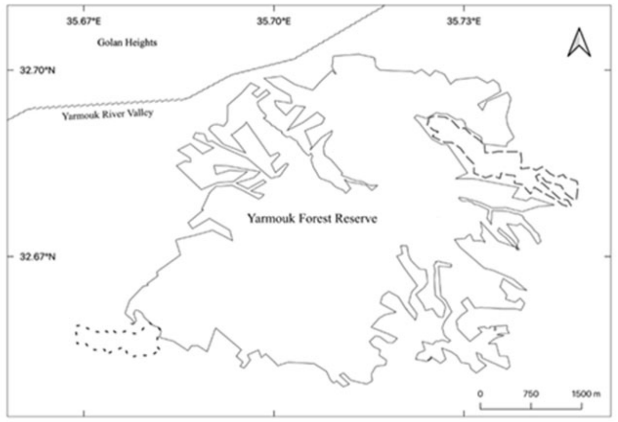

Figure 1. Map of the study site. The smaller dashed lines represent the border of Umm Qais archaeological park. The solid lines represent the border of Yarmouk protected area, and the longer lined dash represents the border of the modern olive tree farm.

The purpose of the surveys was not to comprehensively document species richness, but instead to obtain values for comparison between sites. We thus surveyed six, GIS randomly selected 300 m transects, with a minimum distance of 200 m apart, in each habitat. In order to standardise topography, all the transects were located on plateaus, given that the archaeological site only occurs on a plateau. Habitat data was collected at 30 m intervals, for a total of 10 points for each transect. For each sampling point, we recorded measurements of available tree and rock microhabitat and percent of green, ground vegetation cover.

The tree microhabitat measurements included diameter at breast height (DBH), maximum tree height, and maximum canopy diameter of the nearest tree to the sampling point. Regarding rock structure, we recorded the percent of exposed rock substrate along a 6 m length using a flexible tape measure, the maximum height of the nearest stone with a height greater than 15 cm, and a vertical heterogeneity index within a three-metre radius of the survey point. The vertical heterogeneity index was measured by recording the actual 6 m distance by laying a flexible tape measure along the substrate (bare ground, rocks, ruins, etc.) and then dividing the actual distance by the straight-line distance between the start and end point of the actual distance (actual 6 m distance / straight line distance), with higher values indicating higher vertical habitat heterogeneity. Vertical habitat heterogeneity can be influenced by topography from hills or large vertical rocks. The percent of green vegetation cover was measured on the microhabitat scale and represents availability of green vegetation at the immediate site. We recorded percent green, ground vegetation cover using the smart phone application, Canapeo (Patrignani & Ochsner, 2015), by extending our arm to the side and placing the camera parallel to the ground at a height of roughly 1.45 m above the ground. The percent green ground cover would consist of photosynthetically active annual and perennial herbaceous plants and small, low lying shrubs. Yellow, dormant or dying plants, and bare ground were excluded from the measurement of percent green, ground cover (Patrignani & Ochsner, 2015). We measured tree density post-hoc by counting the number of trees within 15 m of each side of our transects using the satellite imagery from Google Earth. Reptile surveys occurred roughly two to three hours after sunrise and by walking along the length of each transect at an intentionally slow pace of roughly 15 m / minute. For each observation, we recorded the number of each species.

Statistical analysis
We compared mean reptile richness and abundance between the three sites through the use of multiple ANOVAs. Whenever the ANOVA detected a significant difference between the three habitats, we proceeded with follow-up simple contrasts in which the archaeological habitat was the reference and compared to the natural site and olive tree farm. We then used backward stepwise linear regressions to identify which microhabitat variables had a significant relationship with reptile richness and abundance. The microhabitat variables included in the regressions were maximum canopy diameter, percent of exposed rock substrate, maximum rock height of the nearest stone, vertical heterogeneity, percent green, ground vegetation cover, and tree density. We did not include diameter at breast height (DBH) and maximum tree height in the analysis because these variables were highly correlated with maximum tree canopy.

RESULTS

Five tree species were recorded in the archaeological site, four species recorded in the natural site, and three species in the agricultural site. The natural site (n = 60 trees) was dominated by deciduous oak *Quercus aegilops* (77 %, n = 46), spiny hawthorn *Crataegus aronia* (17 %, n = 10), carob tree *Ceratonia siliqua* (5 %, n = 3), and Palestine buckthorn, *Rhamnus palaestina* (2 %, n = 1), whereas the archaeological site (n = 58 trees) was dominated by old olive trees, *Olea europaea* (67 %, n = 39), Atlantic pistachio *Pistacia atlantica* (19 %, n = 11), Syrian Christ-thorn *Ziziphus spina-christi* (10 %, n = 6), and fig *Ficus carica* (3 %, n = 2). The modern olive tree farm (n = 60 trees) was dominated by olive (90 %, n = 50), oak (8 %, n = 5) and Palestine buckthorn *Rhamnus palaestina* (2 %, n = 2). We could not compare the sizes of specific trees between the three habitats because of the different species composition across sites. We therefore combined the measurements of all tree species and compared the tree microhabitat structures (tree height, etc.) between habitats and when examining the relationship between tree structure and species richness or lizard abundance.

The three habitats had similar tree structure as there was no significant difference between mean dbh (ANOVA: $F_{2,170}$ = 1.18, P = 0.31) and height (ANOVA: $F_{2,170}$ = 0.46, P = 0.63) of the three habitats. However, there was a significant difference between the three habitats regarding their mean maximum tree canopy (ANOVA: $F_{2,170}$ = 3.56, P = 0.031), percent of green ground vegetation cover (ANOVA: $F_{2,170}$ = 6.13, P = 0.003), and tree density (ANOVA: $F_{2,15}$ = 20.18, P < 0.0001). Follow-up contrasts showed that the mean maximum tree canopy (Fig. 2) was not significantly different between the archaeological and natural habitat (P = 0.60) and olive tree farm (P = 0.056) but the archaeological habitat did have significantly more green ground vegetation cover than the natural (P = 0.029) and olive tree farm (P = 0.001; Fig. 2). In addition, the archaeological site had similar tree density as the natural site (P = 0.44), but significantly less tree density than the modern olive tree farm (P < 0.0001; Fig. 2).

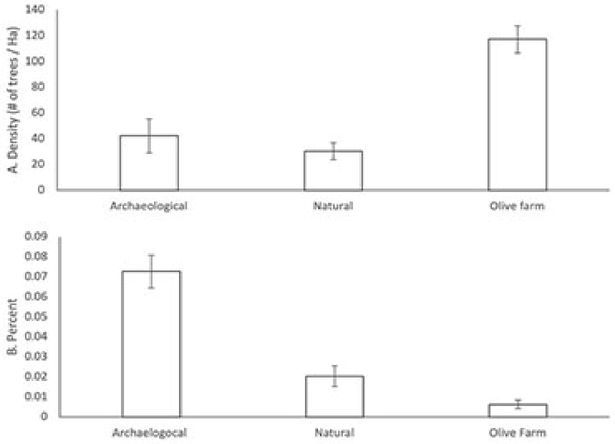

Figure 2. A comparison of mean + SE of tree density and percent green vegetation cover from the three different habitats, an archaeological site, natural site, and modern olive tree farm. **A)** tree density (number of trees / ha). **B)** percent green ground vegetation cover, which was used as an index of food availability.

The overall rock structure (Fig. 3), percent of exposed rock substrate (ANOVA: $F_{2,170}$ = 39.76, P < 0.0001), maximum rock height (ANOVA: $F_{2,170}$ = 14.86, P < 0.0001), and microhabitat rugosity (ANOVA: $F_{2,170}$ = 16.26, P < 0.0001) were significantly different between the three sites. The simple contrasts showed that archaeological site had significantly taller rocks and greater microhabitat rugosity than the natural site (P < 0.0001, P < 0.0001), and olive tree farm (P < 0.0001, P < 0.0001), respectively. The natural site did have significantly more exposed rock substrate than the archaeological site (P < 0.0001) and olive tree farm (P < 0.0001).

The three most common diurnal reptiles in the archaeological and natural sites were the starred agama *Stellagama stellio*, Levant fan footed gecko *Ptyodactylus puiseuxi* and snake eyed lizard *Ophisops elegans*. However, we were not able to compare abundance of *O. elegans* or other reptile species between the three habitats because of the small sample size. A total of six reptile species (including the Forskal's sandsnake *Psammophis schokari*, Mediterranean chameleon *Chamaeleo chamaeleon*, and the nationally endangered and globally threatened Spur-thighed tortoises *Testudo graeca*) were observed at the archaeological site and four species (including the Collared dwarf racer *Platyceps collaris*) were observed at the natural site and zero species of reptiles were observed at the agricultural site. Reptile (ANOVA: $F_{2,18}$ = 19.92, P < 0.0001) richness was significantly different between the three sites. There was no significant difference in mean reptile richness (P = 0.11) between the archaeological and natural sites but the modern olive tree farm had significantly lower reptile (P < 0.0001) richness than the archaeological site (Fig. 3). There was a significant relationship between microhabitat structure with reptile richness ($F_{1,17}$ = 12.44, p = 0.001), with the final model only containing percent green ground vegetation cover and tree density, explaining 62 % (r^2 = 0.62) of the variation of reptile richness. There was no significant relationship between reptile richness and percent green ground vegetation cover (t = 1.83, B = 12.11 ± 6.61, P = 0.087; Fig. 3) but reptile richness significantly decreased as tree density increased (t = -3.74, B = - 0.021 ± 0.006, P = 0.002; Fig. 4).

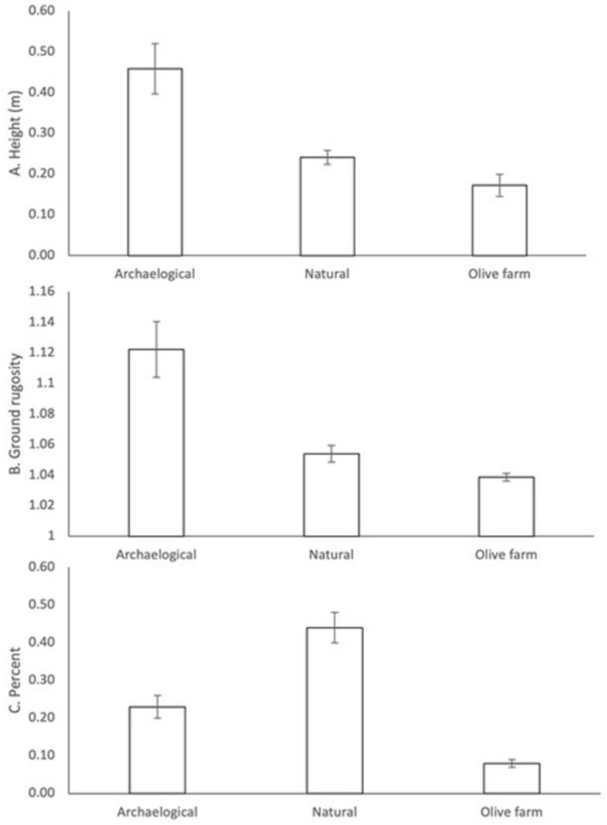

Figure 3. A comparison of mean + SE rock habitat structure of the three habitats, an archaeological site, natural site, and modern olive tree farm. **A)** maximum rock height (m), **B)** ground rugosity. Values closer to one are flatter with less micro-topographical heterogeneity, while larger values represent greater micro-topographical heterogeneity. **C)** percent of exposed rock substrate.

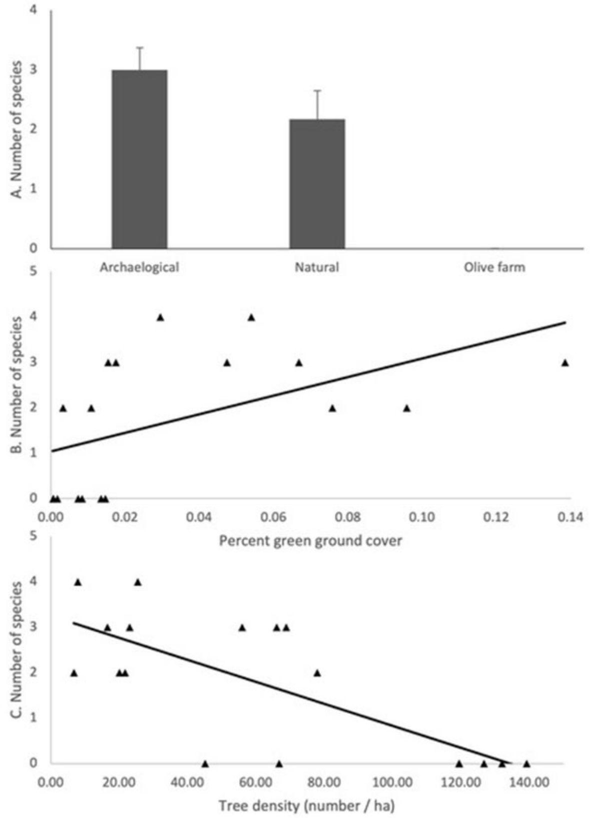

Figure 4. A comparison and relationship of species richness. **A)** Comparison of reptile richness in the three habitats. Olive farm = modern olive tree farm. **B)** Relationship between percent green vegetation cover with reptile richness. **C)** Relationship between three density (number / ha) and reptile richness.

There were significant differences in the number of *S. stellio* (ANOVA: $F_{2,18}$ = 44.52, P < 0.0001) and *P. puiseuxi* (ANOVA: $F_{2,118}$ = 4.86, P = 0.024) observed in the three sites (Fig. 5). Simple contrasts showed that significantly more *S. stellio* and *P. puiseuxi* were observed in the archaeological site than the natural (P < 0.0001, P = 0.025) and the modern olive tree farm (P < 0.0001, P < 0.0001), respectively (Fig. 5). Microhabitat was a significant predictor of the number of *S. stellio* ($F_{1,17}$ = 26.95, P < 0.0001) and *P. puiseuxi* ($F_{1,17}$ = 51.09, P < 0.0001) observed. Percent green ground cover and maximum rock height were the two variables that remained in the final model, explaining 78 % (r^2 = 0.78) and 87 % (r^2 = 0.87) of the variation in the number of *S. stellio* and *P. puiseuxi* observed, respectively. The number of *S. stellio* and *P. puiseuxi* observed increased as the percent of green ground cover (t = 3.89, B = 0.57 ± 0.35, P = 0.001, t = 2.63, B = 0.17 ± 0.066, P = 0.019) and maximum rock height increased (t = 2.68, B = 7.42 ± 2.79, P = 0.017, t = 6.23, B = 7.79 ± 1.24, P < 0.0001), respectively (Fig. 5).

DISCUSSION

The higher reptile richness and densities of starred agama and Levant fan footed gecko at the archaeological site was a result of the habitat mosaic consisting of open

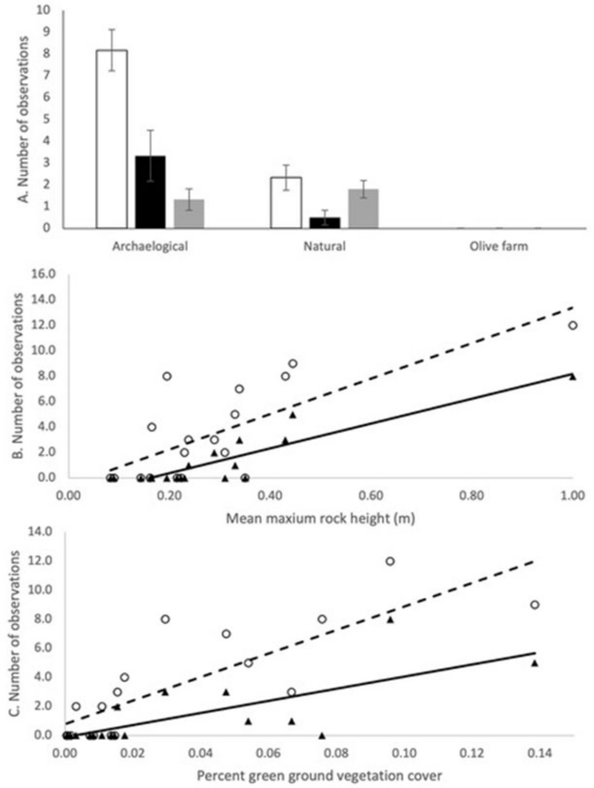

Figure 5. A comparison of the number lizard observations and their relationship with mean maximum rock height and percent green ground vegetation cover. **A)** A comparison of the number of lizard species observations across three different habitats. The hollow bars represent *Stellagama stellio*, the black bars represent *Ptyodactylus puiseuxi*, and the grey bars represent *Ophisops elegans*. **B)** The relationship between the number of observations with the mean maximum rock height (m). The hollow circles represent *S. stellio* and the black triangles represent *P. puiseuxi*. **C)** The relationship between the number of observations with percent green ground vegetation cover. The hollow circles represent *S. stellio* and the black triangles represent *P. puiseuxi*.

areas with relatively low tree density and exposed, tall, rocky ruins that had high potential food availability (Santos & Poquet, 2010). Diurnal reptile richness was negatively associated with tree density (Fig. 3). Artificially high tree density, especially of planted trees used in agriculture or afforestation programs, can lead to a decrease in richness or change the community composition in more arid environments (Shochat et al., 2001; Hawlena & Bouskila, 2006; Schreuder & Clusella-Trullas, 2016; Carpio et al., 2017). The modern olive farm contained an artificially high tree density that was much higher than the natural and archaeological sites, although lower than olive groves in Europe (Metzidakis et al., 2008). Reptiles naturally found in open habitat with low tree densities are likely selected against when the habitat has changed from an open space to a habitat characterised by high tree or vegetation density (Jellinek et al., 2004). The high tree density reduces thermoregulation basking sites for reptiles (Schreuder & Clusella-Trullas, 2016), while potentially increasing predation from avian predators utilising the high availability of once rare perching sites (Shochat et al., 2001; Goode et al., 2005; Hawlena & Bouskila, 2006; Hawlena et al., 2010). The modern olive farm, which had the highest density of trees, had more bird of prey species observations than the other sites (Attum et al., unpublished data).

Although we did not find a relationship between maximum rock height and reptile richness, we believe that the ruins provided rock outcropping habitat to the saxaphilic *S. stellio* and *P. puiseuxi*, as their density increased as mean maximum rock height increased (Jellinek et al., 2004; Fitzsimons & Micheal, 2017). Taller and the greater availability of rock habitat would allow more saxaphilic lizards to utilise the archaeological ruins for thermoregulation and display (Michael et al., 2008, 2010; Monasterio et al., 2010; Norfolk et al., 2010; Croak et al., 2013), while minimising predation risk from the avian predators, such as shrike species that occurred in the archaeological site (Hawlena et al., 2010; Monasterio et al., 2010). In contrast no reptiles were observed in the modern olive tree farm because farmers removed the large rocks in order to facilitate tractor movement which resulted in the modern olive tree farms having the shortest rocks, least habitat rugosity and percent exposed rock substrate (Fig. 2). Saxaphilic reptiles can be negatively impacted by the removal of larger rocks and resultant habitat simplification (Goode et al., 2005; Pike et al., 2010).

Green, herbaceous vegetation was not common in our study sites as the percent of green cover ranged from zero to fourteen (Fig. 4), suggesting that primary productivity that supports higher trophic levels could be a limiting resource. It is believed that in vegetation limited environments, greater percent of green vegetation cover would support more species and higher abundances as result of increased carrying capacity (Carpio et al., 2017). For example, there is often a positive relationship between increased vegetation cover and the number of invertebrates, suggesting that areas with higher vegetation cover provide increased food availability for insectivorous birds and lizards (Robinson, 1981; Sanchez & Parmenter, 2002). Our results supported the assumption that food availability may increase carrying capacity, as both *S. stellio* and *P. puiseuxi* increased in density as percent green, ground vegetation cover increased (White, 1978). In contrast, the modern olive farm had the lowest percent of herbaceous green vegetation cover (Fig. 1) as this site was intentionally heavily grazed to remove herbaceous ground cover that farmers view as competing with young olive trees for water. In addition, the modern olive grove sprayed pesticides to reduce insect populations, which further reduced food availability for insectivores (Cotes et al., 2010).

The archaeological site had the highest percent of green ground vegetation cover, which is likely a result of the lower levels of grazing and the rockiness or heterogeneity of the terrain, which may slow grazing rates or make some areas less accessible (Fitzsimons & Micheal, 2017). Our results suggest that historic olive groves, like those in the archaeological site, are often categorised by relatively low tree density that could potentially be similar in density to natural forests of the region. In addition, historic olive groves likely have more biodiversity value than modern olive tree farms because historic olive groves have lower tree density, more diverse community of native and fruit trees, and older olive trees have a greater number of niches, such as tree cavities, greater branching extant and branch size heterogeneity, all of which contributes to biodiversity potential (Awad & Attum, 2017; Pinto et al., 2018). We observed *S. stello* basking and escaping into the trunk openings in older olive trees. The archaeological site also contained a species of interest, the Greek tortoise, which is endangered within Jordan. Presumably, high food availability and the mixture of old growth olive trees and open areas for thermoregulation in the archaeological site provided suitable Greek tortoise habitat (Attum et al., 2011).

We believe that archeological landscapes can be important areas for reptile conservation in Jordan and the region. Rare reptile species and high reptile richness have been recorded in other archaeological parks in Jordan (Disi et al. 2001; 2014). For example, 40 % of the wildlife species found in Jordan have been recorded in the Petra region that includes Petra Archaeological Park, Jordan's largest archaeological park. (Ruben & Disi, 2006). The Petra region is believed to be biologically rich due to its large size, diverse habitats, availability of springs and waterholes, and diverse plant community (Ruben & Disi 2006; Damhoureyeh et al. 2011). Although the preservation of archaeological sites and biodiversity do not always overlap and in a few instances may have competing priorities, we believe that biodiversity and archeological conservation are mutually beneficial because archaeological sites provide habitat heterogeneity as a result of excavations, herbaceous ground cover, and some level of protection to wildlife (Damhoureyeh et al., 2011; Vanderplank et al., 2014). Promoting the reptile richness of archaeological sites provides another justification for the protection and visitor appreciation of archaeological sites as places of historical, cultural and biodiversity importance (Celesti-Grapow et al., 2006).

ACKNOWLEDGEMENTS

We would like to thank CAORC (Council of American Overseas Research Centers), ACOR (American Council of Oriental Research) and Indiana University Southeast for funding OA's visit. In addition, we would like to thank the Royal Society for Conservation of Nature, Yarmouk Protected Area and Umm Qais Archaeological site for logistical support. We would also like to thank Omar Abed and Tala Maya for their assistance with database management.

Authors contribution

OA devised the project, conducted field work, analysed data, and contributed to the manuscript. SM conducted field work and contributed to the manuscript. NH provided logistical support and contributed to the manuscript.

Ethical statement

This study abided by all local legislation and standard ethical practices.

REFERENCES

Attum, O., Alatoom, M.J., Amr, Z. & Tietjen, B. (2011). Movement patterns and habitat use of soft-released translocated spur-thighed tortoises, *Testudo graeca*. *European Journal of Wildlife Research,* 5, 251–258.

Awad, S.I. & Attum, O. (2017). The biodiversity value of olive groves in the West Bank, State of Palestine. *Jordan Journal of Natural History,* 4, 29–36.

Carpio, A.J., Castro, J., Mingo, V. & Tortosa, F.S. (2017). Herbaceous cover enhances squamate reptile community in woody crops. *Journal for Nature Conservation*, 37, 31–38.

Celesti-Grapow, L., Pysek, P., Jarosík, V. & Blasi, C. (2006). Determinants of native and alien species richness in the urban flora of Rome. *Diversity and Distributions,* 12: 490–501.

Cotes, B., Campos, M., Pascual, F., García, P.A. & Ruano, F. (2010). Comparing taxonomic levels of epigeal insects under different farming systems in Andalusian olive agroecosystems. *Applied Soil and Ecology*, 44, 228–236.

Creech, T.G., Epps, E.W., Monello, R.J. & Wehausen, J.D. (2016). Predicting diet quality and genetic diversity of a desert-adapted ungulate with NDVI.J. *Arid. Environ*., 127, 160–170.

Croak, B.M., Webb, J.K. & Shine, R. (2013). The benefits of habitat restoration for rock-dwelling velvet geckos *Oedura lesueurii*. *Journal of Applied Ecology*, 50, 432–439.

Dambrine, E.J.L., Dupouey, J.L., Laüt, L., Humbert, L., Thinon, M. et al. (2007). Present forest biodiversity patterns in France related to former Roman agriculture. *Ecology,* 88, 1430–1439.

Damhoureyeh, S., Disi, A., Al-Khader, I. & Abu-Dieyeh, M. (2011). Development of a zoning management plan for Petra Archaeological Park (PAP). *Jordan Natural Sciences*, 3, 1040–1049.

Disi A.M., Modry D., Necas P. & Rifai L. (2001). *Amphibians and reptiles of the Hashemite Kingdom of Jordan: An Atlas and Field Guide*, Chimaira, Frankfurt am Main.

Disi A.M., Amr, Z.S. & Hamidan, N. (2014). Diversity, threats, and conservation of the terrestrial and freshwater herpetofauna of Jordan. *Russian Journal of Herpetology,* 21, 221–331.

Fitzsimons, J.A. & Michael, D.R. (2017). Rocky outcrops: A hard road in the conservation of critical habitats. *Biological Conservation*, 211, 36–44.

Goode, M.J., Horrace, W.C., Sredl, M.J. & Howland, J.M. (2005). Habitat destruction by collectors associated with decreased abundance of rock-dwelling lizards. *Biological Conservation*, 125, 47–54.

Hawlena, D. & Bouskila, A. (2006). Land management practices for combatting desertification cause species replacement of desert lizards. *Journal of Applied Ecology*, 43, 701–709.

Hawlena, D., Saltz, D., Abramsky, Z. & Bouskila, A. (2010). Ecological Trap for Desert Lizards Caused by Anthropogenic Changes in Habitat Structurethat Favor Predator Activity.

Conservation Biology, 24, 803–809.

Hunter, M.D. & Price, P.W. (1992). Playing chutes and ladders: bottom-up and top-down forces in natural communities. *Ecology*, 73, 724–732.

Jellinek, S., Driscoll, D.A. & Kirkpatrick, J.B. (2004). Environmental and vegetation variables have a greater influence than habitat fragmentation in structuring lizard communities in remnant urban bushland. *Austral Ecology*, 29, 294–304.

Metzidakis, I., Martinez-Vilela, A., Nieto, G.C. & Basso, B. (2008). Intensive olive orchards on sloping land: good water and pest management are essential. *Journal Environmental Management*, 89, 120–128.

Michael, D.R., Cunningham, R.B. & Lindenmayer, D.B. (2008). A forgotten habitat? Granite inselbergs conserve reptile diversity in fragmented agricultural landscapes. *Journal Applied Ecology*, 45, 1742–1752.

Michael, D.R., Cunningham, R.B. & Lindenmayer, D.B. (2010). The social elite: habitat heterogeneity, complexity and quality in granite inselbergs influence patterns of aggregation in *Egernia striolata* (Lygosominae: Scincidae). *Austral Ecology*, 35, 862–870.

Monasterio, C., Salvador, A. & Díaz, J.A. (2010). Altitude and Rock Cover Explain the Distribution and Abundance of a Mediterranean Alpine Lizard. *Journal of Herpetology*, 44, 158–163.

Newbold, T.A.S. & Macmahon, J.A. (2014). Determinants of habitat selection by desert horned lizards (*Phrynosoma platyrhinos*): the importance of abiotic factors associated with vegetation structure. *Journal of Herpetology*, 48, 306–316.

Norfolk, O., Melotte, A., Gilbert, F., Zalat, S. & Reader, T. (2010). A comparative study of two agamid lizards, *Laudakia stellio* and *Pseudotrapelus sinaitus*, in southern Sinai. *Egypt Journal of Biology*, 12, 27–43.

Patrignani, A. & Ochsner, T.E. (2015). Canopeo: A powerful new tool for measuring fractional green canopy cover. *Agronomy Journal*, 107, 2312–2320.

Pianka, E.R. (1966). Convexity, desert lizards, and spatial heterogeneity. *Ecology*, 47, 1055–1059.

Pike, D., Croak, B., Webb, J. & Shine, R. (2010). Subtle - but easily reversible - anthropogenic disturbance seriously degrades habitat quality for rock-dwelling reptiles. *Animal Conservation*, 13, 411–418.

Pinto, T., Moreira, B., Freitas, H. & Santos, X. (2018). The role of fire history, land-use, and vegetation structure on the response of Mediterranean lizards to fire. *Forest Ecology and Management*, 420, 139–145.

Robinson, J.V. (1981). The effect of architectural variation in habitat on the spider community: an experimental field study. *Ecology*, 62, 73–80.

Ruben, I. & Disi, A.M. (2006): Field guide to the plants and animals of Petra. *Petra National Trust,* 224.

Sanchez, B.C. & Parmenter, R.R. (2002). Patterns of shrub dwelling arthopods diversity across a desert shrubland-grassland ecotone: a test of island biogeographic theory. *Journal of Arid Environments*, 50, 247–265.

Santos, X. & Poquet, J.M. (2010). Ecological succession and habitat attributes affect the postfire response of a Mediterranean reptile community. *European Journal of Wildlife Research*, 56, 895–905.

Schoener, T.W. (1974): Resource partitioning in ecological communities. *Science*, 185, 17–39.

Shochat, E., Abramsky, Z. & Pinshow, B. (2001). Breeding bird species diversity in the Negev: effects of scrub fragmentation by planted forests. *Journal of Applied Ecology*, 38, 1135–1147.

Schreuder, E. & Clusella-Trullas, S. (2016): Exotic trees modify the thermal landscape and food resources for lizard communities. *Oecologia*, 182, 1213–1225.

Vanderplank, S.E, Mata, S. & Ezcurra, E. (2014). Biodiversity and archaeological conservation connected: Aragonite shell middens increase plant diversity. *BioScience,* 64, 202–209.

White, T.R.C. (1978). The importance of relative shortage of food in animal ecology. *Oecologia*, 33, 71–86.

Accepted: 22 April 2022

Herpetological Journal FULL PAPER

https://doi.org/10.33256/32.3.109113

Published by the British Herpetological Society

Egg retention in wild-caught *Python bivittatus* in the Greater Everglades Ecosystem, Florida, USA

Gretchen E. Anderson[1], Frank N. Ridgley[2], Jillian M. Josimovich[1,3], Robert N. Reed[4,5], Bryan G. Falk[6], Amy A. Yackel Adams[4] & Andrea F. Currylow[1]

[1]U.S. Geological Survey, Fort Collins Science Center - South Florida Field Station in Everglades National Park, 40001 SR 9336, Homestead, Florida 33034, USA

[2]Zoo Miami, Conservation and Research Department, 12400 SW 152nd Street, Miami, Florida 33177, USA

[3]Current: U.S. Fish and Wildlife Service, Avon Park Air Force Range, 29 South Boulevard, Avon Park, Florida 33825, USA

[4]U.S. Geological Survey, Fort Collins Science Center, 2150 Centre Avenue, Building C, Fort Collins, Colorado 80526, USA

[5]Current: U.S. Geological Survey, Pacific Island Ecosystems Research Center, Building 344, Hawaii National Park, Hawaii, 96718, USA

[6]National Park Service, Everglades National Park, Homestead, Florida 33034, USA

Retention of eggs in oviducts beyond the normal oviposition period is a common problem for captive reptiles, but the occurrence of egg retention in wild populations is largely unknown. The Burmese python (*Python [molurus] bivittatus*; Kühl 1820) is an oviparous snake native to south-eastern Asia that is now established in southern Florida. From 2011–2019, invasive Burmese pythons were opportunistically removed from Everglades National Park and Big Cypress National Preserve, humanely euthanised, and necropsied to determine reproductive condition. A total of 258 females of reproductive size were found to exhibit various stages of oviposition which generally aligned with purported annual reproductive timing. However, we encountered five pythons during the post-ovulatory period (Aug–Feb) showing signs of recent oviposition with retained eggs. Most of these cases comprised a small number of retained eggs, likely representing some portion of the total clutch. Because this condition is nearly absent in wild animal literature, our observations suggest retained eggs in wild snakes may be more common than previously assumed, possibly slowing or otherwise impacting population growth. However, we recognise that for an invasive species like the Burmese python in Florida, the egg retention rate may be higher in the non-native range compared to the native range due to maladaptation to novel habitats or environmental conditions. Additional research is needed to determine the exact causes of egg retention and investigate the implications for population dynamics on this and other snake species.

Keywords: invasive species, dystocia, snakes, Burmese, reproduction

INTRODUCTION

Egg retention, whereby eggs are held in oviducts beyond the normal oviposition period, is a common reproductive problem in captive reptiles, but reports on its occurrence in wild populations are scarce (Barten, 1985; DeNardo, 2006; Knotek, 2015; Di Girolamo & Selleri, 2017; Govendan et al., 2019). Issues of egg retention are thought to be caused by various factors including physical obstruction, physiological abnormalities, poor maternal body condition, or inadequate captive environmental conditions (DeNardo et al., 2000; DeNardo, 2006; Estrada et al., 2015; Efendić et al., 2017). Although squamates with varying reproductive strategies have occasionally exhibited egg retention (Hoffman, 1970; Lapasha et al., 1985; Plummer, 1996; Blackburn et al., 1998; Blazquez et al., 2000; Bel et al., 2015), the condition is most common in oviparous snakes and often accompanies dystocia (difficulty associated with birth or egg laying; Stahl, 2006). If a snake is incapable of passing eggs (dystocia), then the eggs remain inside the oviduct (egg retention). Because these conditions sometimes lead to death in captive animals, reports of egg retention and dystocia from wild populations of reptiles are scarce, and the natural frequencies are generally unknown (Lapasha et al., 1985; Plummer, 1996; DeNardo et al., 2000; DeNardo, 2006). The impact on oviparous snake populations has the potential to be profound in long-lived species with individually high reproductive output. However, without close monitoring of robust numbers of wild individuals in a population or destructively sampling a cross section, cases of these conditions cannot be identified and documented.

The Burmese python (*Python [molurus] bivittatus*; Kühl 1820) is a large, oviparous snake native to south-eastern Asia (Murphy & Henderson, 1997), but is now an established invasive species across southern Florida, USA, including in Everglades National Park and Big Cypress National Preserve (Snow et al., 2007; Willson et al., 2011; Reed et al., 2012; McCleery et al., 2015). These invasive predators have multiple impacts including predating imperiled species, pets, livestock, and commercially

Correspondence: Gretchen E. Anderson (ganderson@usgs.gov)

important species, outcompeting native predators, and acting as a pathogen or disease vector to native species (Reed & Rodda, 2009).

Although necessary to combat this threat, data on the breeding season across the Burmese pythons' broad native range is limited and varies widely (Van Mierop & Barnard, 1976). Hatchlings are usually seen in late July which places the oviposition period from late spring into early summer (Bhupathy & Vijayan 1989). In southern Florida, the breeding season extends from mid-December through mid-March, and female Burmese pythons appear to oviposit from May through June (Harvey et al., 2008; Reed & Rodda, 2009). Female Burmese pythons are highly fecund, with clutch sizes frequently exceeding 50 eggs in southern Florida (Harvey et al., 2008; Reed & Rodda, 2009; Krysko et al., 2012). However, very little is known about nesting frequency or success in this invasive population and, to the best of our knowledge, we are the first to report egg retention in any (native or invasive) wild-caught Burmese pythons. Because egg retention in female snakes can have fatal consequences or cause sterility in captivity (Ross & Marzek, 1990), it follows that the condition may have deleterious effects on the wild population dynamics. Therefore, focused studies on nesting and clutch success may inform population size, structure, and growth; these are important considerations for conservationists and land managers involved with this invasive species' impacts on native species. These studies may also help to better understand oviparous snakes in general, such as those that are threatened or the focus of conservation efforts.

METHODS

As part of mitigation and removal strategies, Burmese pythons are actively captured from Everglades National Park, Big Cypress National Preserve, and other areas in the Greater Everglades Ecosystem. Some of these specimens are surrendered to the National Park Service (NPS) and U.S. Geological Survey (USGS) for study and are humanely euthanised using a penetrating captive bolt followed by pithing according to American Veterinary Medical Association (AVMA) guidelines (AVMA 2020). Nearly 60 % of these surrendered animals are then necropsied to obtain morphometrics and determine reproductive condition, diet, and other research variables of interest.

For this study we necropsied 258 female Burmese pythons ≥ 210 cm total body length [TL, ~≥186 cm snout-vent length] captured from southern Florida throughout the year, from 2011–2019. Although the sexually mature size for female Burmese pythons in their native range has been reported as 260 cm TL or greater (Wall, 1921; Lederer, 1956; Reed & Rodda, 2009), after necropsying many snakes we found the smallest female containing eggs measured 210 cm. Willson et al. (2014) also encountered a small female (210 cm TL) that contained eggs. Of the 258 females we necropsied, 149 were captured during the post-ovulatory period (Aug–Feb). Nineteen of 149 exhibited oviducts that had not undergone complete involution (post-ovulatory shrinkage or recovery). The hypertrophied oviducts suggest those 19 females had recently oviposited with five of the individuals exhibiting egg retention during post-ovulatory months.

RESULTS

Herein, we examine the cases of egg retention observed in the five females showing signs of recent oviposition and report on possible etiologies and implications (Table 1). Python 1 contained two eggs in the cranial portion of the right oviduct. Python 2 was emaciated with depleted fat bodies and had three retained eggs, two in the right oviduct and one in the left (Table 1a & 1b). Python 3 had five retained eggs that appeared irregular with highly wrinkled shells (Table 1c & 1d). Python 4 had developing primary follicles and 35 densely-packed retained eggs that appeared to have solidified (Table 1e). Python 5 was emaciated with depleted fat bodies, had three retained eggs in the right oviduct, and contained an unidentified mass near the vent. It is worth noting that in four of the five cases only a small number of eggs were retained (n ≤ 5) when clutches from wild Burmese pythons in Florida can contain 62–87 eggs (Krysko et al., 2012, Josimovich et al., 2021, Currylow et al., 2022).

DISCUSSION

In documented cases of dystocia and egg retention, female snakes were usually able to oviposit the majority of their clutch (Barten, 1985; Stahl, 2006), suggesting that the four females with the smaller numbers of eggs had previously oviposited the majority of the clutch. Although the etiologies for our reported cases of egg retention are unknown, evidence at necropsy indicated that these pythons could have experienced dystocia. As mentioned above, dystocia is generally classified into two types, obstructive and non-obstructive. Obstructive dystocia is usually caused by physical abnormalities in or around the female's reproductive tract or by eggs of abnormal shape or size (DeNardo, 2006). It may also result when a small female (e.g. below normal reproductive size) carries average-sized eggs (i.e. the eggs are too large to pass through the oviducts or vent). Non-obstructive dystocia includes that caused by poor physical condition of the mother (e.g. underdeveloped musculature), metabolic imbalances, infections, hormonal interference, nutritional deficiencies, dehydration, or inadequate environmental conditions (DeNardo, 2006; Estrada et al., 2015; Efendić et al., 2017).

As described for Python 5, a mass was discovered near the vent that may have caused an obstructive dystocia and resulted in promoting retention of the three eggs. However, this explanation lacks merit with the assumption that the female was able to pass the rest of the clutch, unless these few remaining eggs were larger or misshapen. Two of the other pythons (Python 1, 210 cm TL and Python 3, 246 cm TL) were at or near the smallest reported reproductive size for this species (210 cm TL; Willson et al., 2014) and it is therefore possible that those two females lacked the size, energy resource accumulation and/or muscle development to successfully oviposit the larger eggs. However, without more information on the relation between female size and egg size and extended specimen observation, it is difficult to determine causes. Python 2 exhibited poor body condition which could support the hypothesis of a non-obstructive dystocia due to some concurrent condition, or that extended retention of the partial clutch negatively affected its health.

Table 1. Capture date, snout-vent length (SVL), total length (TL), number of retained eggs, and photo references of invasive Burmese pythons (*Python bivittatus*) after being removed from the wild in the Greater Everglades Ecosystem, Florida, USA. Capture dates are outside the typical oviposition season of May–June.

	Capture date	SVL (cm)	TL (cm)	# Retained eggs	Photo reference
Python 1	August 2011	216	246	2	None taken
Python 2	August 2014	274	312	3	Figures 1a & 1b
Python 3	December 2016	186	210	5	Figures 1c & 1d
Python 4	August 2019	421	472	35	Figure 1e
Python 5	September 2019	247	282	3	None taken

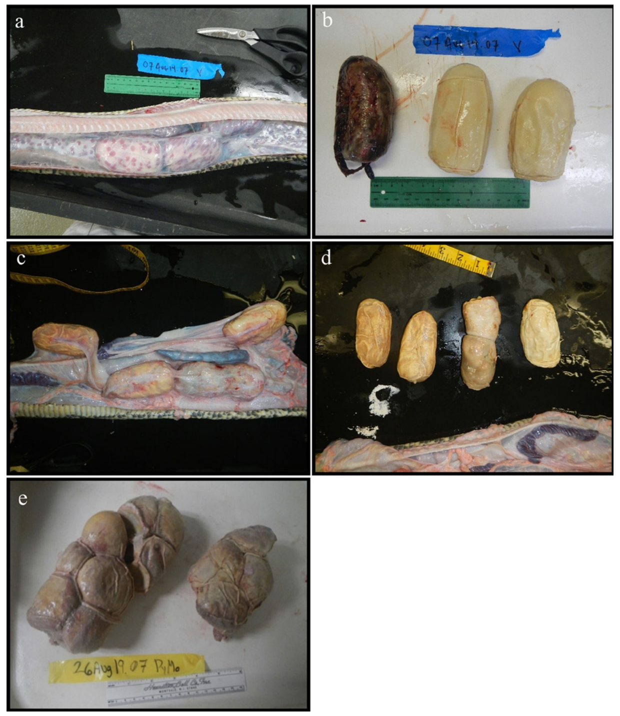

Figure 1. Photos of wild-caught, invasive Burmese pythons (*Python bivittatus*) individuals removed from Everglades National Park, Florida USA. **a)** Three retained eggs in situ within the right oviduct and extremely depleted fat bodies (red dots) in the fascia and **b)** removed from the oviduct of Python 2 **c)** Five retained eggs in situ within the oviduct and **d)** removed from the oviduct of Python 3. This was the smallest animal we detected with this condition. Note the apparent shrinkage of the eggs as evidenced by the significant wrinkling of their surfaces in d). **e)** A subset of the 35 densely-packed and solidified eggs found in Python 4. This animal showed no other abnormalities at necropsy.

Python 4 was the only python to contain a large number of retained eggs (n = 35). Difficulty laying a full clutch, or the majority of a clutch, is documented in captive Burmese pythons (Govendan et al., 2019). Python 4 had no other observed physical abnormalities at necropsy, but we cannot rule out obstructive causes since the original size and shape of the eggs could not be determined. The snake exhibited normal body condition so the high number of retained eggs did not appear to adversely affect the snake during the unknown time of retention. While primary follicles were observed developing in the ovaries, it is possible that the retained eggs could have adversely affected any future reproduction or caused sterility of the female (Ross & Marzek, 1990).

These five cases represent atypical timing for Burmese python oviposition in southern Florida (i.e. Aug–Feb), and all retained eggs were wrinkled or otherwise appeared shrunken in size (Fig. 1). Wrinkled or shrunken appearance is likely caused by water reabsorption from the eggs (Blackburn et al., 1998), but eventual expulsion is far more likely than complete resorption in squamates (Hoffman, 1970; Blackburn, 1998; Blackburn et al., 1998; Blackburn et al., 2003). Barring obstructive complications it is possible that the retained eggs could have been extruded later. However, because nearly all published records of egg retention involve captive animals with subsequent chemically induced or surgical egg removal, successful extrusion or subsequent death rates are not known (Barten, 1985; DeNardo, 2006; Knotek, 2015; Di Girolamo & Selleri, 2017). Retained fertile eggs eventually die and may decompose, which can cause infections, uterine rupture and coelomitis (Ross & Marzek, 1990). Unfertilised retained eggs, although less prone to decomposition complications, can affect future reproduction (Ross & Marzek, 1990). All retained eggs have the potential to cause sterility and death (Ross & Marzek, 1990). It is worth noting that in the other instances of egg retention reported in wild oviparous snakes, one snake underwent surgery and was later released while two others died (Lapasha et al., 1985; Plummer, 1996; DeNardo et al., 2000).

There is limited evidence that snakes may live for several years with retained eggs with no adverse health effects (Ross & Marzek, 1990). We do not know if any of the wild pythons could have later expelled the retained eggs on their own nor whether retained eggs would affect survival of free-ranging pythons. While it is thought that dystocia in wild reptiles is an infrequent occurrence (DeNardo et al., 2000; DeNardo, 2006), our observations suggest it may be more common than previously assumed or reported with 12 % of the adult females captured and necropsied (n = 258) containing eggs. Of those gravid females, 17 % (n = 5 of 30) had retained eggs that were found during atypical timing for oviposition in southern Florida. This suggests a surprisingly high egg retention rate considering the purported risk of sterility or death.

Here we present the first cross-sectional data on this condition in a wild population of invasive snakes. It is unclear if egg retention in wild snakes is more common than previously believed, or if these invasive snakes are experiencing a higher retention rate due to maladaptation to their relatively novel environmental conditions. However, determining the probable causes and natural occurrence rates of egg retention in wild snake species would require additional effort. A clearer understanding of the possible causes or impacts of egg retention is needed to evaluate its impact on population dynamics of both invasive and native snake species, especially those of special concern for conservation.

ACKNOWLEDGEMENTS

We thank T.F. Dean and Ray (Skip) Snow of the National Park Service (NPS), C.M. Romagosa (UF) and N.G. Aumen of the U.S. Geological Survey (USGS) for facilitation of this project in Everglades National Park. Funding for the Everglades work and in-kind support was provided by the U.S. Geological Survey (USGS) Greater Everglades Priority Ecosystem Science Program, NPS, and USGS Invasive Species Program. We thank the many University of Florida interns, NPS staff, volunteers, and Florida Fish and Wildlife Conservation Commission personnel that were involved with the collection of these data. No Institutional Animal Care and Use Committee (IACUC) approval was necessary because the invasive pythons were euthanised as part of mitigation management activities (see USGS IACUC FL_MultipleParks_Currylow_InvasiveHerps_2021.A3), but methods for safe euthanasia were developed in consultation with the National Park Service Wildlife Health Team. Data generated during this study are available within the text of this manuscript. Any use of trade, firm, or product names is for descriptive purposes only and does not imply endorsement by the U.S. Government.

Authors' Contribution

Funding provision: Robert N. Reed, Bryan G. Falk, Andrea F. Currylow, Amy A. Yackel Adams. Research conceptualisation: Andrea F. Currylow, Gretchen E. Anderson. Data collection: Bryan G. Falk, Amy A. Yackel Adams, Robert N. Reed. Data analysis: Andrea F. Currylow, Gretchen E. Anderson. Subject expertise: Frank N. Ridgley, Robert N. Reed. Writing original draft: Gretchen E. Anderson, Andrea F. Currylow, Jillian J. Josimovich. Reviewing and editing: All authors contributed to improving the manuscript.

Ethical Statement

All research was conducted under full compliance with federal and state legislation. Euthanasia methods were developed in consultation with the National Park Service Wildlife Health Team and all euthanasia was humanely performed.

REFERENCES

American Veterinary Medical Association (AVMA). (2020). AVMA Guidelines for the Euthanasia of Animals. Schaumberg, IL, American Veterinary Medical Association.

Barten, S.L. (1985). Oviductal rupture in a Burmese python *(Python molurus bivittatus*) treated with oxytocin for egg retention. *The Journal of Zoo Animal Medicine*, 16, 141–143.

Bel, L., Mihalca, A., Pestean, C., Ober, C. & Oana, L. (2015). Surgical management of dystocia in snakes and lizards. *Bulletin UASVM Veterinary Medicine*, 72, 205–206.

Bhupathy, S. & Vijayan, V.S. (1989). Status, distribution and general ecology of the Indian python *Python molurus molurus* Linn. in Keoladeo National Park, Bharatpur, Rajasthan. *Journal of the Bombay Natural History Society*, 86, 381–387.

Blackburn, D.G. (1998). Resorption of oviductal eggs and embryos in squamate reptiles. *Herpetological Journal*, 8, 65–71.

Blackburn, D.G., Kleis-San Francisco, S. & Callard, I.P. (1998). Histology of abortive egg sites in the uterus of a viviparous placentotrophic lizard, the skink *Chalcides*. *Journal of Morphology*, 235, 97–108.

Blackburn, D.G., Weaber, K.K., Stewart, J.R. & Thompson, M.B. (2003). Do pregnant lizards resorb or abort inviable eggs and embryos? Morphological Evidence From an Australian skink, *Pseudemoia pagenstecheri*. *Journal of Morphology*, 256, 219–234.

Blazquez, C., Diaz-Paniagua, C. & Mateo, J.A. (2000). Egg retention and mortality of gravid and nesting female chameleons (*Chamaeleo chamaeleon*) in southern Spain. *Herpetological Journal*, 10, 91–94.

Currylow, A.F., McCollister, M.F., Anderson, G.E., Josimovich, J.M., Fitzgerald, A.L., Romagosa, C.M. & Yackel Adams, A.A. (2022). Face-off: Novel depredation and nest defense behaviors between an invasive and a native predator in the Greater Everglades Ecosystem, Florida, USA. *Ecology and Evolution*, 12, e8639 https://doi.org/10.1002/ece3.8639.

DeNardo, D. (2006). Dystocias. In: *Reptile Medicine and Surgery*, Mader, D.R. 2nd Ed. Elselvier Inc., St. Louis, USA.787–792.

DeNardo, D., Barten, S.L., Rosenthal, K.L., Raiti, P. & Nathan, R. (2000). Dystocia. *Journal of Herpetological Medicine and Surgery*, 10, 8–17.

Di Girolamo, N. & Selleri, P. (2017). Reproductive disorders in snakes. *Veterinary Clinics of North American Exotic Animal Practice*, 20, 391–409.

Efendić, M., Samardžija, M., Babić, N.P., Bacic, G., Karadjole, T., Lojkic, M., Capak, H., Pećin, M. & Mačešić, N. (2017). Postovulatory egg retention (dystocia) in lizards - Diagnostic and therapeutic options. *Kleintierpraxis*, 62, 754–764.

Estrada, D.M., Mathes, K. & Martínez, P.P. (2015). Distocia en una serpient eratonera amarilla (*Coelognathus flavolineatus*, Schlegel 1837) - reporte de caso. *Revista de la Facultad de Medicina Veterinaria y de Zootecnia*, 62, 75–92.

Govendan, P.N., Kurniawan, L.K.L. & Raharjo, S. (2019). Non-invasive treatment in a case of post-ovulatory egg stasis in a Burmese Python (*Python bivittatus*). *Indonesia Medicus Veterinus*, 8, 282–288.

Harvey, R.G., Brien, M.L., Cherkiss, M.S., Dorcas, M., Rochford, M., Snow, R.W. & Mazzotti, F.J. (2008). Burmese Pythons in South Florida: Scientific Support for Invasive Species Management: UF/IFAS EDIS 2008–4, 10 p., accessed January 15, 2022, at https://doi.org/10.32473/edis-uw286-2008.

Hoffman, L.H. (1970). Observations on gestation in the garter snake, *Thamnophis sirtalis*. *Copeia*, 4, 779–778.

Josimovich, J., Falk, B., Grajal-Puche, A., Hanslowe, E., Bartoszek, I., Reed, R. & Currylow, A.F. (2021). Clutch effects predict Burmese python hatchling growth better than food availability or sex. *Biology Open*, 10, bio058739 https://doi.org/10.1242/bio.058739.

Knotek, Z. (2015). Reproductive surgery in female Asian pythons. In: *40th World Small Animal Veterinary Association Congress, Bangkok, Thailand, 15-18 May, 2015. Proceedings book* (pp. 259–260). World Small Animal Veterinary Association.

Krysko, K.L., Hart, K.M., Smith, B.J., Selby, T.H., Cherkiss, M.S., Coutu, N.T., Reichart, R.M., Nuñez, L.P., Mazzotti, F.J. & Snow, R.W. (2012). Record Length, Mass, and Clutch Size in the Nonindigenous Burmese Python, *Python bivittatus* Kuhl 1820 (Squamata: Pythonidae), in Florida. *IRCF Reptiles & Amphibians Journal*, 19, 267–270.

Lapasha, N.A., Parmerlee, J.S., Powell, R. & Smith, D.D. (1985). *Nerodia erythrogaster transversa* (blotched water snake) Reproduction. *Herpetological Review*, 16, 81.

Lederer, G. (1956). Fortpflanzungs biologie und Entwicklung von *Python molurus* (Linné) und *Python molurus bivittatus* (Kühl). *Die Aquarien-Und Terrarien-Zeitschrift*, 9, 243–248.

McCleery, R.A., Sovie, A., Reed, R.N., Cunningham, M.W., Hunter, M.E. & Hart, K.M. (2015). Marsh rabbit mortalities tie pythons to the precipitous decline of mammals in the Everglades. *Proceedings of the Royal Society* B, 282, 1–7.

Murphy, J.C. & Henderson, R.W. (1997). *Tales of Giant Snakes: A Historical Natural History of Anacondas and Pythons*. Krieger Publishing Company, Malabar, USA.

Plummer, M.V. (1996). *Heterodon platyrhinos* (eastern hognose snake) Mortality. *Herpetological Review*, 27, 146.

Reed, R.N. & Rodda, G.H. (2009). Giant Constrictors: Biological and Management Profiles and an Establishment Risk Assessment for Nine Large Species of Pythons, Anacondas, and the Boa Constrictor: U.S. Geological Survey Open-File Report 2009–1202, 302p., accessed January 15, 2022, at https://doi.org/10.3133/ofr20091202

Reed, R.N., Willson, J.D., Rodda, G.H. & Dorcas, M.E. (2012). Ecological correlates of invasion impact for Burmese pythons in Florida. *Integrative Zoology*, 7, 254–270.

Ross, R.A. & Marzek, G. (1990). Disorders of Reproduction and Pregnancy: Dystocia. In: *The Reproductive Husbandry of Pythons and Boas*, 75–79. Institute for Herpetological Research, U.S.A.

Snow, R.W., Krysko, K.L., Enge, K.M., Oberhofer, L., Warren-Bradley, A. & Wilkins, L. (2007). Introduced populations of *Boa constrictor* (Boidae) and *Python molurus bivittatus* (Pythonidae) in Southern Florida. In: *Biology of the Boas and Pythons*, 365–386. Henderson, R.W. & Powell, R. (eds). Eagle Mountain Publishing, Utah, USA.

Stahl, S. (2006). Reptile obstetrics. *The North American Veterinary Conference*, 20, 1680–1683.

Van Mierop, L.H.S. & Barnard, S.M. (1976). Observations on the reproduction of *Python molurus bivittatus* (Reptilia, Serpentes, Boidae). *Journal of Herpetology*, 10, 333–340.

Wall, F. (1921). Ophidia Taprobanica: Or, The Snakes of Ceylon. Sri Lanka, Government printer.

Willson, J.D., Dorcas, M.E. & Snow, R.W. (2011). Identifying plausible scenarios for the establishment of invasive Burmese pythons (*Python molurus*) in Southern Florida. *Biological Invasions*, 13(7), 1493–1504. https://doi.org/10.1007/s10530-010-9908-3.

Willson, J.D., Snow, R.W., Reed. R.N. & Dorcas, M.E. (2014). *Python molurus bivittatus* (Burmese Python): minimum size at maturity. *Herpetological Review*, 45, 343–34.

Accepted: 22 April 2022

Herpetological Journal
SHORT NOTE
https://doi.org/10.33256/32.3.114119
Published by the British Herpetological Society

A revised system for interpreting great crested newt habitat suitability indices

Andrew S. Buxton[1,2,3] & Richard A. Griffiths[1]

[1]Durrell Institute of Conservation and Ecology, School of Anthropology and Conservation, University of Kent, Marlowe Building, Canterbury, Kent CT2 7NR, UK

[2]Amphibian and Reptile Conservation Trust, 744 Christchurch Road, Boscombe, Bournemouth, Dorset BH7 6BZ, UK

[3]Royal Agricultural University, Stroud Road, Cirencester, GL7 6JS, UK

A widely used system for assessing habitat for the great crested newt uses five categories ranging from 'poor' to 'excellent' based on thresholds for the Habitat Suitability Index (HSI). However, how these categories relate to pond occupancy, at an England-wide scale, is unknown. Equally, the Habitat Suitability Index system has so far only been validated using traditional direct observation methods rather than environmental DNA protocols that are becoming commonplace. Without further validation on a national scale, misleading decisions may be made concerning the likely presence or likely absence of great crested newts. Using environmental DNA data collected from over 5300 ponds distributed across much of England, we show that the existing scoring system underestimates pond occupancy in the lower categories and overestimates pond occupancy in the higher categories, while the median habitat suitability index value was found just within the 'good' category. We found that the median habitat suitability index for occupied ponds was 0.7, confirming this value as a target to aim for when creating or restoring ponds for great crested newts. We suggest a revised system based on the median occupied pond HSI score, whereby the two extreme 'poor' and 'excellent' categories each contain just 10 % of occupied ponds; the 'below average' and 'good' categories each contain 20 % of all occupied ponds, and the 'average' category contains the central 40 % of occupied ponds. Although regional variation in estimated pond occupancy rates using this system may need to be accounted for when interpreting HSI scores, the revised scoring system is generally robust across England. Both the existing and revised HSI scoring systems are no substitute for surveys, and caution is needed when interpreting absence of newts based on habitat suitability data only.

Keywords: Habitat Suitability Index, *Triturus cristatus*, HSI, UK regions, environmental DNA

Assessments of habitat quality are often used to inform conservation recommendations and decisions. Such assessments are frequently constrained by short timeframes needed for decisions, and this has driven the development of simple Habitat Suitability Indices (HSI) that can be rapidly derived and applied by non-specialists (Allen & Hoffman, 1984; U.S. Fish and Wildlife Service, 1976; 1980; 1981; Wesche et al., 1987). The principle underlying the HSI is that it combines a range of easily assessed habitat variables into a single overall score for habitat suitability, based on the requirements of the target species.

The great crested newt *Triturus cristatus* HSI scoring system was developed by Oldham et al. (2000) and is extensively used in ecological impact assessments. Initially developed for use within Great Britain, it is now commonly used across the species range (Unglaub et al., 2015). The HSI assessment focuses on the pond and is based on 10 criteria for 'suitability': geographic location, pond area, frequency of drying, water quality (based on an invertebrate assessment), perimeter shading, waterfowl presence, fish presence, pond density within 1 km, terrestrial habitat quality and macrophyte cover. Each of these Suitability Indices (SIs) are scored between 0.01 and 1 with the geometric mean taken as the final HSI score (Oldham et al., 2000). Although more robust statistical methods are available to assess predictors of species presence and detectability (e.g. Sewell et al., 2010), the Oldham et al. (2000) HSI remains popular amongst practitioners because of its simplicity, and has also been used alongside national surveys such as PondNet (Ewald, 2018) and the National Amphibian and Reptile Recording Scheme (Wilkinson & Arnell, 2013).

A widely-used categorisation system groups ponds with an HSI score below 0.5 as 'poor', 0.5 < 0.6 as 'below average', 0.6 < 0.7 as 'average', 0.7 < 0.8 as 'good' and greater than 0.8 as 'excellent' (ARG UK, 2010). Although there may be inconsistent relationships between HSI score and newt abundance or density (Lewis et al., 2007; Unglaub et al., 2015; Unglaub et al., 2018), the HSI is sometimes used to infer or rule out likely occupancy (Buxton et al., 2021a). In a study of 248 ponds in south-east England - an area known for high pond occupancy (the proportion of sites with species presence) and high pond density - ponds categorised as 'excellent' had a pond occupancy rate of 0.93, 'good' of 0.79, 'average' of 0.55, 'below average' of 0.2 and 'poor' of 0.03 (ARG UK, 2010). Less variation between the categories has been found elsewhere using environmental DNA (eDNA), with ponds categorised as 'excellent' having a pond occupancy rate of 0.17, 'good' of 0.18, 'average' of 0.12, 'below average' of 0.11 and 'poor' of 0.07 (Buxton et al., 2021a). However, there has so far been no evaluation of the likely proportion of ponds falling into each of these categories on an England-wide scale, or the likely occupancy by newts of ponds that fall into each category. This may have far-reaching consequences for conservation decision-making, as cases of 'poor' or 'below average' scores have been used as justification for ruling out occupancy without targeted surveys (see Buxton et al. (2021a) for examples). Furthermore, a value of HSI = 0.7 has been used as a target for 'success' in pond creation and restoration schemes, such as that being undertaken within recent District Level Licencing (DLL) programmes for great crested newts in England (Natural England, 2019; Nature Space Partnership, 2019). The application of thresholds that are not fully understood in terms of likely site occupancy rates carry a risk of inappropriate decisions being made concerning habitat and species protection.

The use of surveys targeting eDNA has revolutionised widespread aquatic species surveys, leading to the ability to conduct national distribution assessments with relative ease, generating quantities of data that were previously unfeasible (Biggs et al., 2015). This permits a review of protocols that were originally developed using traditional surveys of small samples of ponds at limited spatial scales. Here we examine an eDNA based occupancy assessment of 5865 ponds across much of England, with associated HSI information. We examine the relative numbers of great crested newt ponds falling within each

Correspondence: Andrew S. Buxton (andrew.buxton@rau.ac.uk)

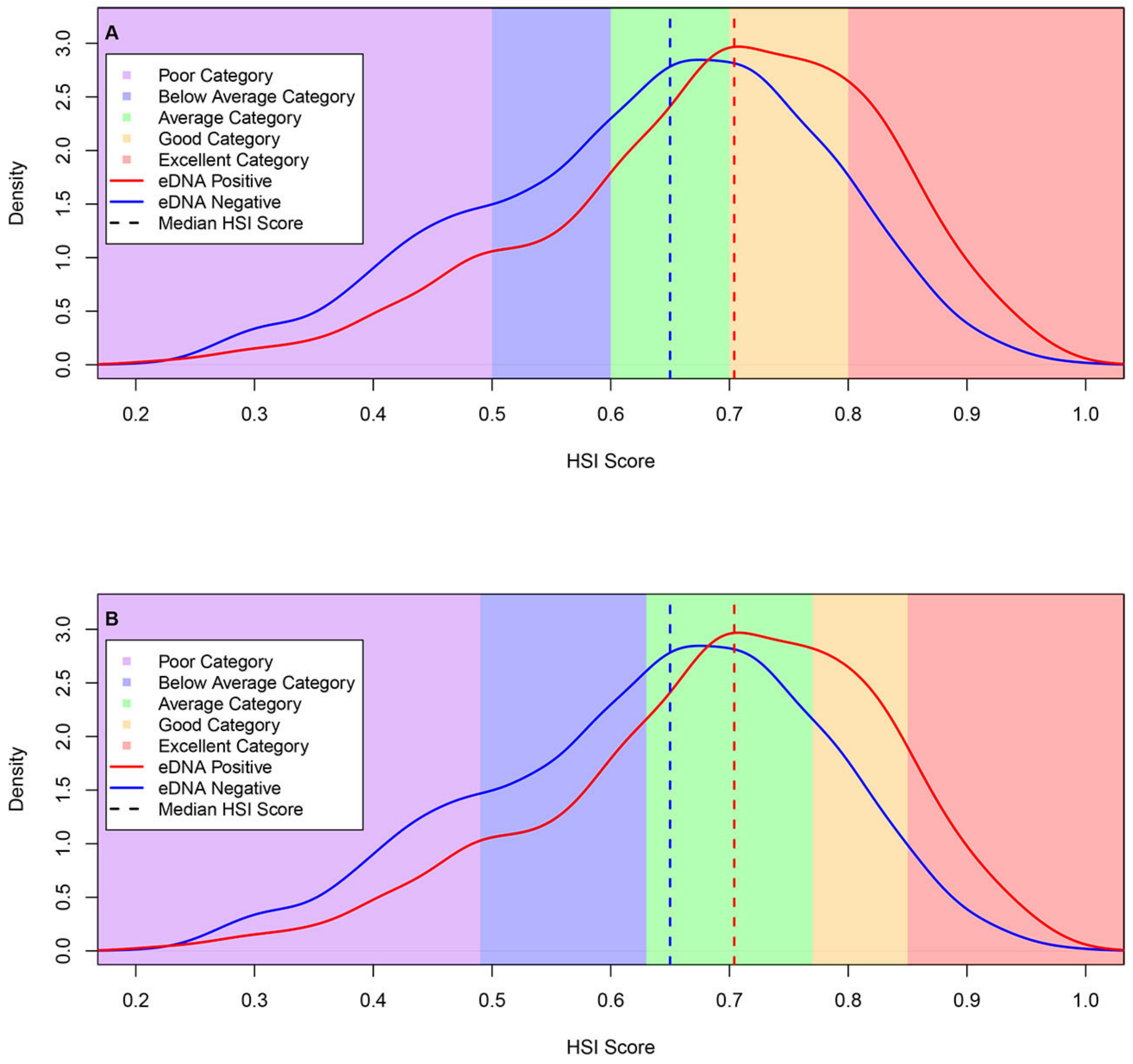

Figure 1. HSI score sample density for ponds with confirmed occupancy (red), and no confirmed occupancy (blue), median HSI for each is indicated by a dashed line. **A)** Existing HSI scoring system (ARG UK, 2010); **B)** Revised HSI scoring system. In both cases the different categories are emphasised by background colour.

Table 1. The observed ('naïve') occupancy rate, percentage of ponds within each category which are occupied and the percentage of all unoccupied ponds when the national eDNA data set was analysed both using the existing ARG UK (2010) categorisation bands and the revised categorisation bands proposed here. The estimated occupancies are based on 5318 ponds sampled using eDNA.

Category	HSI Score ranges	Observed category occupancy percentage	Percentage of all occupied ponds	Percentage of all unoccupied ponds
		Existing categorisation (ARG UK, 2010)		
Poor	< 0.50	20.0	10.8	19.2
Below Average	0.50 < 0.60	23.0	12.2	18.1
Average	0.60 < 0.70	29.1	24.4	26.4
Good	0.70 < 0.80	34.3	29.5	25.0
Excellent	> 0.80	47.6	23.0	11.2
		Proposed categorisation (this study)		
Poor	< 0.49	19.9	10.1	18.1
Below Average	0.49 < 0.63	24.9	19.7	26.4
Average	0.63 < 0.77	31.1	38.9	38.2
Good	0.77 < 0.85	41.6	20.7	12.9
Excellent	> 0.85	51.5	10.5	5.1

of the currently used HSI categories (ARG UK, 2010), and provide adjusted thresholds based on the proportion of ponds falling into these categories nationally. Using the Government Office Regions of England, we further examine regional variation in the proportion of ponds in each category when these revised thresholds are applied.

Ponds were surveyed for great crested newts targeting both eDNA and collecting HSI data. The surveys were commissioned by Natural England as part of a national distribution assessment for the great crested newt, with the data made publicly available through Natural England's Open Data Portal (see acknowledgments for URL). The surveys followed standard UK great crested newt eDNA protocols (Biggs et al., 2014), and great crested newt HSI protocols (ARG UK, 2010; Oldham et al., 2000). Presence was assigned to any site where the eDNA sample showed amplification of at least one qPCR replicate. This threshold is commonly used in assigning occupancy of eDNA samples to increase sensitivity, however there is a risk that a low qPCR replication threshold may exacerbate false positive error (Buxton et al., 2021b; Buxton et al., 2022). We removed 359 records where an HSI score could not be calculated due to missing information, we further removed 188 records that gave an inconclusive eDNA result so could not be assigned to either species presence or absence, which left a total sample size of 5318. 1633 eDNA samples returned in at least one positive qPCR replicate giving an observed (= 'naïve') occupancy of 0.307 across all sites.

The HSI scores for occupied ponds were found not to be normally distributed (Shapiro-Wilks normality test: W = 0.975, P < 0.0001) and had a negative skew (-0.58). We therefore express central tendency and variation in scores as medians and interquartile ranges, plotting density graphs in Base R 4.0.5 (R-Core Team, 2021) to examine the distribution of HSI data for both positive and negative ponds (Fig. 1). Ponds occupied by great crested newts had a median HSI of 0.704 with interquartile range of 0.61–0.79. Unoccupied ponds had a median HSI of 0.65 with interquartile range of 0.63–0.74.(Fig. 1). Occupied ponds do therefore have a higher average HSI score than the ponds with no confirmed occupancy, as has been reported elsewhere (Buxton et al., 2021a).

We calculated observed occupancy within each HSI category as simply the number of great crested newt ponds with confirmed presence divided by the total number of sites in that category. Any categorisation system generated should be examined at a spatial scale similar to that at which it will be applied, i.e. with national data rather than data from only one region. As the data we examined were collected across much of England it is therefore appropriate to suggest a categorisation system at the England-wide scale.

The national eDNA data showed much higher occupancy rates in low scoring HSI categories than would be expected from the ARG UK advice note (ARG UK, 2010). The advice note found just 3 % of ponds to be occupied in the 'poor' category, based on a smaller sample of ponds in south-east England. However, using the ARG UK (2010) categorisation system we observed 20 % observed occupancy in the 'poor' category using the larger eDNA data set (Table 1). Conversely, we found a much lower observed occupancy rate in the higher categories than the ARG UK (2010) advice note. The latter found 93 % of ponds classified as 'excellent' were occupied, compared to 47.6 % observed occupancy for that category using the larger eDNA dataset (Table 1). This general trend of higher occupancy in lower-scoring habitat categories and lower occupancy in higher-scoring habitat categories was also observed by Buxton et al. (2021a). Several factors may contribute to this discrepancy. Firstly - and acknowledging that O'Brien et al. (2017) deemed the HSI scoring system to be generally appropriate in Scotland - habitat suitability may vary across the range (Harper et al., 2019; Miró et al., 2017). Secondly, when high-quality habitat is widespread - such as in parts of south-east England where the ARG UK (2010) data were collected - the species may avoid lower quality ponds in a way they would not if the density of high-quality habitat were lower. Thirdly, the ARG UK (2010) system was based on multiple surveys using traditional survey methods (i.e. visual encounters of all stages and trapping). Small numbers of newts in poor quality ponds, or transient individuals, are more likely to be detected using eDNA than using traditional methods, and this may contribute to the apparently higher pond occupancy in the lower scoring categories using eDNA. Fourthly, using a single positive qPCR amplification to indicate 'presence' may mean occupancy estimates are inflated slightly by a low level of false positives (Buxton et al., 2021b).

We argue that if a categorisation of HSI scores is to be helpful to non-specialists in the interpretation of results, a system with an estimated proportion of occupied ponds likely to fall in each category, and an estimated identifiable occupancy rate on a national scale, would improve the interpretation of results. We therefore determined revised habitat suitability thresholds so that approximately 40 % of the sites fell within the 'average' category; 20 % of sites fell in each the 'below average' and 'good' categories; and the extreme 10 % of ponds at either end of the scale fell in the 'poor' and 'excellent' categories (Table 1).

These new proposed thresholds would limit the categories of 'poor' and 'excellent' to just those sites with exceptionally low or high scores respectively and allow habitat suitability to be interpreted in terms of likely pond occupancy within each category. No occupied ponds were identified with an HSI score below 0.21, but then no ponds at all were identified with a HSI score of 0.20 or less. This is comparable to other great crested newt HSI studies such as Buxton et al. (2021a) which identified occupied ponds with an HSI score of 0.28, with no ponds identified below an HSI score of 1.9. Indeed, only 1 % of all occupied ponds within the present data were found to have an HSI score below 0.31. Nevertheless, great crested newts occupied 20 % of all ponds below HSI = 0.31, and this corresponds with the overall occupancy rate within the 'poor' category of both the existing (ARG UK, 2010) and the revised schemes. As a result, there is no reliable threshold for assuming absence of great crested newts.

HSI thresholds based on an expected proportion of occupied sites within each category permits a more informative interpretation of the index based on the England-wide picture. For example, a suggested interpretation for a pond with a 'good' HSI categorisation may be: "41.3% of ponds with a 'good' HSI score are occupied nationally and this represents 20 % of all occupied ponds". This interpretation can be repeated using information from Table 1 for the other categories and allows non-specialists to assess likely occupancy of a pond and how it compares to ponds in other categories. Nevertheless, the presence of the species should never be ruled out based solely on low HSI score or 'poor' categorisation. Indeed, the fact that 20 % of ponds classified as 'poor' nationally, using either categorisation, return a positive eDNA sample, supports the conclusions of Buxton et al. (2021a) using a separate eDNA data set. Although a positive eDNA sample may occasionally reflect the recent presence of a transitory individual great crested newt, under current legislation such individuals remain protected. We therefore reiterate that ruling out the presence of the species based on a low HSI score is unwise.

The median HSI score for ponds with confirmed occupancy of 0.704, is very close to the boundary between the 'average' and 'good' categories in the existing categorisation (ARG UK, 2010). Indeed, 52.4 % of occupied ponds and 36.3 % of ponds with no confirmed occupancy were found to exceed the 0.7 threshold. Assuming 'above average' is a reasonable target, selection of an HSI = 0.7 as a threshold for successful habitat creation in DLL projects is appropriate. If this were raised to include only 'good' and 'excellent' ponds using the proposed HSI categorisation, a threshold of 0.77 would apply, but this would only encompass 31.8 % of ponds, occupied or not. This is unlikely to be achievable for practical reasons in widespread habitat creation projects, and we recommend that a target based on the median HSI score is maintained.

We further examined how the HSI score performs on a regional scale, based on the Government Office regions of England, in relation to the existing and proposed categorisation. Although the great crested newt HSI accounts for suitability varying between three broad-scale zones (Oldham et al., 2000), finer-scale regional variation may need to be accounted for. The three most northerly regions north-east England (observed occupancy = 0.179), north-west England (observed occupancy = 0.198) and Yorkshire and the Humber (observed occupancy = 0.234) had lower overall observed occupancy than the two most southern regions south-west England (observed occupancy = 0.316) and south-east England (observed occupancy = 0.283), which showed lower occupancy rates than the three central regions west Midlands (observed occupancy = 0.428), east Midlands (observed occupancy = 0.411) and eastern England (observed occupancy = 0.371). All regions had a median occupied pond HSI score within 0.032 of the national median (Supplementary Figure S1; Supplementary Table S1).

The data suggest that the proposed thresholds generated on a national scale are largely appropriate at a regional scale across much of England. However, the three northerly regions showed observed occupancy rates deviating from the national figures (supplementary information Table S1). The north-east had a smaller sample than the other regions and this may represent an outlier, but north-west and Yorkshire and the Humber regions had sample sizes similar to other regions, and may therefore represent true geographic differences. Regional variation may therefore warrant further investigation. Nevertheless, the data do not suggest a simple north-souh divide, as the deviations from the national values varied between northern regions. With most regional HSI categorisation broadly similar to the national categories, we do not currently propose applying region-specific HSI thresholds, but do urge caution when interpreting habitat suitability using the proposed system in under-sampled regions. With only two positive samples and only 20 samples in total, there were insufficient data for the London region to be included.

In conclusion, based on a large national data set, the proposed categorisation for the great crested newt HSI permits a more informative interpretation of the calculated indices using eDNA. The proposed thresholds for different categories of habitat suitability - HSI score below 0.49 as 'poor', 0.49 < 0.63 as 'below average', 0.63 < 0.77 as 'average', 0.77 < 0.85 as 'good'; and greater than 0.85 as 'excellent' - can be interpreted in terms of the estimated proportion of ponds falling within that category and likely pond occupancy. We believe these thresholds are robust enough to be applied across England and, even though there is some regional variation in pond occupancy, median occupied pond HSI score remains stable. Overall, accounting for likely pond occupancy rates within the HSI categories should lead to improved interpretation of HSI scores, more evidence-based decision-making and better conservation outcomes for great crested newts.

ACKNOWLEDGEMENTS

We would like to thank Natural England for making the data they collect freely available online. The raw data used in the model comparison case study was collected by Natural England and is available through the Natural England Open Data Portal https://naturalengland-defra.opendata.arcgis.com/datasets/ffba3805a4d9439c95351ef7f26ab33c_0/data. We would like to thank Dr Eleni Matechou from the School of Mathematics, Statistics and Actuarial Science at the University of Kent for advice with statistical terminology.

Authors contribution

AB - Data analysis and drafting the manuscript. RG – Concept and drafting the manuscript.

Ethical statement

This manuscript contains only the analysis of publicly available data. No additional field surveys were undertaken by the authors, but the data analysed were collected using industry standard protocols approved by Natural England. The collection of eDNA samples did not require the capture or disturbance of individual newts.

REFERENCES

Allen, A.W. & Hoffman, R.D. (1984). Habitat suitability index models: *Muskrat. U.S. Fish and Wildlife Service*, 82, 10.46.

ARG UK. (2010). ARG UK *Advice Note 5: Great Crested Newt Habitat Suitability Index*.

Biggs, J., Ewald, N., Valentini, A., Gaboriaud, C., Griffiths, R., Foster, J. et al. (2014). Analytical and methodological development for improved surveillance of the great crested newt Appendix 5. *Technical advice note for field and laboratory sampling of great crested newt (Triturus cristatus) environmental DNA*. Defra Project WC1067. Oxford; 2014.

Biggs, J., Ewald, N., Valentini, A., Gaboriaud, C., Dejean, T., Griffiths, R., Foster, J., Wilkinson, J.W., Arnell, A., Brotherton, P. et al. (2015). Using eDNA to develop a national citizen science-based monitoring programme for the great crested newt (*Triturus cristatus*). *Biological Conservation*, 183, 19–28.

Buxton, A., Tracey, H. & Downs, N.C. (2021a). How reliable is the habitat suitability index as a predictor of great crested newt presence or absence? *Herpetological Journal*, 31, 51–57.

Buxton, A., Matechou, E., Griffin, J., Diana, A. & Griffiths, R.A. (2021b). Optimising sampling and analysis protocols in environmental DNA studies. *Scientific Reports*, 11, 11637.

Buxton, A., Diana, A., Matechou, E., Griffin, J. & Griffiths, R.A. (2022). Reliability of environmental DNA surveys to detect pond occupancy by newts at a national scale. *Scientific Reports*, 12, 1295.

Ewald, N. (2018). eDNA monitoring for great crested newts 2018. Retrieved from https://freshwaterhabitats.org.uk/wp-content/uploads/2019/04/eDNA-Great-Crested-Newt-2018.pdf

Harper, L.R., Downie, J.R. & McNeill, D.C. (2019). Assessment of habitat and survey criteria for the great crested newt (*Triturus cristatus*) in Scotland: a case study on a translocated population. *Hydrobiologia*, 828, 57–71.

Lewis, B., Griffiths, R.A. & Barrios, Y. (2007). Field assessment of great crested newt *Triturus cristatus* mitigation projects in England. *Natural England Research Report NERR001*. Natural England, Sheffield, England.

Miró, A., O'Brien, D., Hall, J. & Jehle, R. (2017). Habitat requirements and conservation needs of peripheral populations: the case of the great crested newt (*Triturus cristatus*) in the Scottish Highlands. *Hydrobiologia*, 792, 169–181.

Natural England. (2019). *A Framework For District Licensing Of Development Affecting Great Crested Newts: TIN176*. Retrieved from http://publications.naturalengland.org.uk/file/4976658752995328

Nature Space Partnership. (2019). NatureSpace Partnership. 2019. *South Midlands region extension GCN District Licensing project Implementation Strategy*. Stamford, UK.

O'Brien, D., Hall, J., Miró, A. & Wilkinson, J. (2017). Testing the validity of a commonly-used habitat suitability index at the edge of a species' range: great crested newt *Triturus cristatus* in Scotland. *Amphibia-Reptilia*, 38, 265–273.

Oldham, R.S., Keeble, J., Swan, M.J.S. & Jeffcote, M. (2000). Evaluating the suitability of habitat for the great crested newt (*Triturus cristatus*). *Herpetological Journal*, 10, 143–155.

R-Core Team. (2021). R: Language and Environment for Statistical Computing. Vienna, Austria: R Foundation for Statistical Computing.

Sewell, D., Beebee, T.J.C. & Griffiths, R.A. (2010). Optimising biodiversity assessments by volunteers: The application of occupancy modelling to large-scale amphibian surveys. *Biological Conservation*, 143, 2102–2110.

U.S. Fish and Wildlife Service. (1976). *Habitat Evaluation Procedures ESM 101*. Washington DC.

U.S. Fish and Wildlife Service. (1980). *Habitat Evaluation Procedures (HEP) ESM 102*. Washington DC.

U.S. Fish and Wildlife Service. (1981). *Standards for the development of habitat suitability index models for use in the habitat evaluation procedures (HEP)*. Washington DC.

Unglaub, B., Steinfartz, S., Drechsler, A. & Schmidt, B.R. (2015). Linking habitat suitability to demography in a pond-breeding amphibian. *Frontiers in Zoology*, 12, 9.

Unglaub, B., Steinfartz, S., Kühne, D., Haas, A. & Schmidt, B.R. (2018). The relationships between habitat suitability, population size and body condition in a pond-breeding amphibian. *Basic and Applied Ecology*, 27, 20–29.

Wesche, T.A., Goertler, C.M. & Hubert, W.A. (1987). Modified habitat suitability index model for brown trout in southeastern Wyoming. *North American Journal of Fisheries Management*, 7, 232–237.

Wilkinson, J.W. & Arnell, A.P. (2013). *NARRS report* 2007-2012. In ARC.

Accepted: 4 May 2022

Please note that the Supplementary Material for this article is available online via the Herpetological Journal website: https://thebhs.org/publications/the-herpetological-journal/volume-32-number-3-july-2022

Herpetological Journal
FULL PAPER
https://doi.org/10.33256/32.3.120129
Published by the British Herpetological Society

A stable home: Autocorrelated Kernel Density Estimated home ranges of the critically endangered Elongated tortoise

Ysabella Montano[1], Benjamin Michael Marshall[1], Matt Ward[1], Ines Silva[2,3], Taksin Artchawakom[4], Surachit Waengsothorn[5], Colin Thomas Strine[1,6]

[1]Suranaree University of Technology, Nakhon Ratchasima, Thailand
[2](CASUS), Center for Advanced Systems Understanding, Görlitz, Germany
[3](HZDR), Helmholtz-Zentrum Dresden-Rossendorf, Dresden, Germany
[4]Population and Community Development Association, Bangkok, Thailand
[5]Sakaerat Environmental Research Station, Nakhon Ratchasima, Thailand
[6]Dickinson State University, North Dakota, USA

Home range analysis is a standard and fundamental concept in ecology used to describe animal space use over their lifetimes. Connecting home range sizes with animal characteristics, location, and habitat can be used to inform conservation decisions. Reptiles are frequently lacking robust estimates of space use, particularly reptiles in tropical regions. Here we analyse a publicly available dataset, collected by the authors of this study, describing the movements of Critically Endangered Elongated tortoises *Indotestudo elongata*. The tortoise data included the locations of 17 tortoises (12 females, 5 males) collected on average once every three days for an average duration of 353.76 SE ± 33.10 days. We use these data to estimate the home range of Elongated tortoise, and explore how tortoise size and sex influences home range size. To mitigate issues resulting from low effective sample sizes and low temporal resolution of the data, we used a modern home range estimation method – Autocorrelated Kernel Density Estimators (AKDE). We found 14 of 17 individuals appear to be occupying a stable home range (using variograms to determine range residency). The average AKDE home range for all 14 individuals with range residency was 44.81 ± 10.44 ha. Bayesian Regression Models suggest comparable size estimates between male and female home ranges, despite males being physically larger than females in both mass and carapace length. These AKDE home range estimates have the added utility of being more comparable with other studies, less susceptible to errors from a suboptimal tracking regime, and are well positioned for inclusion in future meta-analyses.

Keywords: testudine, autocorrelated kernel density estimator, spatial ecology, space use, Thailand, *Indotestudo elongata*

INTRODUCTION

Understanding an animal's lifetime space use can yield insight into many aspects of its ecology. Most importantly we can identify the spatial requirements for maintaining healthy populations (Di Franco et al., 2018). We can better optimise our limited conservation resources by using methods that quantify animal space use – which is often explored via expensive and long-term datasets – in a more efficient manner (Laver & Kelly, 2008). The most commonly used metric for quantifying an animal's lifetime space use is termed home range (Burt, 1943; Worton, 1989; Fauvelle et al., 2017). Here we follow Silva et al. (2022) and define home ranges as the lifetime space use of an animal.

Information on home range sizes and location can begin to elucidate the decision-making processes animals engage in. Decisions based upon resources (Mitchell & Powell, 2004; 2012; Powell & Mitchell, 2012), topography, and habitat can all filter down to impact animal space use (Fieberg & Kochanny, 2005), and aids in understanding an animal's spatial niche (Xirouchakis et al., 2021). Understanding these phenomena in target species can have implications for both land-use and protected area management (Linnell et al., 2001; Viggers & Hearn, 2005; Houser et al., 2009). For example, Breininger et al. (2011) calculated home ranges for Indigo snakes *Drymarchon couperi* and concluded that the species needed large land tracts with substantial corridors between sites to avoid significant sources of road mortality. However, these tools only have value if the underlying data are treated properly, and the output is interpreted in a biological context.

Traditional approaches for estimating home ranges such as Minimum Convex Polygons (MCP), which essentially draw a polygon around the outermost collected points from a spatial dataset, are still widely used in herpetological research despite serious drawbacks (Crane et al., 2021). Specifically, MCPs tend to mis-estimate true space use (Silva et al., 2020) potentially leading to false conclusions when modelling predictors of home range size (Crane et al., 2021). The MCP approach is often inappropriate for comparisons among studies because it is sensitive to the tracking regime, tracking duration, and location error; and thus may yield flawed comparisons (Silva et al., 2020). If data are autocorrelated, Traditional Kernel Density Estimators (KDE) generate outputs which are not comparable between studies because KDEs are highly sensitive to changes in the duration and intensity of data collection, as well as kernel parameterisation (Averill-Murray et al., 2020; Silva et al., 2020, Noonan et al., 2019). In a simulation study, Silva et al. (2020) found that consecutive datapoints needed to be spaced multiple months apart in order to satisfy the assumption of independence required for traditional methods (e.g. KDEs). Substantial thought should therefore be put into the choice of home range estimator and the methodological approach before quantifying and comparing home range outputs (Signer & Fieberg, 2021). It is also critical to tie the biology of the target study species to the intended estimators and assess whether the tool is applicable given the nature of the animal's movement processes, the techniques used to collect the data, and the research question asked. Avoiding misestimation is particularly important given that spatial ecology research may inform conversation strategies (Fraser et al., 2018).

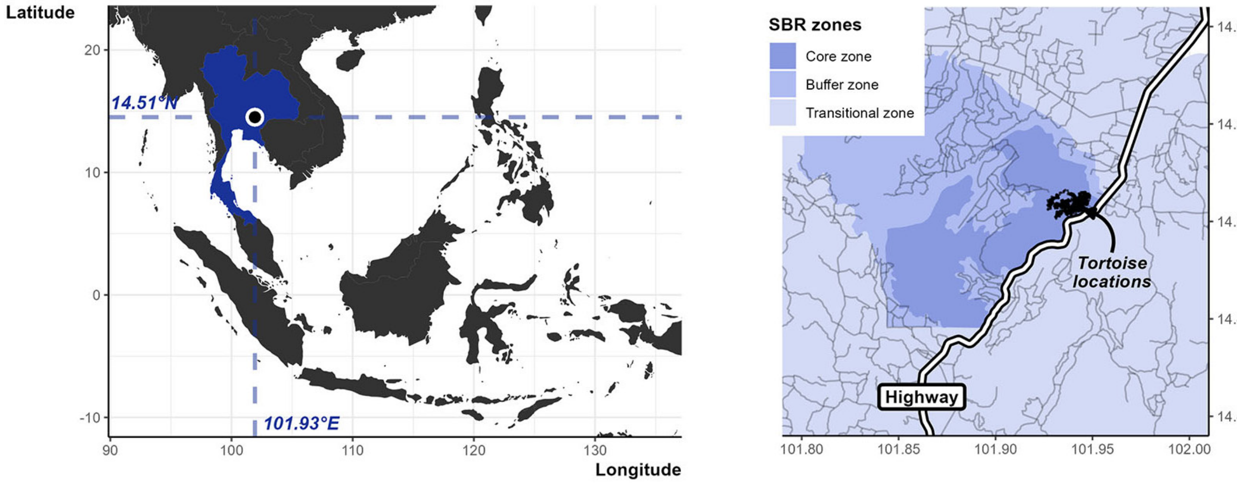

Figure 1. Study location in Thailand. Highlighted in blue is the location of the Sakaerat Biosphere Reserve (SBR) study site: 14.51° N, 101.93° E. The map is north orientated, 0.01° latitude = approx. 1.07 km. Second map shows the SBR in context, with the three zones making up the UNESCO Man & Biosphere Reserve (three levels of blue shading), the highway (black and white line), and minor roads (light grey lines).

Tortoises are long-lived reptiles with a domed bony carapace, capable of moving substantial distances (but typically less than similar sized mammals and considerably slower) over time (Hailey, 1989; Nicholls, 2012). Numerous studies have evaluated tortoise spatial ecology using home ranges (e.g. Yager et al., 2007; McMaster & Downs, 2009; Monadjem et al., 2013; Drabik-Hamshare & Downs, 2017), but most studies have used traditional home range estimators that can impede inter-study comparisons. A review covering 20 years of reptile home range studies found that the reporting of methodological details in the majority of studies were insufficient for meaningful comparisons of home range size (Crane et al., 2021).

In Thailand, the Elongated tortoise *Indotestudo elongata* (Blyth, 1854) is listed as Critically Endangered due to its limited distribution (Rahman et al., 2019). This species is often exploited via illegal markets for local bushmeat, international/regional food, exotic pet, and medicinal trade (Ihlow et al., 2016). At present, we have limited information on home range sizes for *I. elongata*. Studies either lack details concerning range residency, which undermines assertions that the tortoises occupied a stable home range, or the studies use a mix of wild/translocated individuals where the impacts of translocation on home range size or stability are difficult to discern (Tharapoom, 1996; Ihlow et al., 2014; Ihlow et al., 2016). For our study population (Sakaerat Environmental Research Station, Nakhon Ratchasima, Thailand), we previously identified substantial individual overlap of potential movement pathways, a lack of conspecific avoidance or attraction, and potentially evidence of year-round reproductive activity (Ward et al., 2021); but have yet to explore the space requirements of this population occupying a small protected area.

Many factors can influence home range size, such as resource availability (Wasko & Sasa, 2009) or major disturbances such as fire (Drake et al., 2015). Often however, the inherent characteristics of the individual best predict home range size; for example, larger individuals can be expected to require larger areas in order to meet their energetic requirements. Alternatively, reproductively active male tortoises may cover greater distances and move more frequently to maximise access to females. In mating systems where reproductive activity is observed year-round, such as observed for Elongated tortoises (Ward et al., 2021; Ward, 2021), we would expect substantially larger male home ranges than females unless females were also to engage in mate searching behaviour.

Here we investigate home range sizes for the Elongated tortoises in Sakaerat Environmental Research Station, Nakhon Ratchasima, Thailand. To account for the

Correspondence: Colin Strine (strine.conservation@gmail.com)

irregular sampling of our data, we use Autocorrelated Kernel Density Estimators (AKDE) as suggested by Averill-Murray et al. (2020) and Silva et al. (2022). We assess radio-tracked male and female Elongated tortoises movements for range residency (to determine if home range estimation is viable) and provide baseline estimates of home range size. Finally, we attempt to ascertain if individual differences in home range sizes are related to body size or sex.

METHODS

Study site

The study took place within the core area of Sakaerat Biosphere Reserve (SBR), a UNESCO Man and Biosphere site. The site is split into three zones of varying levels of human impact: a transitional zone where agriculture and settlement are permitted, the buffer zone that is predominantly reforestation efforts, and the core zone that consists of primary forest. The protected core area is managed by Sakaerat Environmental Research Station which covers an area of approximately 80 km^2 (Fig. 1). The site primarily consists of seasonal dry evergreen forest and dry dipterocarp forest with patches of mixed deciduous forest and bamboo stands scattered throughout the landscape (Trisurat, 2010). We tracked all tortoises in the core area of the SBR where dry evergreen and dry dipterocarp forest merge to form an ecotone area (Ward et al., 2021). The study site also includes a small single-lane paved access road bisecting the dry dipterocarp forest to the main station grounds which are consistently occupied by staff and visitors but represent less than 1 % of the overall protected area. The protected area of the reserve is adjacent to the major four lane highway that connects Bangkok (south) and Nakhon Ratchasima (north).

Capture and radio-telemetry

We set out to select animals using random encounter surveys, with a total of 10 individuals being sought for a telemetry period of 12 months (n = 10; 2016/17, and n = 8, 2017/18, but one individual appeared in both years). We had great difficulty finding animals during the random surveys, so we supplemented this method with opportunistic findings through road encounters and through other observers who encountered individuals whilst in the reserve conducting other studies. After collecting individuals, we recorded tortoise biometric data (weight, straight carapace length, domed carapace length), took identification photos of the carapace, plastron, and face, and marked the individual with an ID number (M01 - Male 1, F01 - Female 1, etc.) using a white paint pen. After measuring and marking, we attached radio transmitters (Holohil RI-2B 9g glue mount transmitter; Holohil Systems Ltd, 2021; https://www.holohil.com/) using a non-toxic industrial epoxy (Gurit industries Ltd). Using the epoxy resin with a hardening solution (50/50 mix), we coated the underside of the transmitter and placed it firmly to the anterior scute of the animal's carapace above the head and nuchal scute. We then placed globules of the resin mix on the 20 cm long antenna and affixed it to the lateral scutes of the tortoise toward the posterior. The following day we released the animal at the same location they were caught and resumed tracking the individual the day after. We aimed to track 10 individuals, locating each individual once every two days. We undertook tracking in pairs, using one tracking radio receiver. The tracking regime was not always strictly adhered to due to team turnover, weather, and other external factors. During our second telemetry period (2017/18), we focused on female tortoises.

Home range estimates

We used Autocorrelated Kernel Density Estimators (AKDE) to calculate tortoise home ranges (Fleming & Calabrese, 2017; Fleming et al., 2015). The manual collection of radio-tracking data, compared to regimented or automated GPS collection methods, makes AKDE an excellent analysis method to help address unforeseen lapses in data collection (e.g. due to staffing limitations, equipment failure, or inclement weather) particularly with the weighted AKDE function in the ctmm package (Calabrese et al., 2016; Silva et al., 2022; Fleming et al., 2018), which corrects for unrepresentative sampling in time.

We used the ctmm package (Calabrese et al., 2016; Fleming & Calabrese, 2021) to generate variograms for each individual, which visualise the average square distance travelled by the individual within given time lags (termed semi-variance). Using the variograms, we visually determined whether an individual's movements suggested range residency (a flattening of the semi-variance values), which is an assumption required for estimating home ranges with AKDEs (i.e. tortoises tend to remain within their home range areas, and do not exhibit nomadic or migratory behaviours). In further analyses we only included those ranges determined to be stable (n = 14). Via the ctmm package we fit a number of movement models (ctmm's default range of models) using several processes: Ornstein-Uhlenbeck (OU), Ornstein–Uhlenbeck Foraging (OUF), and Independent Identically Distributed (IID). While the IID process is analogous to a traditional KDE approach assuming independent points, the OU process accounts for a central tendency in the animal movement (i.e. range residency or home range). The OUF process is largely similar to OU but also accounts for autocorrelative structures in the velocity of movement. We fit each of these processes in two forms: isotropic and anisotropic, to cover instances where the home range may be more circular or elliptical, respectively.

We fit the movement models (using all of the aforementioned processes) using the perturbative hybrid residual maximum likelihood method (pHREML; Fleming et al., 2019) and used AICc to select the best fitting movement model for each individual. We also recovered the home range crossing time and effective sample sizes (approximately the tracking duration divided by average home range crossing time; Silva et al., 2022). Effective sample size highlights the amount of information available to the home range estimator once redundant location information resulting from autocorrelation is accounted for. Finally, we estimate weighted AKDE home range areas (Silva et al., 2022), selecting the 95 % contour to represent their home range area and using the point estimate of the 95 % contour for comparisons.

Table 1. Tracking summary by individual. ± indicate standard error associated with means

ID	Data points	Start date	End date	Days tracked	Tracking time lag (hour)	Moves
F01	119	16-03-2016	16-03-2017	365	74.24 ± 4.63	94
F02	111	23-03-2016	28-02-2017	342	74.62 ± 8.1	86
F03	121	10-04-2016	19-03-2017	343	68.6 ± 5.19	108
F04	122	08-04-2016	18-03-2017	344	68.23 ± 4.46	115
F05	227	08-04-2016	26-08-2018	870	92.39 ± 25.15	211
F06	98	22-10-2017	28-08-2018	310	76.7 ± 5.04	94
F08	99	22-10-2017	31-08-2018	313	76.65 ± 4.72	95
F09	102	27-10-2017	26-08-2018	303	72 ± 3.17	99
F10	90	21-11-2017	31-08-2018	283	76.31 ± 4.55	76
F12	88	14-11-2017	28-08-2018	287	79.17 ± 5.32	78
F14	89	21-11-2017	01-09-2018	284	77.45 ± 5.27	80
F15	90	22-11-2017	28-08-2018	279	75.24 ± 4.9	64
M01	128	16-03-2016	16-03-2017	365	68.98 ± 4.39	101
M03	129	01-04-2016	19-03-2017	352	66 ± 4.33	84
M04	124	05-04-2016	21-03-2017	350	68.29 ± 5.26	103
M05	130	16-04-2016	19-03-2017	337	62.7 ± 4.26	105
M06	94	03-06-2016	17-03-2017	287	74.06 ± 6.32	81

Comparisons

Due to the small sample size, and lack of a priori hypotheses, we elected to use Bayesian tests of difference to explore how home range size differed between sexes, and in relation to mass (Ellison, 2004). We used the same Bayesian methods to describe differences in mass and carapace length between the sexes. We used a student t-distribution as the response distribution, and the three model formulae were:

1. AKDE 95 % contour point estimate ~ 0 + sex, sigma ~ sex
2. Mass ~ 0 + sex, sigma ~ sex
3. Carapace length ~ 0 + sex, sigma ~ sex

We used weakly informative priors for the three models, based upon means and spreads reported in a previous publication concerning these tortoises (Ward et al., 2021). For a prior describing the home range estimates, we used the previously reported dynamic Brownian Bridge Movement Model (dBBMM) 95 % confidence areas – mean of 26.17 ha, standard deviation (SD) of 33.48 ha (Ward et al., 2021). Although dBBMM estimates do not target home ranges like AKDEs, the way dBBMM confidence areas describe the uncertainty associated with the animal's movement path (calibrated by the animal's movement capacity) can help infer an animal's overall space requirements. We set the carapace length prior to a mean of 37.1 cm and SD of 4.37 cm; and we set the mass prior to a mean of 1.75 kg and SD of 0.5 kg. All three priors were normally distributed with a lower bound limit of 0. For the spread we used two standard deviations to weaken the strength of the prior.

We ran the models with the following setting: 4 chains, 2000 iterations, and 1000 iterations of warmup. Due to convergence issues, we modified two MCMC settings: we increased the adaptive delta to 0.90, and the maximum tree depth to 15.

We also ran a model to explore the relationship between home range area and mass. We included a group effect to account for the possible non-independence of home range sizes within each sex. Our final formula was: AKDE 95 % contour point estimate ~ 1 + Mass + (1|sex). As we had less prior knowledge concerning the home range~mass relationship, we elected to use a very

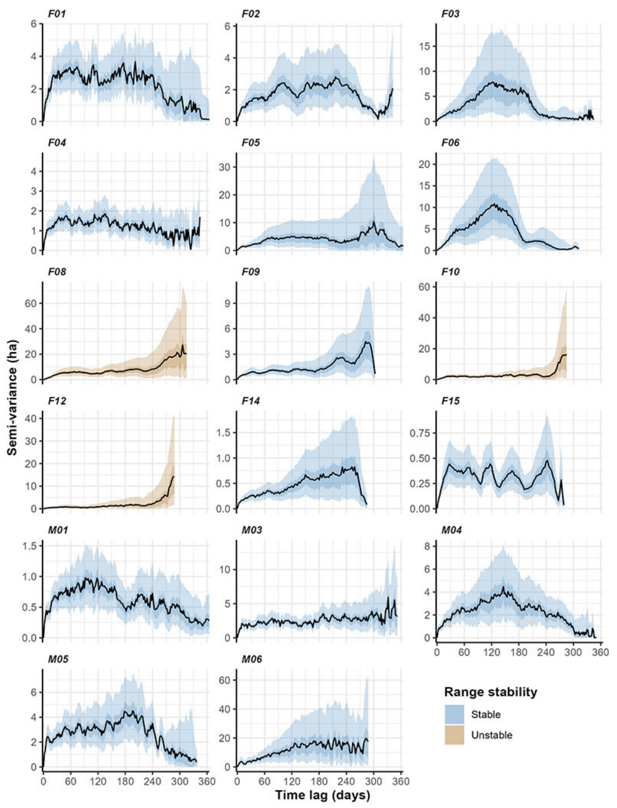

Figure 2. Variograms displaying semi-variance of home range area estimates with x-axis starting at the beginning of each individual's tracking period. Shaded areas display the 50 % (dark shading) and 95 % (light shading) confidence intervals. Blue coloured areas are ranges considered stable; orange coloured areas are ranges considered unstable.

weakly informative prior to constrain the beta coefficient describing the effect of mass (Lemoine, 2019): a Cauchy prior with location 0.1 and scale 5. We ran this model using different settings due to the increased difficulty for the model to satisfactorily converge: 4 chains, 8000 iterations, 2500 warmup iterations, and adaptive delta of 0.95, and a maximum tree depth of 15.

For all models, we used $\hat{R}$ values (~1), trace plots, acf plots, and posterior predictive check plots to check model convergence (see https://osf.io/rxu6f/).

RESULTS

Tracking summary

We tracked 17 individuals (12 females, 5 males) for a mean of 353.76 ± 33.10 days (range 279–870; Fig. S1). We found tortoises frequently relocated between subsequent data points, with a mean of 98.47 ± 7.73 moves (range 64–211) compared to a mean of 115.35 ± 7.94 data points (range 88–227; Table 1). The gap between each data point was approximately 74.25 ± 3.13 hours (range 24–5712; the largest gap was the lag between F05 tracking in 2016/17 and 2017/18; Fig. S2).

Home range

Despite the mean lag time between tracks being over three days (74.25 hours) and high uncertainty associated with semi-variance (e.g. F03 and F06 variograms), we found that 14 out of 17 individuals' ranges appear to be stable – therefore, meeting the range residency assumption required for AKDE home range estimation (Fig. 2). On average the home range crossing time was 17.24 ± 4.37 days, with considerable individual variation (2.71–72.25 days). Males had lower home range crossing times (6.51 ± 1.48 days) than females (21.70 ± 5.73 days). Effective sample size for home range estimation was on average 29.48 ± 4.97, justifying the use of pHREML fitting method and weighting the AKDE areas (Silva et al., 2022). Effective sample size ranged from 3.39 to 75.06, and four individuals had exceptionally low effective sample sizes (<10: F06, F08, F10, F12; Table S2). The low effective sample sizes mirror the lack of stability displayed in the variograms of F08, F10, and F12, and supported our exclusion of these individuals for further analysis.

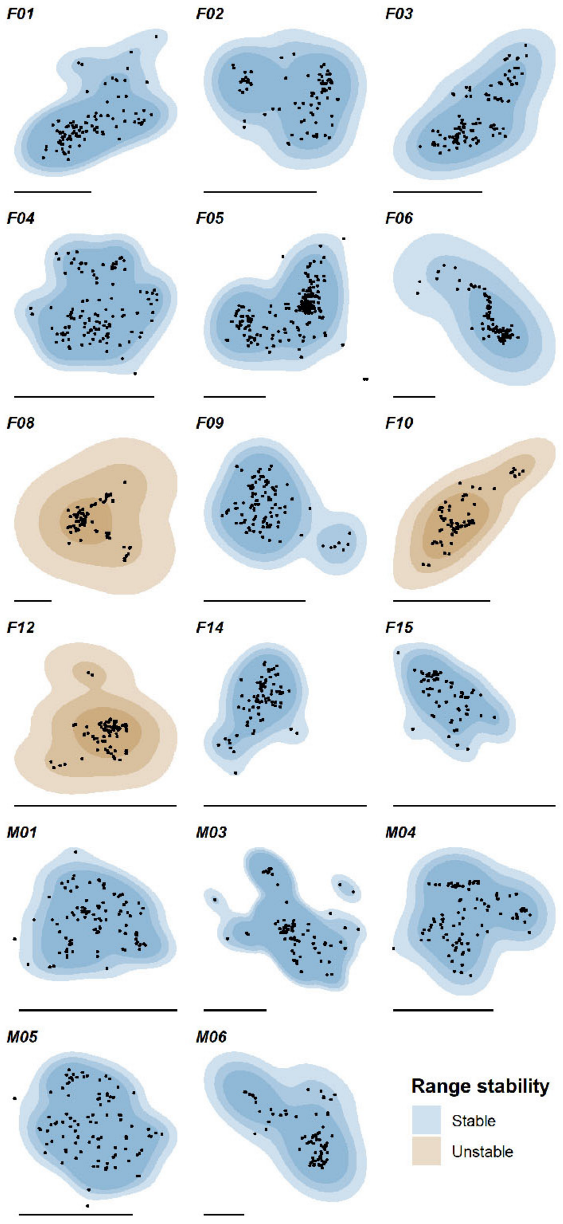

Figure 3. The 95 % contour AKDE area estimates mapped. Upper 95 % confidence level is shown with the darkest shading, the mean point estimate is shown with a medium level of shading, and the lower 95% confidence interval is shown with the lightest shading. Scale bars represent 500 m. Blue coloured areas are ranges considered stable; orange coloured areas are ranges considered unstable.

Table 2. Autocorrelated Kernel Density Estimate (AKDE) results per range resident individual and the movement model used to produce the estimate. Also included are the morphometric data (mass and carapace length). Lower and upper confidence intervals are 95 %. AKDE estimates are in hectares.

ID	Mass (kg)	Carapace length (cm)	AKDE lower CI	AKDE estimate	AKDE upper CI	Movement Model
F01	1.5	37.1	30.31	45.66	64.1	OU anisotropic
F02	1.82	37.2	17.35	25.3	34.72	OU isotropic
F03	1.73	38.6	29.4	48.77	72.97	OU anisotropic
F04	1.72	37.9	16.3	21.61	27.65	OU anisotropic
F05	1.85	37.2	24.75	34.74	46.4	OU anisotropic
F06	1.53	36.2	32.05	86.85	168.49	OU anisotropic
F09	1.67	35.9	11.73	18.81	27.54	OU isotropic
F14	1.25	32.1	4.2	6.56	9.45	OU isotropic
F15	1.6	33	2.99	4.67	6.7	OU anisotropic
M01	2.07	40.3	9.47	12.84	16.72	OU anisotropic
M03	1.84	38.5	31.16	40.94	52.03	OU anisotropic
M04	1.79	38.2	28.07	40.63	55.48	OU anisotropic
M05	1.54	36.8	31.2	39.66	49.12	OU anisotropic
M06	2.05	39.7	61.47	101.12	150.49	OU anisotropic

The 14 individuals who met the range residency assumption suggest a mean 95 % contour home range of 44.81 ± 10.44 ha (varying between the lowest CI of 2.99 ha and a maximum CI 415.36 ha; Fig. 3; Table 2). The top performing movement models selected were either Ornstein-Uhlenbeck (OU) or Ornstein-Uhlenbeck foraging process (OUF), which correspond to correlated positions but uncorrelated velocities, or correlated positions and correlated velocities, respectively (Table S3). Both movement models incorporate restricted space use. Five of the 17 individuals had multiple models within 2 delta AICc (Table S3), but three of these were the non-range resident individuals. The remaining two were F06 where OU AICc was 1.3 lower than OUF, and F09 where both models were OU, and only differed in reflecting more isotropic (more circular) versus anisotropic (more elliptical; delta AICc of 1.5) home ranges. Models that relied on assumptions of Independent Identically Distributed data (IID; i.e., traditional KDE approach) consistently produced the highest dAICc values (Table S2).

Comparisons

The AKDE area estimates did not differ substantially between males and females. Although female ranges were on average 11.09 ± 16.62 ha smaller, the 95 % Highest Density Interval (HDI) suggest that male ranges could be up to 43.66 ha larger, or up to 21.84 ha smaller than female ranges. The wide HDI can be summarised as a 75.23 % chance that males have a larger range (Fig. 4).

Carapace length was considerably more different, with females on average having a 2.34 ± 1.13cm shorter carapace (95 % HDI 0.21–4.60) and a 97.95 % chance that males have a longer carapace. Mass showed a similar pattern. On average females weighed 0.22 ± 0.14 kg less (95 % HDI 0.5 lighter–0.04 heavier), resulting in a 94.63 % chance for males to weigh more (Fig. 4).

The exploration of mass and AKDE area reveal a minor positive relationship between mass and AKDE area (β = 2.88). However, the credible intervals were wide (95 % CRI -19.74–37.05; Fig. 5) and the R^2 values were exceptionally low (Conditional R^2: 0.022, Marginal R^2: 0.001) suggesting the model fails to capture any important variation in home range sizes.

DISCUSSION

We described the home range of a Critically Endangered tortoise species *Indotestudo elongata* using a modern home range estimation method (Autocorrelated Kernel Density Estimators [AKDE]) that is capable of mitigating the biases stemming from low-resolution (and low effective sample size) telemetry data. We found that variograms indicated range residency for 14 of 17

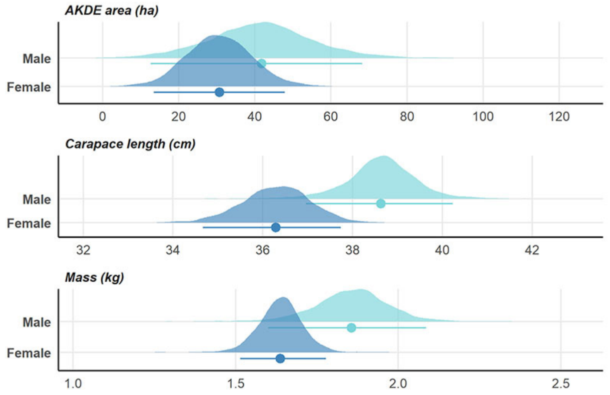

Figure 4. Bayesian comparisons between Female and Male tortoises with stabilised ranges. Point estimates are displayed with 95 % mean Highest Density Continuous Intervals.

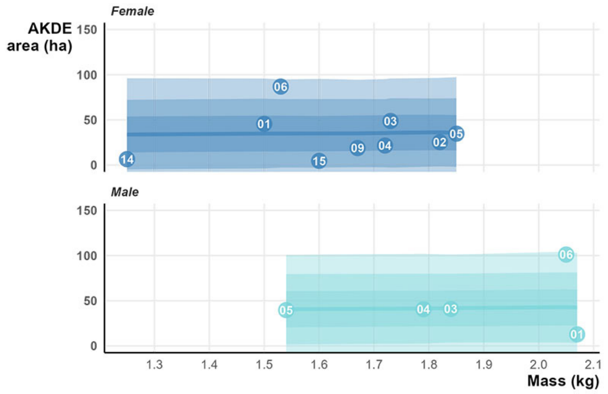

Figure 5. 95 % contour AKDE area in relation to the mass (kg) of female (dark blue) and male (light blue) tortoises. Points are the recorded mass and areas of all individuals with their ID number. Shaded areas indicate the 95 % (lightest shading), 80 % (medium shading), 50 % credible intervals (darkest shading).

tracked tortoises. While Bayesian Regression Models revealed that both mass and carapace length were larger for male tortoises, the AKDE ranges appeared on average only slightly larger for males and are broadly comparable with female tortoise ranges.

Generally, in testudines, there is a slight dimorphism in body size with males being larger than females. This size difference is more apparent in giant tortoise clades, such as the Galapagos and Aldabra tortoises (Chiari et al., 2009; Turnbull et al., 2015), but less apparent in mid-sized forest dwelling species of the tropics including *I.elongata*. Our evidence suggests tracked male individuals were larger than females, which is in line with an earlier study on the same species (Ihlow et al., 2016). However, given the lack of published information on *I. elongata* and due to potential impacts of harvesting, quantifying the size and age ratio (and observable dimorphism from that) within a population remains challenging. In some areas there is no difference between the sizes in adult males or females; however, without accurate age measurement it is impossible to discern whether individuals are still growing adults or at full size (Sriprateep et al., 2013).

As semi-variance represents the average square distance within all given time lags, it ultimately measures the spatial variability in movement behaviour. For short time lags, upward curvature of semi-variance indicates directional persistence. When the semi-variance spikes across intermediate time lags it indicates comparatively faster diffusive behaviour (the animal is covering greater distances), whereas spikes in the furthest/longest time lags typically correlate with migration or range shifting behaviour. While we are unable to pinpoint the cause of the spikes, seasonal variation is a likely candidate. Our study site sees strong seasonal shifts in rainfall that brings forth new vegetative growth, fungal blooms, and *I. elongata* breeding activity (Ihlow et al., 2016, Ward et al., 2021). This species is said to be a water loving testudine, with many anecdotal reports of *I. elongata* frequenting bathing locations and favouring wetlands or riparian habitats where it can be semi-submerged (Ihlow et al., 2016; Ward, 2018). We did not record many areas of such habitats within the current study site, so it is possible that during the heavy rains the tortoises moved into areas of softer clay, shallow pools, or ditches where they could wallow.

As we found an exceptionally low R^2 value while attempting to predict home range sizes based on either tortoise size or sex, we suspect there are alternative, more direct drivers of home range sizes. For example, some individuals spent substantial time along dry stream beds with steep slopes that may have limited movement in certain directions. Other individuals used more complex landscape features; for example, ecotone areas between deciduous dipterocarp forests and dry evergreen forests that could have influenced movements and the resulting home range estimates (Heit et al., 2021). Other factors that may have influenced home range variation – that we were unable to capture with our models and the resolution of our tracking data – could be seasonal shifts in resource availability (e.g. water access, usually provided by depressions along rocks) that might lead tortoises to concentrate movements toward, or cease movements once arriving at, these temporary resources.

Following the suggestions of the STRANGE framework (Webster & Rutz, 2020), we highlight a number of limitations regarding the sampling. The number of animals we could feasibly work with and the absolute (and effective sample size) resulting from our achieved tracking regime limit the inferences we can draw. We conducted this study with a revolving team (of which only two individuals were consistently present) both surveying for study animals and tracking animals. The cryptic camouflage of the carapace in the target species made finding the target species purely via systematic or random surveying unfeasible. We were able to supplement these randomly encountered individuals with animals encountered on the main access road to Sakaerat Environmental Research Station or brought to us by personnel in the area. However, with a limited team and up to 10 simultaneously tracked animals we were limited in the tracking interval we could logistically implement. The initial goal of once-per-two-day tracking became more difficult over time as a result of team turnover. The training period required for new team members ultimately resulted in a team with the capacity to track three individuals per day, thereby limiting each tortoise to three tracks per week. With the inconsistencies of trackers and the occasional absences of members through sickness, conferences or vacations, we produced an inconsistent tracking regime (much like what typically occurs in other radio-tracking studies). Rainy seasons further introduced heterogeneity into our tracking regime, as we were forced to alter protocols to both protect our equipment and keep up with highly mobile animals post rain. The radio-tracking receivers, antennas and accessories are all highly susceptible to water damage, and high humidity causes interference with the radio signal – the latter led to lost animals on numerous occasions. These inconsistencies violate the assumptions of traditional Kernel Density Estimators and make Minimum Convex Polygons fraught with difficulty (due to lack of comparability with other studies that had consistent or differing tracking regimes).

Even with tracking inconsistencies, we were able to yield biologically useful results for 14 of 17 individuals using AKDEs and bias-mitigating measures (pHREML fitting and area weighting). Thereby, providing further evidence that barriers caused by logistic constraints may be overcome when the resulting heterogeneity in sampling are accounted for appropriately. The home range estimates we provide could be used to inform the space requirements for *I. elongata* in protected areas comparable to the Sakaerat Biosphere Reserve, while also providing useful priors for designing spatially explicit capture recapture studies capable of robust estimates of *I. elongata* populations.

ACKNOWLEDGEMENTS

We thank the Suranaree University of Technology (School of Biology, and the Institute of Research and Development) for providing the resources required to undertake this research. We thank Sakaerat Environmental Research Station (SERS) and Thailand Institute of Scientific and Technological Research (TISTR) for logistic support throughout the study and permission for site access. This work was partially funded by the Center of Advanced Systems Understanding (CASUS), which is financed by Germany's Federal Ministry of Education and Research (BMBF) and by the Saxon Ministry for Science, Culture and Tourism (SMWK) with tax funds on the basis of the budget approved by the Saxon State Parliament. We thank numerous simultaneous research teams including the Sakaerat Naja Project, King Mongkut's University of Technology, Thonburi Conservation Ecology Group, Sakaerat Conservation and Snake Education Team as well as SERS staff and visitors for helping to detect additional animals ad hoc to add to the study. We thank Anchalee Awophol for assistance in obtaining research permits for this project. We also thank both the National Research Council of Thailand (NRCT) and the Department of National Parks Thailand for permission to work with this species (Permit Number: 0002/3589). We finally thank Rachel George, Jonathan Clegg, MJ Suriyamongkol, Mark Read, Nate Quarrel, Jizel Miles, Matt Macpherson, Dani Mateo and George Wykes for their assistance in maintaining this project over a consistent two-year period through hard field days and impressive resolve when tracking wild tortoises.

Data availability

Data is available via Movebank (Study ID: 1128208874, originally published as part of Ward et al., 2021; https://www.movebank.org/; Kranstauber et al., 2011; Wikelski et al., 2021), and has been additionally published alongside analysis code and model outputs on the Open Science Framework (https://osf.io/rxu6f/). We conducted all analysis and visualisation using R v.4.0.3 (R Core Team, 2020) via RStudio v.1.4.1103 (R Studio Team, 2020). We used the R packages listed in Table S1 (with citations auto-generated using the grateful v.0.0.3 package; Rodríguez-Sánchez & Hutchins, 2020).

Funding

National Geographic and British Chelonia Group supported field work for this project.

Author contributions

Conceptualisation - YM, MW, CTS; Methodology - YM, MW, CTS, BMM, IS; Formal analysis - BMM, IS; Visualisation - BMM; Investigation - YM, MW; Resources - TA, SW; Writing - original draft - CTS, BMM, MW; Writing - review and editing - YM, MW, CTS, BMM, IS, TA, SW; Supervision - TA, SW; Funding acquisition - YM, MW

Competing interests

The authors declare no competing interests.

REFERENCES

Averill-Murray, R., Fleming, C. & Riedle, J. (2020). Reptile home ranges revisited: a case study of space use of Sonoran Desert Tortoises (*Gopherus morafkai*). *Herpetological Conservation and Biology*, 15, 253–271.

Breininger, D., Bolt, R., Legare, M., Drese, J. & Stolen, E. (2011). Factors Influencing Home-Range Sizes of Eastern Indigo Snakes in Central Florida. *Journal of Herpetology,* 45, 484–490. doi: 10.2307/41415322.

Burt, W.H. (1943). Territoriality and Home Range Concepts as Applied to Mammals. *Journal of Mammalogy,* 24, 346–352. doi: 10.2307/1374834.

Calabrese, J.M., Fleming, C.H. & Gurarie, E. (2016). Ctmm: an R Package for Analyzing Animal Relocation Data As a Continuous-Time Stochastic Process. Methods in *Ecology and Evolution,* 7, 1124–1132. doi: 10.1111/2041-210X.12559.

Chiari, Y., Hyseni, C., Fritts, T.H., Glaberman, S., Marquez, C., Gibbs, J.P., Claude, J. & Caccone, A. (2009). Morphometrics parallel genetics in a newly discovered and endangered taxon of Galápagos tortoise. *PLoS One*, 4(7), p.e 6272. doi: 10.1371/journal.pone.0006272.

Crane, M., Silva, I., Marshall, B.M. & Strine, C.T. (2021). Lots of movement, little progress: a review of reptile home range literature. *PeerJ9,* e11742. doi: 10.7717/peerj.11742.

Di Franco, A., Plass-Johnson, J., Di Lorenzo, M., Meola, B., Claudet, J., Gaines, S., García-Charton, J., Giakoumi, S, Grorud-Colvert, K., Hackradt, C.W. et al. (2018). Linking home ranges to protected area size: The case study of the Mediterranean Sea. *Biological Conservation,* 221. doi: 10.1016/j.biocon.2018.03.012.

Drabik-Hamshare, M. & Downs, C.T. (2017). Aspects of the home range ecology of the leopard tortoise in the semi-arid central Karoo: An area threatened with fracking. *Journal of Arid Environments,* 144, 31–41. doi: 10.1016/j.jaridenv.2017.04.001.

Drake, K.K., Esque, T.C., Nussear, K.E., Defalco, L.A., Scoles-Sciulla, S.J., Modlin, A.T. & Medica, P.A. (2015). Desert tortoise use of burned habitat in the Eastern Mojave desert. *The Journal of Wildlife Management,* 79, 618–629. doi: 10.1002/jwmg.874.

Ellison, A.M. (2004). Bayesian inference in ecology. *Ecology Letters,* 7, 509–520. doi: 10.1111/j.1461-0248.2004.00603.x.

Fauvelle, C., Diepstraten, R. & Jessen, T. (2017). A meta-analysis of home range studies in the context of trophic levels: Implications for policy-based conservation. *PLOS ONE,* 12:e0173361. doi: 10.1371/journal.pone.0173361.

Fieberg, J. & Kochanny, C.O. (2005). Quantifying Home-Range Overlap: The Importance of the Utilization Distribution. *The Journal of Wildlife Management,* 69, 1346–1359. doi: 10.2193/0022-541X(2005)69[1346:QHOTIO]2.0.CO;2.

Fleming, C.H. & Calabrese, J.M. (2017). A new kernel density estimator for accurate home-range and species-range area estimation. *Methods in Ecology and Evolution,* 8, 571–579. doi: 10.1111/2041-210X.12673.

Fleming, C.H. & Calabrese, J.M. (2021). Ctmm: Continuous-Time Movement Modeling. https://CRAN.R-project.org/package=ctmm.

Fleming, C.H., Fagan, W.F., Mueller, T., Olson, K.A., Leimgruber, P. & Calabrese, J.M. (2015). Rigorous home range estimation with movement data: A new autocorrelated kernel density estimator. *Ecology,* 96, 1182–1188.

Fleming, C.H., Sheldon, D., Fagan, W.F., Leimgruber, P., Mueller, T., Nandintsetseg, D., Noonan, M.J., Olson, K.A., Setyawan, E., Sianipar, A. & Calabrese, J.M. (2018). Correcting for missing and irregular data in home-range estimation. *Ecological Applications,* 28, 1003–1010. doi: 10.1002/eap.1704.

Fleming, C.H., Noonan, M.J., Medici, E.P. & Calabrese, J.M. (2019). Overcoming the challenge of small effective sample sizes in home-range estimation. *Methods in Ecology and Evolution,* 10, 1679–1689. doi: 10.1111/2041-210X.13270.

Fraser, K.C., Davies, K.T., Davy, C.M., Ford, A.T., Flockhart, D.T.T. & Martins, E.G. (2018). Tracking the conservation promise of movement ecology. *Frontiers in Ecology and Evolution*, 6(October), 150. doi: 10.3389/FEVO.2018.00150

Hailey, A. (1989). How far do animals move? Routine movements in a tortoise. *Canadian Journal of Zoology,* 67, 208–215. doi: 10.1139/z89-028.

Heit, D., Ortiz-Calo, W. & Montgomery, R. (2021). Landscape complexity persists as a critical source of bias in terrestrial animal home range estimation. *Ecology*. doi: 10.1002/ecy.3427.

Holohil Systems Ltd. 2021. Transmitters. 112 John Cavanaugh Drive, Carp, Ontario. Accessed 2021-010-24. https://www.holohil.com/transmitters/.

Houser, A.M., Somers, M.J. & Boast, L.K. (2009). Home range use of free-ranging cheetah on farm and conservation land in Botswana: research article. *South African Journal of Wildlife Research* - 24-month delayed open access 39, 11–22. doi: 10.10520/EJC117311.

Ihlow, F., Rödder, D., Bochynek, T., Sothanin, S., Handschuh, M. & Böhme, W. (2014). Reinforcement as a conservation tool-assessing site fidelity and movement of the endangered elongated tortoise *Indotestudo elongata* (Blyth, 1854). *Journal of Natural History*, 48(39-40), 2473-85. doi: 10.1080/00222933.2014.925595.

Ihlow, F., Dawson, J., Hartmann, T. & Som, S. (2016). *Indotestudo elongata* (Blyth, 1854) – Elongated Tortoise, Yellow-headed Tortoise, Yellow Tortoise. *Chelonian Conservation and Biology,* 5. doi: 10.3854/crm.5.096.elongata.v1.2016.

Laver, P.N. & Kelly, M.J. (2008). A Critical Review of Home Range Studies. *The Journal of Wildlife Management,* 72, 290–298. doi: 10.2193/2005-589.

Lemoine, N.P. (2019). Moving beyond noninformative priors: why and how to choose weakly informative priors in Bayesian analyses. *Oikos*:oik.05985. doi: 10.1111/oik.05985.

Linnell, J., Andersen, R., Kvam, T., Andrén, H., Liberg, O., Odden, J. & Moa, P. (2001). Home Range Size and Choice of Management Strategy for Lynx in Scandinavia. *Environmental Management,* 27, 869–879. doi: 10.1007/s002670010195.

McMaster, M.K. & Downs, C.T. (2009). Home Range and Daily Movement of Leopard Tortoises (*Stigmochelys pardalis*) in the Nama-Karoo, South Africa. *Journal of Herpetology,* 43, 561–569.

Mitchell, M.S. & Powell, R.A. (2004). A mechanistic home range model for optimal use of spatially distributed resources. *Ecological Modelling,* 177, 209–232. doi: 10.1016/j.ecolmodel.2004.01.015.

Mitchell, M.S. & Powell, R.A. (2012). Foraging optimally for home ranges. *Journal of Mammalogy,* 93, 917–928. doi: 10.1644/11-MAMM-S-157.1.

Monadjem, A., McCleery, R.A. & Collier, B.A. (2013). Activity and Movement Patterns of the Tortoise *Stigmochelys pardalis* in a Subtropical Savanna. *Journal of Herpetology,* 47, 237–242. doi: 10.1670/12-070.

Nicholls, H. (2012). The legacy of Lonesome George. *Nature,* 487, 279–280. doi: 10.1038/487279a.

Noonan, M.J., Tucker, M.A., Fleming, C.H., Akre, T.S., Alberts, S.C., Ali, A.H., Altmann, J., Antunes, P.C., Belant, J.L., Beyer, D. et al. (2019). A comprehensive analysis of autocorrelation and bias in home range estimation. *Ecological Monographs,* 89, e01344. doi: 10.1002/ecm.1344.

Powell, R.A. & Mitchell, M.S. (2012). What is a home range? *Journal of Mammalogy,* 93, 948–958. doi: 10.1644/11-MAMM-S-177.1.

Rahman, S., Platt, K., Das, I., Choudhury, B.C., Ahmed, M.F., Cota, M., McCormack, T., Timmins, R.J. & Singh, S. (2019). *Indotestudo elongata* (errata version published in 2019). *The IUCN Red List of Threatened Species,* 2019, e.T10824A152051190. doi: 10.2305/IUCN.UK.2019-1.RLTS.T10824A152051190.en. Downloaded on 01 November 2021.

R Core Team. (2020). R: *A language and environment for statistical computing*. Vienna, Austria: R Foundation for Statistical Computing. https://www.R-project.org/.

R Studio Team. (2020). RStudio: *Integrated Development Environment for R*. Boston, MA: RStudio, Inc.

Rodríguez-Sánchez, F. & Hutchins, S.D. (2020). grateful: Facilitate citation of R packages.

Signer, J. & Fieberg, J.R. (2021). A fresh look at an old concept: home-range estimation in a tidy world. *PeerJ,* 9, e11031. doi: 10.7717/peerj.11031.

Silva, I., Crane, M., Marshall, B.M. & Strine, C.T. (2020). Reptiles on the wrong track? Moving beyond traditional estimators with dynamic Brownian Bridge Movement Models. *Movement Ecology,* 8, 43. doi: 10.1186/s40462-020-00229-3.

Silva, I., Fleming, C.H., Noonan, M.J., Alston, J., Folta, C., Fagan, W.F. & Calabrese, J.M. (2022). Autocorrelation-informed home range estimation: A review and practical guide. *Methods in Ecology and Evolution*, 13(3), 534–544. doi: 10.1111/2041-210X.13786.

Sriprateep, K., Aranyavalai, V., Aowphol, A. & Thirakhupt, K. (2013). Population structure and reproduction of the elongated tortoise *Indotestudo elongata* (Blyth, 1853) at Ban Kok Village, Northeastern Thailand. *Tropical Natural History*, 13(1), 21–37.

Tharapoom, K. (1996). Radio-Telemetry study of home range size and activities of elongated tortoise *Indotestudo elongata* (Blyth, 1853) at Huai Kha Khaeng Wildlife Sanctuary. Masters Thesis. Department of Biology, Graduate School, Chulalong University.

Trisurat, Y. (2010). Land use and forested landscape changes at Sakaerat Environmental Research Station in Nakhon Ratchasima Province, Thailand. *Ekologia,* 29, 99–109. doi: 10.4149/ekol_2010_01_99.

Turnbull, L.A., Ozgul, A., Accouche, W., Baxter, R., ChongSeng, L., Currie, J.C., Doak, N., Hansen, D.M., Pistorius, P., Richards, H. & van de Crommenacker, J. (2015). Persistence of distinctive morphotypes in the native range of the CITES-listed Aldabra giant tortoise. *Ecology and evolution*, 5(23), pp. 5499–5508. doi: 10.1002/ece3.1764

Viggers, K.L. & Hearn, J.P. (2005). The kangaroo conundrum: home range studies and implications for land management. *Journal of Applied Ecology,* 42, 99–107. doi: 10.1111/j.1365-2664.2005.01001.x.

Ward, M. (2018). *Indotestudo elongata* (Elongated Tortoise). Unusual mortality. *Herpetological Review,* 49, 108–109.

Ward, M. (2021). Spatial ecology and habitat use of the critically endangered Elongated Tortoises (*Indotestudo elongata*) in the Sakaerat Biosphere Reserve. Masters Thesis. Department of Science, School of Biology, Suranaree University of Technology Thailand.

Ward, M., Marshall, B.M., Hodges, C.W., Montano, Y., Artchawakom, T., Waengsothorn, S. & Strine, C.T. (2021). Nonchalant neighbors: Space use and overlap of the critically endangered Elongated Tortoise. *Biotropica*, btp.12981. doi: 10.1111/btp.12981.

Wasko, D.K. & Sasa, M. (2009). Activity Patterns of a Neotropical Ambush Predator: Spatial Ecology of the Fer-de-lance (Bothrops asper, Serpentes: Viperidae) in Costa Rica. *Biotropica,* 41, 241–249. doi: 10.1111/j.1744-7429.2008.00464.x.

Webster, M.M. & Rutz, C. (2020). How STRANGE are your study animals? *Nature*, 582(7812), pp. 337–340. doi: 10.1038/d41586-020-01751-5.

Wikelski, M., Davidson, S.C. & Kays, R. (2021). Movebank: archive, analysis and sharing of animal movement data. Hosted by the Max Planck Institute of Animal Behavior. www.movebank.org, accessed on 2021-11-18.

Worton, B.J. (1989). Kernel Methods for Estimating the Utilization Distribution in Home-Range Studies. *Ecology,* 70, 164–168. doi: 10.2307/1938423.

Xirouchakis, S.M., Grivas, C., Andreou, G. & Georgopoulou, E. (2021). Home range size, space use and resource selection of griffon vultures in an insular environment. *Journal of Zoology,* 314, 116–131. doi: 10.1111/jzo.12868.

Yager, L.Y., Hinderliter, M.G., Heise, C.D. & Epperson, D.M. (2007). Gopher Tortoise Response to Habitat Management by Prescribed Burning. *Journal of Wildlife Management,* 71, 428–434. doi: 10.2193/2006-337.

Accepted: 26 May 2022

Please note that the Supplementary Material for this article is available online via the Herpetological Journal website: https://thebhs.org/publications/the-herpetological-journal/volume-32-number-3-july-2022

Herpetological Journal

FULL PAPER

https://doi.org/10.33256/32.3.130141

Published by the British Herpetological Society

Temporal partitioning of hatching, maturation, and surface activity by reptiles in Florida longleaf pine-wiregrass sandhills

Sky T. Button[1], Cathryn H. Greenberg[2] & James D. Austin[1]

[1]Department of Wildlife Ecology and Conservation, University of Florida, Gainesville, Florida 32611, USA
[2]USDA Forest Service, Southern Research Station, Bent Creek Experimental Forest, 1577 Brevard Road, Asheville, North Carolina 28806, USA

Temporal partitioning of life history traits among syntopic reptiles can facilitate co-occurrence, but may be influenced by environmental factors and evolutionary history. We used 24 years of continuous capture data in the Florida sandhills to evaluate the timing and duration of hatching, maturation and/or surface activity for ten reptile species, spanning multiple clutch strategies, taxonomic relationships, and habits. We hypothesised: i) species would differ in seasonal timing of hatching and maturation; ii) hatching and maturation periods would be more seasonally-synchronised in fossorial than terrestrial or semi-aquatic reptiles; iii) monthly and annual temperature anomalies would be positively related to hatching, maturation, and surface activity anomalies, and iv) groupings of reptiles by clutch strategy, taxonomic relationship, and habit, would explain more variation in the timing and duration of hatching and maturation than species alone. Seasonal timing of response variables varied widely among species. Hatching peaked for > 1 species during most calendar months. Maturation and surface activity periods ranged from aseasonal to highly-seasonal among species. Hatching began 1.5 months earlier and was more prolonged for terrestrial than fossorial species overall. Hatching peaked in early to mid-summer for terrestrial and fossorial species, and winter for the semi-aquatic *Kinosternon subrubrum*. Terrestrial and fossorial species did not differ in average timing, duration, or overlap of maturation periods; semi-aquatic *Liodytes pygaea* matured more consistently across all seasons than other species. Monthly temperature anomalies were negatively correlated with monthly maturation for *Plestiodon egregius*. Annual temperature and precipitation anomalies were related to annual hatching, maturation, and surface activity trends for several species. Taxonomic relationship, habit, and species explained some variation in hatching and maturation timing and duration. Our results illustrate the influence of environment and evolutionary relationships on the timing of important life history traits.

Keywords: Age class, Drift fence, Community, Interspecific, Life history

INTRODUCTION

Niche partitioning and life history traits are major factors regulating species coexistence.Several studies demonstrate how syntopic reptile species partition microhabitats for thermoregulation (Tadevosyan, 2007; Buckley & Jetz, 2010), and food (Schoener, 1968; Pianka, 1973; Lelièvre et al., 2012), but temporal partitioning of hatching and maturation has received little attention (Post, 2019). Information on ontogenetic life history traits and their variation across syntopic reptile species is needed to better understand how they coexist. For example, taxonomic relationships related to physiology and ecological habit (fossorial, terrestrial, or semi-aquatic) may influence temporal partitioning of hatching and maturation by affecting thermal preferences (Brattstrom, 1965; Clusella-Trulas & Lee, 2014), and dependence on warm temperatures to accelerate embryonic development and juvenile growth rates (Sinervo & Adolph, 1989; Van Damme et al., 1992; Georges et al., 2005).

Habit modifies exposure to environmental conditions (e.g. temperature) and may, in turn, influence the timing of life history traits. For example, subterranean temperature is relatively constant year-round compared to surface temperature (Burda et al., 2007; Pike & Mitchell, 2013), potentially allowing for greater seasonal synchronisation of hatching and maturation by fossorial than terrestrial reptile species. In addition, species inhabiting subtropical regions (e.g. central Florida) may vary more widely in their timing of hatching, maturation, and surface activity than those limited by cold winter temperatures in temperate regions. Conversely, the paucity of cold weather adaptations found in many subtropical reptiles (Clusella-Trulas & Lee, 2014) may increase the sensitivity of hatching, maturation, or surface activity periods to monthly or annual temperature anomalies.

We used 24 years of continuous trapping data from longleaf pine-wiregrass sandhills to examine the temporal partitioning of hatching, maturation and surface activity among 10 reptile species within three categories representing fossorial, terrestrial and semi-aquatic habits. Florida sandhills are an ideal ecosystem to assess patterns of temporal partitioning among reptiles bound by similar ecological conditions, as reptile diversity is high (Dodd, 1992; Greenberg et al., 1994; Pearlstine et al., 2002; Means et al., 2004), and a warm climate offers a long 'season' for potential hatching, maturation, and surface activity (Myers, 1990; Button et al., 2019). We hypothesised:

i) reptile species would differ in their seasonal timing of hatching, maturation, and surface activity;
ii) hatching and maturation periods would be more seasonally synchronised in fossorial than terrestrial or semi-aquatic reptiles;
iii) monthly and annual temperature anomalies would be positively correlated with monthly anomalies in reptile hatching, maturation, and surface activity, and
iv) clutch strategy, taxonomic relationship, and habit would provide more information about hatching and maturation periods than species alone.

Correspondence: Sky Button (sky.button@wsu.edu)

METHODS

Study area

We captured reptiles adjacent to eight small (0.10–0.37 ha), ephemeral, groundwater-driven sinkhole ponds, embedded within xeric longleaf pine *Pinus palustris* and wiregrass *Aristida sp.* uplands of the Floridan Aquifer System region, in Ocala National Forest, Marion County, Florida (Greenberg et al., 2015). Six ponds were located within ~0.7 km of one another; two were ~9.5 km south of the others (Fig. S1). Average monthly temperatures (February 1997–December 2017) ranged from 13.5 ˚C in January to 28.6 ˚C in August (Fig. S2). Average annual precipitation (1995–2017) was 140.7 cm, with more than half occurring during late spring and summer. Wetland depths were generally highest in winter and lowest in summer because of rainfall patterns, groundwater recharge (Greenberg et al., 2015; 2017), and low evapotranspiration in winter (Knowles et al., 2002). The upland forest matrix surrounding the study ponds consisted mostly of savanna-like sandhills with wiregrass-forb ground cover and widely-spaced longleaf pine trees with patches of hardwood trees and sand pine *Pinus clausa*. Common soils were well-to-excessively drained Entisols with < 5 % silt plus clay in the upper profile, classified in the hyperthermic, uncoated families of Spodic (Paola series) and Typic (Astatula series) Quartzipsamments (Aydelott et al., 1975). Study pond elevations ranged from 4–26 m.

Field methods

We installed 7.6 m-long drift fences spaced 7.6 m apart around the perimeter of each pond such that 50 % of each pond was fenced. We installed pitfall traps (19-litre buckets) on the inside and outside of each fence at both ends (four per fence), and positioned a double- or single-ended funnel trap (one each per fence) at its midpoint on opposite sides. We embedded a PVC pipe (5-cm diameter; ~1.4 m height) at one end of each fence to attract anoles. We placed a sponge in each pitfall trap and moistened as needed during trap checks to reduce the likelihood of animal desiccation. We checked traps three times weekly from 1 February 1994–31 December 2017, or sometimes less frequently (one to two times weekly) during cold months (November–early March), when capture rates were low. We identified, measured snout-vent length (SVL), and marked all captured individuals using toe- (lizards) or scale-clipping (snakes), or scute-notching (turtles). We used a max-min thermometer to measure maximum and minimum air temperature weekly, and used a rain gauge to measure precipitation approximately three times weekly (February 1997–December 2017).

Study species and categories

We focused our analyses on ten commonly captured species representing three ecological habit categories: terrestrial (Southeastern five-lined skink *Plestiodonin expectatus*, six-lined racerunner *Aspidoscelis sexlineata,* green anole *Anolis carolinensis*, Florida scrub lizard *Sceloporus woodi*, Eastern garter snake *Thamnophis sirtalis*); fossorial (mole skink *P. egregius*, little brown skink *Scincella lateralis,* Florida crowned snake *Tantilla relicta*); and semi-aquatic (Eastern mud turtle *Kinosternum subrubrum*, black swamp snake *Lyodytes pygaea*). These species spanned five major clades, including Testudines (*K. subrubrum)*; Scincomorpha (*P. egregius*, *P. inexpectatus*, *S. lateralis)*; Laterata (*A. sexlineata)*; Iguanomorpha (*A. carolinensis*, *S. woodi)*; and Serpentes (*L. pygaea*, *T. relicta*, *T. sirtalis)*. Four species (*P. egregius, P. inexpectatus, L. pygaea, T. relicta*) are known to produce one clutch per year, while six (*K. subrubrum, S. lateralis, A. sexlineata, A. carolinensis, S. woodi, T. sirtalis*) can produce multiple clutches per year.

Adjustments for flooding

We used only first captures (i.e. no recaptures) in all data analyses. We divided each year into 12, month-long periods to assess seasonal timing of hatching and maturation for each species, pooling data from all ponds. Trap closures due to infrequent flooding necessitated adjustments to capture data during some months at some ponds. We considered a pond to be 'closed' during a given month if flooding reduced its number of monthly trap-nights by > 50 %. Data were adjusted by dividing total monthly first-captures (by age class and species) by the proportion of 'open' ponds. For example, if we captured 100 adults of a species in October 2008, but only five of eight ponds were 'open', the number of captures was adjusted to 160 (100/0.625). We also grouped capture data by year for annual-scale analyses of hatching, maturation, and surface activity, correcting for flood-related trap closures as described above. Flood-related closures that reduced monthly trap-nights at a pond by > 50 % were rare (mean ± SE = 9 % ± 2 %; range = 4–24 % of months) and occurred most often during September–December.

Age class delineation

We assigned individuals to a hatchling, intermediate juvenile, maturing juvenile, or adult age class based on SVL cutoffs derived from published literature (Palmer & Braswell, 1995; Conant & Collins, 1998) and professional judgement (Table 1). We defined 'hatchlings' as individuals with SVLs less than the sum of the minimum SVL plus 15 % of the range of SVLs recorded for all captures of the same species. For example, if SVLs of a given species ranged 10–110 mm (range = 100 mm), individuals < 25 mm (10 + 100*0.15) SVL were classified as 'hatchlings' (Table 1). 'Maturing juveniles' comprised individuals within +10 %

Table 1. Age-class size (snout-vent length) cutoffs and ecological groupings (clutch strategy, taxonomic relationship, and habit) used in analyses, and total (February 1994–December 2017) number of first-captured hatchling, intermediate juvenile, maturing juvenile, and adult age classes for 10 reptile study species, Ocala National Forest, Marion County, Florida[1]. S = single-clutch and M = multi-clutch.

				Hatchlings		Intermediate Juveniles		Maturing Juveniles		Adults		Total
Species[2]	**Clutch Strategy**	**Taxonomic Category**	**Habit[3]**	**Size (mm)**	**n**	**Size (mm)**	**n**	**Size (mm)**	**n**	**Size (mm)**	**n**	**n**
P. egregius	S	Scincomorpha	F	< 23.7	39	23.7–35.0	144	35.1–42.9	185	> 42.9	206	574
S. lateralis	M	Scincomorpha	F	< 18.1	90	18.1–25.1	305	25.2–30.8	346	> 30.8	1,596	2,337
T. relicta	S	Serpentes	F	< 64.8	8	64.8–108.8	99	108.9–133.1	443	> 133.1	529	1,079
Habit Subtotal			F		137		548		974		2,331	3,990
K. subrubrum	M	Testudines	SA	< 33.6	270	33.6–48.9	10	49.0–59.9	13	> 59.9	196	489
L. pygaea	S	Serpentes	SA	< 103.2	13	103.2–188.9	194	189.0–231.0	235	> 231	321	763
Habit Subtotal			SA		283		204		248		517	1,252
A. carolinensis	M	Iguanomorpha	T	< 24.7	18	24.7–32.3	158	32.4–39.6	327	> 39.6	912	1,415
A. sexlineata	M	Laterata	T	< 30.9	135	30.9–45.8	1,152	45.9–56.1	1,134	> 56.1	1,334	3,755
P. inexpectatus	S	Scincomorpha	T	< 30.5	272	30.5–49.9	908	50.0–61.1	354	> 61.1	368	1,902
S. woodi	M	Iguanomorpha	T	< 27.1	13	27.1–37.2	48	37.3–45.4	114	> 45.4	104	279
T. sirtalis	M	Serpentes	T	< 191.9	82	191.9–259.9	78	260.0–317.6	58	> 317.6	92	310
Habit Subtotal			T		520		2,344		1,987		2,810	7,661
Total					940		3,096		3,209		5,658	12,903

[1] Due to low sample sizes we omitted *K. subrubrum* from maturation analyses, and omitted *A. carolinensis, L. pygaea, S. woodi*, and *T. relicta* from hatchling analyses; intermediate juveniles were omitted from both hatchling and maturation analyses.
[2] *P. egregrius = Plestiodon egregius* (mole skink), *S. lateralis = Scincella lateralis* (little brown skink), *T. relicta = Tantilla relicta* (Florida crowned snake), *K. subrubrum = Kinosternon subrubrum* (eastern mud turtle), *L. pygaea = Liodytes pygaea* (black swamp snake), *A. carolinensis = Anolis carolinensis* (green anole), *A. sexlineata = Aspidoscelis sexlineata* (six-lined racerunner), *P. inexpectatus = Plestiodonin expectatus* (southeastern five-lined skink), *S. woodi = Sceloporus woodi* (Florida scrub lizard), and *T. sirtalis = Thamnophis sirtalis* (common gartersnake).
[3] F = fossorial, SA = semi-aquatic, and T = terrestrial.

of an a priori juvenile-adult SVL cutoff. 'Adults' were all individuals larger than maturing juveniles. We defined 'intermediate juveniles' as individuals with SVLs falling above the upper size cutoff for hatchlings but below the lower size cutoff for maturing juveniles, defined above and in Table 1.

Data formatting

We calculated monthly anomalies in temperature and precipitation, and in hatching, maturation, and surface activity to assess their possible correlations. We treated first captures of all age classes except hatchlings (which often diverge in their responses to temperature/precipitation) as a proxy for surface activity. We calculated monthly anomalies of minimum, average, and maximum temperatures, or precipitation, by subtracting average monthly minimum, average, and maximum temperatures, or precipitation (n = 23 for January, n = 24 for all other months), from year-specific monthly temperatures or precipitation. For example, if the annual mean maximum July temperature was 40 ˚C and the maximum July 2010 temperature was 38 ˚C, the anomaly for maximum temperature in July 2010 was -2 ˚C. Similarly, we calculated monthly anomalies in the timing of hatching, maturation, or surface activity for each species by subtracting average monthly estimates of hatching, maturation, or surface activity from estimates within each specific month of the study.

Data analyses: timing of hatching

We used monthly hatchling captures to assess timing of hatching for each species (hypothesis i)) and habit category (fossorial and terrestrial; hypothesis ii)) within a given year. We assumed that a pulse of hatchling captures indicated recent hatching. We converted monthly hatchling captures to monthly proportions of total hatchling captures within a given year to standardise the scale (0–1) among years and species. For example, if we captured 20 of 50 total 2010 hatchlings during April, the proportion of April 2010 hatchling captures was 0.4. We averaged year-specific monthly proportions of hatchling captures (n = 23 for January; n = 24 for all other months) across all years to infer the timing of hatching. We recognise that two of our study species, *L. pygaea and T. sirtalis*, are viviparous and give birth to neonates but use the term 'hatchling' for simplicity.

Data analyses: timing of maturation

We used adult and maturing juvenile captures to estimate timing of maturation for each species (hypothesis i)) and habit (fossorial and terrestrial; hypothesis ii)); smaller age classes (hatchlings and intermediate juveniles) were omitted. We standardised capture data across all years and species by z-scoring (i.e. subtracting by the mean then dividing by the standard deviation) flooding-adjusted captures of age classes (adults and maturing juveniles) and species for each month, relative to the number of flooding-adjusted captures for other months within the same year. We treated z-scored adult captures as a proxy for a species' average monthly catchability, and subtracted z-scored adult captures from z-scored maturing juvenile captures to estimate the relative number of maturing juveniles in the population each month, compared to other months within the same year. For example, we interpreted high capture numbers (positive z-score) of maturing juveniles during a month of low catchability (negative z-score for adult captures) as an above-average number of maturing juveniles for that month relative to other months within the same year. We averaged relative monthly z-scores of maturing juveniles across all years (n = 23 for January and n = 24 for all other months) for each species to estimate seasonal timing of maturation.

Data analyses: environmental correlates of life history traits

We used generalised linear models (GLMs; Nelder & Wedderburn, 1972) to assess relationships of monthly temperature or precipitation anomalies with monthly hatching, maturation, or surface activity anomalies (hypothesis iii)). Minimum, average, and maximum temperature anomalies were highly correlated with one another, so we never included more than one in the same model. We constructed three GLM sets (hatching, maturation, and surface activity) for each species, each consisting of three initial, single predictor-based (minimum, average, or maximum temperature, or precipitation) GLMs, plus a null model. We used Akaike's Information Criterion (AICc) to rank models within each set (Akaike, 1998) and concluded null results if ΔAICc was < 3.0 for the null model relative to the highest-ranking model. Otherwise, we accepted the top-ranking model, and added season (winter, spring, summer, or autumn) as an interactive, second predictor variable if it improved the model's AICc score, to determine whether relationships of temperature or precipitation anomalies with hatching, maturation, or surface activity anomalies varied seasonally.

We also assessed environmental correlates of hatching, maturation, and surface activity across years. We calculated the median month of hatching and maturation for each species and year, then calculated these values relative to the average annual median hatching or maturation times across all study years. We repeated this procedure for the narrowest possible span of months within each year covering 95 % of all hatchling and maturing juvenile captures for each species. For example, if 95 % of hatchlings were captured over a span of 5 months (e.g. May–September) in 2015, compared to an average span of 4 months across all study years, the departure from normal for 'hatching period duration' was 5-4 = 1 month in 2015. For surface activity analyses, we subtracted the number of non-hatchling captures for each species within each year from the average annual number of non-hatchling captures across all years. For example, if we captured 100 non-hatchling *T. relicta* in an average year and captured 80 in 2015, then the departure of non-hatchling *T. relicta* captures in 2015 was -20. We used the same GLM and AICc procedures as above to compare models relating annual hatching, maturation, and surface activity to annual minimum, mean, and maximum temperatures, and precipitation. Years lacking temperature data for part of the year or lacking sufficient hatchling or maturing juvenile captures (i.e. n< 5 within a given year) were excluded from these analyses.

Data analyses: sensitivity of life history traits to clutch strategy, taxonomic relationship, and habit

We categorised each species within each of three groupings including clutch strategy (categories: single- or multi-clutch annually), taxonomic relationship (categories: Testudines, Iguanomorpha, Scincomorpha, Laterata, or Serpentes), and habit (categories: terrestrial or fossorial) to explore the relative importance of grouping method in explaining annual hatching and maturation patterns compared to species alone (hypothesis iv)). We calculated the standard deviation (sd) of average annual hatching or maturation parameters across categories within each grouping for both median hatching/maturation time and the duration of hatching/maturation (described previously). For example, if the collective median hatching time (month) was 5 (May) for the fossorial habit category, and 7 (July) for the terrestrial category, sd of the vector (5, 7) and the relative importance of habit for predicting median hatching time (i.e. sensitivity of median hatching time to habit) would be 1.4. If sd of this vector was 2.4 for the taxonomic relationship grouping, we considered median hatching time to be more sensitive to taxonomic relationship than habit (2.4 > 1.4).

RESULTS

We captured 12,903 total individuals of our ten study species over the 24-year study period, including 940 hatchlings, 3,096 intermediate juveniles, 3,209 maturing juveniles, and 5,658 adults (Table 1, Fig. 1). Hatchlings accounted for < 5 % of total captures for *A. carolinensis, L. pygaea, S. woodi,* and *T. relicta*, and maturing juveniles accounted for < 3 % of total captures for *K. subrubrum* (Table 1); this prevented analysis of hatching or maturation time, respectively, for these species.

Total detection frequency (all years and age classes combined for each species) exceeded its overall mean during early or mid spring (March or April), early or mid autumn (September or October) for *A. sexlineata, L. pygaea, P. inexpectatus, S. lateralis*, and *T. sirtalis*; mid–late spring (May) for *A. carolinensis*, and early spring–early summer (June) for *S. woodi*. The remaining three species had bimodal detection frequencies, with above-average

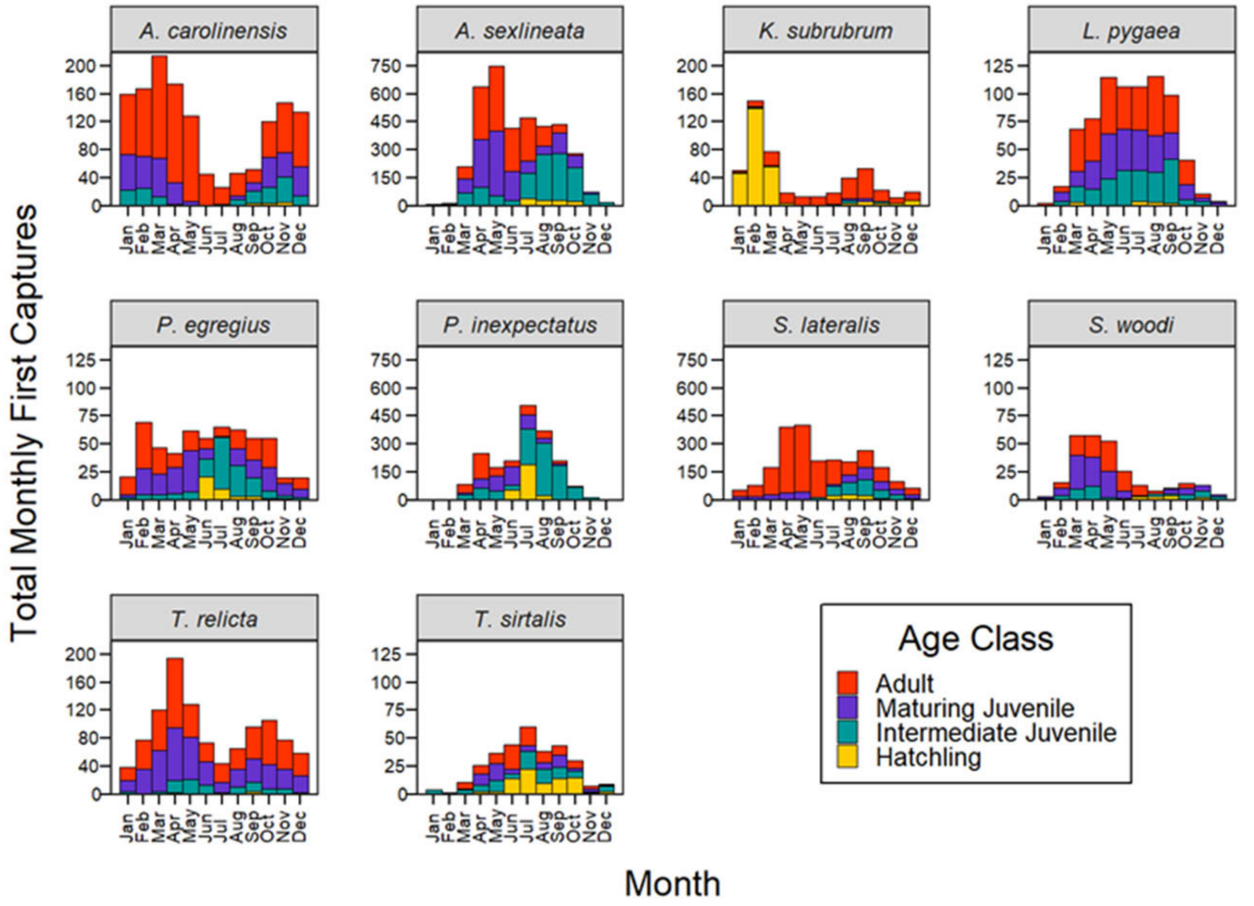

Figure 1. Total monthly number of first captured individuals (1994–2017 combined) by age class (see Table 1) for 10 reptile species, Ocala National Forest, Marion County, Florida. Note, first capture scales are not constant.

detections occurring throughout winter (December–February) and early autumn for *K. subrubrum*; late winter (February) and late spring–mid autumn for *P. egregius*, and; spring (March–May) and early–mid autumn for *T. relicta* (Fig. 1). Captures declined sharply in winter for most species but occurred with moderate frequency almost year-round for *A. carolinensis, P. egregius*, and *T. relicta*.

Interspecific variation in hatching and maturation

Average seasonal timing of hatching and maturation varied widely among species (n = 10; Figs. 2 & 3). Hatching periods spanned several months and overlapped among most species, but peaked in different months for different species, with peaks occurring for at least one species during all months except April, November, and December (Fig. 2). Hatching peaked in mid summer–mid autumn for *A. sexlineata, S. lateralis*, and *T. sirtalis*; late spring–mid summer for *P. egregius and P. inexpectatus*, and throughout winter and early spring for *K. subrubrum*. *Thamnophis sirtalis* hatching exhibited multiple small seasonal peaks during both mid summer and mid autumn (Fig. 2). The duration of seasonal peaks for hatching ranged from approximately 1–2 months for *P. egregius* and *P. inexpectatus*, to 5–6 months for *A. sexlineata* and *T. sirtalis*. Timing of maturation peaked in early–mid autumn for *A. carolinensis, A. sexlineata*, and *S. lateralis*; early summer for *P. inexpectatus*; late autumn–early spring for *S. woodi*, and biannually in late spring and early or late autumn for *P. egregius* and *T. sirtalis* (Fig. 3). Maturation was aseasonal (i.e. sd < 0.3 for average z-scored maturation values across the 12 months) for *T. relicta* and *L. pygaea*; weakly seasonal (sd = 0.3–0.4) for *P. egregius, S. woodi*, and *T. sirtalis*; moderately seasonal (sd = 0.4–0.6) for *A. carolinensis* and *A. sexlineata*, and; highly seasonal (sd > 0.6) for *P. inexpectatus* and *S. lateralis* (Fig. 3).

Influence of habit on hatching and maturation timing

Timing of hatching within a given year varied in relation to habit (n = 3) in multiple ways. For the terrestrial habit category (*A. sexlineata, P. inexpectatus*, and *T. sirtalis*), hatching exceeded 5 % of its annual total and began to sharply increase by mid March – nearly 1.5 months earlier than for the fossorial habit category (*P. egregius* and *S. lateralis*) (Fig. 4). The hatching period (middle 95 % of estimated hatching) was also 1.2 months longer for the terrestrial (7.7 months) than the fossorial (6.5 months) habit category. Fossorial and terrestrial habit categories both reached peak category-wide hatching in early–mid summer, whereas the only semi-aquatic species in our hatching analyses (*K. subrubrum*) hatched almost exclusively during winter (Fig. 2). Nonetheless, species was a better predictor of annual hatching times than terrestrial or fossorial habit categories.

In contrast to hatching periods, the average timing, overlap, and duration of maturation periods were similar in the terrestrial and fossorial habit categories (Fig. S3).

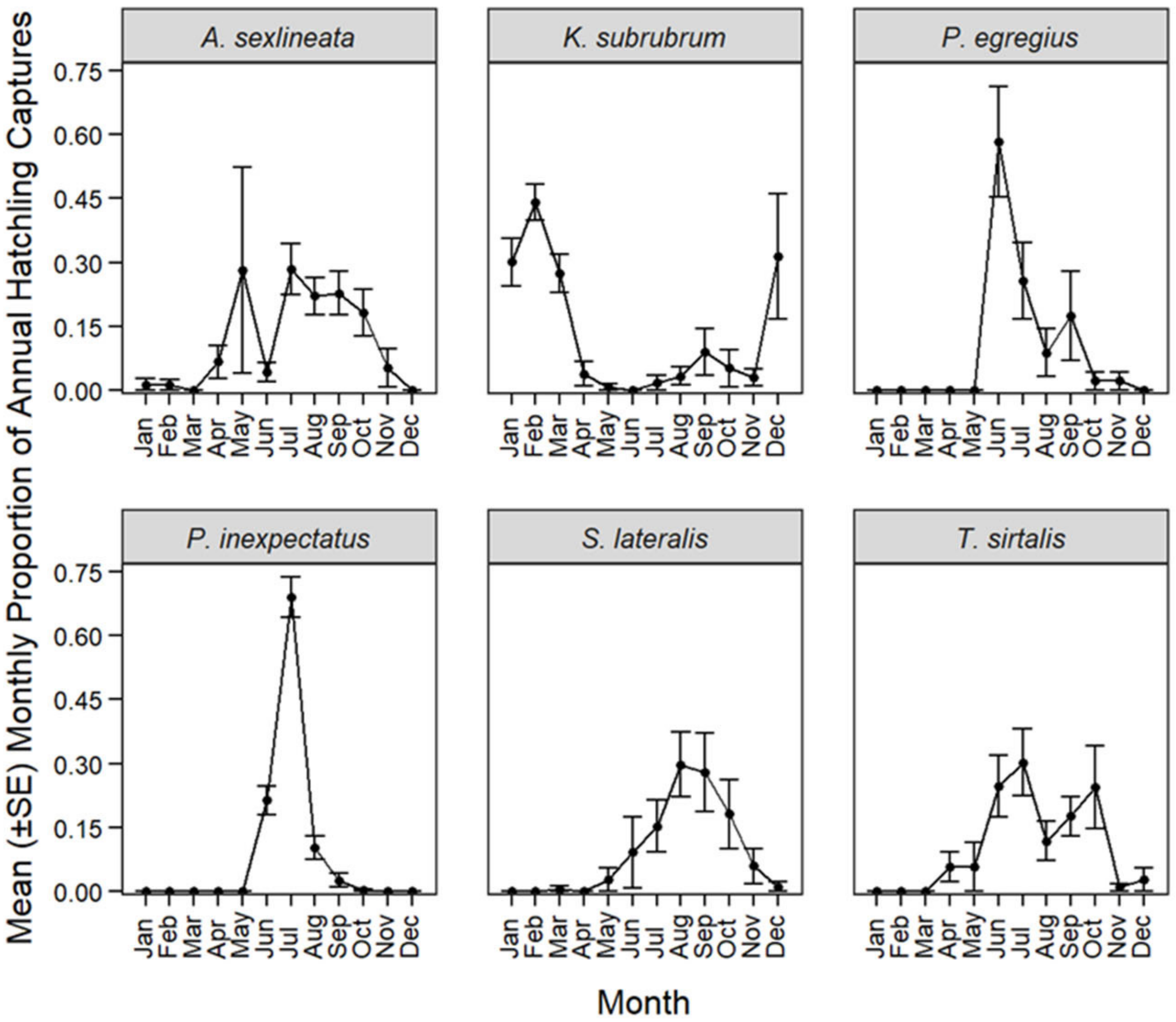

Figure 2. Mean (black points) (+SE; error bars) monthly proportions of annual hatchling captures (n = 23 years for January; 24 years for all other months) for six reptile species; Ocala National Forest, Marion County, Florida. Terrestrial species included *A. sexlineata, P. inexpectatus*, and *T. sirtalis*; fossorial species included *P. egregius* and *S. lateralis*; semi-aquatic species included only *K. subrubrum*. Proportions of hatchlings were calculated by dividing hatchling first captures (defined in Table 1) by total first captures.

Liodytes pygaea (the only semi-aquatic species included in our maturation analyses) maturation occurred more consistently across all seasons than fossorial or terrestrial habit categories (Fig. 3).

Influence of temperature anomalies on hatching, maturation, and surface activity

Monthly maturation anomaly (i.e. difference in monthly maturation compared to average for a given month) was negatively correlated with monthly average temperature anomaly for *P. egregius* (n = 240 months, P = 0.00623; AICc = 620.29; Fig. 5), though the effect size was modest (r = -0.197; 95 % CI = (-0.257, -0.043)) and interactions between temperature anomaly and season did not improve models for predicting maturation anomaly (ΔAICc = 6.16). Monthly temperature or precipitation anomalies did not influence monthly hatching, maturation, or surface activity anomalies for any other (n = 9) study species (i.e. ΔAICc< 3.0 for the null model; Table 2).

Annual temperature or precipitation anomalies were related to annual hatching, maturation, or non-hatchling surface activity patterns for several tested species (all age classes were not analysed for all species due to insufficient sample sizes). Model comparisons (i.e. >3 AICc units better [lower] than a null model) suggested that high annual mean temperature (i.e. positive annual temperature anomaly) was associated with delayed *S. lateralis* hatching, high weekly minimum temperatures across the year were associated with delayed *P. inexpectatus* maturation, and high weekly maximum temperatures across the year were associated with reduced *K. subrubrum* surface activity. In addition, high annual precipitation was associated with delayed birth of *T. sirtalis* neonates and reduced surface activity by *A. sexlineata*, (Table 2; Figs. 6 & 7). We found no evidence that annual temperature or precipitation anomalies influenced annual maturation, hatching, or surface activity anomalies (differences in these variables relative to average) for other study species.

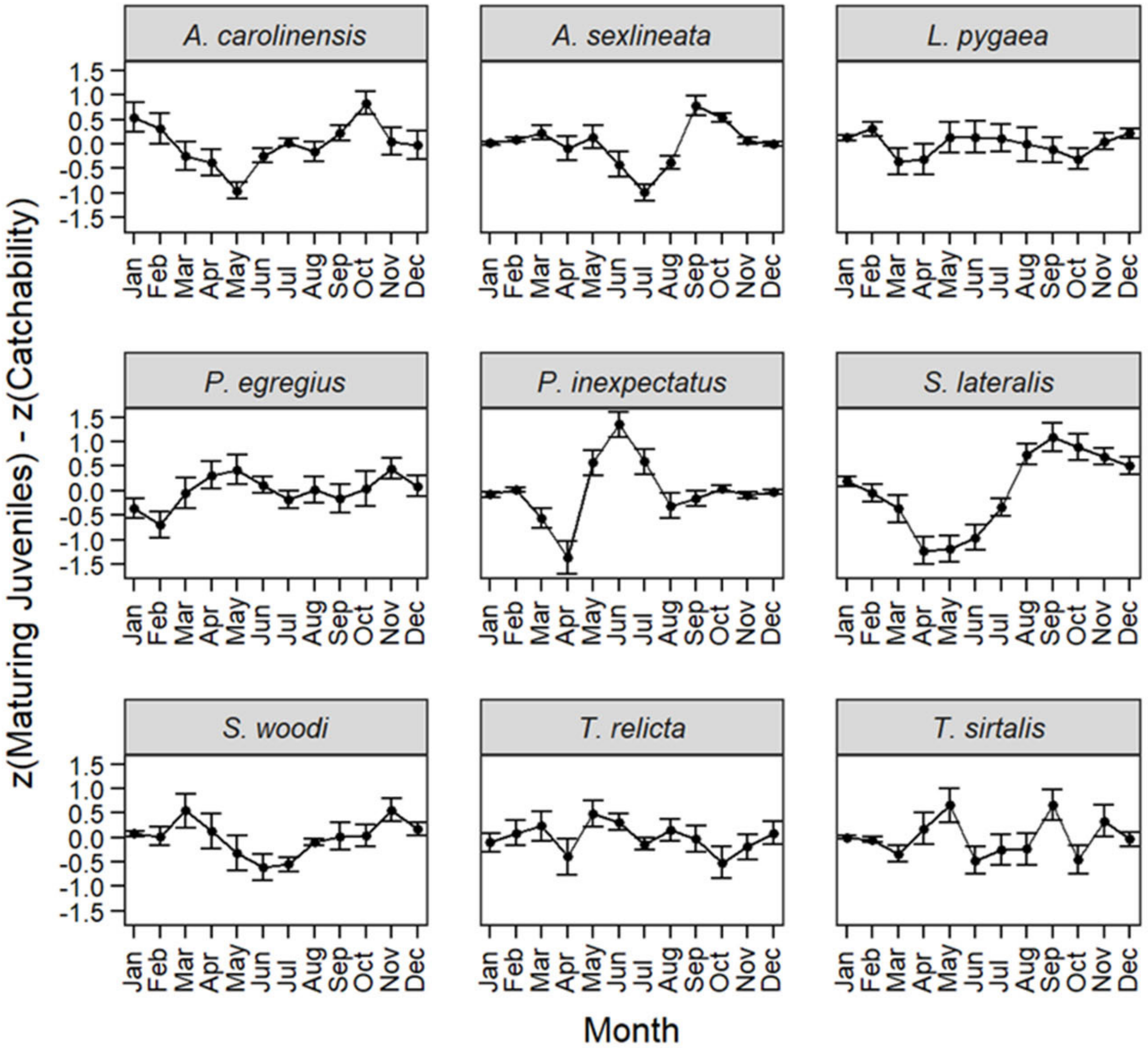

Figure 3. Estimated, standardized mean (black points) (+SE; error bars) monthly (n = 23 years for January; 24 years for all other months) maturation z-scores, for reptile species used in maturation analyses; Ocala National Forest, Marion County, Florida.

Influences of clutch strategy, taxonomic relationship, and habit on species' hatching and maturation patterns

Average hatching and maturation parameters (median timing and duration) varied widely in their sensitivity to clutch strategy, taxonomic relationship, and habit groupings relative to species alone (Fig. S4). Median hatching time and hatching period duration were both more sensitive to species than any of other grouping, but species, taxonomic relationship and/or habit were all similar in their relative influence on median maturation time and maturation period duration. All hatching and maturation parameters were relatively insensitive to clutch strategy.

DISCUSSION

Our results showed wide variation in the timing, duration, and seasonal peaks of hatching and maturation periods among study species (hypothesis i)), and generally supported our hypothesis ii): that habit (e.g. terrestrial or fossorial) may be an important influence on these life history traits. The longer hatching period seen in the terrestrial than fossorial habit category could ensure that at least some hatchlings survive by avoiding stochastic, unfavourable short-term conditions (e.g. unusually cold weather) that are more frequent in terrestrial than fossorial environments (Burda et al., 2007; Pike & Mitchell, 2013). Winter hatching by semi-aquatic *K. subrubrum*, and consistent year-round maturation by semi-aquatic *L. pygaea* also suggested that cold air temperatures are less limiting on hatching and maturation for the semi-aquatic than the fossorial or terrestrial habit categories. In addition, overall higher water levels in winter (Greenberg et al., 2015) increase the likelihood of aquatic habitat availability. Maturation periods were similar between fossorial and terrestrial habit categories, indicating that a relatively constant year-round subterranean temperature in the sandy soils of our study area (Burda et al., 2007; Pike & Mitchell, 2013) was not an important driver of maturation period for the fossorial species group.

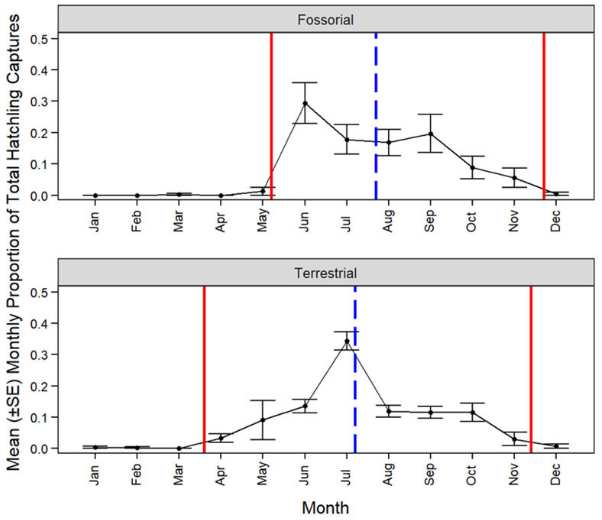

Figure 4. Mean (black points) (+SE; error bars) monthly proportion (n = 23 years for January; 24 years for all other months) of total hatchling captures of fossorial (*P. egregius* and *S. lateralis*) and terrestrial (*A. sexlineata*, *P. inexpectatus*, and *T. sirtalis*) reptile habit categories, Ocala National Forest, Marion County, Florida. Dashed blue lines reflect peak (i.e., mean) hatching time; solid red lines represent cutoffs used to determine an approximate 'start' and 'end' of the hatching period, based on 95 % of estimated hatching falling between these cutoffs.

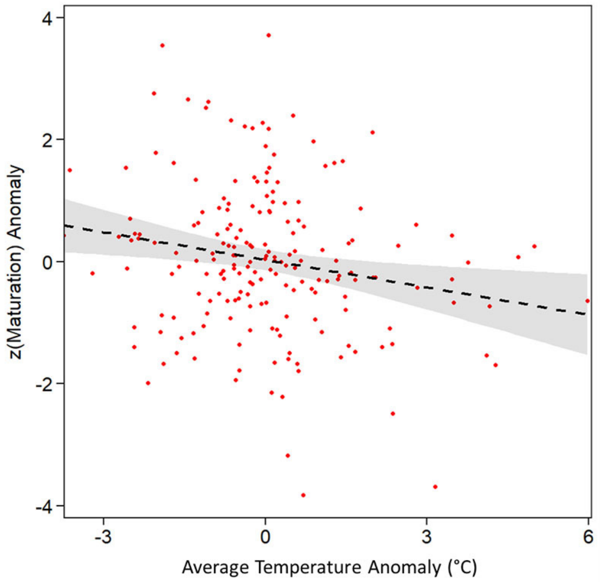

Figure 5. The relationship between average monthly temperature anomaly and z-scored maturation for P. egregious, Ocala National Forest, Marion County, Florida. The black line and gray shading represent the fitted model (r =-0.197) and its 95% confidence interval, respectively. Red points represent monthly temperature anomaly and maturation anomaly data used to model the fitted relationship (i.e., observed values).

Therefore, our hypothesis that hatching and maturation periods would be more seasonally-synchronised in the fossorial than terrestrial or semi-aquatic species groups received mixed support overall. As the climate warms, habit may therefore attenuate changes in hatching periods more for fossorial than terrestrial reptiles, but is less likely to attenuate changes in the timing or duration of maturation.

Monthly anomalies of minimum, average, or maximum temperatures or precipitation compared to normal had no detectable effect on the monthly timing of hatching, maturation, or surface activity for most study species, suggesting that seasonal timing of these life history traits is either relatively inelastic or not vulnerable to temperature deviations within the ranges tested. This did not support our original hypothesis of a positive relationship between temperature anomaly and hatching or maturation anomaly (hypothesis iii)) and was surprising, since warm temperatures are known to accelerate the embryonic development and/or juvenile growth of many reptile species (Sinervo & Adolph, 1989; Van Damme et al., 1992; Georges et al., 2005). Our study species may not be able to capitalise on abnormal short-term (monthly) weather patterns that would benefit their survival during life history transitions or surface activity under climate change. Instead, our study species' patterns of hatching, maturation, and surface activity appeared relatively inflexible over monthly timespans, and were only (for some species) modified when abnormal temperatures or precipitation persisted over much longer (e.g. annual; see below) periods. *Plestiodon egregius* was an exception; z-scored monthly maturation anomaly increased for this species during months of unusually cool weather, suggesting that moderately cool soil temperatures accelerated its maturation. Mount (1963) also suggested that *P. egregius* prefer cooler temperatures, noting they were active near the ground surface of pocket gopher mounds most often during "cooler months of the year."

Although monthly hatching, maturation, and surface activity trends appeared unrelated to monthly temperature and precipitation anomalies for most species, multiple species varied in their annual hatching, maturation, and surface activity trends across annual temperature and precipitation departure gradients (Figs. 6 & 7). Thus, our hypothesis iii) was supported across annual, but not monthly timescales. For example, non-hatchling *K. subrubrum* reduced their surface activity during hot years, which may have indicated a reduced ability to disperse in search of suitable aquatic habitats. In addition, higher than normal annual temperatures were associated with delayed *S. lateralis* hatching and *P. inexpectatus* maturation; future studies of these species' thermal optima during embryonic and juvenile development are thus warranted. Annual temperatures in our study region are projected to increase by 2–4 ˚C by 2071–2099 under climate change (Melillo et al., 2014), which may impact *K. subrubrum, S. lateralis*, and *P. inexpectatus*. For example, *K. subrubrum* populations may become more fragmented if increasing temperatures limit future dispersal between wetlands. In addition, delayed hatching in *S. lateralis* and delayed maturation in *P. inexpectatus* under climate change may lead to overall smaller body sizes in young-of-year individuals during winter, and thus fewer prey options due to smaller gape size during a period of the year when foraging opportunities are already limited. However, *S.*

Table 2. AICc tables for GLMs relating annual species maturation, hatchling, or non-hatchling surface activity to annual temperature and precipitation trends, Ocala National Forest, Marion County, Florida. Only models where the top-ranking model was at least three AICc units lower than the null model are shown. K = number of model parameters; AICc = AICc score of model; ΔAICc = difference in AICc score between a given model and the top-ranking model; ModelLik = model likelihood; AICcWt = AICc-based model weight. See Table 1 footnotes for species codes.

Analysis	Model	K	AICc	ΔAICc	ModelLik	AICcWt
P. inexpectatus Annual Maturation	Median Maturation Time ~ Minimum Temperature	3	35.78	0.00	1.00	0.73
	Median Maturation Time ~ Average Temperature	3	39.25	3.46	0.18	0.13
	Median Maturation Time ~ 1 (Null Model)	2	40.04	4.25	0.12	0.09
	Median Maturation Time ~ Annual Precipitation	3	42.24	6.46	0.04	0.03
	Median Maturation Time ~ Maximum Temperature	3	42.56	6.78	0.03	0.02
A. carolinensis Annual Hatching	Median Hatching Time ~ Annual Precipitation	3	39.60	0.00	1.00	0.85
	Median Hatching Time ~ 1 (Null Model)	2	43.51	3.91	0.14	0.12
	Median Hatching Time ~ Minimum Temperature	3	47.48	7.88	0.02	0.02
	Median Hatching Time ~ Average Temperature	3	48.83	9.23	0.01	0.01
	Median Hatching Time ~ Maximum Temperature	3	49.11	9.51	0.01	0.01
S. lateralis Annual Hatching	Median Hatching Time ~ Average Temperature	3	35.59	0.00	1.00	0.73
	Median Hatching Time ~ Minimum Temperature	3	39.05	3.46	0.18	0.13
	Median Hatching Time ~ 1 (Null Model)	2	39.51	3.93	0.14	0.10
	Median Hatching Time ~ Annual Precipitation	3	42.44	6.85	0.03	0.02
	Median Hatching Time ~ Maximum Temperature	3	43.41	7.83	0.02	0.01
T. sirtalis Annual Hatching[1]	Median Hatching Time ~ Annual Precipitation	3	57.49	0.00	1.00	0.80
	Median Hatching Time ~ 1 (Null Model)	2	61.64	4.15	0.13	0.10
	Median Hatching Time ~ Minimum Temperature	3	62.81	5.32	0.07	0.06
	Median Hatching Time ~ Average Temperature	3	64.46	6.97	0.03	0.02
	Median Hatching Time ~ Maximum Temperature	3	64.65	7.16	0.03	0.02
A. sexlineata Annual Surface Activity	Total Non-hatchling Captures ~ Annual Precipitation	3	227.25	0.00	1.00	0.93
	Total Non-hatchling Captures ~ 1 (Null Model)	2	234.46	7.21	0.03	0.03
	Total Non-hatchling Captures ~ Average Temperature	3	234.50	7.25	0.03	0.02
	Total Non-hatchling Captures ~ Maximum Temperature	3	235.62	8.37	0.02	0.01
	Total Non-hatchling Captures ~ Minimum Temperature	3	236.86	9.61	0.01	0.01
K. subrubrum Annual Surface Activity	Total Non-hatchling Captures ~ Maximum Temperature	3	56.78	0.00	1.00	0.70
	Total Non-hatchling Captures ~ 1 (Null Model)	2	60.44	3.66	0.16	0.11
	Total Non-hatchling Captures ~ Average Temperature	3	60.66	3.88	0.14	0.10
	Total Non-hatchling Captures ~ Annual Precipitation	3	61.63	4.85	0.09	0.06
	Total Non-hatchling Captures ~ Minimum Temperature	3	63.01	6.23	0.04	0.03

[1] Our results for *A. carolinensis* should be treated with caution because no years of our study had simultaneously below-average precipitation and sufficient (>10) *A. carolinensis* hatchling captures to be included in this analysis.

lateralis foraging may be less affected by seasonal changes in resource availability than for *P. inexpectatus*, due to more stable abiotic conditions (e.g. soil temperature, which directly impacts body temperature and may indirectly impact foraging by affecting prey availability) experienced underground versus aboveground. In addition to temperature-related trends, non-hatchling *A. sexlineata* were less surface active during wet than dry years, consistent with the dependence of teiids on sunlight (precluding cloudy skies and rain) for thermoregulation (Sartorius et al., 1999). Higher than normal annual precipitation was also associated with delayed birth of *T. sirtalis* neonates, but potential reasons for this trend are less clear. Compared to temperature, current climate projections suggest modest (<10 %) changes in mean annual precipitation for Florida by 2071–2099 (Melillo et al., 2014), suggesting minor-to-moderate impacts on *A. sexlineata* and *T. sirtalis*. We found no support for annual weather-related hatching, maturation, or surface activity trends for any other species, possibly due to < 20 years

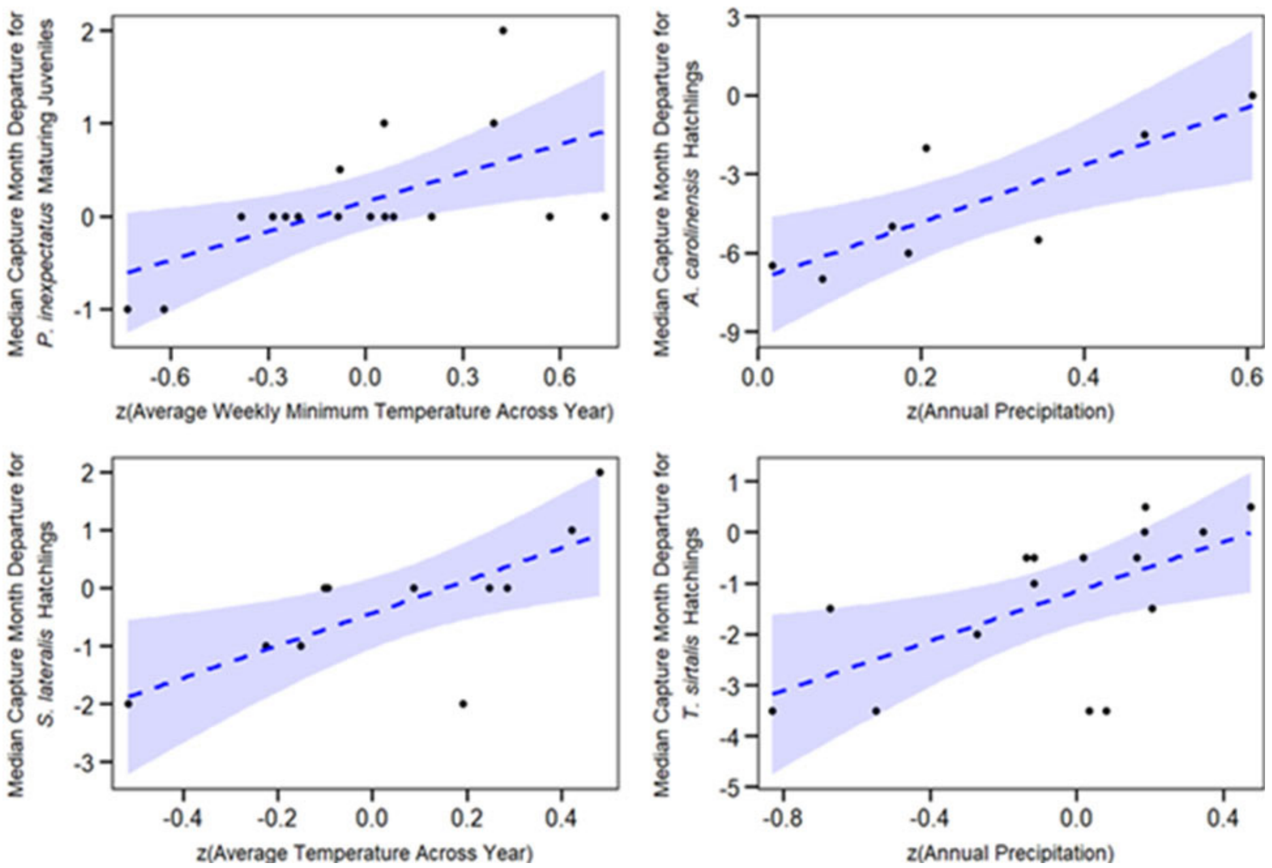

Figure 6. Generalised linear models showing potential effects of annual temperature and precipitation departures on changes in the timing of maturation and hatching, for selected species (Table 2), Ocala National Forest, Marion County, Florida. Negative or positive numbers for median hatchling captures represent years in which the median capture month of hatchlings occurred earlier or later in the year than average (1994–2017), respectively. Black points = observed data, dashed blue lines = fitted curves, and blue shading = 95 % confidence intervals.

of data (i.e. < 20 replicates) being usable in our annual analyses.

Infrequent captures of either hatchlings or maturing juveniles for five of our ten study species suggested that detectability varied widely among age classes for some species. Hatchlings comprised < 5 % of total *A. carolinensis, L. pygaea, S. woodi*, and *T. relicta* captures, suggesting they were less surface-active than other age classes. Lower detectability of hatchlings than other age classes has also been reported for *Gopherus polyphemus* (Gopher Tortoise) and *Pituophis melanoleucus mugitus* (Florida Pine Snake) in longleaf-wiregrass sandhills (Burger, 1998; Pike, 2006). Conversely, maturing juveniles comprised < 3 % of total *K. subrubrum* captures, suggesting that they reduced terrestrial activity during maturation. In our study, 94 % (n = 253/270) of *K. subrubrum* hatchlings were captured entering ponds, suggesting that they move into wetlands shortly after hatching and remain there until adulthood. Differential catchability among age classes has been documented in several other species (Lima & Moreira, 1993; Lind & Welsh, 1994; Wikelski & Trillmich, 1994), and presents a challenge for understanding the role that developmental phenology (e.g. timing of hatching and maturation) plays in shaping the temporal partitioning of species and habit-associated traits (e.g. foraging, courtship) during adulthood.

Our study addresses temporal partitioning of hatching and maturation among multiple sympatric reptiles, and relates species-specific hatching, maturation, and surface activity patterns to fluctuating temperatures and precipitation. Our results thus provide otherwise scarce information for several reptile species and an improved framework for future studies addressing causal mechanisms of temporal differences in these important life history traits. In addition, our findings highlight the potential for climate change to impact life history traits of Florida reptiles and illustrate the need for continued monitoring. Future research should consider how reptile hatching, maturation, and surface activity patterns may change given different emissions scenarios, and should clarify roles of thermal and moisture-related preferences as mechanisms underlying the patterns we observed among species and habit categories.

ACKNOWLEDGEMENTS

The findings and conclusions in this publication are those of the author(s) and should not be construed to represent any official USDA or US Government determination or policy. Funding was provided by the USDA Forest Service, Ocala National Forest; Longleaf Pine Ecosystem Restoration Program; Southern Research Station's

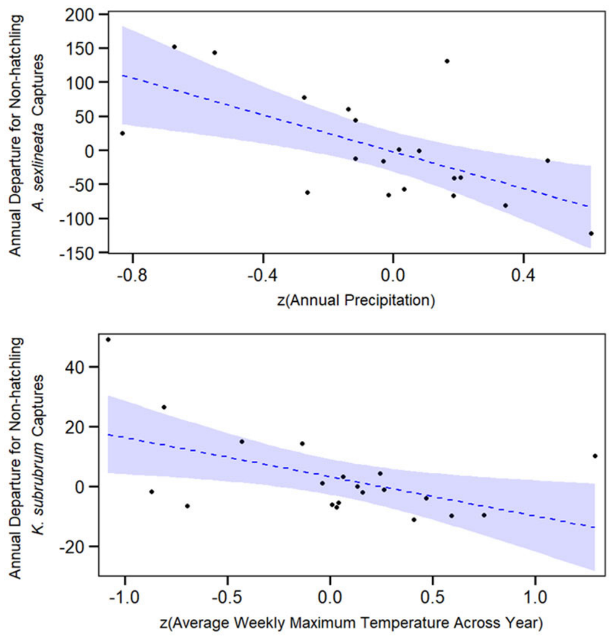

Figure 7. Generalized linear models showing potential effects of annual precipitation departures on changes on the total number of non-hatchlings captured, for selected species, Ocala National Forest, Marion County, Florida. For both of these species, model comparison revealed that the top-ranking models shown above had AICc scores > 3 units lower than the null model (Table 2). Departures in non-hatchling captures represent the number of new non-hatchling captures in a given year minus the average number of annual new non-hatchling captures across all years (1994–2017). Black points = observed data, dashed blue lines = fitted curves, and blue shading = 95% confidence intervals.

Intensive Management Practices Assessment (now defunct) and Upland Hardwood Ecology and Management research work units; Southern Region (R8); Department of Energy-Savannah River Operations (IA Agreement DE-AI09-76SR00056); and the Florida Fish and Wildlife Conservation Commission (contracts NG99-014 and C1195). We thank the many field assistants/site managers over the years, without whom this study would not have been possible: K. Garren, J. Weibe, S.A. Johnson, D.A. Johnson, J.S. Staiger, T. Sheltra (deceased), R.E. Ashton (deceased), D. Wooten, S. Wazny, M. Welker, C. Bugbee, S. Doucette-Riise, C.J. Kovach, R. Lara, L. Tirado, I. Luque-Montes, A. Heh, M. Bainum, C. Hartmann, G. Kamener, and R. Barker. J. Beach (deceased) volunteered full-time, 1994–2006. Many others helped as volunteers or short-term substitutes. We also thank University of Florida professors G.W. Tanner (retired) and A. Storfer, and Ocala National Forest staff L. Lowery (deceased), R. Lowery, C. Sekerak, J. Hinchee, and the fire crew for assistance. This research was approved by IACUC (permit No. 004-09WEC) and the Florida Fish and Wildlife Conservation Commission (permit No. LSSC-12-00021A).

Authors' contribution

Sky T. Button conducted all analyses, drafted the manuscript, and assisted with fieldwork during 2015–2016. Cathryn H. Greenberg procured funding, materials, and labour for the project, oversaw the project's operations, and edited the manuscript. James D. Austin helped procure funding and materials for the project, edited the manuscript, and helped provide local oversight of the project's operations.

REFERENCES

Akaike, H. (1998). Information theory and an extension of the maximum likelihood principle. In: *Breakthroughs in Statistics*. Kotz, S. & Johnson, N. (Eds.), Berlin: Germany. 610–624 p.

Aydelott, D.G., Bullock, H.C. & Furman, A.L. (1975). Soil survey of Ocala National Forest Area, Florida. United States *Department of Agriculture Report*, Florida, USA.

Brattstrom, B.H. (1965). Body temperatures of reptiles. American Midland Naturalist, 73(2), 376–422.

Buckley, L.B. & Jetz, W. (2010). Lizard community structure along environmental gradients. *Journal of Animal Ecology*, 79(2), 358–365.

Burda, H., Šumbera, R. & Begall, S. (2007). Microclimate in burrows of subterranean rodents - revisited. In: *Subterranean Rodents*. Begall, S., Burda, H. & Schleich, C. (Eds.). Berlin: Germany. 21–33 p.

Burger, J. (1998). Effects of incubation temperature on hatchling pine snakes: implications for survival. *Behavioral Ecology*, 43(1), 11–18.

Button, S.T., Sovie, A.R., Greenberg, C.H. & Austin, J.D. (2019). Evaluating the Ecology of *Tantilla relicta* in Florida Pine-Wiregrass Sandhills Using Multi-Season Occupancy Models. *Journal of Herpetology*, 53(3), 179–186.

Clusella-Trullas, S. & Lee, S.L. (2014). Lizard thermal trait variation at multiple scales: a review. *Journal of Comparative Physiology* B, 184(1), 5–21.

Conant, R. & Collins, J.T. (1998). *A Field Guide to Reptiles and Amphibians*: Eastern and Central North America. Boston: USA.

Dodd, C.K. (1992). Biological diversity of a temporary pond herpetofauna in north Florida sandhills. *Biodiversity Conservation*, 1(3), 125–142.

Georges, A., Beggs, K., Young, J.E. & Doody, J.S. (2005). Modelling development of reptile embryos under fluctuating temperature regimes. *Physiological Biochemical Zoology*, 78(1), 18–30.

Greenberg, C.H., Goodrick, S., Austin, J.D. & Parresol, B. (2015). Hydroregime prediction models for ephemeral groundwater-driven sinkhole wetlands: a planning tool for climate change and amphibian conservation. *Wetlands*, 35(5), 899–911.

Greenberg, C.H., Zarnoch S. & Austin, J.D. (2017). Weather, hydroregime, and breeding effort influence juvenile recruitment of anurans: implications for climate change. *Ecosphere*, 8(5), e01789.

Greenberg, C.H., Neary, D.G. & Harris, L.D. (1994). Effect of high-intensity wildfire and silvicultural treatments on reptile communities in sand-pine scrub. *Conservation Biology*, 8(40), 1047–1057.

Knowles Jr, L., O'Reilly, M.A. & Adamski, J.C. (2002). Hydrogeology and simulated effects of the ground-water withdrawals from the Floridan aquifer system in lake county and in the Ocala National Forest and vicinity, north-central Florida, *Water-Resources Investigations Report*, 2(1), 4207.

Lelièvre, H., Legagneux, P., Blouin-Demers, G., Bonnet, X. & Lourdais, O. (2012). Trophic niche overlap in two syntopic colubrid snakes (*Hierophis viridiflavus* and *Zamenis longissimus*) with contrasted habits. *Amphibia-Reptilia*, 33(1), 37–44.

Lima, A.P. & Moreira, G. (1993). Effects of prey size and foraging mode on the ontogenetic change in feeding niche of *Colostethus stepheni* (Anura: Dendrobatidae). *Oecologia*, 95(1), 93–102.

Lind, A.J. & Welsh, H.H. (1994). Ontogenetic changes in the foraging behavior and habitat use of the Oregon garter snake, *Thamnophis atratus hydrophilus*. *Animal Behaviour*, 48(6), 1261–1273.

Means, D.B., Dodd, C.K., Johnson, S.A. & Palis, J.G. (2004). Amphibians and fire in longleaf pine ecosystems: response to Schurbon & Fauth. *Conservation Biology*, 18(4), 1149–1153.

Melillo, J.M., Richmond, T. & Yohe, G. (2014). *Climate Change Impacts in the United States*. Vol. 3. U.S. Global Change Research Program.

Mount, R.H. (1963). The natural history of the red-tailed skink, *Eumeces egregius* Baird. *American Midland Naturalist*, 70(2), 356–385.

Nelder, J.A. & Wedderburn, R.W. (1972). Generalized linear models. *Journal of the Royal Society*: Series A, 135(3), 370–384.

Palmer, W. & Braswell, A. (1995). Reptiles of North Carolina. Chapel Hill: USA.

Pearlstine, L., Smith, S., Brandt, L.A., Allen, C.R., Kitchens, W. & Stenberg, J. (2002). Assessing state-wide biodiversity in the Florida Gap Analysis Project. *Journal of Environmental Management*, 66(2), 127–144.

Pianka, E.R. (1973). The structure of lizard communities. *Annual Review of Ecology & Systematics*, 4(1), 53–74.

Pike, D.A. & Mitchell, J. (2013). Burrow-dwelling ecosystem engineers provide thermal refugia throughout the landscape. *Animal Conservation*, 16(6), 694–703.

Pike, D.A. (2006). Movement patterns, habitat use, and growth of hatchling tortoises, *Gopherus polyphemus*. *Copeia*, 2006(1), 68–76.

Post, E.S. (2019). Time in Ecology. Princeton: USA.

Sartorius S.S., Vitt, L.J. & Colli, G.R. (1999). Use of naturally and anthropogenically disturbed habitats in Amazonian rainforest by the teiid lizard *Ameiva ameiva*. *Biological Conservation*, 90(2), 91–101.

Schoener, T.W. (1968). The Anolis lizards of Bimini: resource partitioning in a complex fauna. *Ecology*, 49(4), 704–726.

Sinervo, B. & Adolph, S.C. (1989). Thermal sensitivity of growth rate in hatchling Sceloporus lizards: environmental, behavioral and genetic aspects. *Oecologia*, 78(3), 411–419.

Tadevosyan, T. (2007). The role of vegetation in microhabitat selection of syntopic lizards, *Phrynocephalus persicus*, *Eremias pleskei*,and *Eremias strauchi* from Armenia. *Amphibia-Reptilia*, 28(3), 444–448.

Van Damme, R., Bauwens, D., Braña, F. & Verheyen, R.F. (1992). Incubation temperature differentially affects hatching time, egg survival, and hatchling performance in the lizard *Podarcis muralis*. *Herpetologica*, 48(2), 220–228.

Wikelski, M. & Trillmich, F. (1994). Foraging strategies of the Galapagos marine iguana (*Amblyrhynchus cristatus*): adapting behavioral rules to ontogenetic size change. *Behaviour*, 128(3), 255–279.

Accepted: 4 May 2022

Please note that the Supplementary Material for this article is available online via the Herpetological Journal website: https://thebhs.org/publications/the-herpetological-journal/volume-32-number-3-july-2022

Volume 32 (July 2022), 142-175

Herpetological Journal

FULL PAPER

https://doi.org/10.33256/32.3.142175

Published by the British Herpetological Society

A review of torrent frogs (*Amolops*: Ranidae) from Bhutan, the description of a new species, and reassessment of the taxonomic validity of some *A. viridimaculatus* group species aided by archival DNA sequences of century-old type specimens

Stephen Mahony[1,2], Tshering Nidup[3], Jeffrey W. Streicher[1], Emma C. Teeling[2] & Rachunliu G. Kamei[1]

[1]Department of Life Sciences, The Natural History Museum, London SW7 5BD, UK
[2]School of Biology and Environmental Science, University College Dublin, Belfield, Dublin D04 V1W8, Ireland
[3]Department of Environment & Life Sciences, Sherubtse College, Kanglung, Trashigang, Royal University of Bhutan, Bhutan

Seven species of the Asian torrent frogs (genus *Amolops*) have previously been reported from the eastern Himalayan country of Bhutan. Species identifications from the region have been largely based on photographed animals with few voucher specimens available and no molecular sampling. Understanding the taxonomic status of Bhutan's torrent frogs has also been hampered by the poorly understood distributional limits of species from surrounding regions. Herein we utilised molecular phylogenetic and morphological data for vouchered specimens from Bhutan and provide a complete literature review of all *Amolops* populations reported from the country. Phylogenetic relationships were estimated by combining available sequence data (from GenBank) with newly generated sequences from recently collected Bhutanese *Amolops* populations. We also obtained archival DNA sequences from the type specimens of *Amolops formosus*, *A. himalayanus*, and *A. kaulbacki*, collected between 82 and 151 years ago. Our comparative analyses revealed a large, new (to science) species of the *Amolops viridimaculatus* group from eastern Bhutan. Morphological examinations of related taxa revealed that *A. senchalensis* from India is not a synonym of *A. marmoratus*. Molecular phylogenetic results supplemented by morphological data unambiguously demonstrate i) that *A. himalayanus* is present in eastern Nepal, ii) the presence of a previously undocumented population of *A. nepalicus* in eastern Nepal, iii) a 200 km range extention for *A. kaulbacki* into Yunnan, China, iv) that *A. gyirongensis* should be considered a junior subjective synonym of *A. formosus*, and v) that *A. splendissimus* from Vietnam should be considered a junior subjective synonym of *A. viridimaculatus*. Based on our results, we expand the *Amolops viridimaculatus* group to include nine species, including *A. formosus, A. himalayanus, A. kaulbacki*, and the new species described herein. We provisionally include a further three species in the *viridimaculatus* group based on morphology, *A. longimanus, A. nidorbellus,* and *A. senchalensis*. Combining our data with the literature review allowed us to identify several unidentified *Amolops* species from recent phylogenetic studies and remove nine frog species (including *Hyla, Sylvirana*, and seven *Amolops* species) from Bhutan's amphibian checklist. We recognise four species of *Amolops* in Bhutan, three of which cannot be confidently identified to the species level based on currently available data.

Keywords: Anura, taxonomy, Himalayas, conservation, vouchered-specimens

INTRODUCTION

The large radiation of Asian torrent or waterfall frogs, genus *Amolops* Cope, 1865 currently contains 72 valid species (Che et al., 2020; Wu et al., 2020; Jiang et al., 2021; Patel et al., 2021; Zeng et al., 2021; Zhang et al., 2021; Table 1) distributed throughout the hilly regions of mainland south-east Asia, much of southern and eastern China and along the southern Himalayas as far west as northern India (Dubois, 1974; Ray, 1999; Anders, 2002; Orlov et al., 2002; Wogan et al., 2008; Biju et al., 2010; Fei et al., 2012; IUCN Bangladesh, 2015; Chan et al., 2018; Streicher et al., 2020). Recent molecular phylogenetic analysis has identified eight distinct evolutionary radiations now treated as species groups, of which the *marmoratus*, *monticola* and *viridimaculatus* groups are represented in the southern Himalayas where they are broadly sympatric (Wu et al., 2020). Each of these species groups contain numerous species that are morphologically conserved and can be difficult or even impossible to reliably identify in the field. Several species remain poorly defined morphologically and the recent use of DNA sequence data as the primary means of species delimitation (Che et al., 2020; Wu et al., 2020) has complicated comparisons with older, morphology-based literature records. Nonetheless, there has been a flood of new species descriptions in recent years from the region (e.g. Zhao et al., 2005; Qi et al., 2019; Che et al., 2020; Khatiwada et al., 2020; Patel et al., 2021).

The Kingdom of Bhutan is a small country (38,394 km²) nestled between the Brahmaputra River Valley and the Tibetan Plateau in the eastern Himalayas, bordered by Tibet and the four Indian states of Arunachal Pradesh, Assam, Sikkim and West Bengal. The mountainous terrain with broad elevational range from 160 m up to 7,500 m a.s.l. (Ramashray & Dorji, 2011) creates varied environments with rich biodiversity potential (NBC, 2019). The amphibian fauna of Bhutan remained poorly studied, but a recent drive by local wildlife enthusiasts, academics, and research staff of the forest department has seen a rapid rise in the number of species reported from the country (DoFPS, 2020; Wangyal et al., 2020; 2021). Unfortunately, the amphibians of Bhutan are poorly represented in museum collections both nationally and internationally, and reports of species are largely based on anecdotal evidence and/or photographs of animals (Wangyal et al., 2020). The presence of morphologically cryptic species complexes and poorly described species named in the 19th and early 20th centuries in the region have contributed to a situation where many species identifications reported in the literature require taxonomic revision. Such revisions require the collection of vouchered specimens from the originally reported populations, direct morphological comparison to taxonomic descriptions in modern literature (when available) or type specimens (spread internationally across museum collections), or through molecular comparison with reliably identified published DNA sequences.

In this paper, we provide a comprehensive review of literature records for the genus *Amolops* from Bhutan to determine the basis of each reported population, and whether species identifications require revision. We sequenced mitochondrial DNA (mtDNA) from eleven specimens of *Amolops* collected in Bhutan (referable to the *marmoratus*, *monticola*, and *viridimaculatus* groups) to compare with available sequence data from other studies. Due to extensive confusion in the literature with respect to the identifications and taxonomic status of several poorly known *viridimaculatus* group species from the southern Himalayas, we also utilised a high-throughput DNA sequencing methodology to obtain mitochondrial data from the 82–151 year old type specimens of three species, *A. formosus* (Günther, 1876), *A. himalayanus* (Boulenger, 1888) and *A. kaulbacki* (Smith, 1940) from the collection of the Natural History Museum, London, UK. Our literature review demonstrates extensive confusion relating to the identification of *Amolops* species reported from Bhutan and allows us to recommend corrections to the national species checklist. Based on morphological and molecular analyses, we identified a new species of the *viridimaculatus* group from eastern Bhutan and we formally describe it herein. Morphological studies of related taxa demonstrate that one synonym, *Rana senchalensis* Chanda, 1987, required taxonomic re-evaluation and is here provisionally treated as valid. Molecular data obtained from the historical type specimens provide insights into the systematic status and distributions of several species, highlight some species identification errors on GenBank, and also necessitate the synonymisation of two species, one from Tibet Autonomous Region, China and one from Vietnam and adjacent Yunnan, China.

Correspondence: Stephen Mahony (stephenmahony2@gmail.com)

MATERIALS & METHODS

Taxon sampling

Fieldwork was carried out in Bhutan by Tshering Nidup, Nub Tshering Lepcha, Penjor, Dawa Gyeltshen, Namgay Dorji and Namgay Rinchen during the spring to monsoon season (March to August) between 2015 and 2019 (Research Permit No. 205474365BFF950D3594C; MTA Reference No. NBC/BRD-7/2019-2020). Specimens were collected during opportunistic visual surveys during both daytime and night-time. Search time was predominantly spent in the vicinity of streams flowing through natural (forested) habitat. Global Positioning System (GPS) coordinates and elevation (metres above sea level) were determined using a Garmin eTrex 10 hand-held GPS device. Representative specimens from each population were photographed live either in-situ (in the field, as observed when encountered) or ex-situ under staged conditions within 24 hours of collection, to provide data on colouration in life. Animals were humanely euthanised using the anaesthetics, aqueous solution of ethyl 3-aminobenzoic methane sulfonate salt (MS 222), or lidocaine. Specimens were fixed in absolute (99.99 %) ethanol (EtOH) for 12 hours and then transferred to 70 % EtOH for long-term storage in the collections of the Sherubtse College Zoology Museum (SCZM), Royal University of Bhutan, Trashigang, Bhutan. A portion of thigh muscle was excised from representative specimens of each population for molecular analyses. Tissue samples were stored at -20 °C in PCR grade absolute EtOH. For this study, we collected eleven specimens of *Amolops* from three localities in eastern Bhutan that we tentatively identified in the field as *A.* aff. *himalaynaus* (n=9), *A.* cf. *gerbillus* (n=1), and *A.* cf. *putaoensis* (n=1).

Museum collection acronyms mentioned in this study are as follows: AMNH (American Museum of Natural History, New York, USA); AMS (Australian Museum, Sydney, Australia); BMNH (British Museum [Natural History]: now the NHMUK - Natural History Museum, London, UK); BNHS (Bombay Natural History Society, Mumbai, Maharashtra, India); CAS (Department of Herpetology, California Academy of Sciences, San Francisco, California, USA); CDZMTU (Central Department of Zoology, Tribuvan University, Kirtipur, Kathmandu, Nepal); CIB (Chengdu Institute of Biology, Chinese Academy of Sciences, Chengdu, Sichuan, China); CUMZ (Chulalongkorn University Museum of Zoology, Bangkok, Thailand); FMNH (Field Museum of Natural History, Chicago, Illinois, USA); GXNU (Guangxi Normal University, Guilin, Guangxi, China); KIZ (Kunming Institute of Zoology, Chinese Academy of Sciences, Kunming, Yunnan, China); HLNP (Hoang Lien National Park headquarters, Lao Cai, Vietnam); KUHE (Graduate School of Human and Environmental Studies, Kyoto University, Kyoto, Japan); KU KUH (University of Kansas Natural History Museum, Lawrence, Kansas, USA); LSUHC (La Sierra University Herpetological Collection, Riverside, California, USA); MCBT (Madras Crocodile Bank Trust, Mahabalipuram, Tamil Nadu, India); MNHN (Museum National d'Histoire Naturelle, Paris, France); NRM (Swedish Museum of Natural History, Stockholm, Sweden); RMB (Lee Kong

Chian Natural History Museum, Singapore); ROM (Centre for Biodiversity and Conservation Biology, Royal Ontario Museum, Toronto, Ontario, Canada); SDB (Systematics Lab, University of Delhi, Delhi, India); SWFU (Southwest Forestry University, Kunming, Yunnan, China); SYNU (Shenyang Normal University, Shenyang, Liaoning, China); SYS (The Museum of Biology, Sun Yat-sen University, Guangzhou, Guangdong, China); VNMN (Vietnam National Museum of Nature, Hanoi, Vietnam); WIIADA (Wildlife Institute of India, Dehradun, Uttarakhand, India); ZISP (Zoological Institute of St. Petersburg, St. Petersburg, Russia); ZSIK (Zoological Survey of India, Kolkata, West Bengal, India). Authors abbreviations are as follows: ECT (Emma C. Teeling); JWS (Jeffrey W. Streicher); RGK (Rachunliu G. Kamei); SM (Stephen Mahony); TN (Tshering Nidup).

Molecular analyses

Whole genomic DNA was extracted from the recently collected tissue samples from Bhutan using a DNeasy Blood and Tissue Kit® (Qiagen) following manufacturer's instructions. A mtDNA sequence that comprises a portion of the 16S ribosomal subunit (*16S*) gene was selected for phylogenetic analyses since it is available for all bar seven currently valid species of *Amolops* at the time of analyses (8 April 2022; see Table 1). We amplified either a continuous portion of the 12S ribosomal subunit, complete tDNA-Valine (*t-Val*) and a portion of the 16S ribosomal subunit (*12S-tVal-16S*) for seven samples (SCZM 2015.03.15.4; SCZM 2015.03.15.5; SCZM 2019.07.18.1; SCZM 2019.07.18.2; SCZM 2019.08.02.1; SCZM 2019.07.20.1; SCZM 2019.07.27.1) using the primers 12SAL(f), 16S2000H(r), LX12SN1(f) and LX16S1R(r) (Zhang et al., 2008), or just the *16S* sequences for four samples (SCZM 2014.07.19.1; SCZM 2015.06.29.1; SCZM 2015.03.28.1; SCZM 2015.03.28.2) using primers 16SAR(f) and 16SBR(r) (Palumbi, 1996). For the *12S-tVal-16S* sequences, we used a PCR reaction recipe of 25 µL aliquots comprised of 1.5 µL extracted DNA, 10 µL PCR grade water, 12.5 µL MyTaq™ Mix (Bioline) and 0.5 µL each of forward and reverse primers (10 µM). For the *16S* only sequences, we used a PCR reaction recipe of 20 µL aliquots comprised of: 2.0 µL extracted DNA; 5 µL Promega 5X Green GoTaq® Flexi Buffer; 4 µL 25 mM Mg CL$_2$; 0.2 µL dNTPs (10 mM each); 1 µL each of forward and reverse primers (10 mM concentrations); 0.1 µL GoTaq® G2 Flexi DNA Polymerase (Promega); 6.7 µL PCR grade H$_2$O. The following PCR reaction protocols were used: (1) for 12SAL, 16S2000H, LX12SN1 and LX16S1R primers, TD 55: initial denaturation at 95 °C for 3 minutes, 10 cycles of denaturation at 95 °C for 30 seconds, annealing at 65 °C (with a reduction of 1 °C each cycle) for 40 seconds, extension at 72 °C for 1 minute, followed by 35 cycles of denaturation at 95 °C for 3 minutes, annealing at 55 °C for 40 seconds, extension at 72 °C for 1 minute; (2) for 16SAR and 16SBR primers, initial denaturation at 95 °C for three minutes, then 35 cycles of denaturation at 95 °C for 30 seconds, annealing at 50 °C for 30 seconds, and extension at 72 °C for 1 minute. The final extension for both protocols was at 72 °C for 10 minutes. PCR products were purified, and Sanger sequenced for forward and reverse strands using PCR primers by the Core Research Labs at the Natural History Museum (London; NHMUK). Chromatograms of raw sequences were checked for quality, trimmed and assembled into contigs using Geneious® V.8.1.9 (Kearse et al., 2012) and sequences were checked on BLAST (Altschul et al., 1990) using the NCBI BLAST (website http://blast.ncbi.nlm.nih.gov) for verifying approximate identities against the GenBank nucleotide database (Benson et al., 2017).

For archival DNA sampling, small portions of muscle tissue (typically the triceps femoris or adductor magnus + gracilis major) from type specimens of three species, *A. formosus* (holotype, BMNH 1947.2.4.18), *A. himalayanus* (syntype, BMNH 1947.2.3.83) and *A. kaulbacki* (holotype, BMNH 1940.6.1.1; Table 1) were excised from the ventral thighs and stored in absolute EtOH at -20 °C for approximately one week before beginning DNA extractions. Samples were digested at 55 °C in a solution of 20 µL of proteinase K and 180 µL of lysis buffer (100 mM NaCL, 100 mM Tris, 25 mM EDTA, 0.5 % SDS), and checked at 10-minute intervals until fully digested. DNA extraction was performed using Sera-Mag™ SpeedBeads™ (Thermo Fisher Scientific) at a concentration of 2.1X (200 µL of digested tissue to 420 µL of beads) and eluted into 40 µL of 10 mM Tris Buffer. We quantified the amount of double-stranded DNA (dsDNA) using 1 µL of each extraction with a Qubit® dsDNA HS (High Sensitivity) Assay Kit on a Qubit® 2.0 Fluorometer (Thermo Fisher Scientific) which indicated the following concentrations: *A. formosus* (0.80 ng/µL), *A. himalayanus* (0.56 ng/µL), and *A. kaulbacki* (0.19 ng/µL). Given these relatively low concentrations, we used the entirety of the DNA extract as template for the library construction which was approximately 31.2 ng (*A. formosus*), 21.8 ng (*A. himalayanus*), and 7.41 ng (*A. kaulbacki*). We used a modified version of the shotgun preparation described in Streicher et al. (2016) to produce Illumina NextSeq® libraries. We used NEBNext® DNA Library Prep Master Mix Sets (New England Biolabs Inc.) for end-repair (NEB #E6050), dA-tailing (NEB #E6053), ligation (NEB #E6056) and PCR (NEB #E7805) to construct libraries. We did not fragment DNA prior to library construction because archival DNA from ethanol-preserved specimens is already highly degraded (McGuire et al., 2018).

End-repair reactions each contained 5 µL 10X Reaction Buffer, 2.5 µL enzyme mix, 2.5 µL PCR water and 40 µL degraded museum specimen DNA. Reactions were held for 30 minutes at 20 °C and then were cleaned using the same bead protocol as the DNA extraction (2.1X) eluting the cleaned, end-repaired fragments into 21 µL 10 mM Tris Buffer. For dA-tailing, each reaction contained 2.5 µL of 10X Reaction Buffer, 1.5 µL Klenow fragment, and 21 µL of cleaned, end-repaired sample. The dA-tailing reactions were held for 30 minutes at 37 °C and then were cleaned using the standard bead protocol (2.1X) and eluted into 12.5 µL of 10 mM Tris Buffer. For ligation, each reaction contained 5 µL of 5X Reaction Buffer, 2.5 µL Quick T4 DNA Ligase, 5 µL 1mM adapter (unique to each sample), and 12.5 µL cleaned, dA-tailed reaction. Adapters sequences for each sample are reported in Streicher et al. (2016)

Table 1. Complete list of valid *Amolops* species (as per 12 April 2022) giving relevant details for GenBank/Sequence Read Archive sequences (*12S-tVal-16S*, or *16S* only) used in maximum likelihood analysis, and *nd2* and *co1* used in *p*-distance analyses. NA, not applicable; NSA, no sequences available; Dist., District; Au. Co., Autonomous County; N.R., Nature Reserve; N.P., National Park; Mt., Mount; Prov., Province.

Species	**Locality**	**Specimen #**	***12S-tVal-16S / 16S***	***nd2***	***co1***	**Reference & Notes**
A. adicola Patel, Garg, Das, Stuart & Biju, *2021*	India: Arunachal Pradesh: Upper Siang Dist.	BNHS 6121 (holotype)	MZ229772.1	-	-	Patel et al. (2021)
A. afghanus (Günther, 1858a)	China: Yunnan: Yingjiang Co.	SYS a003852	MK604837.1	-	-	Lyu et al. (2019b); as *A. "marmoratus"* on GenBank
A. akhaorum Stuart, Bain, Phimmachak & Spence, 2010	Laos: LuangNamtha: Vieng Phou Kha.	FMNH 271355 (paratype)	FJ417158.2	-	-	Stuart et al. (2010); as *A.* "sp. BLS-2009" on GenBank
A. albispinus Sung, Hu, Wang, Liu & Wang, 2016	China: Guangdong: Shenzhen City: Mt. Wutong.	SYS a003452 (paratype)	MK263247.1	-	-	Lyu et al. (2019a)
A. aniqiaoensis Dong, Rao & Lü, 2005 (in Zhao et al., 2005)	China: Tibet.	KIZ 011136	MN953658.1	-	-	Wu et al. (2020)
A. archotaphus (Inger & Chan-ard, 1997)	Thailand: Chiang Mai: Doi Inthanon.	CUMZ A 2000.62	FJ417124.1	-	-	Stuart et al. (2010)
A. assamensis Sengupta, Hussain, Choudhury, Gogoi, Ahmed & Choudhury, 2008	NA	NSA	-	-	-	NA
A. australis Chan, Abraham, Grismer & Grismer, 2018	Malaysia: Peta, Endau-Rompin N.P.	LSUHC 7673 (paratype)	MF061745.1	-	-	"Chan K.O. direct submission" on GenBank, published in Chan et al. (2017); as *A.* "*larutensis*" on GenBank
A. beibengensis Jiang, Li, Zhou, Yan & Che, 2020 (in Che et al., 2020)	China: Tibet: Medog.	KIZ 016397 (paratype)	MN953662.1	MN958721.1	MN961359.1	Wu et al. (2020: as *A.* "sp. 2")
A. beibengensis	China: Tibet: Medog.	KIZ 011061 (topotype)	-	MN958722.1	MN961360.1	Wu et al. (2020: as *A.* "sp. 2")
A. bellulus Liu, Yang, Ferraris & Matsui, 2000	China: Yunnan: Lushui Co.	KIZ 9810021 (paratype)	DQ204473.1	-	-	Ngo et al. (2006)
A. chakrataensis Ray, 1992	NA	NSA	-	-	-	NA
A. chaochin Jiang, Ren, Lyu & Li, 2021	China: Sichuan: Chongzhou City	CIB 116971 (holotype)	MZ702027.1	-	-	Jiang et al. (2021); as *A.* "sp. c JLR-2021" on GenBank
A. chayuensis Sun, Luo, Sun & Zhang, 2013	China: Tibet: Baxoi Co.	SYS a007509	MK573820.1	-	-	Lyu et al. (2019b)
A. chunganensis (Pope, 1929)	China: Jiangxi: Mt. Jinggang.	SYS a004212	MK263263.1	-	-	Lyu et al. (2019a)
A. compotrix (Bain, Stuart & Orlov, 2006)	Vietnam: Kon Tum: Dak Glei Dist.	ZISP A7367 (paratype)	FJ417142.2	-	-	Stuart et al. (2010)
A. cremnobatus Inger & Kottelat, 1998	Vietnam: Nghe An: Khe Moi.	ROM 14528	DQ204477.1	-	-	Ngo et al. (2006)
A. cucae (Bain, Stuart & Orlov, 2006)	Vietnam: Lao Cai: Van Ban Dist.	AMNH 168727 (paratype)	FJ417144.2	-	-	Stuart et al. (2010)
A. daiyunensis (Liu & Hu, 1975)	China: Fujian: Dehua Co.	KIZ F93069 (topotype)	DQ204479.1	-	-	Ngo et al. (2006)
A. daorum (Bain, Lathrop, Murphy, Orlov & Ho, 2003)	Laos: Huaphahn: Vieng Tong Dist.	FMNH 255353	FJ417147.2	-	-	Stuart et al. (2010)
A. deng Jiang, Wang & Che, 2020 (in Che et al., 2020)	China: Tibet: Zayü.	KIZ 014116 (paratype)	MN953695.1	-	-	Wu et al. (2020: as *A.* "sp. 1")
A. formosus (Günther, 1876)	India: Meghalaya: "Khassya".	BMNH 1947.2.4.18 (holotype, *A. formosus*)	**SAMN28238801**	**SAMN28238801**	**SAMN28238801**	This study; Appendix I for assembled sequences.
A. formosus	Nepal: Prov. 1: Sankhuwasabha: Dobhan.	CDZMTU 0145	MT124521.1	-	-	Khatiwada et al. (2020); as *A.* "*nepalicus*" on GenBank
A. formosus [syn. *A. gyirongensis* Jiang, Wang, Wang, Pan & Che, 2020 (in Che et al., 2020)]	China: Tibet: Gyirong.	KIZ 012533 (paratype, *A. gyirongensis*)	MN953682.1	MN958739.1	MN961382.1	Wu et al. (2020: as *A.* "sp. 4")
A. formosus [syn. *A. gyirongensis*]	China: Tibet: Gyirong.	KIZ 012537 (paratype, *A. gyirongensis*)	MN953683.1	MN958740.1	MN961383.1	Wu et al. (2020: as *A.* "sp. 4")
A. formosus [syn. *A. gyirongensis*]	China: Tibet: Gyirong.	KIZ 012534 (paratype, *A. gyirongensis*)	MN953684.1	MN958741.1	MN961384.1	Wu et al. (2020: as *A.* "sp. 4")
A. formosus [syn. *A. gyirongensis*]	China: Tibet: Gyirong.	KIZ 012535 (paratype *A. gyirongensis*)	MN953685.1	MN958742.1	MN961385.1	Wu et al. (2020: as *A.* "sp. 4")
A. formosus [syn. *A. gyirongensis*]	China: Tibet: Gyirong.	KIZ 012536 (holotype *A. gyirongensis*)	MN953686.1	MN958743.1	MN961386.1	Wu et al. (2020: as *A.* "sp. 4")
A. cf. *gerbillus* (Annandale, 1912)	Bhutan: Trashigang: Bodidrang Chhu/Stream	SCZM 2015.06.06.1 (tissue no. D18)	**ON462437.1**	-	-	This study

Species	Locality	Specimen #	*12S-tVal-16S / 16S*	*nd2*	*co1*	Reference & Notes
A. gerutu Chan, Abraham, Grismer & Grismer, 2018	Malaysia: Terengganu: Gunung Tebu.	RMB 21077 (topotype)	MF061721.1	-	-	"Chan K.O. direct submission" on GenBank, published in Chan et al. (2017); as *A.* "*larutensis*" on GenBank
A. granulosus (Liu & Hu, 1961)	China: Sichuan: Mt. Guangwu.	SYS a005399	MK573811.1	-	-	Lyu et al. (2019b)
A. hainanensis (Boulenger, 1900)	China: Hainan: Lingshui.	KIZ 970512	DQ204481.1	-	-	Ngo et al. (2006)
A. himalayanus (Boulenger, 1888a)	India: West Bengal: Darjeeling.	BMNH 1947.2.3.83 (syntype)	**SAMN28238802**	-	-	This study; Appendix I for assembled sequence.
A. himalayanus	Nepal: Prov. 1: Ilam Dist.: Rakse Village.	SH 2789	MN953712.1	MN958770.1	MN961414.1	Wu et al. (2020: as *A.* "sp. 5") ["SH" abbreviation not explained]
A. himalayanus	Nepal: Prov. 1: Ilam Dist.: Mabu.	KIZ 040227	-	MN958771.1	MN961415.1	Wu et al. (2020: as *A.* "sp. 5")
A. himalayanus	Nepal: Prov. 1: Ilam Dist.: Maimajhuwa.	KIZ 040228	-	MN958772.1	MN961416.1	Wu et al. (2020: as *A.* "sp. 5")
A. hongkongensis (Pope & Romer, 1951)	China: Hong Kong.	ROM 16300 (topotype)	AF206453.1	-	-	Chen et al. (2005)
A. indoburmanensis Dever, Fuiten, Konu& Wilkinson, 2012	Myanmar: Chin: Mindat.	CAS 234720 (topotype)	MG909571.1	-	-	Arifin et al. (2018)
A. iriodes (Bain & Nguyen, 2004)	Vietnam: Ha Giang: Vi Xuyen Dist.	AMNH 163926 (paratype)	FJ417152.2	-	-	Stuart et al. (2010)
A. jaunsari Ray, 1992	NA	NSA	-	-	-	NA
A. jinjiangensis Su, Yang & Li, 1986	China: Yunnan: Mt. Gaoligong.	SYS a004571	MK573801.1			Lyu et al. (2019b)
A. kaulbacki (Smith, 1940)	Myanmar: Kachin: Pangnamdim.	BMNH 1940.6.1.1 (holotype)	**SAMN28238803**	-	-	This study; Appendix I for assembled sequence.
A. kaulbacki	China: Yunnan: Pianma.	SCUM 050402CHX	MN953736.1	MN958793.1	MN961437.1	Wu et al. (2020: as *A.* "*viridimaculatus*")
A. kaulbacki	China: Yunnan: Pianma.	SCUM 050403CHX	MN953737.1	MN958794.1	MN961438.1	Wu et al. (2020: as *A.* "*viridimaculatus*")
A. kohimaensis Biju, Mahony & Kamei, 2010	India: Nagaland: Kohima Dist.	WIIADA 751 (topotype)	MZ229774.1	-	-	Patel et al. (2021)
A. larutensis (Boulenger, 1899a)	Malaysia: Perak.	KUHE 15488	AB211484.1	-	-	Matsui et al. (2006)
A. lifanensis (Liu, 1945)	China: Sichuan: Lixian Co.	SYS a005374	MK573809.1	-	-	Lyu et al. (2019b)
A. loloensis (Liu, 1950)	China: Sichuan: Zhaojue City.	SYS a005346	MK604854.1	-	-	Lyu et al. (2019b)
A. longimanus (Andersson, 1939)	NA	NSA	-	-	-	NA
A. mahabharatensis Khatiwada, Shu, Wang, Zhao, Xie & Jiang, 2020	Nepal: Bagmati: Chitwan Dist: Hattibang.	CDZMTU 0110 (holotype)	MT124507.1	-	-	Khatiwada et al. (2020)
A. mantzorum (David, 1872)	China: Sichuan: Fengtongzhai.	SYS a005365	MK573808.1	-	-	Lyu et al. (2019b)
A. marmoratus (Blyth, 1855)	Myanmar: Mon.	CAS 240593 (topotype)	JF794456.1	-	-	Dever et al. (2012)
A. medogensis Li & Rao, 2005 (in Zhao et al., 2005)	China: Tibet: Medog Co.	SYS a006657 (topotype)	MK573813.1	-	MK568328.1	Lyu et al. (2019b)
A. medogensis	China: Tibet: Medog Co.	SYNU 04II6219 (paratype)	-	MN958769.1	MN961413.1	Wu et al. (2020)
A. medogensis	China: Tibet: Medog Co.	SYNU 04II6216 (paratype)	-	MN958768.1	MN961412.1	Wu et al. (2020)
A. medogensis	not mentioned.	SYS a007531	-	-	MK568332.1	"Lyu et al. 2019[b]" according to GenBank, but not mentioned in this paper.
A. medogensis	not mentioned.	SYS a007530	-	-	MK568331.1	"Lyu et al. 2019[b]" according to GenBank, but not mentioned in this paper.
A. medogensis	China: Tibet: Medog Co.	KIZ 06638 (topotype)	-	-	KU243077.1	Jiang et al. (2016)
A. medogensis	China: Tibet: Medog Co.	KIZ 06635 (topotype)	-	-	KU243076.1	Jiang et al. (2016)
A. mengdingensis Yu, Wu & Yang, 2019	China: Yunnan: Mengding.	KIZ 20160266 (holotype)	MK501809.1	-	-	Yu et al. (2019)
A. mengyangensis Wu & Tian, 1995	Vietnam: Lao Cai: Sa Pa.	MNHN[?] 1999.5811	KR827703.1	-	-	Grosjean et al. (2015: museum collection not explicitly stated in reference)
A. minutus Orlov & Ho, 2007	NA	NSA	-	-	-	NA
A. monticola (Anderson, 1871)	India: Sikkim: Tarku Forest Block	WIIADA 544	MZ229773.1	-	-	Patel et al. (2021)
A. nepalicus Yang, 1991	Nepal: Prov. 1: Ilam: Mabu.	KIZ 040269	MN953750.1	-	-	Wu et al. (2020: as *A.* "sp. 7")
A. nepalicus	Nepal: Prov. 1: Taplejung: Lamatar.	CDZMTU 0135	MT124519.1	-	-	Khatiwada et al. (2020); as *A.* "*formosus*" on GenBank
A. nidorbellus Biju, Mahony & Kamei, 2010	NA	NSA	-	-	-	NA
A. nyingchiensis Jiang, Wang, Xie, Jiang & Che, 2016 (in Jiang et al., 2016)	China: Tibet: Medog Co.	SYS a006679 (topotype)	MK573814.1	-	-	Lyu et al. (2019b)
A. ottorum Pham, Sung, Pham, Le, Ziegler & Nguyen, 2019	NA	NSA	-	-	-	NA
A. pallasitatus Qi, Zhou, Lyu, Lu & Li, 2019 (in Qi et al., 2019)	China: Tibet: Dinggyê Co.	SYNU 1507034 (paratype)	MK573816.1	-	-	Qi et al. (2019); as *A.* "sp. n. ZTL-2019" on GenBank
A. panhai Matsui & Nabhitabhata, 2006	Myanmar: Tanintharyi: Dewei Dist.	CAS 229816	MG909606.1	-	-	Arifin et al. (2018)
A. putaoensis Gan, Qin, Lwin, Li, Quan, Liu & Yu, 2020	Myanmar: Kachin: Putao Co.	GXNU QT 20170200 (holotype)	MT901382.1	-	-	Gan et al. (2020b)
A. cf. *putaoensis*	Bhutan: Trashigang: Khaling Chhu/Stream (also called Mongnagkhola).	SCZM 2015.06.29.1 (tissue no. D17)	**ON462438.1**	-	-	This study
A. ricketti (Boulenger, 1899b)	China: Jiangxi: Wuyishan N.R.	SYS a001605	KX507303.1	-	-	Sung et al. (2016)
A. senchalensis (Chanda, 1987)	NA	NSA	-	-	-	NA
A. shuichengicus Lyu & Wang, 2019 (in Lyu et al., 2019b)	China: Guizhou: Shuicheng Co.	SYS a004956 (paratype)	MK604845.1	-	-	Lyu et al. (2019b)
A. sinensis Lyu, Wang & Wang, 2019	China: Guangdong: Shimentai N.R.	SYS a007107 (holotype)	MK263299.1	-	-	Lyu et al. (2019a)
A. spinapectoralis Inger, Orlov &Darevsky, 1999	Vietnam: Kon Tum: Ngoc Linh.	ROM 27424	DQ204488.1	-	-	Ngo et al. (2006)
A. teochew Zeng, Wang, Lyu & Wang, 2021	China: Guangdong: Mt Fenghuang	SYS a008705 (holotype)	MZ447970.1	-	-	Zeng et al. (2021)
A. torrentis (Smith, 1923)	China: Hainan: Lingshui.	KIZ 970543	DQ204489.1	-	-	Ngo et al. (2006)
A. tuanjieensis Gan, Yu & Wu, 2020	China: Yunnan: Gengma Dai and Wa Au. Co.	GXNU YU 110003 (paratype)	MN832772.1	-	-	Gan et al. (2020a)
A. tuanjieensis	China: Yunnan: Gengma Dai and Wa Au. Co.	GXNU YU 110005 (holotype)	MN832773.1	-	-	Gan et al. (2020a)
A. tuberodepressus Liu & Yang, 2000	China: Yunnan: Mt. Ailao.	SYS a003900	MK573797.1	-	-	Lyu et al. (2019b)
A. viridimaculatus (Jiang, 1983)	China: Yunnan: Mt. Gaoligong.	SYS a003753	MK573793.1	-	MK568310.1	Lyu et al. (2019b)
A. viridimaculatus	China: Yunnan: Mt. Gaoligong.	SYS a003754	MK573794.1	-	MK568311.1	Lyu et al. (2019b)
A. viridimaculatus	China: Yunnan: Mt. Gaoligong.	SYS a003812 (topotype)	MK604835.1	-	MK605596.1	Lyu et al. (2019b)
A. viridimaculatus	China: Yunnan: Mt. Gaoligong.	SYS a003813 (topotype)	MK604836.1	-	MK605597.1	Lyu et al. (2019b)
A. viridimaculatus	China: Yunnan: Tengchong.	KIZ 93501	DQ204490.1	-	-	Ngo et al. (2006)
A. viridimaculatus	China: Yunnan: Tengchong.	KIZ 048487	MN953731.1	MN958788.1	MN961434	Wu et al. (2020)
A. viridimaculatus	China: Yunnan: Tengchong.	KIZ 048488	MN953732.1	MN958789.1	MN961434	Wu et al. (2020)
A. viridimaculatus	China: Yunnan: Pingbian.	KIZ 047019	MN953734.1	MN958791.1	-	Wu et al. (2020)
A. viridimaculatus	China: Yunnan: Pingbian.	KIZ 047020	MN953735.1	MN958792.1	-	Wu et al. (2020)
A. viridimaculatus	China: Yunnan: Pianma.	SCUM 050423CHX	MN953733.1	MN958790.1	MN961436.1	Wu et al. (2020)
A. viridimaculatus	China: Yunnan: Gongshan.	CAS 242607	MN953738.1	-	-	Wu et al. (2020); *A.* "*medogensis*" on CAS Herpetology Collection Database
A. viridimaculatus	China: Yunnan: no locality given.	"C-green 05"	AB211480.1	-	-	Matsui et al. (2006)
A. viridimaculatus [syn. *A. splendissimus* Orlov & Ho, 2007]	Vietnam: Lao Cai: Bat Xat Dist.	VNMN 010923 [EBU 85309]	MZ484725.1	-	-	Zhang et al. (2021)
A. viridimaculatus [syn. *A. splendissimus*]	Vietnam: Lao Cai: Bat Xat Dist.	AMS R188526 [EBU 85336]	MZ484726.1	-	-	Zhang et al. (2021)
A. viridimaculatus [syn. *A. splendissimus*]	Vietnam: Lao Cai: Bat Xat Dist.	HLNP2017100900016 [EBU 95337]	MZ484727.1	-	-	Zhang et al. (2021)

Species	Locality	Specimen #	*12S-tVal-16S / 16S*	*nd2*	*co1*	Reference & Notes
A. viridimaculatus [syn. *A. caelumnoctis* Rao & Wilkinson, 2007]	China: Yunnan: Luchun Co.	SWFU 003995 [Yuan 16267]	MZ484728.1	-	-	Zhang et al. (2021)
A. viridimaculatus [syn. *A. caelumnoctis*]	China: Yunnan: Luchun Co.	SWFU 004525 [Yuan 16268]	MZ484729.1	-	-	Zhang et al. (2021)
A. viridimaculatus [syn. *A. caelumnoctis*]	China: Yunnan: Wenshan Co.	SWFU 004524 [Yuan 16447]	MZ484730.1	-	-	Zhang et al. (2021)
A. vitreus (Bain, Stuart & Orlov, 2006)	Laos: Phongsaly: Phongsaly Dist.	FMNH 258187 (paratype)	FJ417164.2	-	-	Stuart et al. (2010)
A. wangyali sp. nov.	Bhutan: Trashigang: Jere Chhu/Stream.	Specimen not collected (tissue no. D4)	**ON462439.1**	-	-	This study
A. wangyali sp. nov.	Bhutan: Trashigang: Jere Chhu/Stream.	Specimen not collected (tissue no. D7)	**ON462440.1**	-	-	This study
A. wangyali sp. nov.	Bhutan: Trashigang: Jere Chhu/Stream.	SCZM 2015.03.28.1 (tissue no. D10; field no. TND011)	**ON462446.1**	-	-	This study
A. wangyali sp. nov.	Bhutan: Trashigang: Jere Chhu/Stream.	SCZM 2015.03.28.2 (tissue no. D11; field no. TND012)	**ON462447.1**	-	-	This study
A. wangyali sp. nov.	Bhutan: Trashigang: Bodidrang Chhu/Stream.	SCZM 2019.07.18.1 [field no. MW 11585] (holotype)	**ON462441.1**	-	-	This study
A. wangyali sp. nov.	Bhutan: Trashigang: Bodidrang Chhu/Stream.	SCZM 2019.07.18.2 [field no. MW 11587] (paratype)	**ON462442.1**	-	-	This study
A. wangyali sp. nov.	Bhutan: Trashigang: Bodidrang Chhu/Stream.	SCZM 2019.08.02.1 [field no. SC0034] (paratype)	**ON462445.1**	-	-	This study
A. wangyali sp. nov.	Bhutan: Trashigang: Rongthong.	SCZM 2019.07.20.1 [field no. SC0001]	**ON462443.1**	-	-	This study
A. wangyali sp. nov.	Bhutan: Trashigang: Kanglung.	SCZM 2019.07.27.1 [field no. SC0017]	**ON462444.1**	-	-	This study
A. wangyufani Jiang, 2020 (in Che et al., 2020)	China: Tibet: Zayü.	KIZ 014067 (paratype)	MN953740.1	MN958796.1	MN961440.1	Wu et al. (2020: as *A.* "sp. 3")
A. wangyufani	China: Tibet: Zayü.	KIZ 014068 (holotype)	-	MN958797.1	MN961441.1	Wu et al. (2020: as *A.* "sp. 3")
A. wenshanensis Yuan, Jin, Li, Stuart & Wu, 2018	China: Guangxi: Jingxi City.	KU KUH 292045 (paratype)	FJ417129.2	-	-	Stuart et al. (2010)
A. wuyiensis (Liu & Hu, 1975)	China: Anhui: Qingyang.	[CIB] QLY53	KF771291.1	-	-	Xia et al. (2014)
A. xinduqiao Fei, Ye, Wang & Jiang, 2017	China: Sichuan: Kangding.	"KIZ041127" (fide Wu et al. 2020) / "KIZ 014127" (fide Fei et al. 2017) (paratype)	MN953764.1	-	-	Wu et al. (2020)
A. yarlungzangbo Jiang, Wang, Li, Qi, Li & Che, 2020 (in Che et al., 2020)	China: Tibet: Medog.	KIZ 014086 (paratype)	MN953744.1	-	-	Wu et al. (2020: as *A.* "sp. 6")
A. yatseni Lyu, Wang & Wang, 2019 (in Lyu et al., 2019a)	China: Guangdong: Zhongshan City.	SYS a006807 (holotype)	MK263290.1	-	-	Lyu et al. (2019a)
A. yunkaiensis Lyu, Wang, Liu, Zeng & Wang, 2018 (in Lyu et al., 2018)	China: Guangdong: Ehuangzhang N.R.	SYS a003979 (paratype)	MK263253.1	-	-	Lyu et al. (2019b)

and we used indexes 20, 22, and 23 on *A. formosus*, *A. himalayanus*, and *A. kaulbacki*, respectively. Reactions were held for 15 minutes at 20 °C, and then pooled together (also with some additional samples not reported here, see below) for size selection. We performed size selection using a BluePippin™ (Sage Science) and 2 % Agarose Gel Cassette (No. BDF2010) with internal size standards. Pooled ligations were cleaned using the standard bead protocol (2.1X) and eluted into 30 µL of 10 mM Tris, which was mixed with 10 µL of BluePippin™ size standard before being loaded into the sample well of the BluePippin™. We selected for a size range of 270–370 base pairs (bp) in order to target DNA insert sizes that were < 300 bp in length. We then performed an enrichment PCR using the size-selected sample by combining 6 µL water, 1 µL each of Illumina TruSeq® primers (i5 and i7), 10 µL Q5® HotStart HiFi PCR Master Mix, and 2 µL of sample. This recipe was repeated 15 times to use all 30 µL of size-selected adapter-ligated samples extracted from the BluePippin™. We ran the 15 PCRs along with a negative control for 18 cycles. Following the PCR-enrichment, we combined all reactions and cleaned them using the standard bead protocol (2.1X), eluting into 15 µL of 10 mM TRIS. We confirmed the successful enrichment of the pooled library using an Agilent® TapeStation System.

The three *Amolops* samples were processed with 45 additional anuran and squamate archival DNA samples (results will be discussed in detail elsewhere; Mahony et al., in litt.). Sequencing was performed on an Illumina NextSeq® 500 using a mid-output paired end 150 kit (300 cycles) at the Core Research Labs at the NHMUK. Sequencing output was demultiplexed and converted into FASTQ format using the bcl2fastq v2.15.0.4 software from Illumina® (https://github.com/brwnj/bcl2fastq). Resulting paired-end FASTQ files were then processed through Illumiprocessor using Trimmomatic (Faircloth, 2013; Del Fabbro et al., 2013), to remove low quality bases and adapter contamination.

Sequence assembly for the three archival *Amolops* samples was performed by mapping read 1, read 2, and singleton reads to a reference mtDNA sequence. Reference mapping was conducted in Geneious® V.8.1.9 using the 'Map to reference' feature with the 'Medium sensitivity / Fast' setting and fine tuning of up to five iterations. Morphologically, *A. formosus*, *A. himalayanus* and *A. kaulbacki* most closely resemble *viridimaculatus* species group taxa, so *A. viridimaculatus* (Jiang, 1983), GenBank number DQ204490.1 was selected as the reference sequence. This sequence also represented the longest continuous sequence of the *12S-tVal-16S* for a *viridimaculatus* species group taxon available on GenBank which maximised the area for read mapping. We then inferred the *12S-tVal-16S* sequence of each type specimen by exporting the consensus sequence of all mapped reads.

Sequencing errors, environmental contamination and crosstalk (index hopping) can cause issues for consensus sequence inference when using reference mapping. These issues can be problematic in regions with low read coverage, when mapped reads are relatively short and when a reference sequence is not available for a closely related species. To mitigate erroneous mapping of reads, the following quality control measures were taken to avoid assembling chimeric sequences: i) we used a reference sequence from a morphologically-similar species (see above), ii) reads suspected to be erroneous because they contained many polymorphisms not observed in overlapping and adjacent mapped reads (particularly an issue for the *A. formosus* sample) were deleted from the assembly, and iii) reads from low coverage regions were compared (using BLAST) to the whole GenBank nucleotide database to confirm that they were most similar to other available *Amolops* sequences (instead of human and/or bacterial contaminants, or the other anuran and squamate species included in the NextSeq® 500 run).

Homologous sequences that comprise either *12S-tVal-16S*, or just the partial *16S* sequence were downloaded from GenBank, targeting at least one representative of all available species and particularly sequences for type specimens when available. As exceptions, we included all available sequences for *A. viridimaculatus* and all unique sequences for other *viridimaculatus* group taxa in order to identify additional populations of *A. formosus*, *A. himalayanus* and *A. kaulbacki* which may have been sequenced in previous studies but misidentified (Table 1). Downloaded sequences were generated in the following studies: Chen et al. (2005); Matsui et al. (2006); Ngo et al. (2006); Stuart et al. (2010); Dever et al. (2012); Xia et al. (2014); Grosjean et al. (2015); Sung et al. (2016); Arifin et al. (2018); Lyu et al. (2019a; 2019b); Qi et al. (2019); Yu et al. (2019); Gan et al. (2020a; 2020b); Khatiwada et al. (2020); Wu et al. (2020); Jiang et al. (2021); Patel et al. (2021); Zeng et al. (2021); Zhang et al. (2021). The dataset comprising newly generated and downloaded sequences was aligned using MUSCLE (Edgar, 2004) in MEGA7 (Kumar et al., 2016; Tamura & Nei, 1993) with default settings. The alignment was visualised in MEGA7 and ambiguously aligned regions were further adjusted by eye where necessary to ascertain homology. Phylogenetic relationships were estimated using RAxML-HPC2 (Stamatakis, 2014) on XSEDE (CIPRES platform: Miller et al., 2010), using default settings with the GTR CAT model on an unpartitioned alignment and 1000 rapid bootstrap (bs.) replicates. The resulting maximum likelihood phylogenetic tree was viewed using FigTree (Rambaut, 2009). The south-eastern China clade comprising *A. spinapectoralis* Inger, Orlov & Darevsky, 1999, and the *hainanensis*, *daiyunensis* and *ricketti* species groups, has been demonstrated to be the sister taxon to the clade containing all remaining *Amolops* species in phylogenetic studies that utilised high-throughput sequencing techniques (i.e. 330 loci in Wu et al. [2020]; 242 nuclear loci + mitogenomes in Zeng et al. [2020]). Therefore, we rooted the tree ("user selected" option in FigTree) with the south-eastern China clade.

Sequence comparisons involving additional mitochondrial genes were required to compare *A. gyirongensis* Jiang, Wang, Wang, Pan & Che, 2020 (in Che et al., 2020) to *A. formosus* due to limited *16S* data from the holotype of *A. formosus*. We used a NADH dehydrogenase 2 (*nd2*) and a cytochrome c oxidase subunit 1 (*co1*) sequence (MN958739.1 & MN961382.1, respectively; Wu et al., 2020) from a paratype (KIZ012533) of *A. gyirongensis* as the reference sequences for mapping archival DNA reads from the holotype of *A. formosus*. Read mapping was performed on Geneious as described above. The resulting consensus (assembled) sequences of *A. formosus* were aligned (as described above) against all available *nd2* and *co1* sequences on GenBank for other *viridimaculatus* species group taxa (Table 1): comparative sequences were generated in the following studies: Jiang et al. (2016); Lyu et al. (2019b); Wu et al. (2020). Uncorrected *p*-distances were generated for the resulting *nd2* and *co1* alignments in MEGA7 using default settings (Kumar et al., 2016; Tamura & Nei, 1993), to estimate distance between *A. gyirongensis* and the holotype of *A. formosus* relative to intraspecific and interspecific distances within and between other valid *viridimaculatus* species group taxa. All newly generated Sanger sequences and Illumina® reads are available on GenBank and the Sequence Read Archive (Leinonen et al., 2010) with the accession numbers ON462437–ON462447, and SAMN28238801–SAMN28238803, respectively (Table 1). Assembled sequence contigs used in analyses for the arcDNA samples are given in Appendix I.

Taxonomy and morphology

Specimens of geographically relevant species were directly examined from the following museum collections: BMNH, BNHS, CAS, SDB, ZSIK; images of type specimens were also obtained from NRM (Appendix II). Due to a prevalence of misidentifications in the literature for *Amolops* (SM, pers. obs.), for species that could not be directly examined, relevant taxonomic literature is cited for each morphological character used in the 'Morphological comparisons' section. Only characters verified on all examined specimens are utilised to represent the new and known species in the 'Morphological comparisons' sections. Sex and maturity of specimens were confirmed by direct examination of the gonads. Sex is not provided for the character/s being discussed where characters are compared based on a combination of male, female and juvenile specimens. To assess dermal microstructures such as asperities coverage, the entire skin surface (of all examined specimens) was viewed under binocular microscope. All measurements on specimens examined in this study were made by SM using digital calipers, in millimetres rounded to the nearest 0.1 mm. Measurements were taken on the right side of the specimen, except when a character was damaged, in which case the measurement was taken on the left side (as noted in text). In the 'Morphological comparisons' section, percentages given for min.–max. ranges are rounded up or down to the nearest whole number. Morphometric abbreviations used in the text and tables are as follows: snout to vent length, from snout tip to cloacal opening (SVL); maximum head width, measured at posterior angle of jaws (HW); head length, measured from retroarticular process of mandible to snout tip (HL); snout depth, measured at anterior border of orbit (SD); snout length, measured from snout tip to anterior bony orbital border (SL); snout to nostril, distance from centre of nostril to snout tip (SN); orbit to nostril, distance from anterior bony orbital border to centre of nostril (EN); minimum distance between nostrils (IN); eye length, horizontal distance between anterior and posterior bony orbital borders (EL); inter upper eyelid width, shortest distance between upper eyelids (IUE); maximum upper eyelid width (UEW); internal front of eyes, distance between anterior (/inner) canthi (IFE); internal back of eyes, shortest distance between posterior (/outer) canthi (IBE); maximum tympanum diameter (TD); tympanum to eye, distance from anterior border of tympanum to posterior bony orbital border (TE); forearm length, from elbow to proximal border of inner metacarpal tubercle (FAL); hand length, from proximal border of inner metacarpal tubercle to tip of third digit (HAL); first finger length, from tip of first digit to its base where it joins second digit (FIL); second finger length, from tip of second digit to its base where it joins first digit (FIIL); third finger length, from tip of third digit to its base where it joins second digit (FIIIL); fourth finger length, from tip of fourth digit to its base where it joins third digit (FIVL); minimum third finger width, taken at approximately half distance between distal subarticular tubercle and base of disc (FIIIW); maximum disc widths of fingers I–IV (FIDW, FIIDW, FIIIDW, FIVDW); fourth toe width, taken dorsally on digit proximal to disc (TIVW); maximum disc widths of toes I–V (TIDW, TIIDW, TIIIDW, TIVDW, TVDW); thigh length, from centre of cloacal opening to knee taken when femur is flexed at right angle to body (TL); shank (containing tibia) length, from knee to tibio-tarsal articulation taken when leg is held in naturally folded position (SHL); maximum width of shank (SHW), tarsus and foot length, from tibio-tarsal articulation to tip of fourth digit (TFL); foot length, from proximal edge of inner metatarsal tubercle to tip of fourth digit (FOL); maximum length of inner metatarsal tubercle (IMT). Digits are numbered from preaxial (inner-FI/TI) to postaxial (outer-FIV/TV) side. Webbing formula between toes follows Savage & Heyer (1997). To supplement morphometric data for the type series of the newly described species, SVL and SHL measurements for four males and four females from Nidup et al. (2016) are included in the 'Morphological comparisons' section as these standard measurements are not expected to be excessively subject to methodological differences between the studies (Hayek et al., 2001). We sequenced four of the measured animals in Nidup et al. (2016: i.e. TND005, TND008 [both not collected], TND011 [SCZM 2015.03.28.1], TND012 [SCZM 2015.03.28.2]) to confirm that they represent the new species described herein.

Map

The software Quantum GIS (QGIS v.2.14.3-Essen) was used to make a topographic map using the 250 m spatial resolution Shuttle Radar Topography Mission (SRTM) layer available from DIVA-GIS (http://www.diva-gis.org), and other basic layers from the Natural Earth Quick Start Kit (http://www.naturalearthdata.com). GPS coordinates and elevation given herein for localities reported in literature without this information were estimated using Google Maps (https://maps.google.com/, accessed April 2021). All coordinates plotted on the map are given in Table 2.

RESULTS & DISCUSSION

Molecular phylogenetics

The shotgun high-throughput sequencing of the three archival DNA samples was successful. These results demonstrate that standard DNA library preparation is a viable method for obtaining archival DNA sequence data from museum specimens. Further discussion of our findings for other taxa and suggestions for improving the protocol will be discussed elsewhere. Total post trimming reads for each sample were 1,914,338 for *A. formosus*, 7,525,416 for *A. himalayanus* and 32,886,900 for *A. kaulbacki*. The final *12S-tVal-16S* alignment used in the phylogenetic analyses had a total length of 1401 bp, in which the sequences of *A. himalayanus* and *A. kaulbacki* were complete, however, the *A. formosus* sequence had a total of 497 bp of missing data. The consensus sequences were generated using variable coverage depths from 2–777 reads per nucleotide for the three samples (read depth 2–59, n=146 total reads for *A. formosus*; read depth 8–120, n=614 total reads for *A. himalayanus*; read depth 29–777, n=3125 total reads for *A. kaulbacki*). The consensus sequence for the holotype of *A. formosus* (collected ca. 1870 based on the timing of Jerdon's visit to 'Khasia' fide, Mahony et al., 2018) and a syntype of *A. himalayanus* (collected sometime between 1870 and 1888; SM, unpublished) were identical to *16S* sequences identified as *A. formosus* in Kathiwada et al. (2020) and as *Amolops* "sp. 5" in Wu et al. (2020), respectively, generated from recently collected tissue samples of populations from eastern Nepal. The consensus sequence for the holotype of *A. kaulbacki* (collected between 82 and 84 years ago; Smith, 1940) was identical to two *16S* sequences from Wu et al. (2020) identified as *A. "viridimaculatus"* from Yunnan, China (Fig. 1).

Table 2. Localities plotted in the distribution map (Fig. 7) for *Amolops wangyali* sp. nov. and for populations suspected to be conspecific with this species but requiring further taxonomic attention. NA. not applicable.

Species	Country	State	District	Locality	GPS	Elevation [m a.s.l.]	GPS / elevation notes	Reference
A. wangyali sp. nov.	Bhutan	N/A	Trashigang	"Jere Chhu (27°12'21.90"N, 91°36'12.20"E), Khaling, … 2,073 m"	27.206083, 91.603389	2073	GPS & elevation as reported in the reference.	Nidup et al. (2016)
A. wangyali sp. nov.	Bhutan	N/A	Trashigang	"Khaling [Chhu/Stream] (27°11´26.18´´N,91° 36´09.40´´E)"	27.190606, 91.602611	2070	GPS as reported in the reference, elevation & coordinate conversion based on plotted GPS point in Google Maps.	Nidup et al. (2016)
A. wangyali sp. nov.	Bhutan	N/A	Trashigang	"Bodidrang [Chhu/Stream] (27°17´20.33´´N, 91°30´56.28´´E)"	27.288981, 91.515633	1640	GPS as reported in the reference, elevation & coordinate conversion based on plotted GPS point in Google Maps.	Nidup et al. (2016); Limbu et al. (2020)
A. wangyali sp. nov.	Bhutan	N/A	Trashigang	"Kanglung: Road from Sherubtse College to Trashigang: Bodidrang [Chhu/Stream]: Namla"	27.27223, 91.53129	1750	GPS & elevation as reported in the reference.	Streicher et al. (2020)
A. wangyali sp. nov.	Bhutan	N/A	Trashigang	"Kanglung: Road from Sherubtse College to Trashigang: Bodidrang [Chhu/Stream]: Namla"	27.27023, 91.53043	1738	GPS & elevation as reported in the reference.	Streicher et al. (2020)
A. wangyali sp. nov.	Bhutan	N/A	Trashigang	"Rongthong"	27.2808, 91.53937	1520	GPS & elevation as reported in the reference.	Streicher et al. (2020)
A. wangyali sp. nov.	Bhutan	N/A	Trashigang	Thragom, a small stream above Kanglung BHU Hospital, Kanglung Gewog (village block)	27.28031, 91.51456	1950	GPS & elevation as reported herein.	This study.
A. wangyali sp. nov.	Bhutan	N/A	Trashiyangtse	"Serkang Chu, … Choetenkora town [27°36'50.00"N,91° 29'32.00"E], … Trashiyangtse District … 1745 m"	27.605298, 91.493766	1745	GPS as reported in the reference, plotted and converted in Google Maps.	Wangyal (2013)
A. cf. *wangyali*	India	Arunachal Pradesh	West Kameng	Bompu (1950–2200 m a.s.l.), Eaglenest Wildlife Sanctuary	27.066411, 92.405947	1950	GPS taken as Bompu camp ca. 1950 m a.s.l., coordinates estimated from Google Maps.	Athreya (2006)
A. cf. *wangyali*	India	Arunachal Pradesh	West Kameng	"New Khellong (1250 m)", Eaglenest Wildlife Sanctuary	27.022367, 92.414367	1250	GPS taken as "New Khellong" 27° 01.342 N 92° 24.862 E, 1270 m from Sondhi & Kunte (2016) though the plotted point is at an elevation of ca. 1040 m a.s.l. in Google Maps.	Athreya (2006)
A. cf. *wangyali*	India	Arunachal Pradesh	West Kameng	"Sessni (1250 m)", Eaglenest Wildlife Sanctuary	27.047500, 92.418611	1250	GPS taken as "Sessni (27° 02'51" N, 92° 25'07" E; 1250 m)" from Agarwal et al. (2010), plotted and coordinate converted in Google Maps.	Athreya (2006)

Our overall phylogeny of *Amolops* resolved an identical systematic arrangement of major species groups identified elsewhere (Wu et al., 2020; Zeng et al., 2020; Fig. 1). Support for monophyly was moderate to high (bs. 76–100) for most species groups except the *mantzorum* group (bs. 63) as observed elsewhere (Wu et al., 2020, Fig. 1). Within the various species groups the topology of our tree differed slightly from the mitochondrial tree in Wu et al. (2020, fig. 1), and support values for relationships within the species groups were generally low (Fig. 1). Our phylogeny placed the recently named *A. pallasitatus* Qi Zhou, Lyu, Lu & Li, 2019 (in Qi et al., 2019) as a member of the *viridimaculatus* group, which was previously placed within the broader concept of the '*mantzorum* group' where it was sister to a clade containing *A. viridimaculatus* and *A. medogensis* Li & Rao, 2005 (in Zhao et al., 2005) (Qi et al., 2019). The expanded phylogeny of Wu et al. (2020) included *A. viridimaculatus* and *A. medogensis* and four unidentified taxa labelled as *Amolops* sp. 2–5, the six lineages forming a distinct clade which they defined as the '*viridimaculatus* group'. Wu et al's. (2020) analyses did not include sequences for *A. pallasitatus* or *A. formosus* (from Qi et al., 2019 & Khatiwada et al., 2020, respectively) which might not have been available to them due to the short timeframe in which the three studies were published. Our study demonstrates that specimen numbers associated with sequences for three of the unidentified species (*Amolops* sp. 2–4) in Wu et al. (2020) match three of the recently described species in Che et al. (2020). Our archival DNA sequencing also confirms the identity of the lineage *Amolops* "sp. 5" of Wu et al. (2020; labelled *A.* "cf. *monticola*" in Che et al., 2020: fig. 59) represented by sequences from three localities in eastern Nepal ("Rakse Village", "Mabu", and "Maimajhuwa" in Ilam District, Province No. 1) as *A. himalayanus* (Fig. 1), representing the first genetically verified populations of this species from Nepal.

Amolops kaulbacki is another enigmatic species

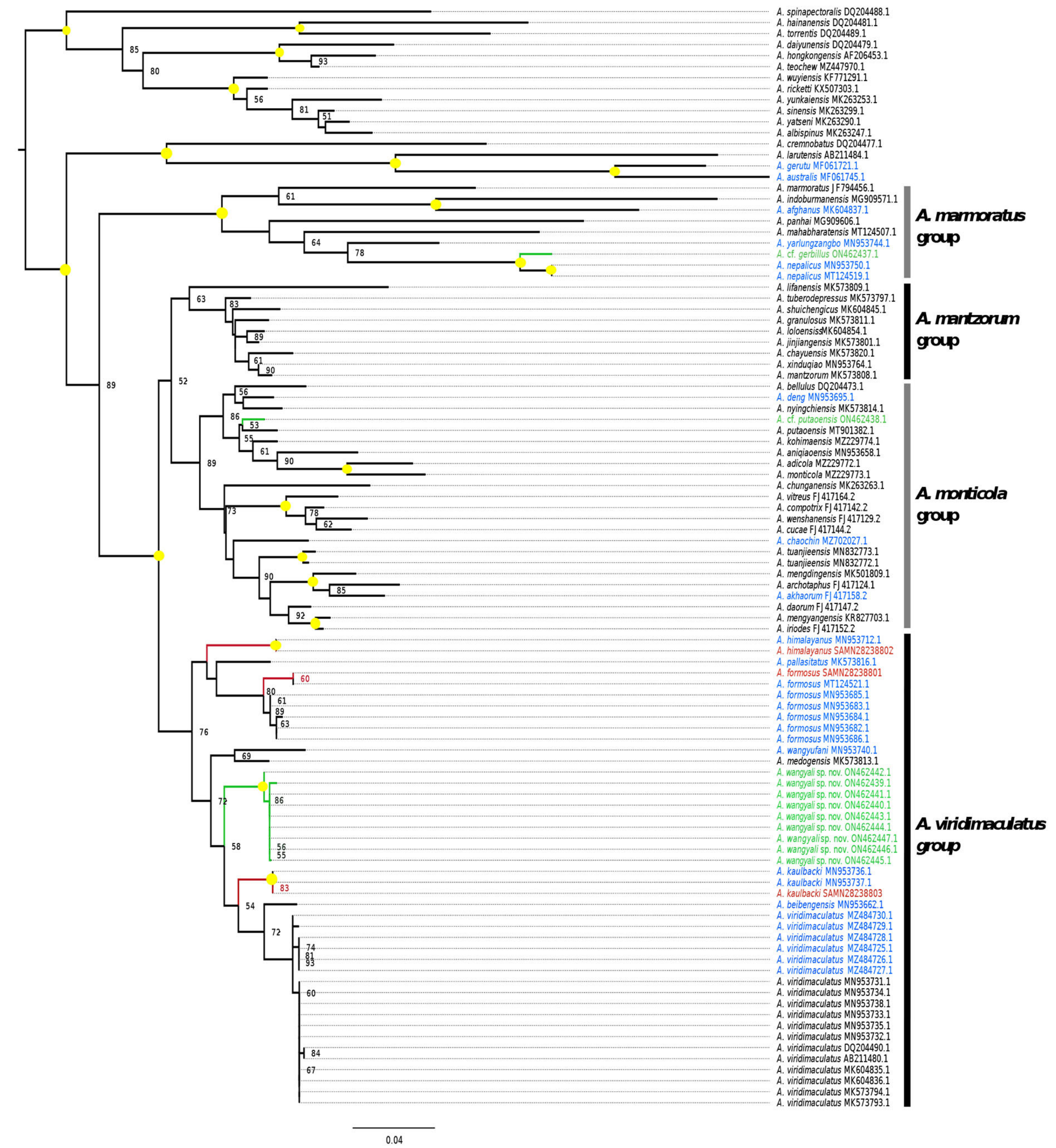

Figure 1. Maximum likelihood phylogeny based on the *12S-tVal-16S* genes for the genus *Amolops* showing the systematic position of the eleven Bhutan samples (green) and the archival DNA sequences for the three type specimens (red). Species identifications in blue differ from those given in GenBank which were misidentified, not identified, or required updating based on the results of this study (Table 1). GenBank/Sequence Read Archive numbers follow species names. Bootstrap support values ≥95 are represented by yellow spots, values >50 are given next to relative nodes, values <50 are not given.

described based on two specimens from Pangnamdim (27° 42′ N, 97° 54′ E), Kachin State in northern-most Myanmar (Smith, 1940). Aside from a questionable report of this species from north-east India (see Lalronunga et al., 2020), no verifiable subsequent accounts of this species are known since its original description (Smith, 1940). Our archival DNA sequencing of the holotype allowed us to correct the identification of two sequences previously identified as *A. "viridimaculatus"* from China (Wu et al., 2020). These two sequences are reported to have come from "Pianma", Yunnan, which could either refer to Pianma Town, Zhenyuan County, Puer Prefecture-level City, central Yunnan Province (according to Google Maps), or more likely Pianma Township (ca. 26° 01.9' N, 98° 38.01' E), situated close to the China-Myanmar border, in Lushui County, Nujiang Prefecture, north-western Yunnan Province (Liu et al., 2000). The latter locality lies ca. 200 km southeast of the type locality of *A. kaulbacki*, and represents a new country record for China and a second verified locality for the species. Wu et al. (2020) also included a sequence from *A. viridimaculatus* sensu stricto (hereafter s.s.) from "Pianma" Yunnan, indicating that the two species might even be sympatric at this locality (assuming the authors were not referring to a different place called "Pianma"), and Liu et al. (2000) mentioned that *A. "viridimaculatus"* was collected at Pianma (Lushui) along with the type specimens of *A. bellulus* (Liu et al., 2000). We recommend that specimens in museum collections previously identified as *A. "viridimaculatus"* from western Yunnan be re-examined to determine which species they represent. We also recommend that authors of molecular phylogenetic studies either provide specific locality information (e.g. GPS coordinates) for all newly sequenced specimens, or refer to a permanent source for this information (e.g. a publication/accessible online museum collection database) to enable georeferencing of sequenced specimens.

The recently collected eastern Bhutan populations of *Amolops* we sequenced represent three distantly related species. One of the species (formally described below as new to science) is nested within the *viridimaculatus* group though its relationship with other members of the group is not clear due to poor support for internal nodes within this clade. Our analysis demonstrates that the *viridimaculatus* group now contains the following nine species confirmed by DNA sequence data: *A. baibengensis* Jiang, Li, Zhou, Yan & Che, 2020 (in Che et al., 2020), *A. formosus* (including *A. gyirongensis*, see taxonomic discussion below), *A. himalayanus*, *A. kaulbacki*, *A. medogensis*, *A. pallasitatus*, *A. viridimaculatus* (including *A. splendissimus* Orlov & Ho, 2007, see taxonomic discussion below), *A. wangyufani* Jiang, 2020 (in Che et al., 2020) and the new species described below (Fig. 1). The second Bhutan species (SCZM 2015.06.06.1 [tissue no. D18]), collected from Bodidrang Chhu/Stream, Trashigang District, is resolved as sister to the closely related Nepal population identified as *A. nepalicus* Yang, 1991 (Khatiwada et al., 2020; Fig. 1). The Bhutan population lies geographically closer to the type locality of *A. gerbillus* (Annandale, 1912) (360 km to the east) than to the nearest reported locality of *A. nepalicus* (the type locality, ca. 417 km to the west). Until further comparisons can be made, we recommend the use of "*A.* cf. *gerbillus*" for populations representing the *marmoratus* group from Bhutan. Our phylogenetic analysis (Fig. 1) demonstrates that the sequence from "Mabu", Ilam District, Province No. 1, Nepal referred to as *Amolops* "sp. 7" in Wu et al. (2020) is conspecific with the species identified as *A. nepalicus* in Khatiwada et al. (2020). This adds a third population to the known distribution of this species (Khatiwada et al., 2021) which lies ca. 76 km south-east of the nearest previously reported locality (type locality), and only ca. 5 km from the border with West Bengal State, India, where this species is likely to be present in the mountainous Darjeeling and Kalimpong districts. The third Bhutan species (SCZM 2015.06.29.1 [tissue no. D17]), collected from Khaling Chhu (27.190606, 91.602611, ~2,070 m a.s.l), Trashigang District, included in our phylogenetic analyses is a member of the *monticola* group. Low bootstrap support obtained for relationships within this group prevent us from determining its closest relative, but the analysis suggests that it might be closest to *A. putaoensis* (Gan et al., 2020) from northern Myanmar (Gan et al., 2020b; Fig. 1).

At the time of writing (06 July 2021), GenBank records for *Amolops* were difficult to navigate due to species identification errors and a large number of sequences for unidentified species. For example, the *16S* sequences identified as *A. "nepalicus"* on GenBank from Khatiwada et al. (2020) represented *A. formosus*, and their *A. "formosus"* sequences represented *A. nepalicus* (Table 1). The sequences on GenBank generated in Wu et al. (2020) identified as *Amolops* "sp. 1–7" must now be updated to reflect the new species descriptions in Che et al. (2020) and the results presented herein as follows: *Amolops* "sp. 1" = *A. deng* Jiang, Wang & Che, 2020 (in Che et al., 2020); *Amolops* "sp. 2" = *A. baibengensis*; *Amolops* "sp. 3" = *A. wangyufani*; *Amolops* "sp. 4" = *A. gyirongensis* (herein considered a synonym of *A. formosus*, see discussion below); *Amolops* "sp. 5" = *A. himalayanus*; *Amolops* "sp. 6" = *A. yarlungzangbo* Jiang, Wang, Li, Qi, Li & Che, 2020 (in Che et al., 2020); *Amolops* "sp. 7" = *A. nepalicus* (Table 1). Outdated and erroneous species identifications are common with GenBank sequences (Mahony et al., 2017: suppl. info.; Mahony & Kamei, 2022; Streicher et al., 2020; Fig. 1; Table 1). Until such time as GenBank incorporates required corrections identified in published literature, the responsibility of maintaining the accuracy of GenBank data is retained by the submitting authors (see Mahony & Kamei, 2022 for detailed discussion).

The taxonomic status of *Amolops gyirongensis*

The assembled *16S* sequence from the *A. formosus* holotype and sequences from recently collected samples identified as this species from Nepal (Khatiwada et al., 2020) comprised of 139 bp of homologous sequence and were found to be identical in nucleotide composition. The same 139 bp sequence of *16S* obtained from the holotype of *A. formosus* was found to be 99–100 % identical to those of the recently described *A. gyirongensis* from Tibet, though the missing data in our alignment produced the erroneous impression on the phylogenetic tree that these taxa are as deeply diverged from each other as other sister taxa on the tree (Fig. 1). A BLAST comparison of a *16S* sequence of *A. formosus* from Khatiwada et al. (2020: MT124521.1, 434 bp length) against homologous sequences for all five available *A. gyirongensis* samples (Table 1) demonstrated that they are only marginally divergent (98.2–98.6 % similar).

To further test whether *A. formosus* and *A. gyirongensis* are genetically distinct we used *nd2* and *co1* sequences (Wu et al., 2020) for a paratype (KIZ012533) of *A. gyirongensis* as reference sequences for mapping archival DNA reads from the holotype of *A. formosus*. For the *nd2* gene, 93 *A. formosus* reads mapped to the reference, and the consensus sequence had a total length of 572 bases (excluding two short stretches of missing data; read depth 2–27 reads). Uncorrected *p*-distance analyses on a *nd2* alignment comprising all available *viridimaculatus* group sequences (572 homologous nucleotide loci), demonstrated that the *A. formosus* holotype differed from *A. gyirongensis* sequences by only 2.1–2.6 % (Table S1). The lowest interspecific *p*-distance for *nd2* between *A. formosus* and other *viridimaculatus* group taxa was 12.1 % (i.e. 13.1 % from *A. baibengensis*, 12.2–12.8 % from *A.*

himalayanus, 12.1 % from *A. medogensis*, 12.4–14.0 % from *A. viridimaculatus*, 12.1–12.2% from *A. wangyufani*). The minimum interspecific *p*-distance observed using this *nd2* alignment was 6.6 % both between *A. viridimaculatus* and *A. baibengensis* and between *A. medogensis* and *A. wangyufani*.

For the *co1* gene, 87 *A. formosus* reads mapped to the reference, and the consensus sequence had a total length of 539 bases (excluding two short stretches of missing data; read depth 2–54 reads). Uncorrected *p*-distance analyses on a *co1* alignment comprising all available *viridimaculatus* group sequences (448 homologous nucleotide loci) demonstrated that the *A. formosus* holotype differed from *A. gyirongensis* sequences by only 2.2 % (Table S2). The lowest interspecific *p*-distance for *co1* between *A. formosus* and other *viridimaculatus* group taxa was 8.0 % (i.e. 9.6 % from *A. baibengensis*, 8.7 % from *A. himalayanus*, 8.7–8.9 % from *A. medogensis*, 8.3–8.5 % from *A. viridimaculatus*, 8.0 % from *A. wangyufani*). The minimum interspecific *p*-distance observed using this alignment dataset is 5.6 % each between *A. viridimaculatus* and *A. baibengensis, A. medogensis* and *A. wangyufani* and *A. viridimaculatus* and *A. kaulbacki*. Our results demonstrate that the genetic distance based on mitochondrial DNA sequences between the holotype of *A. formosus* and the type series of *A. gyirongensis* is significantly lower than that seen between closely related species in the *viridimaculatus* species group and is likely representative of intraspecific variation within a single species. The archival DNA sequencing of the *A. formosus* holotype did not produce homologous reads to compare nuclear sequence data between the two populations. We recommend considering *A. gyirongensis* as a junior subjective synonym of *A. formosus* (also see 'Taxonomic accounts' section below).

The taxonomic status of *Amolops splendissimus* and *Amolops caelumnoctis*

Our phylogeny identified a second taxonomic issue in the *viridimaculatus* group based on sequences obtained from GenBank, where six *Amolops splendissimus* Orlov & Ho, 2007 sequences were nested within a clade otherwise comprising *A. "viridimaculatus"*. The *A. splendissimus* sequences were recently published in a study that aimed to resolve the taxonomic status of *A. splendissimus* named from northern Vietnam and the morphologically indistinct species *A. caelumnoctis* Rao & Wilkinson, 2007 named from neighbouring Yunnan, China (Zhang et al., 2021). Zhang et al. (2021) concluded, based on morphological and molecular *16S* data, that *A. caelumnoctis* represents a junior subjective synonym of *A. splendissimus*. Their phylogeny included only two sequences of other *viridimaculatus* group taxa, *A. medogensis* and *A. "viridimaculatus"* (MN953737: identified in our study as *A. kaulbacki*; Fig. 1). Our phylogeny, that includes all sequences identified as *A. "viridimaculatus"* and *A. splendissimus* available on GenBank demonstrates minimal divergences between the most north-western population nearby the China-Myanmar border from Gongshan County in Yunnan Province to the most south-eastern population from Lao Cai District in northern Vietnam (straight line distance >800 km). A BLAST search for one of the *A. splendissimus 16S* sequences (MZ484729.1) against the 17 other sequences of these two 'species' show they are >99.4 % identical. These sequenced populations include topotype specimens of *A. viridimaculatus* (MK604835.1 and MK604836.1 from Lyu et al., 2019b; see Yang et al., 2019 for account and more precise locality information for these specimens) and *A. splendissimus* (from Zhang et al., 2021). Orlov & Ho (2007) and Rao & Wilkinson (2007) relied primarily on details of markings and colouration to diagnose *A. splendissimus* (and *A. caelumnoctis*) from *A. viridimaculatus*: small yellow spots on a dark purple/black/black-brown background (vs. larger green or yellowish green spots on a red-brown background), fore and hindlimbs spotted (vs. with transverse bands). Zhang et al. (2021: figs. 4 & 5) show individuals of *A. splendissimus* with distinctly larger green spots and one individual having banded forelimbs, demonstrating considerable plasticity in colouration range and markings, with some individuals looking more like *A. viridimaculatus* from the type locality (e.g. Yang et al., 2019: fig. 3f) than the type series of *A. splendissimus* and *A. caelumnoctis* (Orlov & Ho, 2007; Rao & Wilkinson, 2007). Rao & Wilkinson (2007) further diagnosed *A. caelumnoctis* from *A. viridimaculatus* by absence (vs. presence) of a pineal body. The presence or absence of a pineal body was not mentioned by Orlov & Ho (2007), but considered to be absent on all specimens examined by Zhang et al. (2021). Based on comparative specimens examined in this study (Appendix II), the pineal body can be externally visible or appear absent (i.e. probably present, just not visible through the skin) within species, e.g. *A. kaulbacki* visible on holotype, not visible on paratype, visible or not visible within the type series of *A. nidorbellus* Biju, Mahony & Kamei, 2010, and in the referred specimens of *A. viridimaculatus*, not externally visible (CAS 242251), indistinct (CAS 242250, CAS 242252) or distinctly visible (CAS 242214, CAS 242215, CAS 242249). Presence/absence of an externally visible pineal body should therefore not be considered a reliable diagnostic character in *viridimaculatus* group taxa. Considering the lack of species-level genetic differentiation in the *16S* sequences, largely overlapping colouration and markings, and a lack of other clearly diagnostic characters to suggest that the sequences represent more than one species, we formally recognise *A. splendissimus* Orlov & Ho, 2007 (including its junior subjective synonym *A. caelumnoctis* Rao & Wilkinson, 2007) to represent a junior subjective synonym of *A. viridimaculatus* (Jiang, 1983).

Taxonomic accounts

The southern Himalayan *marmoratus* and *monticola* groups require a more comprehensive taxonomic review which is beyond the scope of this current paper (see Patel et al., 2021 for progress on the *monticola* group), thus we refrain from further discussions on the identifications of the two Bhutan species sampled herein from these groups. The holotype of *A. gerbillus* is a juvenile, and no additional specimens representing the *marmoratus* group were available for us to study from the vicinity of the type locality, preventing us from morphologically comparing the Bhutan population with *A. gerbillus* s.s. The Bhutan *viridimaculatus* group species, however, has been studied extensively by one of us (TN: Nidup et al., 2016; Limbu et al., 2020) and the morphological comparison of specimens with regional congeners enabled the identification of sufficient characters to demonstrate that this species represents a previously undescribed taxon (formally described below). The morphological examination of type specimens from the southern Himalayas (Appendix II) included *Rana senchalensis* which has been considered conspecific with *Amolops marmoratus* (Blyth, 1855) (Dubois, 2000). We provide an account for this species below to summarise the current state of knowledge on the taxon and make a recommendation for its treatment as valid (see 'Remarks' section of *Amolops senchalensis*).

Consistent with the small divergence in mitochondrial genes we described above, we found no obvious morphological differences between the holotype of *A. formosus* (examined herein, Appendix II) and the original description of *A. gyirongensis* (Jiang et al., 2020 [in Che et al., 2020]). However, we recommend further morphological study including more specimens of *A. formosus* and/or molecular analyses that includes a combination of mitochondrial and nuclear sequence data to reassess the validity of *A. gyirongensis* in the future. We have compared the newly described species with both *A. formosus* s.s. and *A. gyirongensis* (Jiang et al., 2020 [in Che et al., 2020]) separately in case our proposal for synonymisation is not universally accepted by the community.

Amolops senchalensis (Chanda, 1987)

Rana senchalensis Chanda, 1987 ("1986"). J. Bombay Nat. Hist. Soc., 5(2): 140, 146–147, fig. 1: cited by Dutta (1992:2); Sarkar et al. (1992:67, 81); Duellman (1993:275); Dutta (1997:162–163); Chanda & Deuti (1998:72); Ray (1999:3); Chanda (2002:133–134).

- *Rana sinchalensis*[sic]: Chanda & Ghosh (1988:626); Swan (1993:143).
- *Amolops senchalensis*: Das & Dutta (1998:64).

Holotype

Adult male (ZSI A8753, formerly ZSI KZ 982; Fig. 2), from "Senchal Lake, Darjeeling District, West Bengal" that currently refers to Senchal Lake (ca. 26.993902, 88.264908, 2,260–2,280 m a.s.l.; estimated from Google Maps), Senchal Wildlife Sanctuary, Darjeeling Sadar Sub-division, Darjeeling District, West Bengal State, India, collected by S.K. Dey on 8 October 1983 (Chanda, 1987; Dutta, 1997; specimen jar label).

Etymology

The specific epithet '*senchalensis*' is a toponym, meaning from/of Senchal, with reference to the type locality, Senchal Lake. Considering all *Amolops* species are torrent frogs, thus not associated with lentic waterbodies, presumably the holotype was collected from a stream associated with/nearby the lake, rather than the lake itself.

Suggested common name

The following three alternative common names have been suggested for this species during the short period that it was considered valid (between 1987 and 2000): "Senchal Lake Frog" (Frank & Ramus, 1995), "Senchal Stream Frog" (Das & Dutta, 1998), "Senchal Frog" (Chanda, 2002). Though any of these names could be considered suitable, we favour using common names that indicate the systematic position of species to facilitate the end users of common names to distinguish between different taxonomic groups. Species of the genus *Amolops* are commonly referred to as "torrent frogs", a suitable group name that reflects the lotic habitat in which they are found and morphologically adapted to (e.g. tadpoles possess a large ventral gastromyzophorus disc and post metamorphic frogs possess expanded discs on digits), so we suggest a modification to the common name that reflects this - Senchal torrent frog.

Condition of type specimen

The holotype specimen was in poor preservation condition when examined in 2008 (by SM), appearing to have been completely dehydrated at some point, and then placed back into EtOH (Fig. 2). It might be possible that this specimen can be mostly restored via water or trisodium phosphate rehydration (e.g. Moore, 1999) so that some taxonomic characters can be assessed that are not discernible in its current condition. Chanda (1987) did not mention that the specimen was desiccated in the description, and the illustration provided indicated that the specimen examined by Chanda was probably in reasonably good condition (assuming artistic interpretation was not excessive). We provide measurements taken in this study (by SM) for the holotype in Table 3, but we caution the reader to not overly rely on many of these measurements (particularly soft characters like HL, disc widths, etc.) which would differ significantly if the specimen was hydrated.

Remarks

Chanda (1987) first named the species in the then catchall genus *Rana* Linnaeus, 1758, which at the time included *Amolops* as a synonym. Chanda (1987) primarily used the keys provided by Boulenger (1920) to infer the taxonomic affinities of *Rana senchalensis*, leading to several misleading comparisons, i.e. *Rana senchalensis* was compared with the dicroglossid *Nanorana annandalii* (Boulenger, 1920) rather than other sympatric species of *Amolops*. Duellman (1993:275) erroneously credited "Pillai and Chanda, 1990. J. Bengal Nat. Hist. Soc, N.S., 9:146." as the authorship of the name. We have confirmed that the J. Bengal Nat. Hist. Soc., volume 9 (not available online) comprises issues 1 and 2 which are separately paginated and neither of the two issues reach 146 pages. In addition, the indexes of both issues have been searched and no paper by these authors were published in either issue (H. Pethers, pers. comm. 01/02/2022). Dubois (2000) is typically credited for the synonymisation of *Rana senchalensis* under *Amolops marmoratus* (Blyth, 1855) (e.g. Chanda et al., 2001; Deuti & Ayyaswamy, 2008; Frost, 2021, online). However, Dubois (2000) merely placed the name as a

Figure 2. *Amolops senchalensis* adult male holotype (ZSIK A8753) showing preservation condition in 2008 at the time of examination: A. dorsal view; B. ventral view; C. dorsolateral view; D. profile view of head; E. dorsal view of right forearm; F. posterior view of left thigh. Images not to scale.

synonym of *Amolops marmoratus* without any discussion or justification, and with the wrong authorship (i.e. "*Rana senchalensis* Chanda, 1990"- reference not provided) and therefore this action should not have been regarded as a formal synonymisation of *Rana senchalensis* Chanda, 1987. Dutta (1997) gave the holotype number as "ZSI A8753" which is the number on the specimen label that was still attached to the specimen when examined by SM in December 2008 (Fig. 2). Morphologically this specimen corresponds relatively well with the original description, and details present on the specimen jar label regarding the specimen's collector and collection date agree with details provided for the holotype by Chanda (1987). Chanda et al. (2001) inexplicibly and erroneously gave the holotype number as "ZSI A8474", which has since been followed by Frost (2021).

Despite the poor condition of the holotype, the following characters are obvious enough to determine that *Amolops senchalensis* is not conspecific with either of the *marmoratus* group species likely to be present in Darjeeling (i.e. *A. nepalicus* and *A. mahabharatensis* Khatiwada, Shu, Wang, Zhao, Xie & Jiang, 2020 from neighbouring Nepal): 1) external vocal sacs absent (vs. present and distinct in males of *A. nepalicus* and *A. mahabharatensis*; Wang et al., 2020 and Kathiwada et al., 2020, respectively); 2) third finger distinctly elongated, FIIIL/SVL = 27.7% (vs. <24 % in *A. nepalicus* and *A. mahabharatensis*; Wang et al., 2020 and Kathiwada et al., 2020, respectively); 3) outer metatarsal tubercle absent (vs. present in *A. nepalicus* and *A. mahabharatensis* Wang et al., 2020 and Kathiwada et al., 2020, respectively); 4) forearms are very enlarged relative to upper arms (Fig. 2E) (vs. much less enlarged relative to upper arms in *A. nepalicus* and *A. mahabharatensis*; Wang et al., 2020: figs. 3 & 4 and Kathiwada et al., 2020: figs. 4 & 5, respectively). Though some of these character states observed on the holotype of *A. senchalensis* (i.e. 1, 3 & 4) are also observed on a few geographically distant members of the *marmoratus* group (Dever et al., 2012; examined specimens), all are more typically seen in mature male *viridimaculatus* group taxa (Che et al., 2020; examined specimens, Appendix II), so we consider it more likely that *A. senchalensis* is a member of the *viridimaculatus* group.

Within the *viridimaculatus* group, the systematic position of *A. senchalensis* cannot be confirmed due to the poor preservation condition of the holotype (as described above). Based on adult size alone, the holotype (SVL 46.2 mm) approaches the adult male size for *A. formosus* (SVL 53–65 mm, n=2; Dubois, 1974), a species known from the vicinity of the type locality in Darjeeling (Boulenger, 1920) that also has the smallest adult male size in the group. However, the posterior thighs of *A. senchalensis* appear to have transverse broad dark brown stripes separated by narrow lighter intervening areas (Fig. 2F), whereas *A. formosus* has narrow dark brown stripes separated by broad green intervening areas (e.g. on the examined holotype; see also Dubois, 1974: fig. 4 and Kathiwada et al. 2020: fig. 10), so based on some apparent differences in markings we refrain from considering *A. senchalensis* as a junior subjective synonym of *A. formosus*. We therefore recommend that *Amolops senchalensis* (Chanda, 1987) is considered valid pending the collection of fresh material from the type locality that can permit a further evaluation of its taxonomic status.

Amolops wangyali sp. nov.

{urn:lsid:zoobank.org:pub:729D12FC-6EAD-49C5-B17A-B901FD636FCA}

- *Amolops mantzorum* (nec. *Polypedates mantzorum* David, 1872): Wangyal (2013:4774, 4777, 4779, 4780, image 14): cited by Wangyal (2014:29, as "*Amolops mantzarum*" [sic.]); Nidup et al. (2016:13); Wangyal & Gurung (2017:52).
- *Amolops himalayanus* (nec. *Rana himalayana* Boulenger, 1888): Nidup et al. (2016:13–18, fig. 2 & possibly fig. 3: cited by Wangyal & Gurung (2017:52); Khatiwada et al. (2020:87); Nokhbatolfoghahai et al. (2020:326); Limbu et al. (2020:57, 59, 62).
- *Amolops* aff. *himalayanus*: Streicher et al. (2020:494, 495, fig. 1 [S10 & S11]).
- *Amolops himalayanus* (nec. *Rana himalayana* Boulenger, 1888): Streicher et al. (2020:494; error, should read "*Amolops* aff. *himalayanus*").
- *Amolops himalayanus* (nec. *Rana himalayana* Boulenger, 1888): Limbu et al. (2020:56–64, figs. 2B, 2G, 2H & 6 [left upper & lower]).

Holotype

Adult male (SCZM 2019.07.18.1 [field no. MW 11585]; Figs. 3, 4A & 4B), from Bodidrang Chhu/Stream (27.27023, 91.53043, 1,740–1,750 m a.s.l.), Namla Village, Kanglung Gewog (village block), Trashigang District, eastern Bhutan, collected by Tshering Nidup on 18 July 2019.

Paratypes

Adult female (SCZM 2019.07.18.2 [field no. MW 11587]; Figs. 4C, 4D & 5), collection details same as for holotype; adult female (SCZM 2019.08.02.1 [field no. SC 0034]; Figs. 4E, 4F & 6F), from Bodidrang Chhu/Stream (27.27223, 91.53129, 1,700 m a.s.l.), Namla Village, Kanglung Gewog (village block), Trashigang District, eastern Bhutan, collected by Tshering Nidup and Namgay Rinchen on 2 August 2019.

Etymology

The specific epithet is a patronym, named in recognition of Mr. Jigme Tshelthrim Wangyal, a Forest Officer with the Department of Forest and Park Services, Ministry of Agriculture and Forests, Government of Bhutan. Jigme is an accomplished Bhutanese herpetologist and has published many papers on the subject (Wangyal, 2011, 2013, 2014; Wangyal & Gurung, 2012, 2017; Wangyal & Das, 2014; Wangyal et al., 2020). Jigme's extensive network of Forest Officers, researchers and wildlife enthusiasts have supplemented his extensive personal observations in several of his publications, and as a consequence, many of the species currently on Bhutan's amphibian and reptile checklist were first documented in the country through his efforts. He continues to support and inspire interest in amphibian and reptile research through seminars and field training workshops and is a vocal proponent for improving standards of herpetological research in Bhutan.

Suggested common name

Wangyal's torrent frog.

Condition of type series

All specimens are fully intact, except for a portion of the ventral thigh muscle removed for molecular analysis. Specimens are well hydrated and in a good state of preservation (Fig. 4).

Description of holotype

Adult male, body habitus slender (Figs. 3A, 3C, 3E, 4A & 4B); head dorsally subovoid, wider than long, flat above; snout rounded and strongly protruding in profile (Fig. 3B), its length, longer than horizontal diameter of eye; canthus rostralis distinct, rounded, loreal region concave, obtuse; interorbital space flat, interorbital distance less than width

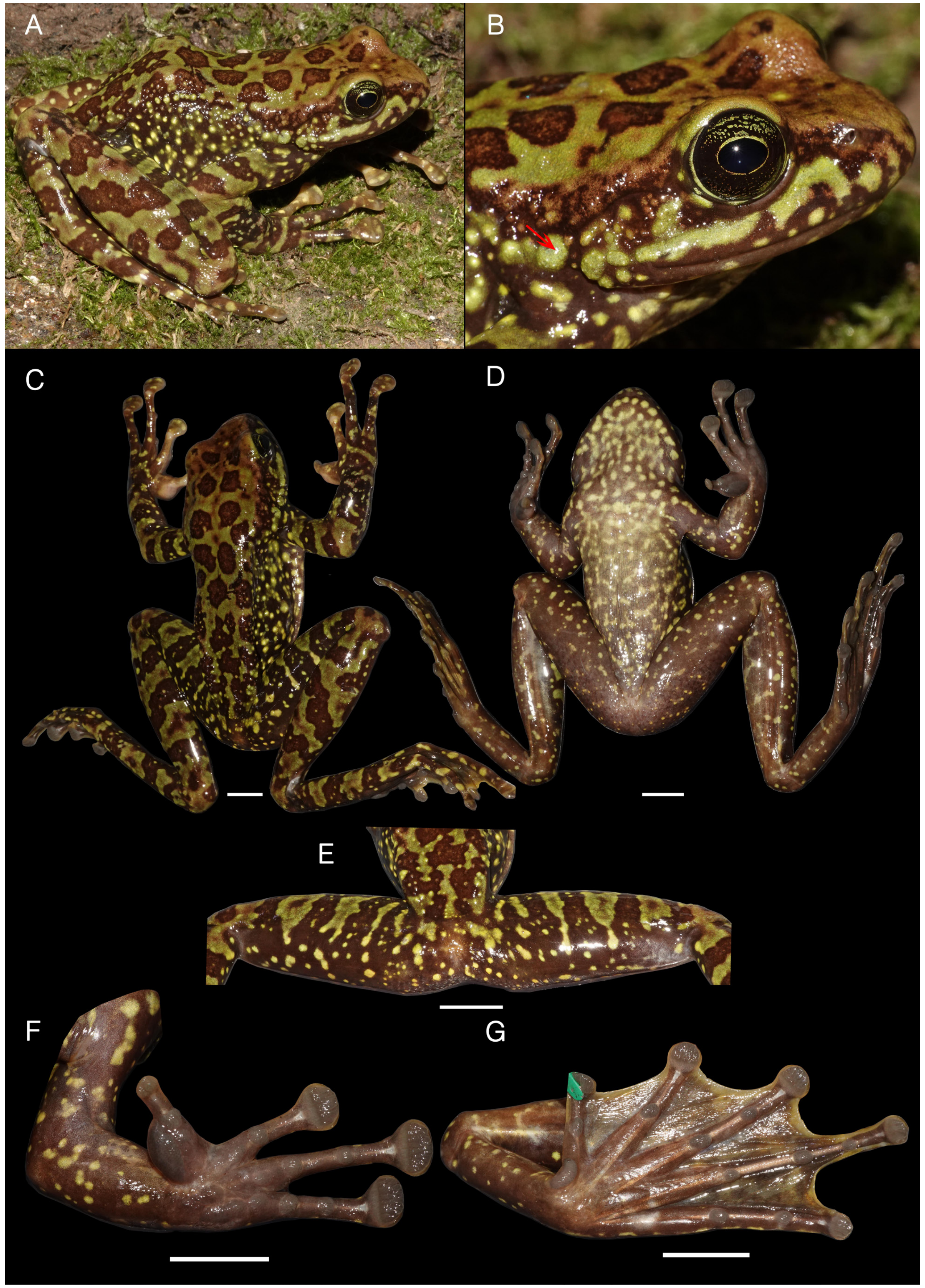

Figure 3. *Amolops wangyali* sp. nov. adult male holotype (SCZM 2019.07.18.1) in life (A & B: images taken ex-situ) and immediately after euthanisation, prior to fixation (C–G): A. dorsolateral view; B. lateral view of head, red arrow shows the shoulder gland; C. dorsolateral view; D. ventral view; E.posterior view of thighs; F. palmar view of left hand; G. plantar view of left foot. Scale bars represent 10 mm.

of upper eyelids, narrower than internarial distance; nostrils laterally positioned, obtusely oval with raised rim (Fig. 3B), closer to eye than snout; pupil horizontal (Fig. 3B); tympanum fully exposed, oval, obliquely orientated, flat, slightly recessed relative to temporal region, rim barely distinct (Fig. 3B), tympanum-eye distance greater than maximum tympanum diameter; pineal ocellus distinct (Figs. 3A–C, 4A); vomerine ridges well developed, more raised posteriorly, narrow, slightly obtuse, equidistant from each other and choanae, anterior ends positioned between choanae, transversely orientated; vomerine teeth small; choanae oval; tongue large, deeply emarginated distally with tips bluntly pointed, covered with tiny papillae, lingual processes absent; external vocal pouch indistinct, represented by patch of longitudinally wrinkled skin near posterior axis of mandible on each side (Figs. 3D & 4B), internal vocal slits small, one positioned on floor of mouth near posterior articulation of jaw on each side.

Forelimbs moderately long, thick, forearms significantly enlarged relative to upper arms (Figs. 3C & 4A), forearm length shorter than hand length; actual and relative finger length formula same, FI<FII<FIV<FIII; fingers relatively long and thin, all finger tips dilated with oval discs, but disc considerably reduced on FI (Fig. 3F), circummarginal grooves present on FII–FIV only (absent on FI); terminal phalange shape not determined; lateral dermal fringes absent on all fingers (Fig. 3F); webbing between fingers absent; subarticular tubercles prominently domed, circumference circular (FI–FIV: 1, 1, 2, 2); supernumerary tubercles prominent, circumference circular to longitudinally oval, one present on base of all digits (Fig. 3F), a secondary smaller supernumerary tubercle present between primary supernumerary tubercle and subarticular tubercle on FIII of left hand and FIV of right hand; prepollex absent; thenar tubercle long, preaxial half obscured by ventral portion of nuptial pad (Fig. 3F); outer and inner metacarpal tubercles distinct, separate, circumference oval, flat, outer long and thin, inner wider and ~30 % shorter (Fig. 3F); smooth nuptial pad restricted to FI, moderately large (notably larger on right hand than on left - asymmetry considered atypical; Fig. 4A & 4B), covering preaxial dorsal surface of proximal phalange extending ventrally on digit (Fig. 3F).

Hindlimbs long, shanks thin (Fig. 3C & 3D), longer than thighs and feet; toes long and thin (Fig. 3G), relative lengths TI<TII<TIII=TV<TIV; tips of all toes expanded with relatively small transversely oval discs, all with circummarginal grooves; webbing between toes extensive, webbing formula: I0–0II0–0III0–1IV1–0V (Fig. 3G); postaxial fringe on TV absent, preaxial groove on TI extends from base of disc to subarticular tubercle (Fig. 3G); subarticular tubercles all present (TI–TV: 1, 1, 2, 3, 2), prominent, circumference longitudinally oval; inner metatarsal tubercle flat, oval, relatively short (Fig. 3G); outer metatarsal tubercle absent; tarsal glandular ridge and supernumerary tubercles absent.

Skin on dorsal surface of head, body and limbs smooth (Figs. 3A–C, 3E & 4A); posterior lateral surface of head below supratympanic ridge and entire flanks covered with small dense tubercles, few small scattered tubercles on posterior dorsum and surrounding cloacal opening (Fig. 3E); supratympanic ridge well developed; a distinct patch of rictal glands at rear of jaw on either side (Fig. 3B); a distinctly enlarged gland positioned anterodorsally above forelimb insertion on either side (hereafter "shoulder gland"; Fig. 3B, indicated by an arrow); dorsolateral ridges absent; a weak parotoid-like swelling posterior to upper supratympanic ridge level with arm insertion, upper edge of parotoid-like swelling straight, lower edge curved and in contact with upper border of shoulder gland (Fig. 3A & 3B); ventral surfaces smooth except a patch of weakly granular skin on proximal posteroventral thighs (Figs. 3D & 4B); small white dermal spinules present, dense on tympanic region and rear of jaw, located on tips of tubercles (Fig. 3B), a moderately dense patch dorsolaterally above forelimb insertions, few scattered on granules of upper flanks, absent on remaining surfaces; other obvious macroglands absent.

Colouration in life (Fig. 3): Dorsum of head light brown anteriorly, blending to light green posteriorly, remaining dorsum of the body light green; large brown irregularly shaped blotches on dorsum of head and body; lateral surfaces of head and snout light green with dark brown mottling and blotches; a broken irregular stripe from tip of snout to eye passing along lateral edge of canthus rostralis on either side; pupil with near continuous pale metallic green border, remaining iris mottled metallic green and chocolate brown, more green than brown on dorsal third and ventral most portions of iris; supratympanic fold and parotoid region light brown; flanks evenly mottled green and brown, with contrasting light green tubercles; gular region, chest and abdomen brown with dense pale green spots anteriorly, becoming more mottled posteriorly on abdomen; dorsum of forelimbs and hindlimbs green with contrasting dark brown transverse to oblique cross-bands, all cross-bands with distinct light green specks; dorsum of fingers (including expanded discs) dark brown with irregularly arranged green specks; posterior surface of thighs and entire ventral surfaces of forelimbs and hindlimbs dark brown with irregularly arranged pale green spots and speckling (spots absent from palmar and plantar surfaces); nuptial pads yellowish-grey dorsally, dark grey ventrally.

Colouration in preservation (Fig. 4A & 4B): Dorsum of head and body primarily pale grey with large dark brown blotches, blotches with slightly darker borders, those on posterior half of body with cream coloured speckles; lateral surfaces of head marbled dark brown and light grey; flanks densely mottled grey and dark brown with creamish yellow granules; dorsum of fore and hindlimbs pale grey banded with dark brown transverse or obliquely transverse stripes; dorsum of hands and feet primarily dark brown with pale greyish cream speckles that increase in density distally onto expanded discs; inner/posterior surface of thighs dark brown with irregular small yellowish-cream spots and speckles; ventral surfaces of head, body and limbs primarily dark brown with dense yellowish-cream spots and speckles; ventral surfaces of hands and feet plain brown with tubercles and discs light

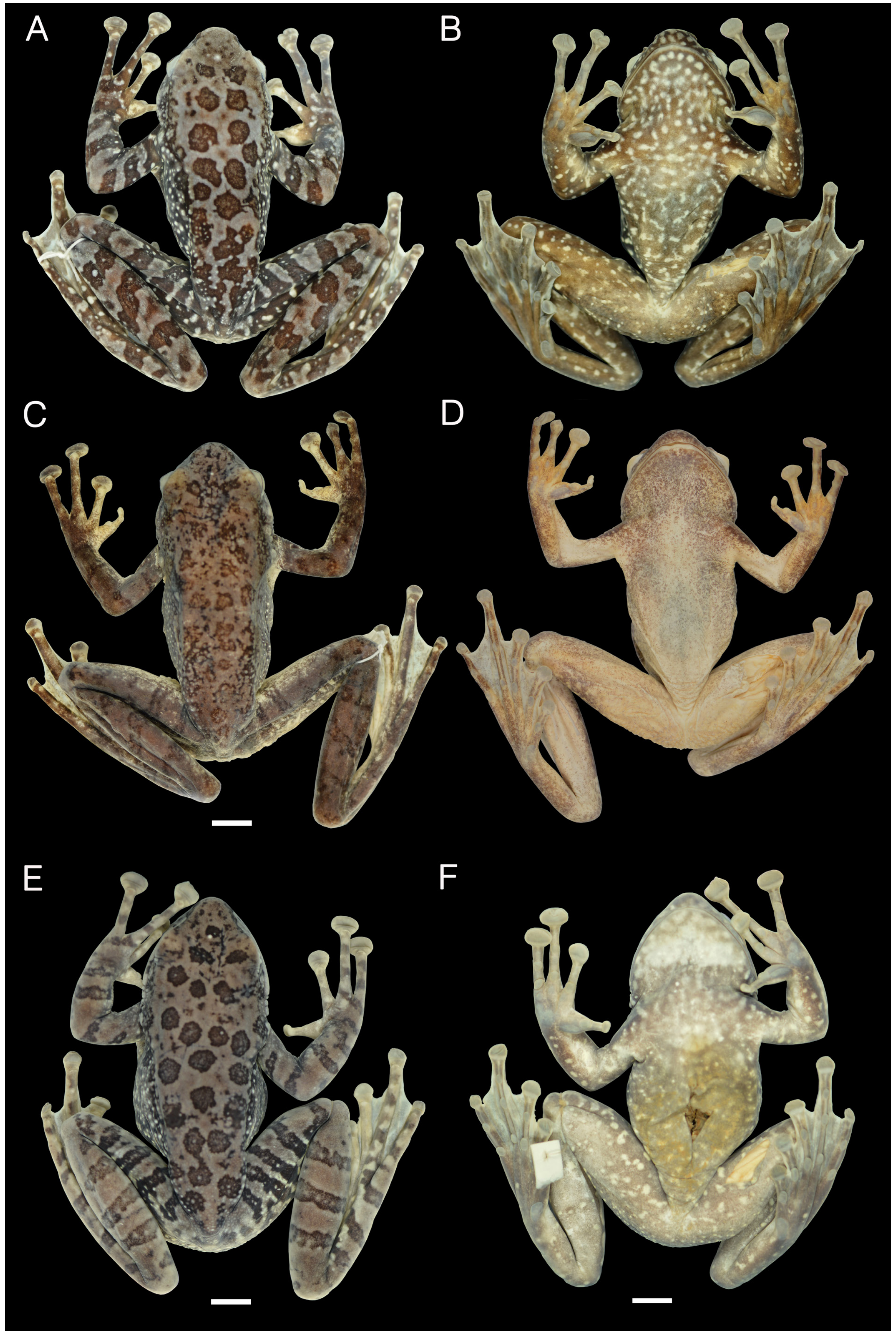

Figure 4. *Amolops wangyali* sp. nov. dorsal and ventral views of the type series in preservation showing variation in colouration and markings: A & B. adult male holotype (SCZM 2019.07.18.1); C & D. adult female paratype (SCZM 2019.07.18.2); E & F. adult female paratype (SCZM 2019.08.02.1). Scale bars represent 10 mm. A, B & D not to scale.

Table 3. Specimen morphometrics for *Amolops wangyali* sp. nov. and the holotype of *A. senchalensis*. Refer to the 'Methods & materials' section for explanation of measurement abbreviations and collection acronyms. HT holotype; PT paratype; M adult male; F adult female; – measurement not taken; * for measurements taken on left side.

Species	*A. wangyali* sp. nov.			*A. senchalensis*	Species	*A. wangyali* sp. nov.			*A. senchalensis*
Specimen #	SCZM 2019.07.18.1	SCZM 2019.07.18.2	SCZM 2019.08.02.1	ZSIK A8753	Specimen #	SCZM 2019.07.18.1	SCZM 2019.07.18.2	SCZM 2019.08.02.1	ZSIK A8753
Status	HT	PT	PT	HT	Status	HT	PT	PT	HT
Sex	M	F	F	M	Sex	M	F	F	M
SVL	71.4	87.5	89.6	46.2	SHW	10.3	10.8	13.1	–
HW	25.7	30.5	31.6	13.9	TFL	61.5	69.8	70	brittle
HL	24.8	30.3	31.6	15.9	FOL	42.1	47.3	47.6	26.6
SD	7.5	8.7	9.5	4.8	IMT	4.2	4.6	5.2	2.3
IFE	11.8	13.8	15	7.7	FIL	8.8	10.3*	13.2	6.3
IBE	20.1	23.9	25.1	12.5	FIIL	13.2	15.7*	17.9	8.4
EL	8.6	10.8	9.8	5.5	FIIIL	19.3	23.3*	24.9	12.8
TD	2.8	3.2	3.3	1.8	FIVL	15.4	16.4*	18.2	9.3
TE	3.6	4.1	3.6	2.1	FIDW	2.3	2.9*	3.3	1.1
SL	9.9	11.3	13.1	5.6	FIIDW	4.8	5.6*	6	1.9
EN	4.3	4.5	5	3.1	FIIIDW	5.1	6.6*	7.1	2.2
SN	5.8	7.2	8.1	2.8	FIVDW	5.5	6.9*	7.2	2.2
IN	7.9	8.4	9.6	5.2	FIIIW	2.2	2.3*	2.4	–
IUE	5.8	6.5	7.0	4.6	TIDW	3.4	3.9	4	–
UEW	6.3	8.4	9.3	3.9	TIIDW	4.1	4.8	4.3	–
FAL	17.6	21.8*	20.3	12.2	TIIIDW	3.4	4.7	5.2	1.5
HAL	25.7	30.6*	33.5	16.7	TIVDW	3.3	4.5	4.9	1.6
TL	41.5	48.9	48.2	26.1	TVDW	3.1	3.7	4.1	1.2
SHL	46.5	51.4	51	28.8	TIVW	2.6	2.7	3	–

grey; webbing between toes mottled grey and brown.

Variation

Mensural data for the type series is provided in Table 3. Paratypes morphologically agree with the holotype description with the following exceptions: webbing between toes slightly less extensive on the two paratypes, I0–1II0–1III0–1.5IV1.5–0V in SCZM 2019.07.18.2 (Fig. 5G) and I0–1II0–1III0–1IV1–0V on SCZM 2019.08.02.1; on SCZM 2019.07.18.2, vomerine ridges are slightly closer to the choanae than to each other, and on SCZM 2019.08.02.1, vomerine ridges are notably more developed (than the holotype and the other paratype), are linear (not obliquely orientated), positioned posterior to the choanae, are much closer to each other than to the choanae, and are evenly raised throughout their length (i.e. posterior ends more raised than anterior ends in the holotype and the other paratype); on SCZM 2019.07.18.2, tubercles are absent from the posterior dorsum and surrounding the cloacal region (Fig. 5E), and on SCZM 2019.08.02.1, tubercles are more dense on the posterior dorsum (than on the holotype), and surrounding the cloacal region, and the loreal region is very weakly granular (this specimen was not fixed in 90 % EtOH so some skin characters are more distinct than on the holotype and the other paratype); on SCZM 2019.07.18.2, a distinct dorsolateral row of tubercles is present on the body (Fig. 5A–C); on SCZM 2019.08.02.1, the tympanum is not distinctly sunken relative to the surrounding tympanic region; on SCZM 2019.07.18.2, dermal asperities are absent from all surfaces, and on SCZM 2019.08.02.1, the tips of some of the upper flank tubercles appear to have small, flat calcifications; on SCZM 2019.07.18.2, the shoulder gland is positioned directly above the forelimb insertion (Fig. 5A–C); colouration and markings vary extensively between specimens, see Figs. 3–6 and the following figures published elsewhere: Wangyal (2013: image 14); Nidup et al. (2016: figs. 2 & possibly 3); Limbu et al. (2020:56–64, figs. 2B, 2G, 2H & 6 [left upper & lower]); Streicher et al. (2020: fig. 1 [S10 & S11]).

Secondary sexual characters

Male (the holotype) with a large nuptial pad on F1; forearms significantly enlarged relative to upper arms; external paired subgular vocal sacs indistinct (e.g. not opaque relative to surrounding skin colour) but present as longitudinal folds; internal vocal slits small, one positioned on each side on floor of mouth close to posterior axes of jaws; testes yellow in colour. Female paratypes have forearms only slightly enlarged relative to upper arms; fallopian tubes convoluted; ova pigmentless; nuptial pads, external vocal sacs and internal vocal slits absent. Examination of additional specimens is required to determine whether presence of dermal asperities is unique to males.

Morphological comparisons

Amolops wangyali sp. nov. is herein compared to the following species confirmed to be members of the *viridimaculatus* group based on molecular phylogenetic analyses: *A. baibengensis*, *A. formosus* (*A. gyirongensis* is compared separately), *A. himalayanus, A. kaulbacki, A. medogensis, A. pallasitatus, A. viridimaculatus* (including *A. caelumnoctis* and *A. splendissimus*), and *A. wangyufani*. Based on the examination of specimens (Appendix II), photographs of specimens or the original descriptions, we consider the following species to likely be members of the *viridimaculatus* group but await confirmation based on molecular data: *A. longimanus* (Andersson, 1939), *A. nidorbellus* and *A. senchalensis*. The new species is not compared with the following *Amolops* species from Bhutan and surrounding regions of the southern Himalayas (north and north-east India, Nepal, Myanmar, and Tibet Autonomous Region and Yunnan Province in China) that have not yet been assigned to a species group based on molecular data as they are not here considered to represent *viridimaculatus* group members: *A. assamensis* Sengupta, Hussain, Choudhury, Gogoi, Ahmed & Choudhury, 2008, *A. gerbillus* and *A. jaunsari* Ray, 1992 are clearly *marmoratus* group members (examined specimens, Appendix II; Ray, 1999); and based on the original morphological description, *A. chakrataensis* Ray, 1992 is either a *marmoratus* or *monticola* group member (Ray, 1999). SVL and SHL measurements for additional *Amolops wangyali* sp. nov. are from Nidup et al. (2016), see 'Materials & Methods' section.

Amolops wangyali sp. nov. differs from *A. baibengensis* by smaller adult female size, female SVL 80.5–89.6 mm, n=6 (vs. female SVL 90.2–93.2, n=2; Jiang et al., 2020 [in Che et al., 2020]; note: English language diagnosis erroneously stated "SVL 75.8 mm in females, SVL 90.2–93.2 in females" in Jiang et al., 2020 [in Che et al., 2020] - should read "SVL 75.8 mm in male, SVL 90.2–93.2 in females" based on data given in their table 27), tympanum distinct, larger TD/EL 30–34 %, n=3 (vs. "tympanum indistinct", TD/EL 20–27 %, n=3; Jiang et al., 2020 [in Che et al., 2020]), adult colouration in life - dorsum of body primarily green with brown blotches (vs. adult colouration in life - dorsal and lateral surfaces of body brown with small green spots; Jiang et al., 2020 [in Che et al., 2020:184–185 figs. [x5]]); from *A. formosus* by larger adult size, male SVL 71.4–76.7 mm, n=5, female SVL 80.5–89.6 mm, n=6 (vs. male SVL 53–65 mm, n=2, female SVL 53–75 mm, n=6; Boulenger, 1920; Dubois, 1974), higher SN/EN 135–162 %, n=3 (vs. SN/EN 125 % on holotype, n=1; examined specimen, Appendix II), lower IUE/IN 73–77 % and IUE/UEW 75–92 %, n=3 (vs. IUE/IN 89 % and IUE/UEW 112 % on holotype, n=1; examined specimen, Appendix II), lower FOL/SHL 91–93 %, n=3 (vs. FOL/SHL 100 % on holotype, n=1; examined specimen, Appendix II), tympanum oval, n=3 (vs. circular on holotype, n=1; examined specimen, Appendix II); from *A. gyirongensis* by larger adult male size, SVL 71.4–76.7 mm, n=5 (vs. male SVL 61.3–63.1, n=3; Jiang et al., 2020 [in Che et al., 2020]), relatively longer shanks, male SHL/SVL mean 63.6 %, min.–max. range 61–66 %, n=5, female SHL/SVL mean 58.7 %, min.–max. range 57–61 %, n=6 (vs. male SHL/SVL mean 58.3 %, n=3, female SHL/SVL mean 54.9 %, n=7; Jiang et al., 2020 [in Che et al., 2020] - measurements for individual specimens were not provided so min.–max. SHL/SVL ranges cannot be determined), tympanum distinct (vs. "indistinct"; Jiang et al., 2020 [in Che et al., 2020]); from *A. himalayanus* by lower TE/TD 109–129 %, n=3 (vs. TE/TD 136–150 %, n=3; examined specimens, Appendix II; tympanum border indistinct on fourth examined specimen, BMNH 1947.2.3.83, so measurement was not taken), lateral dermal fold on preaxial edge of TI extends from disc to subarticular tubercle, n=3 (vs. extends from disc to inner metatarsal tubercle, n=4; examined specimens, Appendix II); from *A. kaulbacki* by higher SN/EN 135–162 % and FIIIL/SVL 27–28 %, n=3 (vs. SN/EN 120–127 % and FIIIL/SVL 24–25 %, n=2; examined specimens, Appendix II), lower FOL/SHL 91–93 %, n=3 (vs. FOL/SHL 88–90 %, n=2; examined specimens, Appendix II), adult dorsal colouration of body in life primarily green with dark brown blotches (vs. primarily dark brown with green reticulations, n=2; examined specimens, Appendix II); from *A. longimanus* by skin on flanks distinctly tubercular, n=3 (vs. smooth on holotype, n=1; determined from photograph, Appendix II), nostril closer to eye than to snout tip, SN/EN 135–162 %, n=3 (vs. "nostrils a little nearer the tip of the snout than the eye" on holotype, n=1; Andersson, 1939), interorbital distance narrower than upper eyelid width, IUE/UEW 75–92 %, n=3 (vs. "Interorbital space….broader than the upper eyelid" on holotype, n=1; Andersson, 1939); from *A. medogensis* by skin on flanks with small dense tubercles (vs. smooth, n=6; Fei et al., 2012:424 figs. [6x]), smaller adult size, male SVL 71.4–76.7 mm, n=5, female SVL 80.5–89.6 mm, n=6 (vs. male SVL 95 mm, n=1, female SVL 93 mm, n=1; Fei et al., 2012), dorsum of body primarily green with dark brown blotches (vs. primarily dark brown with dense green speckling and mottling, n=6; Fei et al., 2012:424 figs. [6x]); from *A. nidorbellus* by typically smaller adult size, male SVL 71.4–76.7 mm, n=5, female SVL 80.5–89.6 mm, n=6 (vs. male SVL 76.4–82.3 mm, n=3, female SVL 85.4–98.0 mm, n=3; examined specimens, Appendix II; Biju et al., 2010), lower TE/TD 109–129 % and IUE/UEW 75–92 %, n=3 (vs. TE/TD 163–230 % and IUE/UEW 105–144 %, n=6; examined specimens, Appendix II; Biju et al., 2010), typically longer SHL/SVL, male 61–66 %, n=5, female 57–61 %, n=6 (vs. SHL/SVL, male 57–60 %, n=3, female 52–57 mm, n=3; examined specimens, Appendix II; Biju et al., 2010), dorsal colouration primarily green with dark brown blotches (vs. chocolate brown with small iridescent green rosette shaped spots, n=6; examined specimens, Appendix II; Biju et al., 2010), skin on flanks tubercular (vs. smooth, n=6; examined specimens, Appendix II; Biju et al., 2010); from *A. pallasitatus* by larger adult female size, SVL 80.5–89.6 mm, n=6 (vs. female SVL 70.6–72.3 mm, n=2; Qi et al., 2019), skin on flanks tubercular (vs. smooth, n=2; Qi et al., 2019), smaller TD/EL 30–34 %, n=3 (vs. TD/EL 40–42 %, n=2; Qi et al., 2019), longer female SHL/SVL 57–61 %, n=6 (vs. female SHL/SVL 53–55 %, n=2; Qi et al., 2019); from *A. senchalensis* by larger adult male size, SVL 71.4–76.7 mm, n=5 (vs. adult male SVL 46.2 mm on holotype, n=1; examined specimen, Appendix II), lower IUE/IN 73–77 % and FAL/HAL 61–71 %, n=3 (vs. IUE/IN 89 % and FAL/HAL 73 % on holotype, n=1; examined specimen, Appendix II);

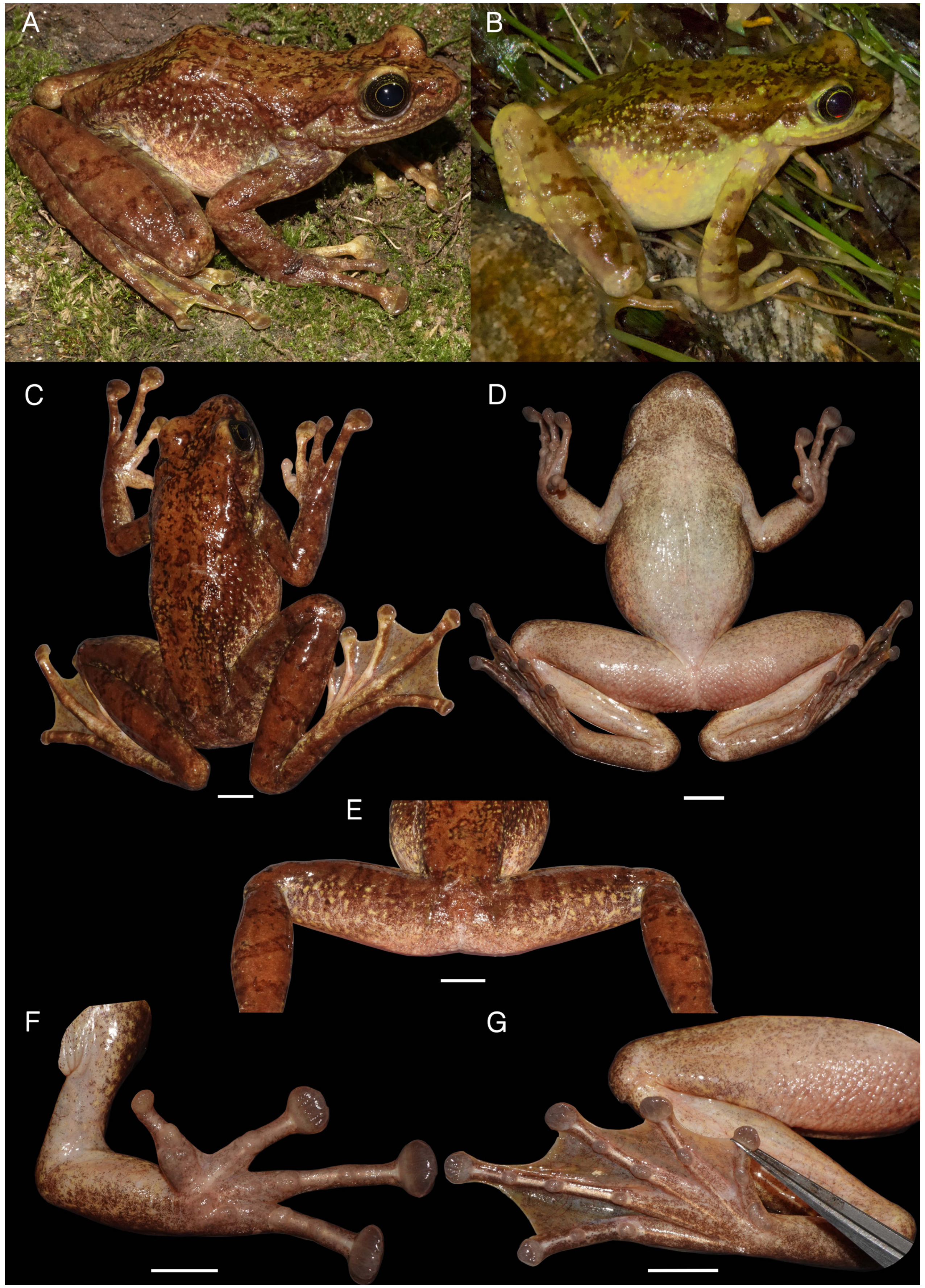

Figure 5. *Amolops wangyali* sp. nov. adult female paratype (SCZM 2019.07.18.2) in life (A & B) and immediately after euthanisation, prior to fixation (C–G): A. dorsolateral view, image taken ex-situ; B. dorsolateral view, image taken in-situ; C. dorsolateral view; D. ventral view; E. posterior view of thighs; F. palmar view of left hand; G. plantar view of right foot. Scale bars represent 10 mm.

from *A. viridimaculatus* (including *A. caelumnoctis* and *A. splendissimus*) by lower IUE/UEW 75–92 %, n=3 (vs. IUE/UEW 110–150 %, n=6; examined specimens, Appendix II; IUE/UEW 93–125 %, n=10, of which only two specimens had IUE/UEW<108 %; Orlov & Ho, 2007; IUE or UEW not measured; Zhang et al., 2021; Rao & Wilkinson, 2007), higher male SHL/SVL 61–66 %, n=5 (vs. male SHL/SVL 55–60 %, n=4; examined specimens, Appendix II; SHL/SVL 52–62 %, n=18, of which only one specimen had SHL/SVL>59 %; Orlov & Ho, 2007; Rao & Wilkinson, 2007; SHL not measured; Zhang et al., 2021), lower FOL/SHL 91–93 %, n=3 (vs. FOL/SHL 96–100 %, n=5 [FOL not taken for one specimen CAS 242252 due to missing digits]; examined specimens, Appendix II; FOL/SHL 89–105 %, n=8 of which only one specimen had FOL/SHL<94 %; Rao & Wilkinson, 2007; FOL not measured; Orlov & Ho, 2007; Zhang et al., 2021), TVL=TIIIL, n=3 (vs. TVL>TIIIL, n=5 [not taken for one specimen CAS 242252 due to missing digits]; examined specimens, Appendix II; TVL>TIIIL, n=1; Orlov & Ho, 2007; not mentioned; Rao & Wilkinson, 2007; Zhang et al., 2021), supratympanic fold well-developed, n=3 (vs. weakly developed, n=6; examined specimens, Appendix II; Orlov & Ho, 2007; Rao & Wilkinson, 2007), tympanum oval shaped, n=3 (vs. circular, n=6; examined specimens, Appendix II; "round"; Orlov & Ho, 2007; shape not mentioned; Rao & Wilkinson, 2007; Zhang et al., 2021), skin on flanks distinctly tubercular (vs. weakly granular, n=6; examined specimens, Appendix II; or "smooth"; Orlov & Ho, 2007; Rao & Wilkinson, 2007; Zhang et al., 2021), adult dorsal colouration in life primarily green with dark brown blotches (vs. in life, reddish-brown/dark purple/black/black-brown with very small to moderately large yellow, yellowish-green or iridescent green smooth edged rounded spots; Orlov & Ho, 2007; Rao & Wilkinson, 2007; Yang et al., 2019; Zhang et al., 2021); from *A. wangyufani* by larger adult male size, SVL 71.4–76.7 mm, n=5 (vs. male SVL 68.3–69.0, n=2; Jiang, 2020 [in Che et al., 2020]), relatively longer shanks, male SHL/SVL mean 63.6 %, min.–max. range 61–66 %, n=5, female SHL/SVL mean 58.7 %, min.–max. range 57–61 %, n=6 (vs. male SHL/SVL mean 60.6 %, n=2, female SHL/SVL mean 56.5 %, n=1; Jiang, 2020 [in Che et al., 2020] - individual specimen measurements were not provided so min.–max. SHL/SVL range cannot be determined for males), adult dorsal colouration of body in life primarily green with dark brown blotches (vs. primarily brown with green reticulations; Jiang, 2020 [in Che et al., 2020]:226, 228–229 figs. [x7]); shanks with 3–4 distinct dark brown transverse stripes (vs. 6–7 distinct dark brown transverse stripes; Jiang, 2020 [in Che et al., 2020]:226, 228–230 figs. [x8]).

Distribution

This species is currently known with certainty based on the results of sequence data from four localities in Trashigang District, Bhutan (Table 1): 1) the type locality at Bodidrang Chhu/Stream (1,640–1,750 m a.s.l.), Kanglung Gewog (village block) (Figs. 6E & 7; Nidup et al., 2016; Limbu et al., 2020; Streicher et al., 2020; results herein); 2) Jere Chhu/Stream (27.206083, 91.603389; 2,073 m a.s.l.), Khaling Town, Khaling-Kharungla Forest Management Unit (Nidup et al., 2016: fig. 2B & 2C); 3) a small perennial stream (27.2808, 91.53937; 1,520 m a.s.l.) that bisects the Trashigang-Samdrumjongkhar Highway (the stream eventually joins the Bodidrang Chhu/Stream further north at ca. 1,300 m a.s.l.), Rongthong Village (Streicher et al., 2020; Fig. 6C); 4) Thragom, a small stream above Kanglung BHU Hospital (27.28031, 91.51456; 1950 m a.s.l.), Kanglung Gewog (village block). We also consider the following localities to be included in the distribution based on published photographs that we regard as identifiable to this species (see 'Review of *Amolops* reports from Bhutan' section below for more details; Table 2; Fig. 7): 1) Serkang Chhu/Stream, a tributary of the Kulong Chhu/River, Choetenkora Town (ca. 27.605298, 91.493766; 1,745 m a.s.l.), Trashiyangtse District (Wangyal, 2013: image 14); 2) Khaling Chhu/Stream (27.190606, 91.602611; ca. 2,070 m a.s.l.), 1.7 km south of the Khaling Town, Khaling-Kharungla Forest Management Unit, Trashigang District (Nidup et al., 2016: fig. 2F). All six of these streams are within the Drangme Chhu/River Basin indicating that the species is likely to be widespread along tributaries on both sides of the Drangme Chhu/River in Mongar, Trashigang and Trashiyangtse districts of eastern Bhutan, at least within the elevation range 1,520–2,073 m a.s.l. The species possibly ranges further east into Tawang District, Arunachal Pradesh State, India where the Drangme Chhu/River is known as the Tawang Chhu/River.

Populations of *Amolops* photographed in Athreya (2006:145–146) referred to as "*Staurois* cf *viridimaculatus*" (adults) from "Bompu (2200 m) to New Khellong (1250 m)" and "*Amolops* sp." (juvenile) from "Sessni (1250 m)" in Eaglenest Wildlife Sanctuary, West Kameng District, Arunachal Pradesh State, India, superficially resemble *Amolops wangyali* sp. nov. These Eaglenest Wildlife Sanctuary populations are ca. 90 km east of the type locality of *Amolops wangyali* sp. nov. Measurements provided for two adult individuals from the Eaglenest Wildlife Sanctuary population differ from the type series of *Amolops wangyali* sp. nov., most notably by the head being considerably wider than long, however, HL measurements in Athreya (2006) may have been taken differently to our study. We suggest that the taxonomic status of populations from West Kameng District be reassessed to verify their identities.

Natural history and conservation

Nidup et al. (2016) and Limbu et al. (2020) discussed details on the general habitat, ecology and reproductive biology of this species. Limbu et al. (2020) reported the breeding season as March to June based on field observations, however, one of the paratypes (SCZM 2019.07.18.2) contained large pigmentless ova extending the reproductive season at least to late July when it was collected. Nidup et al. (2016) provided an image of an uncollected tadpole (fig. 3) from Bodidrang Chhu/Stream which they identified as *A. "himalayanus"*, however, at least two, or possibly three species of *Amolops* are sympatric in this stream (Limbu et al., 2020), so the identity of this photographed tadpole would require verification. Nidup et al. (2016) identified domestic stream

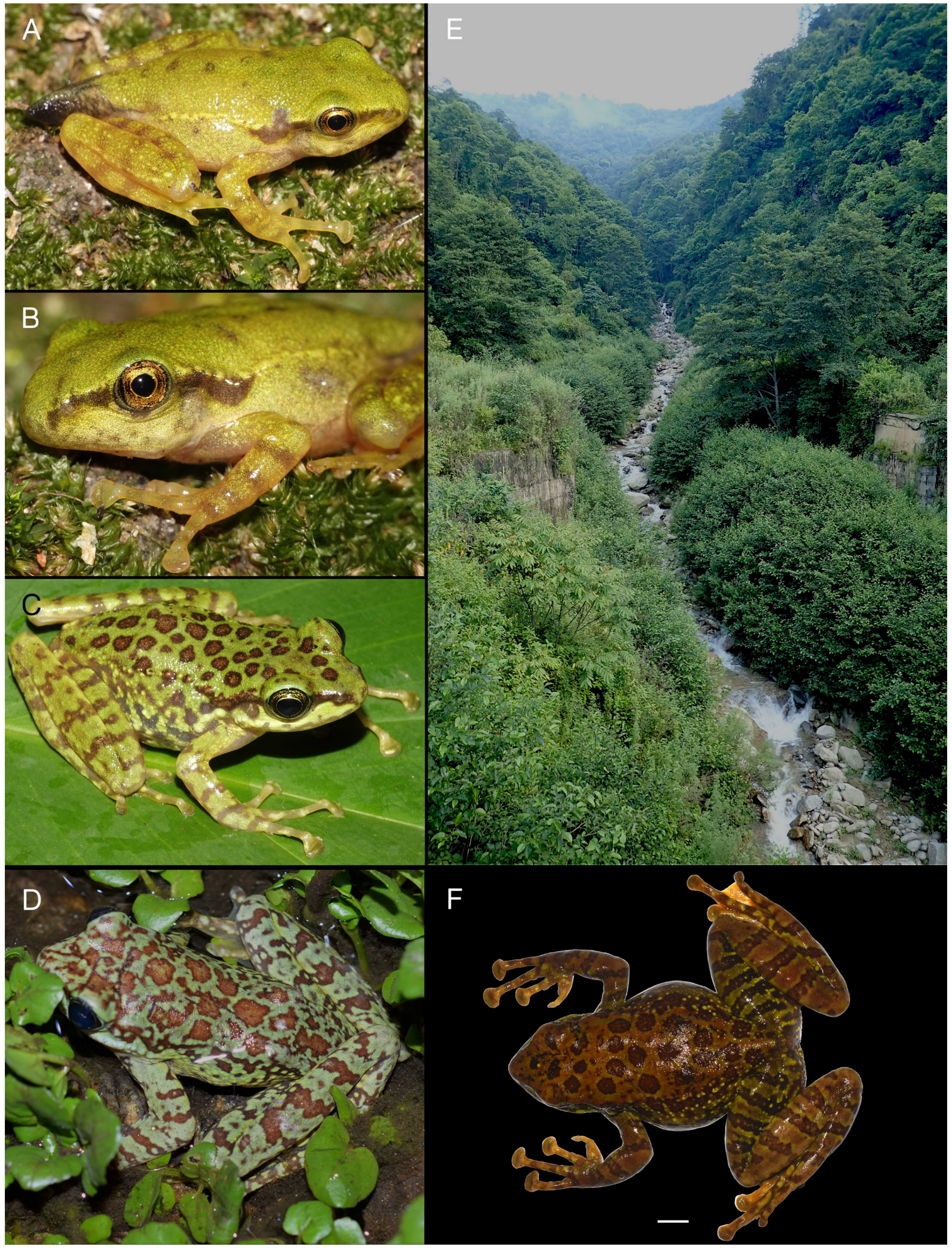

Figure 6. *Amolops wangyali* sp. nov. juveniles in life (A–D) showing ontogenetic variation in colouration and markings: A & B. dorsolateral and profile views of a nearly metamorphosed juvenile (SCZM 2019.07.18.3), from the type locality, images taken ex-situ; C. dorsolateral view of larger juvenile (SCZM 2019.07.20.1), from Rongthong (27.2808, 91.53937, ca. 1,520 m a.s.l.), Trashigang District, Bhutan, image taken ex-situ; D. dorsal view of uncollected halfgrown juvenile, from Jere Chhu/Stream, Khaling Town, Bhutan, image taken in-situ; E. habitat at the type locality, Bodidrang Chhu/Stream, taken from the Singye Thegchog Bridge two days after the collection of the holotype (20 July 2019); F. adult female paratype (SCZM 2019.08.02.1) from Bodidrang Chhu/Stream, image taken immediately after euthanisation, prior to fixation. Scale bar represents 10 mm.

pollution as a potential threat to the population at the Jere Chhu/Stream locality. Streicher et al. (2020) included the holotype and one of the paratypes in a preliminary survey for the amphibian pathogen *Batrachochytrium dendrobatidis* (Longcore et al., 1999), in Bhutan, which found no positive infections. The forested areas in Bhutan are afforded considerably more protection than in surrounding countries and frogs are not commonly collected for food/medicinal consumption in Bhutan, so deforestation and overharvesting are unlikely to threaten this species. However, a growing body of research is finding catastrophic biodiversity decline in even pristine and protected habitats worldwide (e.g. Hallmann et al., 2017; Zipkin et al., 2020) demonstrating the immediate need for long term monitoring of amphibian populations and extensive biodiversity surveys to understand the taxonomic diversity of the region. Patel & Das (2020) obtained high success rates for identifying and counting individuals of *Amolops formosus* during a multiday minimally invasive photographic survey using pattern recognition software. This could be a valuable tool of determining population sizes of adult individuals of *Amolops wangyali* sp. nov. (and other taxa with contrasting markings). However, juveniles are almost plain green becoming blotched as they mature (Fig. 6A–D; Nidup et al., 2016: fig. 2F; Limbu et al., 2020: fig. 2G & 2H) demonstrating that ontogenetic changes in colouration and markings are observable in this species. More work would be necessary to determine the extent of individual ontogenetic change, and at which point (if at all) adult colour pattern stabilises to assess the usefulness of Patel & Das's (2020) technique for long term studies (over months or years).

Review of *Amolops* reports from Bhutan

In this section, we review the *Amolops* species reported from Bhutan in the literature. Based on thus-far available published data, we clarify some misidentifications (provisionally) of species referred to this taxon in an effort to reduce taxonomic confusion of Bhutanese anurans. A relatively recent surge in progress among Bhutan's herpetological researchers to document the amphibians of this historically poorly studied country has led to a dramatic increase in the numbers of publications and number of species reported from the country. The following publications have provided original information relating to members of the genus *Amolops* from Bhutan: Das & Palden (2000); Wangyal & Gurung (2012, 2017); Wangyal (2013; 2014); Wangyal & Das (2014); Nidup et al. (2016); Tshewang & Letro (2018); Koirala et al. (2019); Limbu et al. (2020); Streicher et al. (2020); Wangyal et al. (2020).

Das & Palden (2000) provided the first country record of an *Amolops* species in Bhutan, *A. marmoratus*, based on two specimens collected from "Sershong, Sarpang District" and deposited in the Royal Manas National Park Museum, Gelephu, Sarpang District, Bhutan. The name *Amolops marmoratus* has long been a catch-all name that comprised a complex of superficially similar species reported from throughout much of the southern and eastern Himalayas from Nepal, through north-east India, Myanmar and neighbouring parts of Thailand and southern China. Dever et al. (2012) subsequently restricted the geographic distribution of *A. marmoratus* s.s. to eastern Myanmar and western Thailand. Pending further molecular verification and taxonomic scrutiny of the populations in Bhutan from the *marmoratus* species group, we recommend that species in this group are provisionally referred to as *A.* cf. *gerbillus*.

Wangyal & Gurung (2012) reported *A.* cf. *monticola* for the first time in Bhutan from "Rurichu [or Ruri Chhu/Stream] (27020.30' N & 89054.49' E), Wangdue Phodrang District at an altitude of 982m", however, the photograph provided of an example of the species (Wangyal & Gurung, 2012: image 7) represents a *marmoratus* species group member most similar to a species we have elsewhere identified as *A.* cf. *gerbillus* (Streicher et al., 2020). *Amolops monticola* (Anderson, 1871) is a poorly known species with few known specimens that are correctly identified in museum collections (SM pers. obs.; Patel et al. 2021). The name *A. monticola* has commonly been used to refer to *Amolops* that have dorsolateral ridges (e.g. Stuart et al., 2010) but many individuals of *A.* cf. *gerbillus* can possess weak dorsolateral ridges, and thus the confusion may arise.

Wangyal (2013: image 14) identified a photograph of a live frog as *A. mantzorum* that we consider to morphologically resemble a female *A. wangyali* sp. nov. The photographed individual was reported from a "perennial stream called Serkang Chu, that runs through the suburban Choetenkora Town [also called Chorten Kora, ca. 27.605298, 91.493766], the headquarters of Trashiyangtse District at an altitude of 1745m" (Wangyal, 2013). Serkang Chhu is a tributary of the Kulong Chhu, and the reported locality lies ca. 40 km north of the type locality of the new species, *A. wangyali* sp. nov. Wangyal (2013: image 17) identified a photograph of a pair of frogs as "*Sylvirana* cf. *guentheri*" from "Zhonggarchu, Lingmethang, Mongar [District]". Wangyal (2014) cautioned that this report of *Sylvirana* cf. *guentheri* required confirmation. The distinctly expanded discs on the digit tips and overall morphology of the photographed individuals (Wangyal, 2013: image 17) agree well with members of the *Amolops monticola* species group (possibly conspecific with the species included in our molecular analyses as "*A.* cf. *putaoensis*"; Fig. 1). *Hylarana (Sylvirana) guentheri* (Boulenger, 1882) has not been reported elsewhere in the southern Himalayas and should be removed from the faunal list of Bhutan. Wangyal & Das (2014) listed *A. formosus, A. gerbillus, A. himalayanus, A. marmoratus* and *A. monticola* in a checklist with no clarification regarding the basis for the inclusion of these species and thus must be regarded as anecdotal. They provided a figure (Wangyal & Das, 2014: fig. 3b) of a live frog identified as *Nanorana liebigii* (Günther, 1860) which we here identify as a female *A.* cf. *gerbillus*. Wangyal (2014) listed *Amolops "farmosus"* [sic.], *A. himalayanus* and *A. gerbillus* as expected to occur in Bhutan based on the proximity of their known distributions bordering Bhutan, indicating that their inclusion of these species on the aforementioned checklist (Wangyal & Das, 2014) was premature.

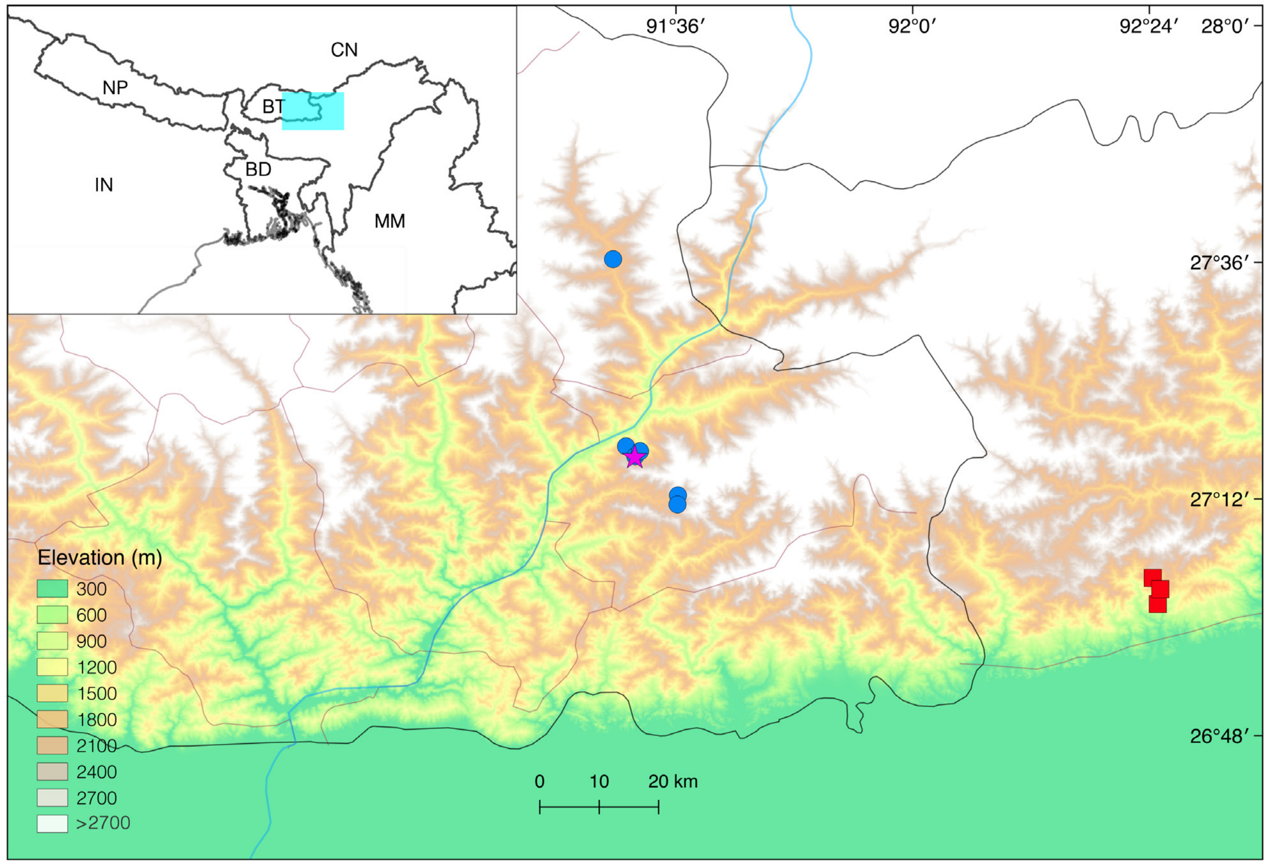

Figure 7. Topographic map of eastern Bhutan and bordering areas of north-east India showing the distribution of *Amolops wangyali* sp. nov. (star for type locality, circles for additional localities) and populations suspected to be conspecific with this species (squares). Inset: map of Bhutan and neighbouring north-east India with cyan box representing the area depicted in the main map. Country borders in black; district/state borders in brown; major river in blue; BD Bangladesh; BT Bhutan; CH China; IN India; MM Myanmar; NP Nepal.

Nidup et al. (2016) reported *A. himalayanus* for the first time in Bhutan giving the first in-depth study on an *Amolops* species in the country. This paper gave some basic specimen measurements, details of biology and conservation concerns and a summary of several previous reports of *A. himalayanus* from the literature. The authors discussed differences in SVL between their new material and specimens of *A. himalayanus* at BMNH, but other subtle morphological differences between the BMNH type specimens and the Bhutan populations were overlooked by the authors (see 'Morphological comparisons' section above). This is understandable as species diversity within the group was not known to be so high at the time of their study, and subtle morphological differences may have been considered as intraspecies variation when not informed by molecular data. The populations discussed in Nidup et al. (2016) represent *A. wangyali* sp. nov. Therefore, subsequent listing of *A. himalayanus* in Bhutan based on Nidup et al.'s (2016) study are corrected herein (see 'chresonymy of *A. wangyali* sp. nov.'). Limbu et al. (2020) further expanded on the reproductive ecology of *A. wangyali* sp. nov. (as *A. "himalayanus"*), from the type locality, Bodidrang Chhu/Stream. Limbu et al. (2020: fig. 6) also provided four photographs of other unidentified species of *Amolops* from the same locality, their identifications are provisionally revised here as follows: fig. 6, top left, undetermined *viridimaculatus* species group member, superficially similar to *A. formosus* but possibly representing a juvenile *A. wangyali* sp. nov.; fig. 6, bottom left, represents *A. wangyali* sp. nov.; fig. 6, top and bottom right, both represent *A.* cf. *gerbillus*. The morphological examination of specimens preferably accompanied by molecular sampling will be necessary to confirm the identities of these populations.

Tshewang & Letro (2018) reported *A. formosus* from "Langthel" and *A. marmoratus* from "Langthel, Nabji, Taksha, Tingtibi" in the Jigme Singye Wangchuck National Park in central Bhutan. The photograph they provided (Tshewang & Letro, 2018: image 33) of a live frog identified as *A. formosus* does not show diagnosing morphological characters to enable us to determine a reliable species-level identification beyond that it is a member of the *viridimaculatus* species group. The frogs shown in two photographs identified as *A. marmoratus* represent *Duttaphrynus* cf. *himalayanus* and *A.* cf. *gerbillus* (Tshewang & Letro, 2018: images 34a & 34b, respectively). The cited literature used for making species identifications in Tshewang & Letro's (2018) study do not provide adequate details of morphological characters to correctly identify species of *Amolops* so we recommend that the population identified as *A. formosus* should be referred to in future as "*Amolops* sp. 1. (*viridimaculatus* group)" pending a detailed taxonomic study of voucher specimens from the locality.

Koirala et al. (2019) reported four species of *Amolops* (*A. marmoratus, A. mantzorum, A. monticola* and an unidentified *Amolops* species) from Jigme Dorji National Park (but gave no specific localities) in western Bhutan. A photograph of *A. marmoratus* (image 4) represents an *A.* cf. *gerbillus* female, *A. mantzorum* (image 5) represents an *A.* cf. *formosus*, and *Amolops* sp. (image 6) represents another *A.* cf. *gerbillus*. No image of the species they identified as *A. monticola* was given so their report of *A. monticola* must be considered as anecdotal. They also provided an image labelled as "*Hyla* sp." (Koirala et al., 2019: image 8) which represents a juvenile *viridimaculatus* group member, possibly the same species as that shown in their image 4. Wangyal (2011) listed "*Hyla* cf. *annectans*" in a checklist as a new country record from the Royal Manas National Park, Bhutan, but provided no accompanying information. Wangyal (2014) subsequently highlighted the need for verification of his earlier report of a "*Hyla*" (Laurenti, 1768) species in Bhutan, but despite the uncertainty, he included "*Hylo*[sic.] cf. *onnectans*[sic.]" in the checklist of Bhutan species. Wangyal & Gurung (2017) listed "*Hyla annectans*" (Jerdon, 1870) in their updated amphibian checklist for Bhutan, without "cf." therefore implying that the species' identification had been confirmed, but no supporting evidence was provided. We are unaware of a verifiable report for the genus *Hyla* in Bhutan, so this genus should not be included on future national faunal checklists.Wangyal & Gurung's (2017) amphibian checklist of Bhutan listed six species of *Amolops*: *A. formosus, A. gerbillus, A. himalayanus, A. mantzorum, A. marmoratus*, and *A. monticola*.

In a study to determine whether the amphibian pathogen *Batrachochytrium dendrobatidis* was present in Bhutan, Streicher et al. (2020: fig. 1 S10 & S11) provided photographs of frogs identified as *A.* aff. *himalayanus* which represent the holotype and one of the paratypes (SCZM 2019.07.18.2) of *Amolops wangyali* sp. nov., and a specimen of *A.* cf. *gerbillus* (fig. 1, S12). Most recently, *Amolops wenshanensis* Yuan, Jin, Li, Stuart and Wu, 2018 was reported by Wangyal et al. (2020) from Goenshari Rimchu (27.694890 °N, 89.769082 °E) in Punakha District based on a photo voucher (ZRC (IMG) 1.208). The individual photographed is the same as that given in Koirala et al. (2019: image 8) as "*Hyla* sp.", taken from a slightly different angle, but on the same substrate. Wangyal et al. (2020) did not refer to Koirala et al.'s (2019) prior identification. The field work in Koirala et al. (2019) was reported to have been carried out from November 2017 to February 2019, however, the photo voucher in Wangyal et al. (2020) was reported to have been taken on 20 July 2019, indicating a discrepancy in the date that the photo vouchered animal was observed between these two papers. As mentioned above the individual photographed in both studies represents a juvenile *viridimaculatus* species group member; *A. wenshanensis* is a member of the morphologically disparate *monticola* species group (Yuan et al., 2018). The basis for the identification in Wangyal et al. (2020) is not clear and is considered here to be erroneous.

CONCLUSIONS

In summary, we identified four species of *Amolops* from Bhutan: (1) *Amolops* sp. 1. (*viridimaculatus* group: from Tshewang & Letro, 2018), (2) *A.* cf. *gerbillus* (*marmoratus* group), (3) *A.* cf. *putaoensis* (*monticola* group), and (4) *A. wangyali* sp. nov. (*viridimaculatus* group). Outside of the new species described herein, we were unable to determine species identities for these taxa given the available data. Until such time as vouchered specimens are clearly identified from the country by means of a detailed morphological comparison of vouchered specimens with relevant taxonomic literature, and/or with the aid of DNA sequence data, the following nine species must be formally removed from the amphibian checklist of Bhutan: (1) *Amolops formosus*, (2) *A. gerbillus*, (3) *A. himalayanus* (including *A.* aff. *himalayanus*), (4) *A. mantzorum*, (5) *A. marmoratus*, (6) *A. monticola*, (7) *A. wenshanensis*, (8) *Sylvirana* cf. *guentheri*, (9) *Hyla annectans* (including *Hyla* cf. *annectans*). Unintentional misidentifications in the literature can result in significantly overestimated/erroneous geographic distributions for species, a situation which undermines conservation efforts. Inaccuracies in such assessments could even result in the redirection of conservation resources (funds and efforts) away from vulnerable range restricted species that require urgent attention. For these reasons, we encourage authors not to assign species names to taxa in publications if there is any uncertainty regarding the identification of the species. Many populations of amphibians reported from Bhutan (and elsewhere in Asia) are provided non-specific locality details (e.g. lack GPS coordinates, elevation details), are not represented in museum/university collections by vouchered specimens, and are often published without photographic evidence. Locally abundant species can often be dismissed as "common", or of little scientific interest, and subsequently ignored by researchers; however, studies on Himalayan amphibians have demonstrated that "common" or widespread species occasionally represent complexes of morphologically similar species (e.g. Dubois, 1975; Kamei et al., 2009; Dever et al., 2012; Khatiwada et al., 2017; Mahony et al., 2013, 2018, 2020), so careful attention to document every species should be made when possible. Our review of *Amolops* reports in literature demonstrate that some taxonomic information can be obtained from good quality images of uncollected animals, but inevitably an accurate species inventory for Bhutan's amphibian fauna will not be possible without permanently maintained reference collections of vouchered specimens. Range restricted species may be only one drought, forest fire or hydroelectric dam away from extinction, thus the urgency to catalogue the Himalayan biodiversity has never been more urgent.

ACKNOWLEDGEMENTS

The Department of Forest and Park Services, Bhutan kindly provided specimen collection permits to TN (Permit no. 205474365BFF950D3594C) and the National Biodiversity Centre, Ministry of Agriculture & Forests, Royal Government of Bhutan issued the Material Transfer Agreement (Ref. no. NBC/BRD-7/2019-2020) that made this research possible. For logistical support in the field and assistance organising permits TN thanks the Sherubtse College management, particularly Tshering Wangdi (President) and Dendup Tshering (Dean of Research & Industrial Linkages), and Malcolm J. Pearch (previously in Harrison Institute, UK), and for their assistance in the field, Nub Tshering Lepcha, Penjor, Dawa Gyeltshen, Namgay Rinchen, Ash B. Limbu and Namgay Dorji; SM thanks Kaushik Deuti and K. Venkataraman, and staff of the amphibian sections (ZSIK) for access to specimen collections and support during museum visits, Jens Vindum (CAS) for providing specimen loans, Erik Åhlander and Andrea Hennyey (NRM) for providing images for a type specimen, Hellen Pethers (NHM library) for confirming the missing reference in J. Bengal Nat. Hist. Soc. We thank Tshering Wangdi (President) and Karma Wangchuck (Head of Department of Environment & Life Sciences) of Sherubtse College for hosting SM, JWS and RGK. SM, JWS and RGK thank Ugyen Norbu and Parop Wangdi for their companionship and/or logistical assistance during our Bhutan visit. This research was supported by the following funding: Irish Research Council-Marie Skłodowska-Curie CAROLINE Fellowship (CLNE/2017/482) to SM; Natural History Museum, London support from the Department of Life Sciences to JWS and SM; Percy Sladen Memorial Fund from the Linnean Society to SM; first (2015–2016) and second (2018–2019) Rufford Small Foundation Grants to TN. We thank the two anonymous reviewers for their suggestions and comments on our submitted manuscript.

Authors' contribution

SM examined museum specimens, did molecular phylogenetic analyses and drafted the manuscript. SM & JWS designed arcDNA experiments. SM, JWS, RGK did molecular lab work. SM, JWS, ECT obtained funding. TN collected specimens and field data. SM, TN, JWS organised permits. SM, JWS, TN photographed specimens. RGK, SM prepared figures and map. JWS drafted arcDNA lab protocol. SM, RGK, JWS, TN, ECT read, commented and edited working drafts of the manuscript.

REFERENCES

Agarwal, I., Mistry, V.K. & Athreya, R. (2010). A preliminary checklist of the reptiles of Eaglenest Wildlife Sanctuary, West Kameng District, Arunachal Pradesh, India. *Russian Journal of Herpetology*, 17(2), 81–93.

Altschul, S.F., Gish, W., Miller, W., Myers, E.W. & Lipman, D.J. (1990). Basic Local Alignment Search Tool. *Journal of Molecular Biology*, 215, 403–410.

Anders, C. (2002). Class Amphibia (amphibians). In: *Amphibians and Reptiles of Nepal*. Schleich, H.H. & Kästle, W. (eds.). Ruggell: A.R.G. Gantner Verlag K.G., pp. 133–340.

Anderson, J. (1871). A list of the reptilian accession to the Indian Museum, Calcutta from 1865 to 1870, with a description of some new species. *Journal of the Asiatic Society of Bengal*, 40, 12–39.

Andersson, L.G. (1939). Batrachians from Burma collected by Dr. R. Malaise, and from Bolivia and Ecuador collected by Dr. C. Hammarlund. *Arkiv för Zoologi*, *Stockholm*, 30(23 "1938"), 1–24.

Annandale, N. (1912). Zoological results of the Abor Expedition, 1911–1912. I. Amphibia. *Records of the Indian Museum*, 8, 7–36.

Arifin, U., Smart, U., Hertwig, S.T., Smith, E.N., Iskandar, D.T. & Haas, A. (2018). Molecular phylogenetic analysis of a taxonomically unstable ranid from Sumatra, Indonesia, reveals a new genus with gastromyzophorous tadpoles and two new species. *Zoosystematics and Evolution*, 94(1), 163–193.

Athreya, R. (2006). Eaglenest Biodiversity Project (2003–2006): Conservation Resources for Eaglenest Wildlife Sanctuary. Pune: Kaati Trust, 189 p.

Bain, R.H. & Nguyen, T.Q. (2004). Herpetofauna diversity of Ha Giang Province in northeastern Vietnam, with descriptions of two new species. *American Museum Novitates*, 3453, 1–42

Bain, R.H., Lathrop, A., Murphy, R.W., Orlov, N.L. & Ho, C.T. (2003). Cryptic species of a cascade frog from Southeast Asia: taxonomic revisions and descriptions of six new species. *American Museum Novitates*, 3417, 1–60

Bain, R.H., Stuart, B.L. & Orlov, N.L. (2006). Three new Indochinese species of cascade frogs (Amphibia: Ranidae) allied to *Rana archotaphus*. *Copeia*, 2006, 43–50.

Benson, D.A., Cavanaugh, M., Clark, K., Karsch-Mizrachi, I., Lipman, D.J., Ostell, J. & Sayers, E.W. (2017). GenBank. *Nucleic Acids Research*, 45(Database issue), D37–D42. https://doi.org/10.1093/nar/gkw1070.

Biju, S.D., Mahony, S. & Kamei, R.G. (2010). Description of two new species of torrent frog, *Amolops* Cope (Anura: Ranidae) from a degrading forest in the northeast Indian state of Nagaland. *Zootaxa*, 2408, 31–46.

Blyth, E. (1855). Report of the Curator; Zoological Department, for March meeting. *Journal of the Asiatic Society of Bengal*, 24, 187–188.

Boulenger, G.A. (1882) Catalogue of the Batrachia Salientia s. Caudata in the Collections of the British Museum. Second Edition. British Museum (Natural History). London: Taylor and Francis, xvi + 503 p.

Boulenger, G.A. (1888). Descriptions of two new Indian species of *Rana*. *Annals and Magazine of Natural History*, Series 6, 2, 506–508.

Boulenger, G.A. (1899a). Descriptions of new batrachians in the collection of the British Museum (Natural History). *Annals and Magazine of Natural History*, Series 7, 3, 273–277.

Boulenger, G.A. (1899b). On a collection of reptiles and batrachians made by Mr. J. D. Latouche in N.W. Fokien, China. *Proceedings of the Zoological Society of London*, 1899, 159–172.

Boulenger, G.A. (1900). On the reptiles, batrachians, and fishes collected by the late Mr. John Whitehead in the interior of Hainan. *Proceedings of the Zoological Society of London*, 1899, 956–962.

Boulenger, G.A. (1920). A monograph of the South Asian, Papuan, Melanesian and Australian frogs of the genus *Rana*. *Records of the Indian Museum*, 20, 1–226. doi: 10.5962/bhl.title.12471.

Chan, K.O., Alexander, A.M., Grismer, L.L., Su, Y.-C., Grismer, J.L., Quah, E.S.H. & Brown, R.M. (2017). Species delimitation with gene flow: A methodological comparison and population genomics approach to elucidate cryptic species boundaries in Malaysian Torrent Frogs. *Molecular Ecology*, 26(20), 5435–5450. DOI: 10.1111/mec.14296.

Chan, K.O., Abraham, R.K., Grismer, J.L. & Grismer, L.L. (2018). Elevational size variation and two new species of torrent frogs from Peninsular Malaysia (Anura: Ranidae: *Amolops* Cope). *Zootaxa*, 4434, 250–264.

Chanda, S.K. (1987). On a collection of anuran amphibians from Darjeeling and Sikkim Himalayas, with description of a new species of *Rana* (Ranidae). *Journal of Bengal Natural History Society*, 5 (2 "1986"), 140–155.

Chanda, S.K. (2002). Hand book - Indian amphibians. Kolkata: Zoological Survey of India, 335 p.

Chanda, S.K. & Deuti, K. (1998). Endemic amphibians of India. *Records of the Zoological Survey of India*, 96 (1–4 "1997"), 63–79.

Chanda, S.K. & Ghosh, A.K. (1988). Addenda to the amphibian fauna of India. *Journal of the Bombay Natural History Society*, 85 (3), 626–627.

Chanda, S.K., Das, I. & Dubois, A. (2001). Catalogue of amphibian types in the collection of Zoological Survey of India. *Hamadryad*, 25 (2 "2000"), 100–128.

Che, J., Jiang, K., Yan, F. & Zhang, Y. (2020). Amphibians and Reptiles in Tibet—Diversity and Evolution. Beijing: Chinese Academy of Sciences. Science Press. 803 p.

Chen, L., Murphy, R.W., Lathrop, A., Ngo, A., Orlov, N.L., Ho, C.T. & Somorjai, I.L. (2005). Taxonomic chaos in Asian ranid frogs: an initial phylogenetic resolution. *Herpetological Journal*, 15(4), 231–243.

Cope, E.D. (1865). Sketch of the primary groups of Batrachia s. Salientia. *Natural History Review*. *New Series*, 5, 97–120.

Das, I. & Dutta, S.K. (1998). Checklist of the amphibians of India, with English common names. *Hamadryad*, 23 (June), 63–68.

Das, I. & Palden, J. (2000). A herpetological collection from Bhutan, with new country records. *Herpetological Review*, 31, 256–258.

David, A. (1872). Rapport adressé a MM. les Professeurs-Administráteurs du Museum d'histoire naturelle. *Nouvelles Archives du Muséum d'Histoire Naturelle. Paris*, 7 ("1871"), 75–100.

Del Fabbro, C., Scalabrin, S., Morgante, M. & Giorgi, F.M. (2013). An extensive evaluation of read trimming effects on Illumina NGS data analysis. *PLoS ONE*, 8(12), e85024. doi:10.1371/journal.pone.0085024.

Dever, J.A., Fuiten, A.M., Konu, Ö. & Wilkinson, J.A. (2012). Cryptic torrent frogs of Myanmar: an examination of the *Amolops marmoratus* species complex with the resurrection of *Amolops afghanus* and the identification of a new species. *Copeia*, 2012(1), 57–76.

Deuti, K & Ayyaswamy, A.K. (2008). Three new records of amphibians from West Bengal. *Records of the Zoological Survey of India*, 108 (4), 17–20.

DoFPS(2020). Bhutan Herpetofauna Monitoring Protocol. Thimphu: Department of Forests and Park Services, i–ii + 35 pp.

Dubois, A. (1974). Liste commentée d'Amphibiens récoltés au Népal. *Bulletin du Muséum National D'Histoire Naturelle, Series 3*, 213 (Zoologie 143), 341–411.

Dubois, A. (1975). Une nouveau complexe d'espèces jumelles distinguées par le chant: les grenouilles de Népal voisines de *Rana limnocharis* Boie (Amphibienes, Anoures). *Comptes Rendus Hebdomadaires des Séances de l'Académie des Sciences*, 281, 1717–1720.

Dubois, A. (2000). Synonymies and related lists in zoology: general proposals, with examples in herpetology. *Dumerilia*, 4 (2), 33–98.

Duellman, W.E. (1993). Amphibian species of the world: additions and corrections. *Natural History Museum, University of Kansas. Special Publication*, 21, i–iii, 1–372 pp.

Dutta, S.K. (1997). Amphibians of India and Sri Lanka (Checklist and Bibliography). Bubaneswar: Odyssey Publishing House, XIII + 342 + XXII pp.

Edgar, R.C. (2004). Muscle: a multiple sequence alignment method with reduced time and space complexity. *BMC Bioinformatics*, 5, 113.

Faircloth, B.C. (2013). Illumiprocessor: A trimmomatic wrapper for parallel adapter and quality trimming. http://dx.doi.org/10.6079/J9ILL.

Fei, L., Ye, C.Y. & Jiang, J.P. (2012). Colored Atlas of Chinese Amphibians and their Distributions. Chengdu: Sichuan Publishing House of Science and Technology, 620 p.

Fei, L., Ye, C.-y., Wang, Y.-f. & Jiang, K. (2017). A new species of the genus *Amolops* (Anura: Ranidae) from high-altitude Sichuan, southwestern China, with a discussion on the taxonomic status of *Amolops kangtingensis*. *Zoological Research*, 38, 138–145.

Frank, N. & Ramus, E. (1995). A Complete Guide to Scientific and Common Names of Reptiles and Amphibians of the World. Pottsville: NG Publishing, Inc., 377 p.

Frost, D.R. (2021). Amphibian Species of the World: an online reference. Version 6. New York: American Museum of Natural History. Downloaded on 16 September 2021. https://amphibiansoftheworld.amnh.org/index.php.

Gan, Y.-L., Yu, G.-H. & Wu, Z.-J. (2020a). A new species of the genus *Amolops* (Anura: Ranidae) from Yunnan, China. *Zoological Research*, 41(2), 188–193.

Gan, Y.-L., Qin, T., Lwin, Y.H., Li, G.-G., Quan, R.-C., Liu, S. & Yu, G.-H. (2020b). A new species of *Amolops* (Anura: Ranidae) from northern Myanmar. *Zoological Research*, 4(6), 1–7.

Grosjean, S., Ohler, A., Chuaynkern, Y., Cruaud, C. & Hassanin, A. (2015). Improving biodiversity assessment of anuran amphibians using DNA barcoding of tadpoles. Case studies from Southeast Asia. *Comptes Rendus Biologies*, 338(5), 351–361.

Günther, A.C.L.G. (1858). Neue Batrachier in der Sammlung des britischen Museums. *Archiv für Naturgeschichte*, 24, 319–328.

Günther, A. (1860). Contributions to a knowledge of the reptiles of the Himalaya mountains. I. Descriptions of the new species. II. List of Himalayan reptiles, with remarks on their horizontal distribution. *Proceedings of the Zoological Society of London*, 1860, 148–175.

Günther, A.C.L.G. (1876). Third report on collections of Indian reptiles obtained by the British Museum. *Proceedings of the Zoological Society of London*, 1875, 567–577.

Hallmann, C.A., Sorg, M., Jongejans, E., Siepel, H., Hofland, N., Schwan, H., Stenmans, W., Müller, A., ... de Kroon, H. (2017). More than 75 percent decline over 27 years in total flying insect biomass in protected areas. *PloS ONE*, 12(10), e0185809. https://doi.org/10.1371/journal.pone.0185809

Hayek, L.-A.C., Heyer, W.R. & Gascon, C. (2001) Frog morphometrics: A cautionary tale. *Alytes: International Journal of Batrachology*, 18(3–4), 153–177.

Inger, R.F. & Chan-ard, T. (1997). A new species of ranid frog from Thailand, with comments on *Rana livida* (Blyth). *Natural History Bulletin of the Siam Society*, 45, 65–70.

Inger, R.F. & Kottelat, M. (1998). A new species of ranid frog from Laos. *Raffles Bulletin of Zoology*, 46, 29–34.

Inger, R.F., Orlov, N.L. & Darevsky, I.S. (1999). Frogs of Vietnam: A report on new collections. *Fieldiana. Zoology. New Series*, 92, 1–46.

IUCN Bangladesh. (2015). Red List of Bangladesh Volume 4: Reptiles and Amphibians. Dhaka: IUCN, International Union for Conservation of Nature, Bangladesh Country Office, xvi + 320 p.

Jerdon, T.C. (1870). Notes on Indian herpetology. part 2. *Proceedings of the Asiatic Society of Bengal*, March 1870, 66–85.

Jiang, K., Wang, K., Xie, J., Zou, D.-H., Liu, W.-L., Jiang, J.-p., Li, C. & Che, J. (2016). A new species of the genus *Amolops* (Amphibia: Ranidae) from southeastern Tibet, China. *Zoological Research*, 37, 31–40.

Jiang, K., Ren, J.-L., Lyu, Z.-T., Wang, D., Wang, Z., Lv, K., Wu, J.-W. & Li, J.-T. (2021). Taxonomic revision of *Amolops chunganensis* (Pope, 1929) (Amphibia: Anura) and description of a new species from southwestern China, with discussion on *Amolops monticola* group and assignment of species groups of the genus *Amolops*. *Zoological Research*, 42(5), 574–591.

Jiang, Y.-m. (1983). [A new species of the genus *Staurois* (Ranidae), *Staurois viridimaculatus*]. *Acta Herpetologica Sinica. New Series*, 2(3), 71.

Kamei, R.G., Wilkinson, M., Gower, D.J. & Biju, S.D. (2009). Three new species of striped *Ichthyophis* (Amphibia: Gymnophiona: Ichthyophiidae) from the northeast Indian states of Manipur and Nagaland. *Zootaxa*, 2267(1), 26-42.

Kearse, M., Moir, R., Wilson, A., Stones-Havas, S., Cheung, M., Sturrock, S., Buxton, S.,Cooper, ... Drummond, A. (2012). Geneious Basic: an integrated and extendable desktop software platform for the organization and analysis of sequence data. *Bioinformatics*, 28(12), 1647–1649.doi: 10.1093/bioinformatics/bts199.

Khatiwada, J.R., Shu, G.C., Wang, S.H., Thapa, A., Wang, B. & Jiang, J. (2017). A new species of the genus *Microhyla* (Anura: Microhylidae) from Eastern Nepal. *Zootaxa*, 4254 (2), 221–239.

Khatiwada, J.R., Shu, G., Wang, B., Zhao, T., Xie, F. & Jiang, J. (2020). Description of a new species of *Amolops* Cope, 1865 (Amphibia: Ranidae) from Nepal and nomenclatural validation of *Amolops nepalicus* Yang, 1991. *Asian Herpetological Research*, 11(2), 71–94.

Khatiwada, J.R., Wang, B., Zhao, T., Xie, F. & Jiang, J.P. (2021). An integrative taxonomy of amphibians of Nepal: an updated status and distribution. *Asian Herpetological Research*, 12(1), 1–35. DOI: 10.16373/j.cnki.ahr.200050 .

Koirala, B.K., Cheda, K. & Penjor, T. (2019). Species diversity and spatial distribution of amphibian fauna along the altitudinal gradients in Jigme Dorji National Park, western Bhutan. *Journal of Threatened Taxa*, 11(10), 14249–14258.

Kumar, S., Stecher, G. & Tamura, K. (2016). MEGA7: Molecular Evolutionary Genetics Analysis Version 7.0 for bigger datasets. *Molecular Biology and Evolution*, 33(7), 1870–1874.

Lalronunga, S., Vanramliana, Lalrinchhana, C., Vanlalhrima, Sailo, V., Lalnunhlua, Sailo, L., Zosangliana, ... Lalhmingliani, E. (2020). DNA barcoding reveals a new country record for three species of frogs (Amphibia: Anura) from India. *Science Vision*, 20(3), 106–117.

Laurenti, J.N. (1768). Specimen Medicum, Exhibens Synops in Reptilium Emendatum cum Experimentis Circa Venena et Antidota Reptilium Austriacorum. Wien: Joan. Thom. nob. de Trattnern: i–ii + 1–215, pl. I–V.

Leinonen, R., Sugawara, H., Shumway, M., & International Nucleotide Sequence Database Collaboration. (2010). The Sequence Read Archive. *Nucleic Acids Research*, 39(Database issue), D19–D21.

Limbu, A.B., Dophu, Biswa, A.B., Sonam, L., Norbu, K., Gyeltshen, D., Basnet, D.B., Gyeltshen, J. & Nidup, T. (2020). Breeding ecology of *Amolops himalayanus* (Amphibia: Anura: Ranidae) in Bodidrang Stream, Trashigang District, Bhutan. *Asian Journal of Biology*, 10(1), 56–64.

Linnaeus, C. (1758). Systema Naturae per Regna Tria Naturae, Secundum Classes, Ordines, Genera, Species, cum Characteribus, Differentiis, Synonymis, Locis. 10th Edition. Volume 1. Stockholm, Sweden: L. Salvii, i–iv + 1–824.

Liu, C.-c. (1945). New frogs from West China. *Journal of the West China Border Research Society, Series B*, 15, 28–44.

Liu, C.-c. (1950). Amphibians of western China. *Fieldiana. Zoology Memoires*, 2, 397 p. + 10 pl.

Liu, C.-c. & Hu, S.-q. (1961). Tailless Amphibians of China. *Beijing: Science Press*. [i–ii] + i–xvi + 1–364, pl. 1–6 + 1–28. [In Chinese]

Liu, C.-c. & Hu, S.-q. (1975). Report on three new species of Amphibia from Fujian Province. *Acta Zoologica Sinica*, 21, 265–271.

Liu, W.-z. & Yang, D.-t. (2000). A new species of *Amolops* (Anura: Ranidae) from Yunnan, China, with a discussion of karyological diversity in *Amolops*. *Herpetologica*, 56, 231–238.

Liu, W.-z., Yang, D.-t., Ferraris, C. & Matsui, M. (2000). *Amolops bellulus*: a new species of stream-breeding frog from western Yunnan, China (Anura: Ranidae). *Copeia*, 2000, 536–541.

Longcore, J.E., Pessier, A.P. & Nichols, D.K. (1999). *Batrachochytrium dendrobatidis* gen. et sp. nov., a chytrid pathogenic to amphibians. *Mycologia*, 91(2), 219–227.

Lyu, Z.-T., Wu, J., Wang, J., Sung, Y.-h., Liu, Z.-y., Zeng, Z.-C., Wang, X., Li, Y.-y. & Wang, Y. (2018). A new species of *Amolops* (Anura: Ranidae) from southwestern Guangdong, China. *Zootaxa*, 4418, 562–576.

Lyu, Z.-T., Huang, L.-s., Wang, J., Li, Y.-q., Chen, H.-h., Qi, S. & Wang, Y.-y. (2019a). Description of two cryptic species of the *Amolops ricketti* group (Anura, Ranidae) from southeastern China. *ZooKeys*, 812, 133–156.

Lyu, Z.T., Zeng, Z.C., Wan, H., Yang, J.H., Li, Y.L., Pang, H. & Wang, Y.Y. (2019b). A new species of *Amolops* (Anura: Ranidae) from China, with taxonomic comments on *A. liangshanensis* and Chinese populations of *A. marmoratus*. *Zootaxa*, 4609(2), 247–268.

Mahony, S., Teeling, E.C. & Biju, S.D. (2013). Three new species of horned frogs, *Megophrys* (Amphibia: Megophryidae), from northeast India, with a resolution to the identity of *Megophrys boettgeri* populations reported from the region.

Zootaxa, 3722(2), 143–169.

Mahony, S., Foley, N.M., Biju, S.D. & Teeling, E.C. (2017). Evolutionary history of the Asian horned frogs (Megophryinae): integrative approaches to timetree dating in the absence of a fossil record. *Molecular Biology and Evolution*, 34(4), 744–771 + S.I. 38 p.

Mahony, S., Kamei, R.G., Teeling, E.C. & Biju, S.D. (2018). Cryptic diversity within the *Megophrys major* species group (Amphibia: Megophryidae) of the Asian horned frogs: phylogenetic perspectives and a taxonomic revision of South Asian taxa, with descriptions of four new species. *Zootaxa*, 4523(1), 1–96.

Mahony, S., Kamei, R.G., Teeling, E.C. & Biju, S.D. (2020). Taxonomic review of the Asian horned frogs (Amphibia: *Megophrys* Kuhl & Van Hasselt) of Northeast India and Bangladesh previously mis-identified as *M. parva* (Boulenger), with descriptions of three new species. *Journal of Natural History*, 54, 119–194.

Mahony, S. & Kamei, R.G. (2022). A new species of bent-toed gecko, *Cyrtodactylus* Gray (Squamata: Gekkonidae) from Manipur state, northeast India, with a critical review of extensive errors in literature covering Indo-Burman species. *Journal of Natural History*, 55(39–40 “2021”), 2445–2480.

Matsui, M. & Nabhitabhata, J. (2006). A new species of *Amolops* from Thailand (Amphibia, Anura, Ranidae). *Zoological Science*, 23, 727–732.

Matsui, M., Shimada, T., Liu, W.Z., Maryati, M., Khonsue, W. & Orlov, N. (2006). Phylogenetic relationships of Oriental torrent frogs in the genus *Amolops* and its allies (Amphibia, Anura, Ranidae). *Molecular Phylogenetics and Evolution*, 38(3), 659–666.

McGuire, J.A., Cotoras, D.D., O’Connell, B., Lawalata, S.Z.S., Wang-Claypool, C.Y., Stubbs, A., Huang, X., ... Iskandar, D.T. (2018). Squeezing water from a stone: high-throughput sequencing from a 145-year old holotype resolves (barely) a cryptic species problem in flying lizards. *PeerJ*, 4470.

Miller, M.A., Pfeiffer, W. & Schwartz, T. (2010). Creating the CIPRES science gateway for inference of large phylogenetic trees. In: Proceedings of the Gateway Computing Environments Workshop (GCE). Institute of Electrical and Electronics Engineers (ed.). New Orleans: Piscataway, pp. 1–8. https://doi.org/10.1109/GCE.2010.5676129

Moore, S. (1999). Fluid Preservation. In: Carter, D. & Walker, A. (eds). (1999). Chapter 5: Care and Conservation of Natural History Collections. Oxford: Butterworth Heinemann, pp. 92–132.

National Biodiversity Centre (NBC) (2019). Biodiversity Statistics of Bhutan 2017: A Preliminary Baseline. Thimphu: National Biodiversity Centre. 66 p.

Ngo, A., Murphy, R.W., Liu, W., Lathrop, A. & Orlov, N.L. (2006). The phylogenetic relationships of the Chinese and Vietnamese waterfall frogs of the genus *Amolops*. *Amphibia-Reptilia*, 27(1), 81–92.

Nidup, T., Gyeltshen, D., Penjor, Dorji, S. & Pearch, M.J. (2016). The first record of *Amolops himalayanus* (Anura: Ranidae) from Bhutan. *Herpetological Bulletin*, 136(2016), 13–18.

Nokhbatolfoghahai, M., Conway, K.W., Atherton, L., Budha, P.B., Jowers, M.J. & Downie, J.R. (2020). Larval description and developmental staging of *Amolops* tadpoles from Nepal, including ultrastructure of the oral disc and sucker. *Salamandra*, 56(4), 317–328.

Orlov, N.L. & Ho, T.C. (2007). Two new species of cascade ranids of *Amolops* genus (Amphibia: Anura: Ranidae) from Lai Chau Province (northwest Vietnam). *Russian Journal of Herpetology*, 14(3), 211–228.

Orlov, N.L., Murphy, R.W., Ananjeva, N.B., Ryabov, S.A. & Ho, T.C. (2002). Herpetofauna of Vietnam, a checklist. Part 1. Amphibia. *Russian Journal of Herpetology*, 9(2), 81–104.

Palumbi, S.R. (1996). Nucleic acids II: the polymerase chain reaction. In: Molecular Systematics. 2nd ed. Hillis, D.M., Moritz, C. & Mable, B.K. (ed.) Sunderland: Sinauer Associates, 205–247.

Patel, N.G. & Das, A. (2020). Shot the spots: A reliable field method for individual identification of *Amolops formosus* (Anura, Ranidae). *Herpetozoa*, 33, 7–15.

Patel, N.G., Garg, S., Das, A., Stuart B.L. & Biju, S.D. (2021). Phylogenetic position of the poorly known montane cascade frog *Amolops monticola* (Ranidae) and description of a new closely related species from Northeast India. *Journal of Natural History*, 55(21–22), 1403–1440.

Pham, A.V., Sung, N.B., Pham, C.T., Le, M.D., Ziegler, T. & Nguyen, T.Q. (2019). A new species of *Amolops* (Anura: Ranidae) from Vietnam. *Raffles Bulletin of Zoology*, 67, 363–377.

Pope, C.H. (1929). Four new frogs from Fukien Province, China. *American Museum Novitates*, 352, 1–5.

Pope, C.H. & Romer, J.D. (1951). A new ranid frog (*Staurois*) from the Colony of Hongkong. *Fieldiana. Zoology*, 31, 609–612.

Qi, S., Zhou, Z., Lyu, Z., Lu, Y., Wan, H., Hou, M., Guo, K. & Li, P. (2019). Description of a new species of *Amolops* (Anura: Ranidae) from Tibet, China. *Asian Herpetological Research*, 10(4), 219–229.

Ramashray, P. & Dorji, S. (2011). Earthquake and landslide vulnerability: some selected studies from Bhutan. *Sherub Doenme: The Research Journal of Sherubtse College*, 11(1&2), 23–31.

Rambaut, A. (2009). FigTree version 1.3.1. Downloaded in January 2012. http://tree.bio.ed.ac.uk/software/figtree/.

Rao, D.Q. & Wilkinson, J.A. (2007). A new species of *Amolops* (Anura: Ranidae) from southwest China. *Copeia*, 2007(4), 913–919.

Ray, P. (1992). Two new hill-stream frogs of the genus *Amolops* Cope (Amphibia: Anura: Ranidae) from Uttar Pradesh (India). *Indian Journal of Forestry*, 15, 346–350.

Ray, P. (1999). Systematic studies on the amphibian fauna of the district Dehradun, Uttar Pradesh, India. *Memoirs of the Zoological Survey of India*, 18(3), 1–102.

Sarkar, A.K., Biswas, M.L. & Ray, S. (1992). Amphibia. In: State Fauna Series 3: Fauna of West Bengal. Part 2. (Reptilia, Amphibia, Fishes, Hemichordata and Archaeozoology). Ghosh, A.K. (ed.) Kolkata: Zoological Survey of India, 67–100.

Savage, J.M. & Heyer, W.R. (1997). Digital webbing formulae for anurans: a refinement. *Herpetological Review*, 28(3), 131.

Sengupta, S., Hussain, B., Choudhury, P.K., Gogoi, J., Ahmed, F.M. & Choudhury, N.K. (2008). A new species of *Amolops* (Anura: Ranidae) from Assam, north-eastern India. *Hamadryad*, 32(1), 5–12.

Smith, M.A. (1923). On a collection of reptiles and batrachians from the Island of Hainan. *Journal of the Natural History Society of Siam*, 6, 195–212.

Smith, M.A. (1940). The amphibians and reptiles obtained by Mr. Ronald Kaulback in Upper Burma. *Records of the Indian Museum*, 42, 465–486.

Sondhi, S. & Kunte, K. (2016). Butterflies (Lepidoptera) of the Kameng Protected Area Complex, western Arunachal Pradesh, India. *Journal of Threatened Taxa*, 8(8), 9053–9124.

Stamatakis, A. (2014). RAxML version 8: a tool for phylogenetic analysis and post-analysis of large phylogenies. *Bioinformatics*, 30, 1312–1313. doi:10.1093/bioinformatics/btu033 .

Streicher, J.W., Schulte II, J.A. & Wiens, J.J. (2016) How should genes and taxa be sampled for phylogenomic analyses with missing data? An empirical study in iguanian lizards. *Systematic Biology*, 65, 128–145.

Streicher, J.W., Sadler, R. & Loader, S.P. (2020). Amphibian taxonomy: early 21st century case studies. *Journal of Natural History*, 54(1–4), 1–13.

Streicher, J.W., Mahony, S., Kamei, R.G., Nidup, T., Jervis, P. & Fisher, M.C. (2020). Preliminary survey reveals no evidence of *Batrachochytrium dendrobatidis* in the Kingdom of Bhutan. *Herpetological Review, Amphibian and Reptile Diseases*, 51(3), 494–497.

Stuart, B.L., Bain, R.H., Phimmachak, S. & Spence, K. (2010). Phylogenetic systematics of the *Amolops monticola* group (Amphibia: Ranidae), with description of a new species from northwestern Laos. *Herpetologica*, 66(1), 52–66.

Su, C.-y., Yang, D.-t. & Li, S.-m. (1986). A new species of *Amolops* from the Hengduan Shan Mountains. *Acta Herpetologica Sinica*, 5(3), 204–206.

Sun, G.-z., Luo, W.-x., Sun, H.-y. & Zhang, G.-y. (2013). A new species of cascade frog from Tibet: China [In Chinese with English abstract]. *Forestry Construction*, 20, 14–16.

Sung, Y. H., Hu, P., Wang, J., Liu, H. & Wang, Y.Y. (2016). A new species of *Amolops* (Anura: Ranidae) from southern China. *Zootaxa*, 4170(3), 525–538.

Swan, L.W. (1993). The Satpura Hypothesis - a biogeographical challenge to geology. *Journal of the Bombay Natural History Society*, 90(2), 141–157.

Tamura, K. & Nei, M. (1993). Estimation of the number of nucleotide substitutions in the control region of mitochondrial DNA in humans and chimpanzees. *Molecular Biology and Evolution*, 10(3), 512–526. https://doi.org/10.1093/oxfordjournals.molbev.a040023 .

Tshewang, S. & Letro, L. (2018). The herpetofauna of Jigme Singye Wangchuck National Park in central Bhutan: status, distribution and new records. *Journal of Threatened Taxa*, 10(11), 12489–12498.

Wang, K., Bhattarai, S., Wu, Y., Che, J. & Siler, C.D. (2020). Resurrection of *Amolops nepalicus* Yang, 1991 (Amphibia: Anura: Ranidae), with comments on the record of *A.* cf. *afghanus* in Nepal and China and the validity of two other junior synonyms of *A. marmoratus* (Blyth, 1855). *Zootaxa*, 4819(1), 143–158.

Wangyal, J.T. (2011). Snakes and lizards from the Bumdeling Wildlife Sanctuary region of Bhutan: Review of herpetofaunal information and new country records. *Herpetological Review*, 42(1), 117–122.

Wangyal, J.T. (2013). New records of reptiles and amphibians from Bhutan. *Journal of Threatened Taxa*, 5, 4774–4783.

Wangyal, J.T. (2014). The status of the herpetofauna of Bhutan. *Journal of the Bhutan Ecological Society*, 1, 20–25.

Wangyal, J.T. & Das, I. (2014). Status of Amphibian Studies and Conservation in Bhutan. In: Conservation Biology of Amphibians of Asia: Status of Conservation and Decline of Amphibians, Eastern Hemisphere First Edition. Heatwole, H. & Das, I. (eds.) Borneo: Natural History Publications. 201–207.

Wangyal, J.T. & Gurung, D.B. (2012). Amphibians of Punakha-Wangdue Phodrang Valley, Bhutan. *Frog Leg Newsletter of the Amphibian Network of South Asia and Amphibian Specialist Group - South Asia*, 18, 31–44.

Wangyal, J.T. & Gurung, D.B. (2017). The Current Status of Herpetofauna in Bhutan. In: Introduction to the Biodiversity of Bhutan in the Context of Climate Change and Economic Development. Centre for Rural Development Studies. Gurung, D.B. & Katel, O. (ed.). Punakha: College of Natural Resources, Lobesa. Kuensel Corporation Limited, 39–55.

Wangyal, J.T., Bower, D.S., Sherub, Tshewang, S., Wangdi, D., Rinchen, K., Phuntsho, S., ... Das, I. (2020). New herpetofaunal records from the Kingdom of Bhutan obtained through citizen science. *Herpetological Review*, 51(4), 790–798.

Wangyal, J.T., Gyeltshen & Gower, D.J. (2021). First confirmed record of caecilians (Amphibia: Gymnophiona) from the Himalayan Kingdom of Bhutan. *Journal of Animal Diversity*, 3(1), 127–132.

Wogan, G.O.U., Vindum, J.V., Wilkinson, J.A., Koo, M.S., Slowinski, J.B., Win, H., Thin, T. ... Shein, A.K. (2008). New country records and range extensions for Myanmar amphibians and reptiles. *Hamadryad*, 33(1), 83–96.

Wu, G.-f. & Tian, W.-s. (1995). A new *Amolops* species from southern Yunnan. In: Amphibian Zoogeographic Division of China. A Symposium Issued to Celebrate the Second Asian Herpetological Meeting Held at Ashgabat, Turkmenistan 6 to 10 September 1995. Zhao, E.-m. (ed.), *Sichuan Journal of Zoology, Supplement*, 51–52.

Wu, Y-H., Yan, F., Stuart, B.L., Prendini, E., Suwannapoom, C., Dahn, H.A., Zhang, B-L., ... Che, J. (2020). A combined approach of mitochondrial DNA and anchored nuclear phylogenomics sheds light on unrecognized diversity, phylogeny, and historical biogeography of the torrent frogs, genus *Amolops* (Anura: Ranidae). *Molecular Phylogenetics and Evolution* (148), 106789. doi: https://doi.org/10.1016/j.ympev.2020.106789 .

Xia, Y., Zheng, Y., Miura, I., Wong, P.B.Y., Murphy, R.W. & Zeng, X. (2014). The evolution of mitochondrial genomes in modern frogs (Neobatrachia): nonadaptive evolution of mitochondrial genome reorganization. *BMC Genomics*, 15(1), 1–15.

Yang, D.-t. (1991). Phylogenetic systematics of the *Amolops* group of ranid frogs of southeastern Asia and the Greater Sunda Islands. *Fieldiana. Zoology. New Series*, 63, 1–42.

Yang, J.-H., Huang, X.-Y., Ye, J.-F., Yang, S.-P., Zhang, X.-.C. & Chan B.P.-L. (2019). A report on the herpetofauna of Tengchong section of Gaoligongshan National Nature Reserve, China. *Journal of Threatened Taxa*, 11(11), 14434–14451.

Yu, G., Wu, Z. & Yang, J. (2019). A new species of the *Amolops monticola* group (Anura: Ranidae) from southwestern Yunnan, China. *Zootaxa*, 4577(3), 548–560.

Yuan, Z.-y., Jin, J.-q., Li, J., Stuart, B.L. & Wu, J. (2018). A new species of cascade frog (Amphibia: Ranidae) in the *Amolops monticola* group from China. *Zootaxa*, 4415, 498–512.

Zeng, Z., Liang, D., Li, J., Lyu, Z., Wang, Y. & Zhang, P. (2020). Phylogenetic relationships of the Chinese torrent frogs (Ranidae: Amolops) revealed by phylogenomic analyses of AFLP-Capture data. *Molecular Phylogenetics and Evolution*, 146, 106753.

Zeng, Z.-C., Wang, J., Lyu, Z.-T. & Wang, Y.-Y. (2021). A new species of torrent frog (Anura, Ranidae, *Amolops*) from the coastal Hills of Southeastern China. *Zootaxa*, 5004(1), 151–166.

Zhang, P., Papenfuss, T.J., Wake, M.H., Qu, L. & Wake, D.B. (2008). Phylogeny and biogeography of the family Salamandridae (Amphibia: Caudata) inferred from complete mitochondrial genomes. *Molecular Phylogenetics and Evolution,* 49, 586–597.

Zhang, Y., Rowley, J.J.L., Liu, X., Nguyen, T.T., Nguyen, H.Q., Tapley, B., Nguyen, L.T., ... Yuan, Z. (2021). *Amolops caelumnoctis* Rao & Wilkinson, 2007, a junior synonym of *A. splendissimus* Orlov & Ho, 2007 (Amphibia: Anura: Ranidae). *Zootaxa*, 5057(2), 181–200.

Zhao, W.-g., Rao, D.-q., Lü, S.-q.& Dong, B.-j. (2005). Herpetological surveys of Xizang Autonomous Region 2. Medog. *Sichuan Journal of Zoology*, 24, 250–253.

Zipkin, E.F., DiRenzo, G.V., Ray, J.M., Rossman, S. & Lips, K.R. (2020). Tropical snake diversity collapses after widespread amphibian loss. *Science*, 367(6479), 814–816.

APPENDIX I

***12S-tVal-16S* assembled arcDNA sequences used in Maximum Likelihood analyses**

```
>Amolops_himalayanus_BMNH1947.2.3.83_12S-tVal-16S
ACAAAACATTTTAACATTTTAGTACAGGTGATCGAAAAATT
CCTAGGCGCTTCAGATAAAGTACCGCAAGGGAATAATGAA
ATAGAAATGAAATAATCTTAAAGCCCTAAATAGCAGAGCTT
CCCCCTCGTACCTTTTGCATCATGGTCTAGCCAGTCTCCCCA
GGCAAAATGAAAATTTTAGTCTGTTTCCCCGAAACTAAGCG
AGCTACTTCAAAACAGCCCAAAGGGGCTAACCCGTCTCTGTT
GCAAAAGAGTGGGAAGATTTTTAAGTAGAGGTGACAAGCCT
ACCGAGCTTAGAGATAGCTGGTTGTTCAGGAAAAGAGTCTCA
GCTCTACCTTAAATCTCTTTATTAAACCAAACAAAACACTAA
ATTTAAGAGCTATTCAAATAAGGCACAGCTTATTTGAAGCGG
GGTACAACCCCTAATACTGGGTCAATATAGATGCTATTAATA
AAGTGGGCCTAAAAGCAGCCACCTTCTAAAAAGCGTTAAAG
CTTAATACACCATATCTACAATTCCACAATCTTTAAACAACC
CTTCATTACTACTGAACTATTTTATAACCTTATAAAAGCCATT
ATGCTAGAACTAGTAACAAGAAATTGTCCTTCTCCAAAATGT
ATGTTTAAACCAAAATGGACCCACCACTGGTAGTTAACGCA
AATGTAAAAATTATAGCACCACACGGCCAGAAAACCCTATA
ATCCCCTAACGTTAACCTTACACTAGAACATTACAGGAAAGA
TTAAAAGAGGGAGAAGGAACTCGGCAAATCACAGTCCCGCC
TGTTTACCAAAAACATCGCCTCTTGACTAAACATAAGAGGTC
CAGCCTGCCCAGTGACATAGTTTAACGGCCGCGGTACCCTAA
CCGTGCAAAGGTAGCATAATCACTTGTTCTTTAAATGAGGAC
TCGTATCAACGGCATCACGAGGACTGTACTGTCTCCTCCCTCC
AATCAGTGAAACTGATCCCCCCGTGAAGAAGCGGGGATTAAC
CTATAAGACGAGAAGACCCCATGGAGCTTTAAACCCAACACA
CACCTCTACGCACTCAAATCAACGTAGCCCAAGAGACTTGCGT
GTTGGTTTTAGGTTGGGGGGACCGCGGAGTAAAATTAAACCTC
CACGACAGACGGACTAACACCCTTATCCACGAACTACAATTCT
AAGAGCCAATAAATTGTTGTCTAATGACCCAATTACTTGATCAA
CGAACCAAGTTACCCTGGGGATAACAGCGCAATCTACTTCAAG
AGCCCCTATCGACAAGTGGGTTTACGACCTCGATGTTGGATCAG
GGTATCCTGGTGGTGCAGCCGCTACTAACGGTTCGTTTGTTCAA
CGATTAAAACCCT
```

```
>Amolops_formosus_BMNH1947.2.4.18_12S-tVal-16S
ACAAAACATTTTAACATTTTAGTACAGGTGATCGAAAAATT
TCTAAGCGCTTCAGATAAAGTACCACAAGGGAACAATGAA
ATAGAAATGAAATAATATTAAAGCCCTAAATAGCAGAGTTT
CCCCCTCGTACCTTTTGCATCATGGTCTAGCCAGTCTCCACA
GGCAAAACGAGAATTTTAGTCTGCTTCCCCTAAACTAAGCG
AGCTACTNNNNNNNNNNNNNNNNNGTTAACCCGTCTCTGT
TGCAAAAGAGTGGGAAGATTTTTAAGTAGAGGTGACAAGCC
TACTGAGCTTAGAGATAGCTGGTTGTTCAGGAAAAGAGTCTC
AGCTCTACCTTAAATTTTTCTATTACACCAAACAAAACACTA
AATTTAAGAGCTATTCAAATAAGGCACAGCTTATTTGAAGCG
GGGTACAAACCACAATACTGGGTTAATCCAGATATTATAATT
TAAGTGGGCCTAAAAGCAGCCATCTTCTAAAAAGCGTTAAAG
CTTAATACACCATGTCTACAAATTCCAAAATTTTTAAACAACC
CTTCATTACTACTGAACTATTTTATAACTTTATAAAAGTCATTA
TGCTAGAACTAGTAACAAGAAATTATCCTTCTCCAAAATGTA
TGTTTGAACCAAAATGGACCCACCACTGGTAGTTAACGCAAA
TGTAAAAATCATAGCACACACGCTAGAAAACCCTATGATTTC
TAAGCGTCAACCNNNNNNNNNNNNNNNNNNNNNNNN
NNNNNNNNNNNNNNNNNNNNNNNNNNNNNNNNNN
NNNNNNNNNNNNNNNNNNNNNNNNNNNNNNNNNN
NNNNNNNNNNNNNNNNNNNNNNNNNNNNNNNNNN
NNNNNNNNNNNNNNNNNNNNNNNNNNNNNNNNNN
NNNNNNNNNNNNNNNNNNNNNNNNNNNNNNNNNN
NNNNNNNNNNNNNNNNNNNNNNNNNNNNNNNNNN
NNNNNNNNNNNNNNNNNNNNNNNNNNNNNNNNNN
NNNNNNNNNNNNNNNNNNNNNNNNNNNNNNNNNN
NNNNNNNNNNNNNNNNNNNNNNNNNNNNNNNNNN
NNNNNNNNNNNNNNNNNNNNNNNNNNNNNNNNNN
NNNNNNNNNNNNNNNNNNNNNNNNNNNNNNNNNN
NNNNNNNNNNNNNNNNNNNNNNNNNNNNNNCCTTATC
CACGAACTACAATTCTAAGAGCCAATAAATTGTTGTCTA
ATGACCCAATTACTTGATCAACGAACCAAGTTACCCTGG
GGATAACAGCGCAATCTACTTCAAGAGCCCCTATCGACA
AGTAGGTTTACGACCNNNNNNNNNNNNNNNNNNNNN
NNNNNNNNNNNNNNNNNNNNNNNGGTTCGTTTGTTCA
ACGATTAAAACCCT
```

```
>Amolops_kaulbacki_BMNH1940.6.1.1_12S-tVal-16S
ACAAAACATTTTAACACTTTAGTACAGGTGATCGAAAAATT
TCTAAGCGCTTCAGATAAAGTACCGTAAGGGAATAATGAAA
TAGAAATGAAATAATCTTAAAGCCCTAAATAGCAGAGCTTC
CCCCTCGTACCTTTTGCATCATGGTCTAGCCAGTCCCCCCA
GGCAAAACGAAAATTTTAGTCTGATTCCCCGAAACTAAGCG
AGCTACTTCAAAACAGCCCAAAAGGGCCAACCCGTCTCTGT
TGCAAAAGAGTGGGAAGATTTTTAAGTAGAGGTGACAAGCC
TACCGAGCTTAGAGATAGCTGGTTGTTCAGGAAAAGAGTCTC
AGCTCTACCTTAAATTTTTTTTATTGAAACCAAACAAAACACT
AAATTTAAGAGCTATTCAAATAAGGCACAGCTTATTTGAAGC
GGGGTACAACCCCAAATACTGGGTTAGTCTAGATGTAGTAAA
TAAAGTGGGCCTAAAAGCAGCCATCTTCTGAAAAGCGTTAAA
GCTTAATATACCTTATCTACAATTCCACAATTTTTAAACAACCC
TTCATTACTACTGAACTATTTTATAACCTTATAAAAGTTATTAT
GCTAGAACTAGTAACAAGAAATTGCCCTTCTCCCAAATGTATG
TTTAAACCAAGATGGACCTACCACTGGTAGTTAACGCAAGTGT
AAAAATCATAGCACCACACGGCTAGAAAACCCTATGGTTTCTC
AGCGTTAACCTTACACTAGAACATTACAGGAAAGATTAAAAGA
GAAAGAAGGAACTCGGCAAATCACAGTCCCGCCTGTTTACCAA
AAACATCGCCTCTTGACCAAGTATAAGAGGTCCAGCCTGCCCAG
TGACATAGTTTAACGGCCGCGGTACCCTAACCGTGCAAAGGTAG
```

```
CATAATCACTTGTTCTCTAAATAGGGACTCGTATCAATGGCATCA
CGAGGGCTGTACTGTCTCCTTTCTCCAATCAGTGAAACTGATCTC
CCCGTGAAGAAGCGGGGATTGACCTATAAGACGAGAAGACCCC
ATGGAGCTTTAAACCCAATATACACCTCCTACGCACTCAAATCA
ATATAGCCCAAGAGACTTGTGTATCGGTTTTAGGTTGGGGGACC
GCGGAGTAAAATTAAACCTCCACGACAGACGGATTAACACCCTT
ATCCACGAACTACAATTCTAAGAGCCAATAAATTGTTGTCTAAT
GACCCAATTACTTGATCAACGGACCAAGTTACCCTGGGGATAAC
AGCGCAATCTACTTCGAGAGCCCCTATCGACAAGTAGGTTTACG
ACCTCGATGTTGGATCAGGGTATCCTAGTGGTGCAGCCGCTACT
AAAGGTTCGTTTGTTCAACGATTAAAACCCT
```

***nd2* assembled arcDNA sequence used for *p*-distance analyses**

```
>Amolops_formosus_BMNH1947.2.4.18_nd2
ATTAATACCCTCGCCATCATCCCAATTATAACTAAAACCNN
NNNNNNNNNNGCCATTGAAGCTGCCACAAAATACTTCCTCA
CTCAAGCCACAGCCTCCGCTCTAGTTCTATTTTCAAGTCTCAT
TAATGCCTGACAAGTAGGACAATGAAATATCTCCCACCTAAC
TGACTTACCAATAAATGTACTTGCTATTGCCCTCATAATAAAA
CTAGGCCTAGCCCCCTTACATTTTTNNNNNNNNNNNNNNNNNN
NNNNNATTTCATTGTCTACAGGGCTTATTTTATCAACCTGACAA
AAAATTGCCCCAATAGCCCTTCTTCTCCAAATTTCCCACCTAAT
TGACCTAAATTTAACCATTATTATTGGTCTCACCTCAATTCTAGT
TGGGGGATGAGGCGGCATTGCCCAAACCCAATTACGTAAGATTA
TTGCCTTCTCTTCAATCGGCCACCTTGGGTGAATAGTCATTGTATT
AAAATTTAGCCCCCAGCTCACACTTTTTAACTTTCTACTTTATATC
TTAATAACAACCTCAATATTTATCTCCCTCATAGCAATTTCTGCCA
CAAAAATATCGGAAATCTCCACATCCTGACCAAAAACCC
```

***co1* assembled arcDNA sequence used for *p*-distance analyses**

```
>Amolops_formosus_BMNH1947.2.4.18_co1
ATTGGCACAGCCTTAAGCCTACTCATTCGAGCAGAACTAAG
CCAACCMGGAGCCCTTCTTGGTGATGACCAAATTTACAATG
TAATTGTAACCGCCCACGCATTTGTAATAATTTTTTTTATAGT
AATGCCCATCTTAATCGGAGGCTTCGGAAACTGATTAATCCC
ATTAATAATTGGAGCCCCAGACATAGCTTTCCCCCGGATAAA
TAATATGANNNNNNNNNNNNNNNNNNNNNCATCTTTTTTCCTCCT
CCTAGCATCCTCTGCAGTCGAGGCTGGGGCCGGAACAGGCTGAAC
TGTTTATNNNNNNNNNNNNNNNNNNNNNNNNNNNNNNNNNNN
NNNNNNNNNNNNNNNNNNNNNNNNNNNNNNNNNNNNNNNNN
NNNNNNNCTCATCAATCTTGGGGGCTATTAACTTTATTACAA
CAATTATTAATATAAAACCTGCATCAATTACACAATACCAAA
CACCCCTCTTTGTTTGGTCCGTNTTGATTACTGCCGTCCTATT
ACTACTTTCCCTCCCAGTCTTAGCCGCCGGCATCACAATACTT
TTAACTGACCG
```

APPENDIX II

Comparative specimens examined

Amolops afghanus: BMNH 1947.2.27.93 (previously BMNH 1933.3.7.55: lectotype of *Polypedates afghanus*—Dever et al., 2012), female, “Afghanistan” (in error).

Amolops assamensis: ZSIK 10272 (holotype), adult male, “Mayeng Hill”, Assam, India; ZSIK 10273 (paratype), adult female, “Kolahat R.F.”, Assam, India; ZSIK 10274 (nontype), adult female, “Garbhanga R.F.”, Assam, India.

Amolops formosus: BMNH 1947.2.4.18 (previously BMNH [18]72.4.17.281: holotype), adult female, “Khassya” [=Khasi Hills], Meghalaya, India.

Amolops gerbillus: ZSIK 16925 (holotype of *Rana gerbillus*), juvenile not sexed, “Yembung, alt. 1100 ft”, Arunachal Pradesh, India; ZSIK 16950 (holotype of *Ixalus argus* Annandale, 1912), juvenile not sexed, “Upper Renging, alt. 2150 ft., Abor”, Arunachal Pradesh, India.

Amolops himalayanus: BMNH 1947.2.27.94 and BMNH 1947.2.3.83 (previously BMNH [18]72.4.17.347 and BMNH [18]80.11.10.120, respectively: syntypes), two adult females and BMNH 1947.2.27.95 (previously BMNH [18]87.11.2.20: syntype), adult male, “Darjeeling”, West Bengal, India; ZSIK (unregistered when examined in 2009), adult female, “Gangtok, Sikkim”, India.

Amolops kaulbacki: BMNH 1947.2.3.96 (previously BMNH 1940.6.1.1: holotype) and BMNH 1947.2.3.65 (previously BMNH 1940.6.1.2: paratype), two adult males, “Pangnamdim, Triangle, Upper Burma”, Kachin State, Myanmar.

Amolops kohimaensis: ZSIK A 10972 (holotype), ZSIK A 10966, ZSIK A 10971, BNHS 5282 (paratypes), SDB 2007.129 (referred specimen), five adult males, “Lorü, 25°38’23”N 94°03’31”E, 1,575 m asl., Jotsoma village, Kohima district, Nagaland, northeast India”.

Amolops longimanus: NRM1861 (holotype), “Kambaiti”, Kachin State, Myanmar.

Amolops monticola: ZSIK 10036 (holotype), adult female, “Darjeeling”, West Bengal, India.

Amolops nidorbellus: ZSIK A 10965 (holotype), BNHS 5276 (paratype), SDB 2009.335 (referred specimen), three adult males, and ZSIK A 10968–10970 (paratypes), three adult females, “Lorü, 25°38’23”N 94°03’31”E, 1,575 m asl., Jotsoma village, Kohima district, Nagaland, northeast India”.

Amolops senchalensis: ZSIK A8753 (holotype), adult male, “Senchal Lake, Darjeeling”, West Bengal, India.

Amolops viridimaculatus: CAS 242214, adult male, and CAS 242215, adult female, “XiaoDiFang Village (24°52'51.4" N, 98°45'7.9" E), Zhengding, LongYang Co. [error, should be Tengchong Co.], Baoshan Pref., Yunnan, China”; CAS 242250–242252, three adult males, and CAS 242249, adult female, “XiaoDiFang River (24°51'45.5" N, 98°45'21.7" E, 2133 m) at XiaoDiFang Village, TengChong Co., Baoshan Pref., Yunnan, China”.

Accepted: 17 May 2022

Please note that the Supplementary Material for this article is available online via the Herpetological Journal website: https://thebhs.org/publications/the-herpetological-journal/volume-32-number-3-july-2022

THE HERPETOLOGICAL JOURNAL
SUBMISSION PROCESS

The Herpetological Journal is an international peer-reviewed publication of the British Herpetological Society, with open-access publication options. *The Journal* has a broad focus relating to behaviour, ecology, evolution, systematics, taxonomy, physiology, anatomy, functional morphology, pathology, natural history, method development and conservation of reptiles and amphibians. All articles should appeal to a general herpetological audience and have a solid grounding in natural history. We are committed to open science and avoiding unconscious biases so moving forward we will operate a double-blind peer review process.

Manuscripts that describe natural history observations, range extensions or checklists are not appropriate submissions (unless they address a bigger question) and would be better suited to our sister publication, *The Herpetological Bulletin*.

The Herpetological Journal welcomes contributions in the following categories:

- Full length research articles
- Short communications
- Reviews
- Perspectives/Opinion pieces

Files to be uploaded to the OJS system: Cover Page, Main Text, Tables, Figures, Supplementary Files.

Cover Page:
This will not be seen by peer reviewers in order to comply with a double-blind peer review process. The cover page should include Title, Authors, Author Affiliations, Ethical Statement and Author Contributions (if editors do not deem that authors contributed substantially to the research then the article will be rejected).

Main Text:
Nb. author names or affiliations should not be included in this file.

Full length research articles should be between 2,500 and 6,000 words and include the following sections: Title, Abstract (maximum 300 words), Keywords (five words that are not used in the title), Introduction, Methods, Results, Discussion, Acknowledgements, Data Accessibility, References, Figure captions, Table captions. The word limit excludes Data Accessibility and References. There are no limits to the number of figures and tables.

Short communications should be less than 2,500 words and include the following sections: Title, Abstract (maximum 250 words), Keywords (five words not used in the title), Main Text (NOT separated into Introduction, Methods, Results and Discussion), Acknowledgements, Data Accessibility, References, Figure captions, Table captions. The word limit excludes Data Accessibility, References, and Figure and Table captions. Short communications can have a maximum of ONE figure and ONE table.

Reviews are either solicited by editors or a short email enquiry should be sent to the Editor-in-Chief (bhsherpetologicaljournal@gmail.com) to enquire about the suitability of a proposed review. Reviews should be between 2,500 and 6,000 words. Section headings can be specified at the authors discretion.

Perspectives/Opinion pieces will be considered if they address a new or controversial topic/idea, or if they are comments about newly published articles in *The Herpetological Journal*. Perspectives/Opinion pieces should be a maximum of 1,500 words (excluding references) and can include ONE figure and ONE table.

Tables:
Tables should be provided in a separate Word file. Tables should be numbered in Arabic numerals, e.g. Table 1. Tables should be as simple as possible and typed double-spaced on separate sheets with a title/short explanatory paragraph above the table. Horizontal and vertical lines should be avoided, as should tables that split over more than one page or that need to be set in landscape format.

Figures:
Figures should initially be submitted in a single Word or PDF file. Graphs, line drawings and photographs should be numbered in sequence in Arabic numerals, e.g. Figure 1. If a figure has more than one part, each should be identified as (a), (b), etc. Figure captions should be included at the end of the main text. After acceptance figures should be submitted as separate image or pdf files with a minimum resolution of 300dpi and a maximum file size of 5MB.

Supplementary Data/Files:
To conform with an open science process, it will be necessary for datasets, code, supplementary figures etc. to be deposited in an online repository (e.g. https://osf.io/) and made available after publication. At the initial submission stage, at a minimum, any code and supplementary figures should be uploaded in the submission portal for review. Any new taxonomic changes should be recorded on ZooBank.

It is a fundamental condition that submitted manuscripts have not been published and will not be simultaneously submitted or published in another journal. However, as a journal we do support the submission of articles on preprint servers (e.g., bioRxiv) as long as the preprints are linked to final published articles.

By submitting a manuscript, the authors agree that the copyright for their article is transferred to the publisher if and when the article is accepted for publication. The copyright covers the exclusive rights to reproduce and distribute the article, including reprints and photographic reproductions. Permission to use images after publication will almost always be granted but must be sought in advance from the Editors.

Papers should be written in British English (including figure labels) and spelling should be that of the Oxford English Dictionary.

Times and dates should conform to the following formats: for time of day use 0900, 1000 etc; for dates use 7 July 2017 etc. Please avoid using bold text, all caps or small caps for emphasis. If emphasis is required, use italics. Common names should be in lower case unless a proper noun is used.

All submissions must adhere to the British Herpetological Society's Ethical Policy and Guidelines, which can be found here – https://www.thebhs.org/images/stories/BHS-ethicspolicy.pdf.

Open Access Policy: *The Herpetological Journal* supports "green" open access, as outlined by the Research Councils UK, to facilitate deposition of articles e.g. at institutional repositories. *The Herpetological Journal* also offers the option of "gold" open access for individual articles (free of charge for members of the British Herpetological Society, and at an article processing charge of £97 for non-members).

REFERENCE STYLE

CITATION IN TEXT:

- Chronological then alphabetical
- Use "et al." (not italicised) for more than two authors
- Last name (s) and year separated by comma
- Names separate by "&"
- References separated by semicolon

Ex. 1: (Heyer et al., 1988; Weygoldt et al., 1989; Eterovick et al., 2005)
Ex. 2: (Smith et al., 2004; Jones & Smith, 2008)
Ex. 3: (Smith et al., 2015)
Ex. 4: "Although Smith et al. (2008) did not include -"
Ex. 5: "- as observed by Smith & Jones (2017)"

REFERENCES

- Authors
- Last name separated from initials by comma
- Initials capitalised and separated by period (no space)
- Names separated by commas
- Last name separated by "&"

Ex.: Smith, A.H., Jones, R.D. & Lloyd, K.A.
Ex.: Smith, A.H. & Jones, R.D.

Year:
- In parentheses, followed by a full stop.

Title:
- Only first letter capitalised except book titles (in this case, All First Letters Capitalised).

Journal:
- Journal name should be written in full, italicised, followed by a comma
- Volume and pages separated by comma and ending with full stop (not italicised).

Journal article:
- Authors. (Year). Title. *Journal*, Volume (Issue), xx–xx.

Book:
- Authors. (Year). Book Title. City: Country. Xxx p.

Book chapter:
- Authors. (Year). Chapter title. In: *Book Title*, Book editor (s). (Ed./Eds.) City: Country. Xxx p.

Ex. 1:
Lebboroni, M. & Corti, C. (2006). Road-killing of lizards and traffic density in central Italy. In: *Herpetologia Bonnensis II: Proceedings of the 13th Ordinary General Meeting of Societas Europaea Herpetologica*, 81–82. Vences, M., Köhler, J., Ziegler, T. & Böhme, W. (eds). Bonn: Societas Europaea Herpetologica.

Ex. 2:
Sambrook, J., Fritsch, E.F. & Maniatis, T. (1989). Preparation and Analysis of Eukaryotic Genomic DNA. In: *Molecular Cloning: A Laboratory Manual*, 2nd Eds. Cold spring Harbor Laboratory Press, New York, USA.

Websites:
Lang, J., Chowfin, S. & Ross, J.P. (2019). *Gavialis gangeticus*. The IUCN Red List of Threatened Species 2019: e.T8966A149227430. Downloaded on 3 October 2019. http://dx.doi.org/10.2305/IUCN.UK.2019-1.RLTS.T8966A149227430.en.

Herpetological Journal website: https://www.thebhs.org/publications/the-herpetological-journal